Bulletin
of
The Geological Society of America

VOLUME 68 October 1957 NUMBER 10

CONTENTS

	Pages
Geologic evolution of the Beartooth Mountains, Montana and Wyoming. Part 1: Archean history of the Quad Creek area. By F. Donald Eckelmann and Arie Poldervaart	1225–1262
Weathering of granite and associated erosional features in Hong Kong. By Bryan P. Ruxton and Leonard Berry	1263–1292
Anthracitic coal from Precambrian upper Huronian black shale of the Iron River district, northern Michigan. By S. A. Tyler, E. S. Barghoorn, and L. P. Barrett	1293–1304
Mineralogy, petrography, and radioactivity of representative samples of Chattanooga Shale. By Thomas F. Bates and Erwin O. Strahl	1305–1314
Geology of the Cochise Head and western part of the Vanar quadrangles, Arizona. By Floyd F. Sabins, Jr.	1315–1342
Geological and geophysical synthesis of the tectonics of portions of British Columbia, the Yukon Territory, and Alaska. By Pierre St. Amand	1343–1370
Upland gravels of southern Maryland. By John Schlee	1371–1410
Short Notes	
Girvanella not a guide to the Cambrian. By Richard Rezak	1411–1412
Misconception of the intermediate refractive index. By R. C. Emmons and R. M. Gates	1413–1414

Subscription $15.00 per year.

Printing Office: Mt. Royal & Guilford Aves., Baltimore 2, Md.

Communications for publications should be addressed to The Geological Society of America, Dr. H. R. Aldrich, Secretary, 419 West 117 Street, New York, N. Y.

Please give notice of change of address 4 weeks in advance. Claims for nonreceipt of the Bulletin of a given month must be sent to the Secretary of the Society before the end of the second succeeding month.

Entered as second-class matter at the Post Office at Baltimore, Md., under the Act of Congress of July, 16, 1894.
Accepted for mailing at special rate of postage provided for in Section 1103 Act of October 3, 1917, authorized on July 8, 1918.

PAPERS IN PRESS FOR FORTHCOMING ISSUES

STRUCTURE AND PETROLOGY OF THE CARIBOU LAKE INTRUSIVE BODY, ONTARIO, CANADA. By G. M. Friedman

HALOGEN-ACID ALTERATION OF ASH AT FUMAROLE NO. 1, VALLEY OF TEN THOUSAND SMOKES. By T. S. Lovering

THERMAL EFFECTS OF THE OCEAN ON PERMAFROST. By A. H. Lachenbruch

ORIGIN OF THE CORUNDUM DEPOSITS OF RENFREW COUNTY, ONTARIO, CANADA. By H. D. Carlson

STRATIGRAPHY AND STRUCTURE OF THE ST. ALBANS AREA, NORTHWESTERN VERMONT. By A. B. Shaw

PEBBLE AND SAND LITHOLOGY OF THE MAJOR WISCONSIN GLACIAL LOBES OF THE CENTRAL LOWLAND. By Richard C. Anderson

CORRELATION OF THE TRIASSIC FORMATIONS OF NORTH AMERICA EXCLUSIVE OF CANADA. By J. B. Reeside *et al.*

THERMAL WATERS OF VOLCANIC ORIGIN. By D. E. White

MAGMATIC, CONNATE, AND METAMORPHIC WATERS. By D. E. White

BULLETIN OF THE GEOLOGICAL SOCIETY OF AMERICA
VOL. 68, PP. 1225-1262, 15 FIGS., 5 PLS. OCTOBER 1957

GEOLOGIC EVOLUTION OF THE BEARTOOTH MOUNTAINS, MONTANA AND WYOMING

PART 1. ARCHEAN HISTORY OF THE QUAD CREEK AREA

By F. DONALD ECKELMANN AND ARIE POLDERVAART

ABSTRACT

The Beartooth Mountains form an elongated range with longer axis trending northwest and consist of a core of granitic gneiss flanked by migmatites and metasediments. The Quad Creek area is astride the northeast boundary of granitic gneiss and migmatites and metasediments. The area is 7 square miles in extent and is occupied by a large syncline with axis striking north-northeast and plunging 10°–30°S.-SW.

Detailed field studies indicate the following geologic history. (1) Original deposition of an Archean sedimentary sequence. (2) Emplacement of metagabbro and ultramafic intrusions, followed by folding; fold axes strike north-northeast. (3) Regional metamorphism and granitization, resulting in a core of granitic gneiss and mantle of migmatites and metasediments with boundaries trending northwest. The last expression of granitization was the production of pegmatites; a few metanorite intrusions were emplaced before pegmatite formation. (4) Emplacement of a metabasaltic dike swarm, younger than the pegmatites but probably within the same plutonic cycle, and striking mainly northwest. (5) Emplacement of a younger Precambrian dolerite dike swarm which has the same dominant strike as the older dike swarm. (6) Peneplanation and deposition of Paleozoic sediments. (7) Laramide uplift and thrusting, and emplacement of felsic porphyries early in this cycle. Laramide structures are controlled by basement structures. The dominant northwest trend was established in the Archean cycle of regional metamorphism and granitization, yet the direction of the oldest foldings is unique.

Field and laboratory studies indicate *in situ* formation of granitic gneiss. Fold axes pass continuously and without deflection from the mantle of metasediments and migmatites across the boundary zone into the core of granitic gneiss, although the folds intersect the boundary zone at 40°–50°. The boundary zone consists of interdigitating tongues of migmatites and granitic gneiss, and these rock types grade into one another along and across strike. In the boundary zone more resistant rock types persist at definite horizons, continuous with skialiths of similar rocks in granitic gneiss. Foliation in granitic gneiss and banding in migmatites are parallel throughout to bedding in metasediments. Growth phenomena shown by zircons of different rocks also indicate autochthonous formation of granitic gneiss.

Mineral assemblages of resisters of para-amphibolite, ultramafic rocks, biotite schists, and banded ironstones indicate metamorphism in sillimanite-almandine subfacies of amphibolite facies; temperatures probably were 500°–600° C. Subsequent increase in water concentrations can be traced in seemingly regressive changes in mineral assemblages. This culminated in metasomatic changes which produced granitic gneisses from pre-existing rocks. The writers conclude that granitization was effected by migrating alkaline aqueous solutions during a prolonged Archean cycle of thermal activity. Twenty-three chemical analyses are given, and chemical variation during granitization is discussed.

CONTENTS

TEXT

	Page
Introduction	1226
Regional setting	1226
Beartooth research project	1227
Methods of investigation	1228
Previous work	1229
Acknowledgments	1229
Tectonic structures	1230
Quad Creek syncline	1230

	Page
Attitudes of dikes	1230
Petrography	1233
Granitic gneisses	1233
Migmatites	1236
Metasediments	1237
Meta-igneous rocks	1240
Pegmatites	1242
Mineralogy	1242
Zircon studies	1242
Metamorphic facies	1244
So-called regressive changes	1245
Metasomatic effects	1246
Chemical data	1247
Origin of rocks	1249
Granitic gneiss	1249
Pegmatites	1250
Para-amphibolites	1251
Siliceous biotite-cordierite-bronzite-anthophyllite rocks	1251
Quartzites	1253
Banded ironstones	1254
Granitization in Beartooth Mountains	1254
Type of granitization	1254
Chemical variation	1255
Geologic chronology	1255
General statement	1255
Mae West metagabbro	1256
Ultramafic rocks	1257
Folding and metamorphism	1257
Metamorphism and granitization	1257
Quad Creek metanorite	1258
Metabasaltic dikes	1258
Precambrian dolerite dikes	1258
Laramide revolution	1258
Absolute ages and correlations	1259
References cited	1259

ILLUSTRATIONS

Figure	Page
1. Geologic setting of Beartooth Mountains	1227
2. Area of Beartooth research project	1228
3. Attitudes of 89 felsic porphyry dikes	1231
4. Development of low-angle fractures	1231
5. Attitudes of 89 Precambrian mafic dikes	1231
6. Attitudes of 56 Precambrian pegmatite dikes	1232
7. Granitic gneisses	1233
8. Migmatites	1236
9. Para-amphibolites	1237
10. Metasediments	1238
11. Metasediments	1239
12. Pre-pegmatite mafic intrusives	1241
13. Post-pegmatite mafic dikes	1243
14. Field sketch of siliceous biotite-cordierite-bronzite-anthophyllite rock	1253
15. Differentiation-index diagram for para-amphibolites, migmatites, and granitic gneisses	1256

Plate	Following page
1. Aerial view of Rock Creek face of the Quad Creek area	1240
2. Quartzite, migmatite, and pegmatite	
3. Agmatite, ultramafic, and migmatite	
4. Outgrowths and overgrowths on zircons of granitic gneiss	

	Facing page
5. Map and cross sections of the Quad Creek area	1262

TABLES

Table	Page
1. Chemical and petrographic data	1234
2. Characters of zircons	1244
3. Trace-element standards	1248
4. Trace-element data for ultramafic and mafic rocks of igneous origin	1248
5. Ca-Sr data for mafic rocks of igneous origin	1249
6. Trace-element data for amphibolites and migmatites	1249
7. Compositions of basalts, para-amphibolites and dolomitic shales	1252
8. Siliceous cordierite-anthophyllite rocks	1252
9. Geologic chronology of Quad Creek area	1257

INTRODUCTION

Regional Setting

The Bighorn Basin of Montana and Wyoming (Fig. 1) is surrounded by mountain ranges which expose cores of Archean rocks: the Beartooth Mountains to the northwest, the Owl Creek and Bridger mountains to the south, and the Bighorn and Pryor mountains east and north of the basin. The Absaroka-Shoshone Mountains west of the basin consist of Tertiary lava flows and pyroclastic rocks which accumulated in the Yellowstone structural basin. The Bighorn Basin contains a thick sequence of Paleozoic and younger sediments. In the basin the surface of the crystalline basement is almost 10,000 feet below sea level (Bucher, Thom, and Chamberlin, 1934, p. 187), whereas in the surrounding mountains the basement stands 10,000–12,000 feet above sea level. Fold structures in the basin are related in age, trend, and asymmetry to Laramide structures in the adjacent uplifted mountains (Bucher, Thom, and Chamberlin, 1934, p. 173–174). The axis of the Bighorn Basin is in the western part of the basin and passes underneath the Beartooth thrust just south of Red Lodge (Bucher, Chamberlin, and Thom, 1933, p. 681).

The Beartooth Mountains trend northwest and are approximately 60 miles long by 30 miles wide (Fig. 1). They consist mainly of a core of granitic gneiss flanked by migmatites and metasediments (Lammers, 1939, unpublished ms.). In addition there are basaltic and

metabasaltic intrusions of several ages and felsic porphyry dikes, stocks, and sheets of early Laramide age (Rouse *et al.*, 1937, p. 736–737). A few erosion remnants of Paleozoic sediments are also present, as at Beartooth Butte (Scheufler, 1954, M.S. thesis, Wayne Univ.).

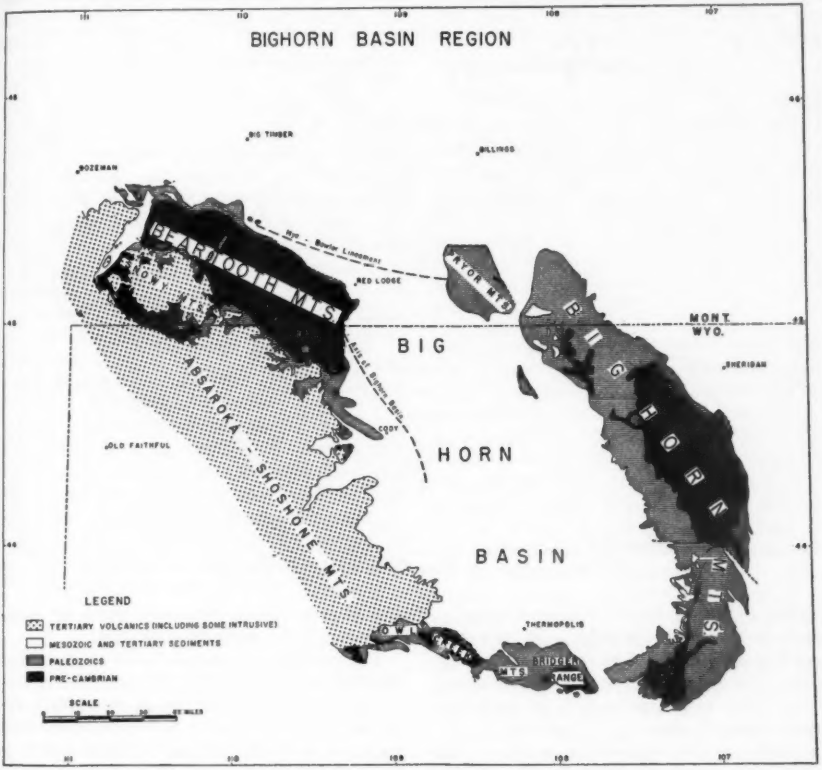

FIGURE 1.—GEOLOGIC SETTING OF BEARTOOTH MOUNTAINS

Structurally the Beartooth Mountains form an archlike uplift, bounded by the Beartooth thrust to the northeast and the Gardner fault to the southwest. During the Laramide Revolution the Beartooth block was tilted to the southwest and thrust northeastward (Bucher, Thom, and Chamberlin, 1934, p. 174).

Beartooth Research Project

The basic research program of the Yellowstone-Bighorn Research Association at Red Lodge, Montana, is the study of the evolutionary history of the Bighorn Basin region as a typical mountain and mountain-border region. The Beartooth research project was initiated in 1952 to augment knowledge of the geologic history and structural and petrogenetic development of Precambrian rocks of this mountain range.

The main area of investigation is a zone about 10 miles wide, which extends across the range from Red Lodge to Cooke City. Reconnaissance work within this larger area and detailed mapping (scale 400 feet to the inch) of a series of carefully selected key areas are in progress. The Quad Creek area is the first of these key areas (Fig. 2). It was selected because of (1) accessibility from U.S. Highway 12 which provides many excellent road cuts, (2) position astride the northeastern boundary of the core of granitic gneiss and mantle of migmatites and metasediments, and (3) the relief of

3000 feet with steep valley walls, which contributes to the high percentage of outcrop in the area and yields opportunities to observe rocks and structures in three dimensions (Pl. 1).

The writers believe that detailed field studies are prerequisite to geologic research and agree with Read (1952, p. 6) that, "if granitization. . . cannot be proved in the field . . . it cannot be proved at all." In this first report of the Beartooth project, emphasis is on field relations. Petrographic work reported is of reconnaissance nature; it serves as background to field observations and defines the various rocks more closely in terms of their mineralogical and chemical composition. Detailed petrologic studies of changes involved in the autochthonous formation of granitic gneiss are reserved for later contributions under the project.

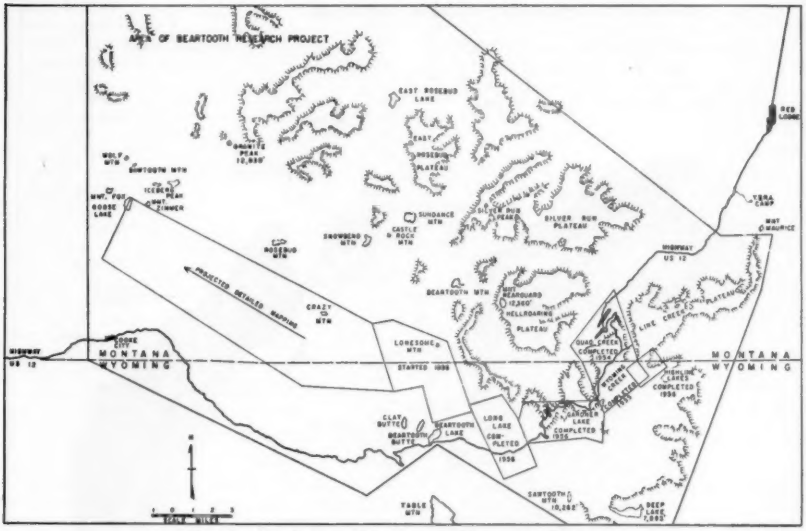

FIGURE 2.—AREA OF BEARTOOTH RESEARCH PROJECT

Methods of Investigation

Field mapping was done with the aid of a surveyed highway map of the Highway Division, Department of the Interior, specially prepared oblique aerial and ground photographs, and enlargements of a vertical U.S. Geological Survey aerial photograph. The scale of the photo enlargements and the highway map (400 feet to the inch) was used in actual field mapping. Traverses were spaced at intervals of 400 feet or less and taken at high angles to the prevailing structural trend. Attitude readings along traverses were recorded at least every 100 feet. In reducing the field map to a scale of 1:6000, the numerous dip and strike symbols have been averaged. On the final map (Pl. 5) each symbol represents about 10 measurements in the immediate vicinity.

The petrographic work is based on more than 700 thin sections. Modes were determined with a Chayes point counter, using three slices cut at right angles for each specimen, with total traverses of 1500–2500 points. Shaw and Harrison (1955) and Chayes (1956, p. 16–30) have shown that modes of foliated and lineated rocks can be determined with accuracy if proper precautions are used. All modes have been checked by calculating bulk chemical compositions from them and comparing calculated compositions with chemical analyses. Discrepancies remain between the analyses and the model compositions (Table 1). For example, CaO in the analysis of specimen 329/53 is nearly twice that calculated from the mode. Again, Al_2O_3 in the analysis of specimen 227/54 is about 4 per cent lower than is calculated from the mode.

Refractive indices were determined by the immersion method using sodium light and a Leitz-Jelley refractometer. Optic axial angles

were measured directly with a universal stage. Compositions of plagioclase are based on refractive indices, checked by extinction angles of albite twin lamellae, determined on the universal stage. Compositions are based on correlation curves published by Hess (1952; orthopyroxenes) and Poldervaart (1950; plagioclases and olivines).

Zircon concentrates were prepared by methods described by Poldervaart (1955a, p. 435–437) and Eckelmann and Kulp (1956, p. 307–308). For each sample the entire concentrate was mounted on a single slide, and zircon characteristics were recorded for 100 grains intersected at spaced intervals along spaced traverses covering the slide. Concentrates prepared from the same rock give nearly identical results for counts of 100 grains for each concentrate.

The spectrographic work was done by Miss H. Scribny under the guidance of Dr. Karl Turekian at the Lamont Geochemical Laboratory. The elements Ga, Ba, Co, Ni, Cr, and Zr were determined by mixing one part of sample with two parts of graphite buffer and arcing 10 mg of the mixture to completion in a platform electrode at 16 amperes. The data are semiquantitative only; they were obtained by visual comparison with two standards. In addition, Dr. Karl Turekian determined Sr and Ca for several samples, using a technique described by Turekian and Kulp (1956).

Previous Work

Previous work on the Precambrian rocks of the Beartooth Mountains has been of reconnaissance nature, with emphasis on either economic or structural geology.

Lovering (1929) studied the Cooke City mining district and reported two ages of intrusive granites: an older formation called the Goose Creek granite and a younger formation known as the Cooke granite.

Lammers (1939, unpublished ms.) recognized Precambrian controls for Laramide structures. He regarded the Goose Creek granite as intrusive but found the Cooke granite to be of the same age and produced by *lit-par-lit* injection, granitization, and partial assimilation by Goose Creek granite of a series of hornblende and biotite schists. The Cooke granite was reported to be similar to the granitic gneiss of the core of the Beartooth range. Biotite schist and gneiss and amphibolite lenses in the granitic gneiss were interpreted as stoped blocks picked up by the granite during emplacement. Foliation was considered to represent platy flow structures. Lammers also recognized the partition of the Beartooth Mountains into a core of granitic gneiss with a mantle of migmatites and metasediments. The Quad Creek area was described by Lammers (1939, unpublished ms.) as consisting mainly of Precambrian

> "... migmatitic injection gneiss in which bands of highly granitized schist alternate with layers of gray biotite granite. Here and there one finds outcrops of pink granite similar to the Cooke granite of the Cooke City Mining District. The relationship between this pink granite and the migmatite could not be ascertained because diagnostic exposures are lacking. In the absence of better evidence its origin is assumed to be the same as that of the Cooke formation."

Cloos and Cloos (1934) found several intrusive granites in the southern part of the Beartooth range. Schafer (1937) reported on the chromite deposits in serpentinites of Hellroaring Plateau and the Quad Creek area. Lane (1938, p. 63–64) gave helium age determinations for the Quad Creek metanorite and two metanorite dikes. Rouse *et al.* (1937) and Stobbe (1952) described the early Laramide felsic porphyries along the northeastern part of the Beartooth Mountains. The present writers have not examined these rocks in further detail. Scheufler (1954, M.S. thesis, Wayne Univ.) mapped the erosion remnant of Paleozoic sediments at Beartooth Butte and compared jointing in sediments with that in the surrounding Precambrian rocks.

Bucher, Thom, and Chamberlin (1934), Bucher, Chamberlin, and Thom (1933), and Thom (1952; 1955) discussed the tectonic setting of the Beartooth Mountains and emphasized Precambrian control of Laramide structures.

Acknowledgments

This investigation forms part of the research program of the Yellowstone-Bighorn Research Association. The camp of the Association at Red Lodge, Montana, has been used as field base throughout the work.

Financial support for the major part of the work was received from the Penrose Bequest of The Geological Society of America. Parts of the work have also been financed by support from the Yellowstone-Bighorn Research Asso-

ciation, the National Science Foundation (project NSF-G-1717), and the Higgins and Kemp funds of Columbia University. Eckelmann also acknowledges tenure of the James Furnam Kemp Fellowship during 1955.

The writers are grateful for the help and stimulation received from many hours of discussions with Profs. Walter H. Bucher and W. Taylor Thom, Jr., both foundation members of the Yellowstone-Bighorn Research Association. They benefited from discussions in the field with Drs. Hans P. Eugster, Richard M. Foose, Gunnar Kullerud, J. Laurence Kulp, E. C. H. Lammers, John C. Maxwell, Willard H. Parsons, J. Frank Schairer, Saurindranath Sen, and Hatten S. Yoder, Jr. They were further privileged by discussions at Columbia University with Prof. H. H. Read.

Mr. Jack Richard of Cody, Wyoming, is responsible for the excellent aerial and ground photographs which greatly facilitated the field work. Ronald E. Wilcox helped in mapping during 1954. The co-operation of Karl Turekian in supervising the spectrographic work at the Lamont Geochemical Laboratory is also gratefully acknowledged. Finally, the writers are indebted to Dr. H. B. Wiik for the chemical analyses.

Tectonic Structures

Quad Creek Syncline

The geologic map (Pl. 5) shows the main synclinal structure of the area. The over-all trend is N. 5°–10° E. with a plunge of 10°–30° S.-SW. This is the over-all plunge of the folds in the Quad Creek area and in adjacent areas. Locally the plunge steepens, as it does just north of the Quad Creek metanorite. The limbs dip at steep angles, generally between 60° and 80°. Maximum separation of limbs is 3 miles, with no evidence of adjacent related structures in the mapped area. Mapping in the Gardner Lake and Long Lake areas (Fig. 2) resulted in recognition of several similar synclinal structures separated by zones of vertically dipping rocks. Thus the Quad Creek syncline is one of a series of folds striking north-northeast and plunging south-southwest.

In the Quad Creek area the structure is continuous across the gradational boundary zone between migmatites and metasediments to the northeast and granitic gneiss to the southwest. Continuity of structure is based on (1) attitudes of biotite-rich bands and streaks, (2) foliation planes, (3) thin, platelike lenses of amphibolite, biotite gneiss, and biotite schist, and (4) bedding planes in metasediments. Wherever observed, foliation in granitic gneiss and migmatites parallels bedding in metasediments. This is especially striking in gradations of quartzite and granitic gneiss (Pl. 2, fig. 1) Several minor folds are found in the synclinal trough (Pl. 5). Two criteria show that the beds are right-side up, and thus that the over-all structure of the Quad Creek area is a syncline: (1) cross-bedding in quartzites and (2) graded bedding as shown by gradual increase upward of hornblende or biotite and corresponding decrease of quartz and feldspar, in individual beds of para amphibolite or biotite schist and gneiss. This type of field evidence is superbly exhibited in only a few localities, but recognition of such features in these localities has enabled the writers to identify and employ the same criteria in localities where they are not so well shown. The symmetry of the syncline (Pl. 5) also provides argument against an overturned or isoclinally folded structure.

Plastic folds, flow folds, and ptygmatic folds are common. Flow folds are most common in the synclinal trough and are characterized by thickening of crests and troughs and complementary thinning of limbs. Ptygmatic folds are usually associated with lenses of amphibolite or biotite schist and probably formed during the cycle of metamorphism and feldspathization.

The longitudinal section B-B′ (Pl. 5) shows a local reversal of the synclinal plunge where the structure is cut by the Quad Creek metanorite intrusive. This reversal in synclinal plunge may be due to emplacement of the metanorite body or may have formed during the earlier folding cycle.

Attitudes of Dikes

EARLY LARAMIDE FELSIC PORPHYRY DIKES: Plate 5 shows that the three most prominent dikes have a common strike of N. 30°—40° W. and dip of 25°–35° E. A contoured plot for 89 smaller dikes is given in Figure 3; only 4 are vertical, and 85 are inclined. The spread of the plotted poles is large, but there are two maxima: one strikes N. 15° W. and dips 36° E., and the other strikes N. 35° E. and dips 48° NW. The acute angle between these two planes is bisected by the fold axis (N. 10° E.). If the maxima are significant, maximum compression has been horizontal and along a direction N. 80° W., and maximum elongation has been up-

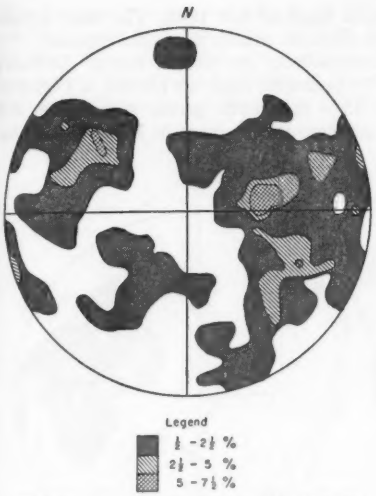

FIGURE 3.—ATTITUDES OF 89 FELSIC PORPHYRY DIKES

ward. Apparently Laramide northeast thrusting has been translated partly in the folded structure into compression at right angles to the fold axis; gliding is along planes of bedding, banding, or foliation within the structure. This indicates influence of the pre-existing structure on the orientation of the smaller dikes. The observed upward elongation probably means that there was little overburden at the time of Laramide movements and emplacement of the dikes. However, the relatively few readings taken in so small an area and the large spread in attitudes of the dikes may not warrant this interpretation.

In the Quad Creek syncline, dip directions for 84 inclined dikes (excluding one dike with attitude E. W., 30° N.) are as follows: of 22 dikes on the east limb, 2 dip east, and 20 dip west; of 62 dikes on the west limb, 53 dip east, and 9 dip west.

These results indicate considerable influence of the synclinal structure on the orientation of the smaller dikes. The three prominent dikes are not related to the synclinal structure but to the Laramide uplift, as their strike parallels the Beartooth thrust front. Figure 4 illustrates how open cracks of similar attitude could have formed on the northeast side of the range during Laramide movements in that direction. Fractures formed in this manner would be open, and large amounts of felsic porphyry magma could be emplaced in such fractures.

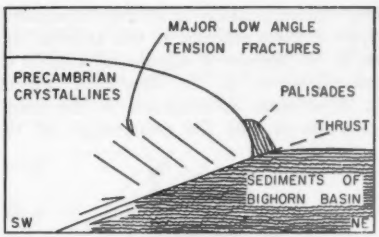

FIGURE 4.—DEVELOPMENT OF LOW-ANGLE FRACTURES

Rouse *et al.* (1937) found that the felsic porphyries along the Beartooth front were emplaced early in the Laramide revolution. Reconnaissance work in the project area has shown that the intrusives are concentrated along the northeastern and southwestern sides of the Beartooth block and are rare in the core. Stocks of felsic porphyry are confined to the thrust front.

PRECAMBRIAN MAFIC DIKES: Figure 5 shows a contoured plot for 89 mafic dikes, including 22 vertical dikes and 67 inclined dikes. A distinct maximum strikes N. 50° W. and dips at 90°. Most of the inclined dikes strike east or north; one maximum is at N. 23° E., 84° SE., another at N. 63° E., 66° SE., and a third at N. 5° E., 73° W.

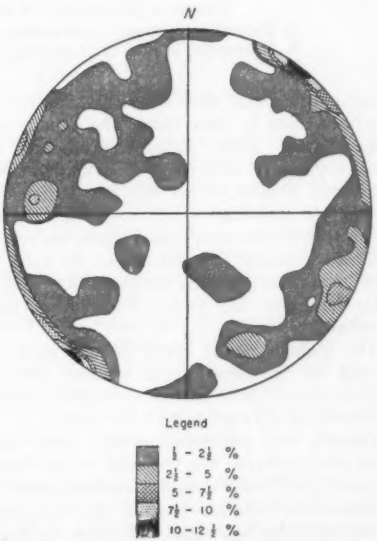

FIGURE 5.—ATTITUDES OF 89 PRECAMBRIAN MAFIC DIKES

The writers hesitate to attempt a detailed analysis of these maxima at this stage of the work. E. W. Spencer is completing a study of fracture systems in the Beartooth project area. A separate investigation of the mafic dikes is also planned The preferred N. 50° W. direction of vertical dikes is clearly defined and can be verified in other areas. The paucity of perpendicular dikes striking northeast is equally apparent and may indicate that the Beartooth Mountains are not due to simple folding by horizontal compression but represent a part of the earth's crust forced up vertically along major fracture planes. In such a unit the best-developed fractures are those that determine the longer direction of the structural block.

The inclined mafic dikes do not show a control by the Quad Creek syncline. Of 38 inclined mafic dikes on the west limb of the structure, 21 dip east, and 17 dip west.

Basaltic and metabasaltic dikes have not been differentiated. The majority of the dikes in the Quad Creek area are metamorphosed. Comparisons between basaltic and metabasaltic dikes do not show differences in attitudes. Mafic dikes have been found throughout the Beartooth block, and in the core some are several hundred feet thick. The most prominent dikes are usually unmetamorphosed.

PRECAMBRIAN PEGMATITE DIKES: Attitudes for 56 pegmatite dikes are plotted in Figure 6: (1) dikes in granitic gneiss, migmatites, and metasediments, (2) dikes in Mae West metagabbro, and (3) dikes in the Quad Creek metanorite. Only the dikes in the Mae West metagabbro have been contoured in Figure 6*B*.

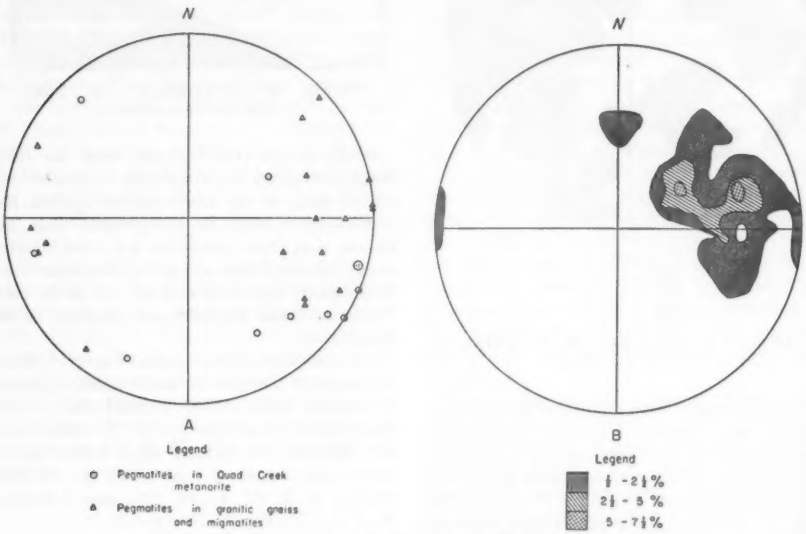

FIGURE 6.—ATTITUDES OF 56 PRECAMBRIAN PEGMATITE DIKES
A. Pegmatites in Quad Creek metanorite and in granitic gneisses and migmatites
B. Pegmatites in Mae West metagabbro

There are only 17 discordant pegmatites in granitic gneiss, migmatites, and metasediments; most pegmatites in these rocks form conformable lenses and stringers (Pl. 2, fig. 3). Three of the 17 discordant pegmatites are vertical. In the Quad Creek syncline dip directions of the 14 inclined pegmatites are as follows: of 3 dikes on the east limb, 1 dips east, and 2 dip west; of 11 dikes on the west limb, 9 dip east, and 2 dip west.

The influence of the synclinal structure on dip directions of pegmatite dikes is evident.

The 26 pegmatites in the Mae West metagabbro show a maximum with strike N. 32° W. and dip 32° E. and another with strike N. 18° W. and dip 58° E. The intrusive is situated on the western limb of the syncline, and nearly all the dikes dip eastward. In several places the metagabbro is foliated, and pegmatite

dikes in these localities conform to the dip of foliation in the host rock. This indicates that the Mae West metagabbro was emplaced before folding. Subsequent formation of the syncline and deformation of the gabbro produced narrow, discontinuous rims of clear albite along boundaries with microcline. Crystals enclosed by microcline or bordering small microcline porphyroblasts have wider albite rims. A few crystals are partly sieved by quartz and show

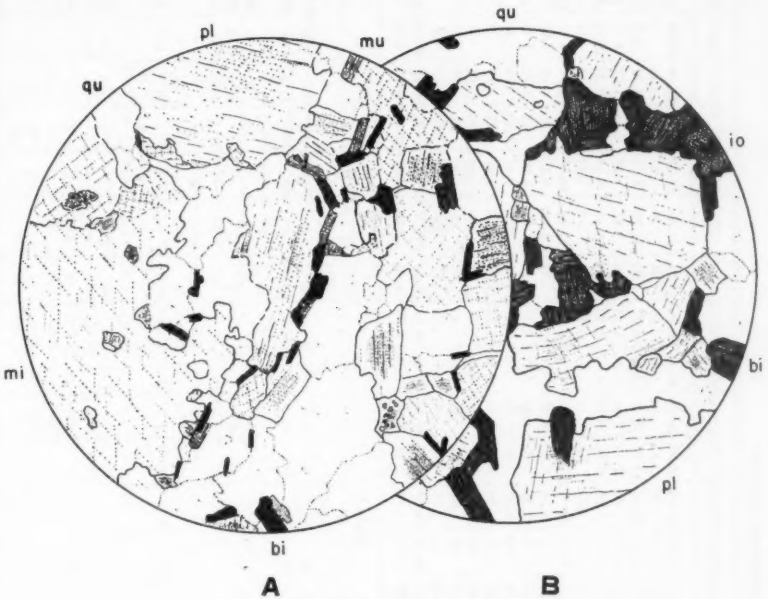

FIGURE 7.—GRANITIC GNEISSES (× 15)
A. Leucogranitic gneiss (248/53)
B. Tonalitic gneiss (329/53)
qu—quartz, pl—plagioclase, mi—microcline, bi—biotite, mu—muscovite, io—iron ores

eastward-dipping planes of weakness which determined the orientation of pegmatites intruded during the later cycle of metamorphism and granitization.

The 13 pegmatites in the Quad Creek metanorite are random in orientation.

PETROGRAPHY

Granitic Gneisses

LEUCOGRANITIC GNEISS: Typical representatives of leucogranitic gneiss are 248/53 and 287/53 (Table 1; Fig. 7*A*). Major constituents are quartz, microcline, and plagioclase. Minor constituents are biotite, muscovite, magnetite and ilmenite, chlorite, apatite, zircon, and green epidote. Plagioclase may show slight bending. Crystals are untwinned or twinned on albite law, and a few show Carlsbad-albite twinning. Plagioclase is slightly turbid and has crude myrmekitic textures. Better-developed petaloid myrmekite is found along plagioclase-microcline borders. Some small plagioclase porphyroblasts contain irregular patches of microcline. Microcline is nonperthitic or slightly perthitic and shows well-developed grid twinning. The amount of microcline varies in different rocks. The more microcline, the more conspicuous are: (1) turbidity of plagioclase, (2) alteration of biotite to chlorite, (3) myrmekite, and (4) albite rims around plagioclase. Microcline appears to have formed later than quartz and plagioclase. Brown or greenish-brown biotite, or chlorite after biotite, is ubiquitous. Biotite is partly altered to pleochroic clinochlore with associated magnetite, muscovite, epidote, and rutile. Rutile needles in biotite and chlorite commonly show sagenite structure. Muscovite is prominent in some rocks but less conspicuous or absent in others.

TABLE 1.—CHEMICAL AND PETROGRAPHIC DATA

Chemical Analyses*

Index Number	287/53	248/53	249/53	329/53	176/54	57/54	281/53	404/53	195/53	125/53	131/54	111/54	41/53	227/54	14/55	127/54	259/54	177/54	24/53	20/53	5/54	69/53	4/53
SiO_2	76.23	74.00	73.11	69.02	68.10	62.10	61.24	55.05	52.54	52.76	50.92	50.77	48.45	48.06	75.84	45.82	53.31	52.63	54.08	52.98	50.62	51.18	50.14
TiO_2	.12	.09	.12	.25	.39	.54	.64	1.36	.54	.40	.42	.34	1.36	.49	.24	.20	.35	.46	.35	.38	1.00	.95	.65
Al_2O_3	12.34	14.04	14.81	16.82	15.01	16.01	18.72	14.92	16.81	12.56	14.07	14.43	16.13	16.57	7.33	10.29	15.71	11.96	8.54	8.28	12.79	14.00	15.67
Fe_2O_3	.71	.44	.41	.27	1.21	1.02	.10	4.27	4.73	1.86	2.23	2.46	1.24	1.83	.16	2.44	1.66	2.46	1.57	1.52	2.05	7.13	1.89
FeO	.78	.46	1.13	1.81	2.27	4.48	2.13	6.07	5.41	7.10	9.96	8.61	10.47	9.32	4.69	6.47	6.19	5.48	9.25	10.32	8.97	9.04	9.71
MnO	.02	.02	.02	.04	.06	.15	.09	.22	.13	.27	.15	.14	.24	.18	.02	.14	.12	.13	.12	.19	.15	.12	.17
MgO	.24	.26	.61	1.11	1.30	3.70	3.07	3.51	5.01	10.79	7.96	8.45	7.82	8.06	7.96	25.00	10.52	9.96	15.97	19.53	11.00	3.97	6.31
CaO	1.29	1.44	3.01	3.95	3.32	4.79	5.40	6.57	6.16	8.14	9.62	10.68	10.30	9.38	.18	6.84	6.17	9.25	6.42	3.98	8.94	6.84	9.64
Na_2O	3.81	3.86	4.67	4.34	4.20	3.64	3.77	3.50	2.39	2.61	2.09	1.20	1.56	3.32	.22	1.00	2.50	3.11	1.32	1.11	2.37	3.08	2.58
K_2O	3.65	4.42	1.38	1.26	2.28	1.58	2.30	1.39	2.80	1.28	.54	.96	.78	.47	.94	tr.	1.18	1.18	.74	.46	.50	.90	.83
H_2O^+	.29	.33	.44	.53	.60	1.15	1.16	1.22	2.09	.93	1.50	1.43	1.32	1.72	1.90	2.28	.69	.71	1.43	.77	.49	2.01	1.95
H_2O^-	nil	.02	nil	nil	.09	nil	.01	.02	.13	nil	.17	.18	.05	.12	.25	.20	.04	.02	.01	.01	.01	.18	.01
P_2O_5	.03	.04	.02	.04	.13	.08	.19	.56	.39	.04	.02	.03	.11	.12	.06	.04	.06	.10	.07	.05	.07	.10	.07
CO_2	.12	.10	.17	.31	.45	nil	.67	1.10	.45	1.01	nil	nil	nil	nil	nil	nil	1.48	2.02	nil	nil	.84	nil	nil
Total	99.63	99.52	99.90	99.75	99.41	99.24	99.49	99.76	99.58	99.75	99.65	99.68	99.83	99.64	99.79	100.72	99.98	99.47	99.87	99.58	99.80	99.50	99.62
Sp. gr.	2.64	2.62	2.65	2.70	2.72	2.76	2.78	2.92	2.92	2.96	3.10	3.10	3.04	3.09	2.85	3.18	2.92	2.94	3.00	3.10	3.04	3.06	3.05

Modes†

olivine	—	—	—	—	—	—	—	—	—	—	—	—	—	—	—	10½	—	—	—	—	—	—	—
quartz	31	34	43	31	24½	24	21	13	20	8	9	6	10½	—	56	—	4½	4½	5	6½	—	—	1½
plagioclase	47	37½	49½	58	54**	45	51**	34	29	21	20	27	13	34	—	—	40	32½**	23½	15½	32	25	42½**
microcline	15	24½	+	—	—	—	1	—	—	—	—	—	—	—	—	—	—	—	—	—	—	—	—
augite	—	—	—	—	—	—	—	—	—	—	—	10	—	5	—	—	—	—	+	+	25	22	43½
hypersthene	—	—	—	—	—	—	—	—	—	—	7	14	—	—	6	32	—	—	34½	54½	22½	—	—
hornblende	—	—	—	—	7	15½	12½	23	3	55	60	34	70	60	—	—	—	54½	23½	15½	12	30	8
actinolite	—	—	—	—	—	—	—	—	—	—	—	—	—	—	—	46	43	—	—	—	—	—	—
anthophyllite	—	—	—	—	—	—	—	—	—	—	—	—	—	—	5	—	—	—	—	—	—	—	—
biotite (chlorite)	4	2	7	10½	10	10	5½	10	30	13	3	8	2	½	14½	—	7½	—	10	4½	3	+	½
muscovite (sericite)	2	1½	+	—	+	—	+	½	—	—	—	—	—	—	—	—	+	+	—	—	—	—	+
epidote††	—	—	+	+	2½	4	9	10½	10	—	—	—	—	½	—	—	+	3	—	—	—	—	+
cordierite	—	—	—	—	—	—	—	—	—	—	—	—	—	—	18	—	—	—	—	—	—	—	—
spinel	—	—	—	—	—	—	—	—	—	—	—	—	—	—	—	8	—	—	—	—	—	—	—
magnetite + ilmenite	1	½	½	½	2	1½	—	6	8	2½	1	1	4½	—	½	3½	1½	½	3	3	5	12	4
sphene	—	—	—	—	—	—	—	1½	—	—	—	—	—	—	—	—	—	—	—	—	—	—	+
apatite	+	+	+	+	+	+	+	1	+	+	+	+	+	+	+	—	½	½	½	½	½	+	+
calcite	—	—	—	—	—	—	—	½	+	½	—	—	—	—	—	—	3	4½	—	—	—	—	—
groundmass	—	—	—	—	—	—	—	—	—	—	—	—	—	—	—	—	—	—	—	—	—	11	—

Mineral Data

Mineral Data

olivine	Fa	—	—	—	—	—	—	—	—	—	—	—	—	—	—	—	18	—	—	—	—	—	—	—
plagioclase	An	13	15	18	18	25	30	32	32	35	30	56	57	65	37	—	—	45	35	50	56	50	40	50
augite	2V(+)	—	—	—	—	—	—	—	—	—	—	—	52	—	54	—	—	—	—	—	—	50	50	49
	γ	—	—	—	—	—	—	—	—	—	—	—	1.722	—	1.720	—	—	—	—	—	—	1.718	1.733	1.720
hypersthene	Of	—	—	—	—	—	—	—	—	—	—	44	28	—	—	30	20	—	—	18	16	24	—	—
amphibole	2V(−)	—	—	—	—	68	71	63	62	66	66	64	68	63	68	73	85	80	75	80	81	70	—	—
	γ	—	—	—	—	1.670	1.673	1.675	1.678	1.678	1.676	1.678	1.674	1.673	1.675	1.651	1.637	1.641	1.661	1.650	1.650	1.668	1.683	1.680
biotite	β	1.621	1.623	1.620	1.622	1.617	1.620	1.611	1.622	1.620	1.624	1.640	1.630	—	—	1.607	—	1.605	—	1.607	1.609	1.623	—	—

* Analyst, H. B. Wiik, Helsinki, Finland

† Weight per cent

** Heavily sericitized plagioclase

†† Epidote in the modes includes pistacite, zoisite, clinozoisite, and allanite.

287/53 Leucogranitic gneiss
248/53 Leucogranitic gneiss
249/53 Tonalitic gneiss
329/53 Tonalitic gneiss
176/54 Banded biotite-hornblende migmatite
57/54 Banded biotite-hornblende migmatite
281/53 Banded biotite-hornblende migmatite
404/53 Banded biotite-hornblende migmatite
195/53 Migmatitic biotite schist

125/53 Para-amphibolite
131/54 Para-amphibolite
111/54 Amphibolite of doubtful origin
41/53 Para-amphibolite
227/54 Para-amphibolite
14/55 Siliceous biotite-cordierite-bronzite-anthophyllite rock
127/54 Ultramafic rock
259/54 Mae West metagabbro
177/54 Mae West metagabbro
24/53 Quad Creek metanorite
20/53 Quad Creek metanorite
5/54 Metanorite dike
69/53 Iron-rich metabasaltic dike
4/53 Basaltic dike

TONALITIC GNEISS: Typical representatives of tonalitic gneiss are 249/53 and 329/53 (Table 1; Fig. 7*B*). Major constituents are quartz and plagioclase. Minor constituents are microcline, biotite, epidote, allanite, sericite, chlorite, magnetite and ilmenite, apatite, and zircon. Small plagioclase porphyroblasts are common. Many crystals are sericitized and epidotized, and others are antiperthitic (249/53). In order of abundance twinning is according to albite, albite-pericline, Carlsbad-albite, and pericline-Carlsbad-albite laws; most crystals are twinned. Microcline builds small interstitial units and partly replaces plagioclase. Crystals are nonperthitic and show grid twinning. Myrmekite is rare. Biotite shows strong preferred orientation; it is brown or greenish brown, commonly exhibits sagenite structure, and may be altered to clinochlore, epidote, magnetite, and muscovite. Allanite is a common accessory. An extreme variety of this rock type is alaskitic and consists mainly of quartz and plagioclase with a few rosettes and tufts of pale-green chlorite.

Migmatites

BANDED BIOTITE MIGMATITE: Biotite migmatites and granitic gneisses differ only in the distribution of biotite. In granitic gneisses, biotite is homogeneously distributed and produces foliation by its preferred orientation. In banded biotite migmatites, biotite is concentrated in bands and streaks, continuous for several inches or several feet, and separated by paler quartzofeldspathic bands, streaks, or lenses with or without accessory biotite (Pl. 3, fig. 3). Banded biotite migmatites include granitic varieties with quartz, microcline, and plagioclase as major constituents, as well as tonalitic varieties in which microcline is absent or minor. In other respects these migmatites (Fig. 8*A*) resemble the granitic gneisses.

BANDED BIOTITE-HORNBLENDE MIGMATITE: These rocks grade into banded biotite migmatites or amphibolites. Typical representatives are 176/54, 57/54, 281/53, and 404/43 (Table 1; Fig. 8*B*). Main constituents are quartz, plagioclase, biotite or chlorite, and hornblende.

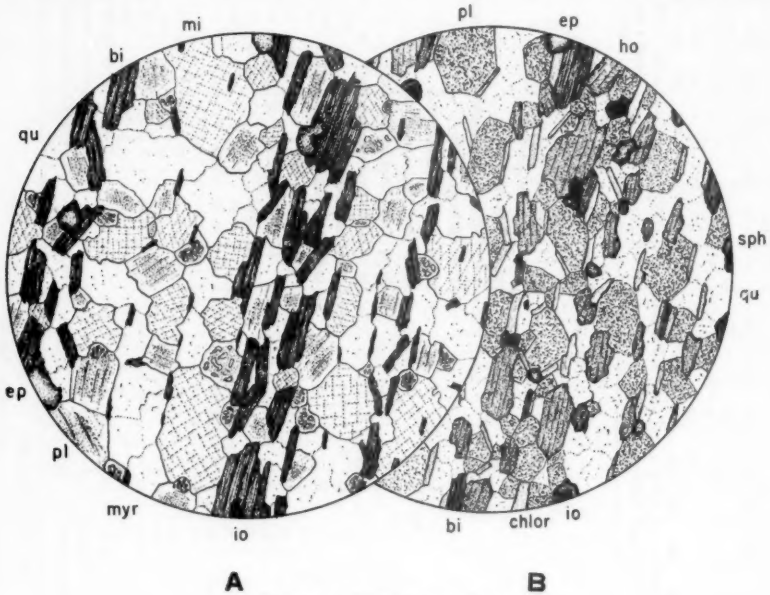

FIGURE 8.—MIGMATITES (× 15)
A. Banded biotite migmatite (9/53)
B. Banded biotite—hornblende migmatite (404/53)
qu—quartz, pl—plagioclase, mi—microcline, myr—myrmekite, bi—biotite, ho—hornblende, ep—epidote, io—iron ores, chlor—chlorite, sph—sphene

Minor constituents are green epidote or clinozoisite, magnetite and ilmenite, sericite, calcite, and apatite. In a few rocks actinolite, allanite, sphene, microcline, rutile, and zircon are accessories. Plagioclase is commonly sericitized, but the extent of alteration varies.

guished in the field. Microcline-biotite migmatites are characterized by numerous large microcline porphyroblasts and small conformable lenses of pegmatite. Agmatites[1] have many lenses and streaks of amphibolite and biotite schist and gneiss (Pl. 3, Fig. 1). They

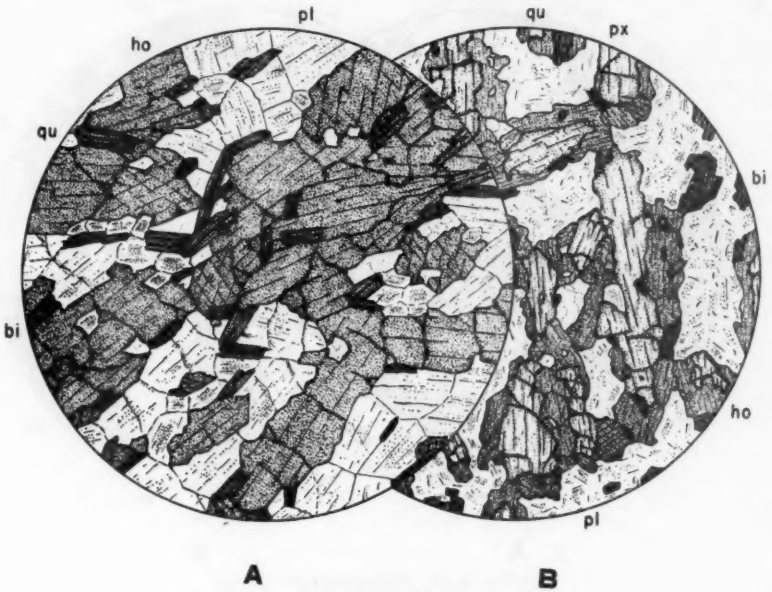

FIGURE 9.—PARA-AMPHIBOLITES (× 15)
A. Hornblende—plagioclase rock (125/53)
B. Hornblende—pyroxene—plagioclase rock (111/54)
qu—quartz, pl—plagioclase, px—pyroxene, bi—biotite, ho—hornblende

Most crystals are equidimensional; lath-shaped individuals occur in hornblende-rich migmatites. Twinning is according to albite, albite-pericline, and albite-pericline-Carlsbad laws, and most crystals are twinned. Biotite is brown or olive green; the latter variety shows sagenite structure. Crystals are usually associated with hornblende and epidote and are commonly altered to clinochlore, sericite, and magnetite. Hornblende shows pleochroism olive green, bluish green, brownish yellow. Green epidote is a common minor constituent, a major constituent in some samples, and associated with clinozoisite in a few samples. Discrete muscovite is rare, but sericite aggregates associated with plagioclase and biotite are common.

OTHER MIGMATITES: Two variations of the above types of migmatites have been distinmay be banded biotite or biotite-hornblende rocks.

Metasediments

PARA-AMPHIBOLITES: The problem of the distinction between para- and ortho-amphibolites is well known. In the Quad Creek area the writers tried to distinguish them on the basis of field relations. Para-amphibolites show banding and interlayering with other metasediments. Ortho-amphibolite outcrops are

[1] The term agmatite (Sederholm, 1926, p. 136) is used here for migmatites with many dark blocks, lenses, and streaks of amphibolite and biotite schist and gneiss—*i.e.*, as the term merismite is used by Central European petrologists (*e.g.*, Vaasjoki, 1953, p. 21).

more uniform. On this basis, and in entire outcrops, larger bodies of ortho-amphibolite, such as the Mae West metagabbro, and larger lenses of para-amphibolite have been identified. On a smaller scale these criteria are insufficient. Small lenses of ultramafic rocks have been found within larger banded units of para-amphibolite (Pl. 3, fig. 2). Detailed sampling of dominantly para-amphibolite outcrops may yield banded, inhomogeneous rocks as well as a few perfectly homogeneous samples, which are indistinguishable from ortho-amphibolites.

Para-amphibolites of the Quad Creek area have a wide range of composition. Main variables are hornblende (30–80 per cent) and pyroxene (Fig. 9 *A*, *B*). Typical representatives are 125/53, 41/53, 131/54, and 227/54 (Table 1). Plagioclase is always present, equidimensional or lath-shaped, and untwinned or twinned according to albite, albite-pericline, and albite-pericline-Carlsbad laws. Green hornblende is ubiquitous and may be accompanied by pale-bluish-green diopsidic augite and/or pleochroic hypersthene and brown or reddish-brown biotite. Quartz is usually present. Minor constituents are magnetite and ilmenite, chlorite, and apatite. Epidote, clinozoisite, allanite, sphene, microcline, and sericite are constituents in a few samples.

Amphibolites of doubtful origin consist of plagioclase, pleochroic bronzite or hypersthene,

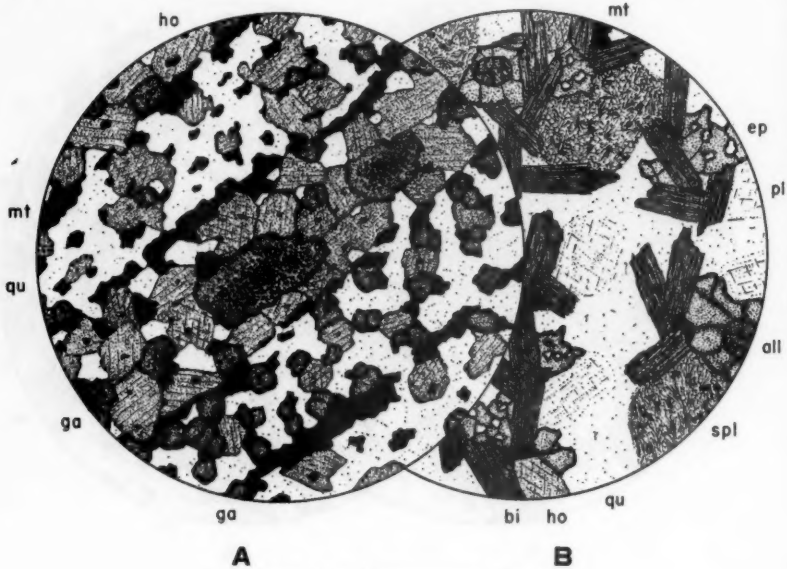

FIGURE 10.—METASEDIMENTS (× 48)
A. Banded ironstone (230/53)
B. Migmatitic biotite schist (195/53)
qu—quartz, pl—albite, spl—sericitized plagioclase, bi—biotite, ep—epidote, all—allanite, mt— magnetite, ho—hornblende, ga—garnet

pale-green augite, green or brownish-green hornblende, reddish-brown biotite, magnetite, and ilmenite. Quartz may be present. A typical sample is 111/54 (Table 1).

BANDED IRONSTONES. Banded ironstones occur in only four localities and are invariably associated with para-amphibolites. The largest outcrop is less than 10 feet wide by 50 feet long. The rocks are medium- to fine-grained and well banded (Fig. 10*A*). Most bands range in thickness between 0.5 and 2.5 mm, but bands in one rock reach a maximum of 12 mm. The light bands consist of quartz or quartz and magnetite. The dark bands are composed of one of the following mineral assemblages: (1) magnetite-garnet-hornblende, (2) magnetite-hedenbergite-hornblende-garnet, (3) magnetite-hedenbergite-cummingtonite-garnet, (4) magnetite-ferrohypersthene-hornblende-

garnet, and (5) magnetite-hedenbergite-hornblende-vesuvianite. Most common are dark bands with magnetite, pink garnet, and bluish-green hornblende. Accessory minerals are rutile, sphene, and apatite.

microcline. A few samples contain quartz, plagioclase, microcline, biotite, cordierite, and sillimanite (Fig. 11*A*). In this group belong also some siliceous cordierite-biotite-bronzite-anthophyllite rocks (Fig. 11*B*) found in one

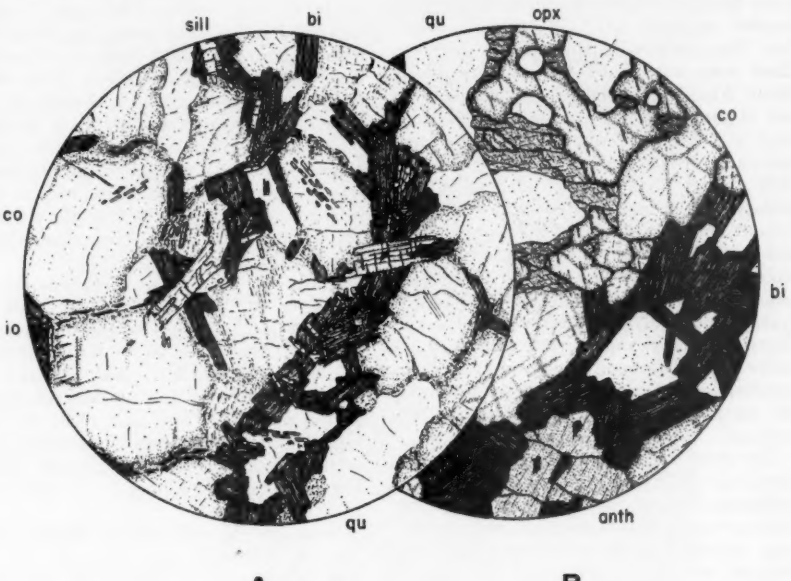

FIGURE 11.—METASEDIMENTS (× 48)
A. Siliceous biotite—cordierite—sillimanite rock (87/53)
B. Siliceous biotite—cordierite—bronzite—anthophyllite rock (14/55)
qu—quartz, co—cordierite, bi—biotite, opx—bronzite, anth—anthophyllite, sill—sillimanite, io—iron ores

BIOTITE SCHIST AND GNEISS: Two types of biotite schist and gneiss can be distinguished: (1) biotite-hornblende schists and gneisses associated with amphibolites and banded biotite-hornblende migmatites, and (2) biotite schists and gneisses associated with biotite-rich quartzites. The first type (Fig. 10*B*) is formed by progressive K metasomatism of amphibolites and is a variety of migmatite. The rocks consist mainly of quartz, plagioclase, greenish-brown biotite, with or without epidote, and bluish-green hornblende. Minor constituents are magnetite and ilmenite, sphene, epidote, clinozoisite, chlorite, sericite, apatite, calcite, and allanite. A typical rock is 195/53 (Table 1).

The second type has as major constituents quartz, plagioclase, and brown biotite. Minor constituents are pink almandine garnet, magnetite and ilmenite, and, in a few samples, locality as a lens associated with major quartzite units. Main constituents are quartz, cordierite, biotite, anthophyllite, and bronzite. Rutile is a characteristic accessory. Also present may be plagioclase and apatite. A representative sample is 14/55 (Table 1).

QUARTZITES: Primary bedding and cross-bedding of quartzites are commonly well preserved. Individual beds range in thickness from a few inches to several feet. Some samples are nearly pure quartz with a few biotite flakes that parallel bedding. Plagioclase and biotite are common minor constituents, and pink almandine garnet is present in some samples. Other accessories are apatite, zircon, magnetite, and muscovite, less commonly microcline, epidote, hornblende, and sphene. By progressive feldspathization the quartzites grade into granitic gneiss (Pl. 2, fig. 1).

Meta-Igneous Rocks

ULTRAMAFIC ROCKS: Small lenses of ultramafic rocks are intimately associated with banded para-amphibolite units (Pl. 3, fig. 2). Only a few of these lenses have been recognized in the field; most have been identified only by detailed sampling and thin-section examination. The largest ultramafic body in the Quad Creek area was mined for chromite during World War II. This body is also included in a unit of para-amphibolite. Collapse of the mine shaft precluded underground inspection, and mine dumps cover much of the outcrop. Schafer (1937, p. 30) gives a sketch map of outcrop geology before mining operations started. Present surface outcrops are of amphibolite, and most of the surface workings are in amphibolite. One cut exposes heavily slickensided serpentinite in contact with amphibolite and granitic gneiss, all intersected by a felsic porphyry dike. The contact with granitic gneiss shows a reaction zone of predominant black hornblende with a less well-developed outer rim composed almost wholly of biotite (vermiculite).

The ultramafic rocks contain different combinations of the following minerals: olivine, pleochroic bronzite, pale-green actinolite, colorless or pale-yellow serpentine, talc, phlogopite, chlorite, green spinel, and magnetite. Bronzite is residual in a few rocks, but in others it is poikiloblastic and metamorphic. Chlorite is pseudomorphous after phlogopite. Yellow serpentine derives its color from numerous minute granules of a mineral that may be magnetite. A representative sample is 127/54 (Table 1).

Chromite deposits of the Beartooth Mountains have been described by Schafer (1937). Poldervaart is preparing a detailed study of exceptionally well-exposed ultramafic lenses in the Highline Lakes area (Fig. 2).

MAE WEST METAGABBRO: Representative samples of Mae West metagabbro are 259/54 and 177/54 (Table 1; Fig. 12*A*). The rocks are coarse-grained with subophitic textures commonly preserved. Main constituents are plagioclase and amphibole, which occur with biotite in some samples. Plagioclase is usually sericitized and in some places, epidotized. Amphibole is either bluish-green hornblende or colorless to pale-green actinolite. Some biotite occurs as nested aggregates associated with quartz, but more commonly it is uniformly distributed. Minor constituents are quartz, chlorite, epidote, sericite, magnetite and ilmenite, calcite, sphene, allanite, apatite, and a colorless garnet. A sample from the contact of the intrusion has quartz, plagioclase, chlorite, epidote, and vesuvianite.

Intrusions of the Mae West type are relatively rare and small in the Quad Creek area, but they are far more common in other areas in the Beartooth core. In the Lonesome Mountain area (Fig. 2), many thick sills and dikes of metagabbro have been metamorphosed and partly granitized. The host rocks have also been folded in these areas, but the folds are more open than in the Quad Creek or Gardner Lake areas and have dips of 15°–40° instead of 60°–80°.

QUAD CREEK METANORITE: Representative samples of Quad Creek metanorite are 24/53 and 20/53 (Table 1; Fig. 12*B*). Plagioclase, bronzite, and hornblende are the main minerals, and minor constituents are quartz, biotite, augite, magnetite and ilmenite, sulfides, and apatite; epidote, chlorite, sericite, and sphene are minor constituents in some rocks. Plagioclase poikilitically encloses pleochroic bronzite prisms. The amount of plagioclase increases from the core of the intrusive toward its margins. Near the contact colorless to pale-green actinolite and sericite are conspicuous, and residual bronzite is strongly clouded and

PLATE 1.—AERIAL VIEW OF ROCK CREEK FACE OF THE QUAD CREEK AREA

Wyoming Creek is to the left. The abandoned chromite mine is on the front part of the plateau, just before the indentation of the Rock Creek face formed by Quad Creek. The cirque in the right background is that of the Twin Lakes and Chain Creek and forms the southwestern boundary of the map area. The skyline is part of the Gardner Lake area.

PLATE 2.—QUARTZITE, MIGMATITE, AND PEGMATITE

FIGURE 1.—Quartzite lens in granitic gneiss. Dark streaks and bands are quartzite; light streaks and bands are granitic gneiss. Note conformity of granitic gneiss bands to bedding in quartzite.

FIGURE 2.—Banded migmatite grading into granitic gneiss. Note lack of discordance in gradational contact. Joint with epidote and chlorite crosses photo from left center to right top.

FIGURE 3.—Conformable pegmatite in migmatite. Note small pegmatite lenses and feldspar eyes in migmatite and relict foliation in main pegmatite.

Photo by Jack Richard, Cody, Wyoming

AERIAL VIEW OF ROCK CREEK FACE OF THE QUAD CREEK AREA

FIGURE 1

FIGURE 2

FIGURE 3

QUARTZITE, MIGMATITE, AND PEGMATITE

FIGURE 1

FIGURE 2

FIGURE 3

AGMATITE, ULTRAMAFIC AND MIGMATITE

OUTGROWTHS AND OVERGROWTHS ON ZIRCONS OF GRANITIC GNEISS

nearly opaque. Near the lowest exposures of the body considerable amounts of sulfides (pyrite, pyrrhotite, and chalcopyrite) occur interstitial to plagioclase and bronzite.

In the upper parts of the intrusive are many schlieren, veins, and dikes of very coarse-grained metanorite pegmatite characterized by plagioclase, quartz, hornblende, actinolite, biotite, magnetite, sphene, chlorite, epidote, sericite, calcite, and apatite. The veins and dikes have borders of biotite against the metanorite. The intrusive is also cut by numerous granite pegmatite dikes which transect both the metanorite and the metanorite pegmatite.

Intrusives of the Quad Creek type are rare in the project area, and only one other body of this type has been found.

MAFIC DIKES: The Mae West metagabbro and Quad Creek metanorite are cut by pegmatites, but the mafic dikes of the area invariably transect the pegmatites. The majority of the dikes are metanorites which have conspicuous prismatic bronzite microphenocrysts and lath-shaped plagioclase (Fig. 13*A*; Table 1, sample 5/54). Other minerals are augite, magnetite and ilmenite, brownish-green hornblende, apatite, and, in a few samples, olivine. A few dikes show evidence of cataclasis. All meta-

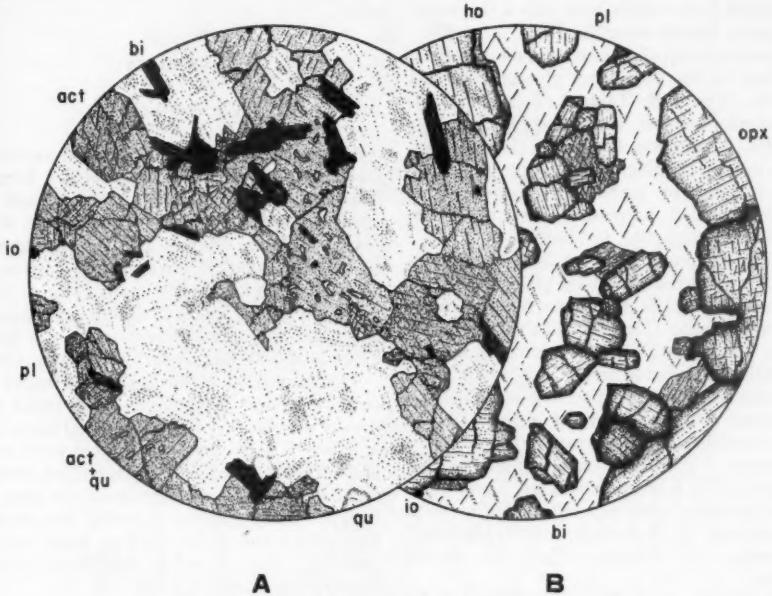

FIGURE 12.—PRE-PEGMATITE MAFIC INTRUSIVES (x 15)
A. Mae West metagabbro (259/54)
B. Quad Creek metanorite (20/53)
qu—quartz, pl—plagioclase, opx—bronzite, ho—hornblende, act—actinolite, bi—biotite, io—iron ores

PLATE 3.—AGMATITE, ULTRAMAFIC, AND MIGMATITE

FIGURE 1.—Agmatite with lenses of amphibolite and biotite schist. The host rock is banded migmatite. Cap to left of center of photo for scale.

FIGURE 2.—Ultramafic lens in para-amphibolite. Boundaries of ultramafic body are outlined. Banding in para-amphibolite is seen on right of photo.

FIGURE 3.—Banded biotite migmatite. Top of beds is toward left of photo.

PLATE 4.—OUTGROWTHS AND OVERGROWTHS ON ZIRCONS OF GRANITIC GNEISS

a-g.—Zircons with distinct cores and shells. Note that length of cores may be skew with respect to *c* axis of shells (b, c); shells fracture independent from cores (e, g).

h-m.—Zircon outgrowths and aggregate crystals.

norites have been thermally metamorphosed. Plagioclase and bronzite are clouded, olivine where present has a corona of small bronzite crystals, and augite is partly recrystallized to a granoblastic aggregate of salite and either hypersthene or hornblende. Along contacts the metanorites are recrystallized to plagioclase-hornblende rocks which have only a few residual, nearly opaque bronzite prisms.

A second group of metabasaltic dikes is characterized by the abundance of magnetite and ilmenite (Fig. 13*B*; Table 1, sample 69/53). Subophitic textures are preserved in most samples. Plagioclase laths are clouded, and some are porphyritic. Original pyroxene has been replaced by granoblastic aggregates of heavily clouded ferroaugite, brownish-green hornblende, magnetite, and biotite.

The third group of dikes is subophitic to ophitic and characterized by plagioclase laths and anhedral augite with cores of early, magnesian pigeonite (Fig. 13*C*; Table 1, sample 4/53). Plagioclase also forms microphenocrysts. Alteration is variable and of a hydrous type; it results in saussuritization of plagioclase, replacement of pyroxene by chlorite and bluish-green hornblende, and alteration of ilmenite to leucoxene. A relatively rare variant in this group of dikes is characterized by microphenocrysts of augite with pigeonite cores, set in a ground-mass of plagioclase, augite, pigeonite, magnetite, and ilmenite (Table 4, sample 40/53).

The last group of dikes is considered to be younger than the metanorite and iron-rich metabasaltic dikes and younger than the metamorphism that recrystallized these last two groups of intrusions. Reasons for this are the preservation of magnesian pigeonite and original augite and the lack of clouding of both plagioclase and pyroxenes (Poldervaart, 1953, p. 261–262).

Pegmatites

Quartz and pink microcline characterize most of the pegmatites. Minor constituents include biotite, albite, ilmenite, muscovite, and, in a few samples, pale-green apatite. A few pegmatites have local concentrations of albite and muscovite. Pegmatites in amphibolite host rocks commonly contain ilmenite crystals up to an inch in diameter. Pegmatites in the Quad Creek metanorite are lined with coarse-grained biotite-chlorite aggregates formed by reaction with the host rock.

In the Gardner Lake area (Fig. 2) being studied by R. L. Harris, a pegmatite has been found which contains beryl crystals up to 10 inches long. Near the Clarks Fork River crossing of U.S. Highway 12, albite-biotite pegmatites associated with amphibolite skialiths[2] in granitic gneiss contain cubic crystals of uraninite.

Mineralogy

Zircon Studies

Zircon studies may shed new light on many aspects of plutonism. If granites are formed from sediments, rounded zircons typical of many sediments (Poldervaart, 1955a, p. 439–441) must show evidence of their transformation to the euhedral zircons characteristic of magmatic granites (Poldervaart, 1956, p. 529–532). The initial stages of this transformation of zircons have been determined in the Quad Creek area (Poldervaart and Eckelmann, 1955).

Transformation of zircons is evidenced by outgrowths and overgrowths on rounded zircons of sedimentary origin (Pl. 4). Figures *a–f* of Plate 5 show complete overgrowths with distinct cores. The zircon shells are pale brown, pink, or colorless, and the cores are gray or brown. Figure *g* shows a partial overgrowth. Figures *h–j* and *l* show various types of outgrowths. Figures *k* and *m* show fusion of two cores by the overgrowth material.

Counts for zircon concentrates of 15 samples, representing different rock types, are given in Table 2. Characters recorded are: (1) rounding of terminal faces; (2) crystals without outgrowths or overgrowths, subdivided into crystals showing distinct crystal faces (euhedral), only residual faces (subhedral), and no crystal faces (anhedral); (3) crystals with outgrowths and partial overgrowths, with or without crystal faces on the new growths, and (4) crystals with complete overgrowths, without new crystal faces, with some new crystal faces, and showing euhedral outlines. The last subdivision is the most advanced stage in the transformation of zircons.

Table 2 shows that the two granitic gneisses from the core of the Beartooth Mountains have a majority of zircons with partial or complete overgrowths. Considerable proportions of

[2] The term skialith (Goodspeed, 1948, p. 516) is used for "relict inclusions in granitized rocks". Similarly, skiacryst is a relict crystal (*c.f.* xenolith and xenocryst).

FIGURE 13.—POST-PEGMATITE MAFIC DIKES (x 48)

A. Metanorite (5/54)
B. Iron-rich metadolerite (69/53)
C. Younger dolerite (4/53)

qu—quartz, pl—plagioclase, px—augite, opx—bronzite, ho—hornblende, bi—biotite, io—iron ores, chlor—chlorite, ms—mesostasis

completely mantled zircons show euhedral outlines. Granitic gneisses in the boundary zone have a majority of zircons without outgrowths and few completely mantled zircons with euhedral outlines. Zircons from the migmatites and metasediments are essentially the same. Thus transformations are shown in zircon concentrates of all rocks examined but are conspicuous and well developed only in granitic gneisses from the Beartooth core. Although granitic gneisses from the boundary zone are as granitic as rocks from the core, the extent of transformation of their zircons is similar to that shown by concentrates of associated migmatites and metasediments. Regional homogenization thus appears to be an important factor in the transformation of zircons during granitization.

TABLE 2.—CHARACTERS OF ZIRCONS

Classification	A		B				C				D			
Index Number	1/53	60/54	29/53	53/53	54/53	244/53	116/53	124/53	469/53	190/53	52/53	246/53	48/53	60/53
1. Rounded	79	90	92	97	97	98	100	94	99	97	99	100	100	100
2. No outgrowths	24	27	64	64	64	64	87	69	56	56	54	49	58	73
anhedral	*13*	*6*	*25*	*20*	*26*	*22*	*42*	*22*	*17*	*26*	*35*	*22*	*26*	*30*
subhedral	*10*	*20*	*36*	*41*	*37*	*39*	*45*	*43*	*39*	*30*	*19*	*27*	*32*	*43*
euhedral	*1*	*1*	*3*	*3*	*1*	*3*	—	*4*	—	—	—	—	—	—
3. Outgrowths and partial overgrowths	5	20	13	26	25	12	11	23	25	18	37	40	37	15
no new faces	*2*	*2*	*5*	*9*	*3*	*5*	*1*	*3*	*6*	*9*	*23*	*9*	*13*	*5*
some new faces	*3*	*18*	*8*	*17*	*22*	*7*	*10*	*20*	*19*	*9*	*14*	*31*	*24*	*10*
4. Complete overgrowths	71	53	23	10	11	24	2	8	19	26	9	11	5	12
no new faces	—	—	—	—	—	*1*	—	—	—	*5*	*4*	*3*	—	*1*
some new faces	*51*	*43*	*18*	*7*	*9*	*21*	*2*	*6*	*18*	*18*	*4*	*8*	*5*	*11*
euhedral	*20*	*10*	*5*	*3*	*2*	*2*	—	*2*	*1*	*3*	*1*	—	—	—

A—granitic gneisses southwest of boundary zone
B—granitic gneisses in boundary zone
C—migmatites northeast of boundary zone
116/53, 124/53, 469/53—banded biotite migmatites
190/53—banded biotite-hornblende migmatite
D—metasediments
52/53—biotite schist
246/53—biotite gneiss
48/53—quartz-plagioclase schist in main quartzite unit
60/53—quartzite, same unit

Metamorphic Facies

Plutonic terrains that have undergone granitization cannot be expected to show a simple metamorphic history. Diffusion of heat is a faster process than diffusion of ions or molecules (Bowen, 1948, p. 84); hence rocks are usually metamorphosed before they are granitized. Traces of the regional metamorphic stamp may be preserved in resister rocks (Read, 1952, p. 7) and may be used to reconstruct the metamorphic facies before granitization. Resister rocks in the Quad Creek area include para-amphibolites, ultramafic rocks, biotite schists, and banded ironstones; these allow accurate interpretation of the metamorphic facies. Mineral assemblages indicative of this are as follows:

Para-amphibolites

quartz-plagioclase-hornblende-biotite-(garnet, epidote)
quartz-plagioclase-augite-hornblende-biotite-(garnet, epidote)
(quartz)-plagioclase-augite-hypersthene-hornblende-(biotite)
plagioclase-augite-hypersthene-(hornblende, biotite)

Ultramafic rocks

olivine-bronzite-actinolite-spinel-magnetite

Biotite schists

quartz-plagioclase-biotite-(garnet, epidote)
quartz-plagioclase-biotite-cordierite-sillimanite-(microcline)
quartz-plagioclase-microcline-biotite-cordierite-hypersthene-sillimanite
quartz-biotite-cordierite-bronzite-anthophyllite-(plagioclase)

Banded ironstones

quartz -hedenbergite-hornblende-garnet-magnetite
quartz - hedenbergite - cummingtonite - garnet-magnetite
quartz - ferrohypersthene - hornblende - garnet-magnetite

Ramberg (1952, p. 150) defined the lower boundary of the amphibolite facies by the association of epidote and a plagioclase more calcic than An_{30}. Para-amphibolites of the Quad Creek area undoubtedly belong to this facies (Table 1). He also concluded (1952, p. 156) that rhombic pyroxene is stable in the highest half of the amphibolite facies. A tentative subsolidus diagram given by Ramberg (1949, p. 39) indicates that mineral assemblages of Quad Creek para-amphibolites are stable at about 500°–600° C.; in another diagram Ramberg (1952, p. 69) shows that these assemblages belong to the border field between the amphibolite and granulite facies. The paucity of garnet is dependent on the Al/Mg, Fe, Ca and the Fe/Mg ratio of the rocks. Apparently there was generally too little Al and too much Mg in the para-amphibolites to produce much garnet.

Bowen and Tuttle's (1949) study of the system MgO-SiO_2-H_2O paved the way to better understanding of the stability of Mg silicates. According to this investigation, enstatite is stable in the presence of water at temperatures above about 650° C., whereas forsterite remains stable until temperatures of about 400° C. are reached. Even small amounts of the corresponding Fe silicates drastically lower these temperatures. Yoder (1955, p. 515) pointed out that the various reactions may proceed at considerably lower temperatures if water pressures are less than rock pressures. In the Quad Creek ultramafic rocks reasonable limits can be placed on these effects; compositions of the constituent minerals are known (Table 1), and it is unlikely that the rock pressure was greatly in excess of water pressure during metamorphism. Thus temperatures of 500°–600° C. seem reasonable for the mineral assemblage of the ultramafic rocks.

Tilley (Metamorphism Symposium, Geophysical Laboratory Wash., March 20–22, 1956) believes that there is a lower and a higher sillimanite isograd, which reflects formation of sillimanite from biotite and muscovite respectively. Yoder and Eugster (1955, p. 262–269) showed that muscovite becomes unstable at temperatures of 600°–700° C. and reacts with quartz to form sillimanite and orthoclase. Sillimanite in Quad Creek biotite schists formed from biotite, as indicated by the intimate association of biotite, sillimanite, cordierite, and hypersthene in these rocks. Temperatures of 500°–600° C. seem reasonable for the production of sillimanite, cordierite, and hypersthene from biotite. The scarcity of garnet may again indicate relatively low Al and high Mg content of biotite schists.

Ramberg (1952, p. 72–73) states that,

"... at a high degree of metamorphism—in the border field between amphibolite facies and granulite facies—sphene undergoes several reversible reactions with common rock-forming minerals under liberation of rutile and/or ilmenite, so that the mineralogical environment under which sphene can exist stably at high pressure and temperature becomes very restricted."

The presence of rutile in many of the Quad Creek resister rocks indicates metamorphism in the highest subfacies of the amphibolite facies.

James (1955, p. 1475) found that the Iron Formation of Michigan is characterized in the sillimanite zone by quartz, magnetite, grunerite, pyroxene, hornblende, and garnet, whereas pyroxene is absent in the garnet and staurolite zones. Mineral assemblages of Quad Creek banded ironstones belong to the sillimanite-almandine subfacies of the amphibolite facies.

Thus mineral assemblages of various resister rocks indicate that before granitization the Quad Creek area was subjected to regional metamorphism of highest amphibolite facies, and temperatures were probably in the range of 500°–600° C.

So-Called Regressive Changes

The pre-granitization metamorphic facies is determined by mineral assemblages of relatively rare resister rocks. In tracing the succeeding granitization, attention must be focused on migmatites and partly metasomatized metasediments which are far more common throughout the Quad Creek area. Studies of

series of thin sections allow recognition of the effects of imbibition and granitization. Mineralogical changes observed in para-amphibolites, ultramafic rocks, and biotite schists are as follows:

Para-amphibolites

(quartz)-calcic plagioclase-augite-hypersthene-(hornblende, biotite)
(quartz)-calcic plagioclase-green hornblende-brown biotite-(garnet, epidote)
quartz-plagioclase An_{30-40}-green hornblende-brown biotite-epidote
quartz-sericitized plagioclase An_{30}-bluish green hornblende-greenish brown biotite-epidote-(chlorite)
quartz-sericitized plagioclase An_{30}-greenish brown biotite-chlorite-(epidote, microcline)

Ultramafic rocks

olivine-bronzite-actinolite-spinel-magnetite
olivine-actinolite-talc-magnetite-(phlogopite)
actinolite-serpentine-phlogopite-chlorite-magnetite
serpentine-phlogopite-chlorite-magnetite

Biotite schists

quartz-plagioclase-brown biotite-cordierite-sillimanite-(hypersthene, microcline)
quartz-plagioclase-brown biotite-(garnet, epidote)
quartz-plagioclase-brown biotite-epidote
quartz-plagioclase-greenish brown biotite-epidote-(chlorite, microcline)
quartz-sericitized plagioclase An_{20-30}-microcline-greenish brown biotite-chlorite-(epidote)

The writers have been unable to determine similar series for the banded ironstones. Equivalent changes are: (1) replacement of bronzite by anthophyllite in biotite-cordierite-bronzite-anthophyllite rocks, and (2) the contrast between microcline in biotite schists containing cordierite and sillimanite (cryptoperthitic; $2V_\alpha$ 70°–80°), and microcline in biotite schists with greenish-brown biotite (only slightly perthitic; $2V_\alpha$ 80°–90°).

These mineral changes occur in many rock series, both along and across strike, from cores of metasedimentary units outward into enveloping migmatites, in skialiths in granitic gneiss, and in gradations from migmatites into granitic gneisses. They can be attributed to: (1) retrograde metamorphism, reflecting lower temperatures, or (2) increased amounts of water at the same temperature and rock pressure as prevailed during the initial water-deficient metamorphism. The first interpretation fails to account for the relationship between mineral changes in the rocks and their degree of feldspathization or distance from tongues or islands of granitic gneiss.

Understanding of the role of water in metamorphism has increased considerably in recent years, especially through two papers by Yoder (1952; 1955). Yoder (1955, p. 516–518) used the system MgO-SiO_2-H_2O (Bowen and Tuttle, 1949) as example to define mineral assemblages of the same composition, stable at the same temperature and rock pressure, in the presence of different amounts of water. By changing the amount of water—*e.g.*, in the divariant field between the univariant curves marked by absence of water and enstatite respectively—a rock consisting solely of enstatite may be converted into: (1) forsterite-enstatite-talc, (2) forsterite-talc, (3) forsterite-talc-serpentine, and (4) either forsterite-serpentine-water or talc-serpentine-water. The first three mineral assemblages characterize the water-deficient region, and the last two are stable in the presence of water as a free phase. The writers believe that all the seemingly regressive mineral changes enumerated can be explained in this manner. This is true also for the Quad Creek metanorite and metabasaltic dikes whose cores consist of plagioclase-pyroxene and margins of plagioclase-hornblende.

The relationship of mineral changes in the rocks and their proximity to tongues and islands of granitic gneiss link the changes caused by increased amounts of water to the granitization process.

Metasomatic Effects

The over-all pattern of mineral changes accompanying granitization in the Quad Creek area is:

(1) (pyroxenes)→ hornblende → hornblende + biotite + epidote → biotite + chlorite + epidote → biotite + (chlorite, epidote)
(2) more calcic plagioclase → oligoclase An_{30} → sericitized oligoclase An_{20-30} → turbid oligoclase An_{10-20} → clear albite
(3) decrease in amounts of ferromagnesian minerals and appearance of "alteration" minerals such as epidote, chlorite, sericite, and calcite
(4) increase in amounts of alkali feldspars in-

cluding nonperthitic to slightly perthitic microcline ($2V_\alpha$: 80°–90°) and quartz

The complexity of the mineral changes is emphasized by epidote which is present in different mineral associations in different rocks, according to its formation: (1) in para-amphibolites and biotite schists during initial metamorphism; (2) feldspathized para-amphibolites and banded biotite-hornblende migmatites during alteration of hornblende to biotite and epidote; (3) in biotite migmatites and granitic gneisses during conversion of oligoclase An_{20-30} into more sodic plagioclase and epidote. Similarly, rutile is present in high-grade metasediments and appears again in sagenite structures shown by greenish-brown biotites of migmatites.

Relations of the alkali feldspars are especially complicated. As Lammers (1939, unpublished ms.) found, the core of the Beartooth block consists predominantly of pink, leucogranitic gneiss similar to samples 287/53 and 248/53 (Table 1). Toward the migmatitic boundary zone tonalitic gneisses (Table 1, samples 249/53 and 329/53) with little or no microcline become associated with the pink granitic gneiss. It seems from this over-all distribution that K metasomatism was concentrated in the core of the Beartooth block, and Na apparently migrated farther outward. Differential movement of Na and K is also indicated by rock series of gradations from quartzites into granitic gneisses that show a progression: (1) quartz-(biotite), (2) quartz-oligoclase-biotite, and (3) quartz-oligoclase-microcline-biotite. Some ultramafic lenses in contact with granitic gneiss have an inner zone of hornblende and a rim of biotite (vermiculite). In para-amphibolites, K metasomatism is as conspicuous as Na metasomatism:

$$\begin{array}{c} \text{Na metasomatism} \\ \downarrow \\ \text{Ca-Na plagioclase} \rightarrow \text{Na-Ca plagioclase} \\ \text{hornblende} \rightarrow Na^{+1} + \text{biotite} + \text{epidote} \\ \uparrow \\ \text{K metasomatism} \end{array}$$

Small-scale differences in type of metasomatism are common. Biotite-cordierite-bronzite-anthophyllite rocks apparently formed by migration of Mg,Fe from para-amphibolites into adjacent quartzites. Irregularities in K *versus* Na metasomatism are very common. Thus alaskitic rocks with quartz-oligoclase (chlorite) may be found near granitic gneisses with abundant microcline. Autochthonous, highly potassic pegmatites are examples of extreme K metasomatism.

The presence of alteration minerals is characteristic of nearly all thoroughly granitized rocks, although alteration is most conspicuous in the migmatites. These features (sericitization, epidotization, turbidity of plagioclase, chloritization of biotite, presence of epidote, chlorite, and calcite associated with hornblende and biotite) are linked with so-called regressive mineral changes and can be attributed similarly to the presence of water as a free phase during granitization.

Chemical Data

Table 1 lists results of 23 chemical analyses, modes, and optical data determined for the major constituents.

Semiquantitative spectrographic data are presented in Tables 4 and 6. Eight orders of abundance have been determined for each element by visual comparison of the samples with two synthetic mixtures. Amounts of the various elements in the standards are given in Table 3.

The eight orders of abundance for each element are: *a* much higher than the amount of that element in standard B, *b* somewhat higher than the amount in standard B, *c* about the same as the amount in standard B, *d* less than the amount in standard B but higher than *e*, *e* higher than the amount in standard A but lower than *d*, *f* about the same as the amount in standard A, *g* less than the amount in standard A, and *h* below the limits of sensitivity. Absolute ranges indicated by these symbols differ for each element (Table 3).

Table 4 shows results for ultramafic and mafic rocks of igneous origin. The three ultramafic rocks are characterized by low Ga, Ba, and Zr and high Ni and Cr. The markedly mafic character of the Quad Creek metanorite is shown by the high values for Ni and Cr of the fresh rocks, represented by the first eight samples. The values are similar to those of the ultramafic rocks. Of the following three samples, 174/53 is a pegmatitic phase of the metanorite, 144/53 a contact phase, and 173/53 a metanorite adjacent to and altered by a later pegmatite dike. Sample 174/53 indicates that trace-element concentrations may be changed radically in the differentiation of pegmatitic phases in a noritic magma, with especially marked decreases in Ni and Cr. Samples 144/53 and 173/53 have been altered after consolida-

tion and now consist mainly of turbid plagioclase and bluish-green hornblende; 173/53 also has some quartz. The results indicate marked decreases in Cr, but Ni has been less sensitive to postconsolidation alteration of the rocks.

TABLE 3.—TRACE-ELEMENT STANDARDS

	A (ppm)	B (ppm)
Ga	14	110
Ba	270	2700
Co	39	640
Ni	70	670
Cr	130	1000
Zr	100	—

The next seven samples are of fresh metanorite dikes. Trace-element data for these rocks are almost identical to those for the Quad Creek metanorite. Of the following four samples, 19/53, 212/53, and 221/53 are contact phases consisting of quartz, plagioclase, hornblende, and epidote with only residual pyroxene, and 138/53 is an altered metanorite adjacent to a Laramide felsic porphyry dike. The altered dike rocks are not much different from the fresh samples.

The following samples are: 69/53, an iron-rich metabasaltic dike; 40/53, a fresh basaltic dike with augite microphenocrysts; 273/53 and 289/53, two basaltic dikes showing hydrous alteration. In three of these rocks trace-element distribution is different from that of the metanorite dikes and the Quad Creek samples, but sample 40/53 is similar to the metanorites in its trace-element content.

In a few rocks Ca and Sr have been determined spectrographically. Results are given in Table 5.

The two Quad Creek metanorites are from the center of the body; 15/53 is from its upper part exposed along the road, and 140/53 is from its lower part near the sulfide-rich phases. The fresh metanorite dikes have Sr/Ca ratios similar to the Quad Creek metanorite. Of the altered contact phases, 19/53 has an exceptionally high Sr content combined with high Zr (Table 4); 221/53, more thoroughly altered than 19/53, has an unusually low Sr content. The iron-rich metabasalt 69/53 is characterized by a very high Sr content, and the younger basaltic dikes, fresh and altered, have normal Sr/Ca ratios.

Trace-element results for amphibolites and migmatites are given in Table 6. Data are arranged in accordance with five petrographic groups:

(1) Amphibolites with quartz <5%, biotite <10%, and hornblende or pyroxene >40%. Sample 33/53 has much hypersthene; 37/53 has augite and hypersthene; remaining samples have hornblende only.
(2) Amphibolites with quartz 5–20%, biotite < 5%, and hornblende >40%.

TABLE 4.—TRACE-ELEMENT DATA FOR ULTRAMAFIC AND MAFIC ROCKS OF IGNEOUS ORIGIN

Sample number	Ga	Ba	Co	Ni	Cr	Zr
Ultramafic rocks						
34/53	g	g	d	c	a	g
58/53	g	g	d	c	a	h
65/53	h	g	f	a	a	h
Quad Creek metanorites						
15/53	g	d	f	c	a	g
18/53	g	g	g	c	a	e
20/53*	g	d	f	c	a	h
22/53	g	f	f	c	a	g
24/53*	f	f	f	c	a	f
128/53	g	f	f	c	a	g
140/53	g	f	d	c	a	g
175/53	f	f	e	c	a	g
174/53	f	e	f	d	f	g
144/53	f	d	f	c	f	f
173/53	f	e	f	a	d	g
Metanorite dikes						
171/53	g	d	f	c	a	f
172/53	g	f	f	c	b	g
222/53	f	f	e	c	a	g
223/53	f	f	e	c	a	g
225/53	f	f	e	c	a	f
226/53	f	f	e	c	a	g
326/53	f	d	f	c	a	g
19/53	f	d	f	c	a	e
212/53	f	g	e	c	a	g
221/53	f	f	e	c	a	g
138/53	f	d	f	c	c	g
Other dikes						
69/53*	f	d	f	f	f	f
40/53	f	d	f	d	a	g
273/53	f	e	f	g	f	f
289/53	f	f	f	g	f	f

* Chemically analyzed samples (Table 1)

(3) Amphibolites with quartz 5–10%, biotite 10-20%, and hornblende 20–40%.

(4) Migmatites with quartz >10%, biotite >10%, and hornblende <5%. All three samples have strongly sericitized plagioclase.

TABLE 5.—CA-SR DATA FOR MAFIC ROCKS OF IGNEOUS ORIGIN

	Ca (per cent)	Sr (ppm)	% Sr/% Ca × 10^3
Quad Creek metanorites			
15/53	2.3	97	4.2
140/53	3.1	103	3.3
Metanorite dikes (fresh)			
223/53	4.6	118	2.6
225/53	5.0	147	2.9
Metanorite dikes (altered)			
19/53	4.6	299	6.5
221/53	4.2	22	.5
Other dikes			
69/53	4.8	403	8.4
40/53	5.6	128	2.3
289/53	6.1	146	2.4

(5) Migmatites with quartz >10%, biotite >5%, and hornblende >5%. Sample 192/53 has strongly sericitized plagioclase; 253/53 has considerable garnet and accessory vesuvianite.

The erratic distribution of trace elements (Table 6) may reflect both the origin and the degree of metasomatism suffered by these rocks.

ORIGIN OF ROCKS

Granitic Gneisses

Field relations in the Quad Creek area (and throughout the Beartooth Mountains) indicate *in situ* formation of granitic gneisses and migmatites from pre-existing sediments:

(1) The synclinial structure of the Quad Creek area is continuous from the migmatites and metasediments to the northeast through the gradational boundary zone and into the granitic gneiss to the southwest. The structure intersects the boundary zone at an angle of 40°–50° yet maintains the same attitude throughout without signs of deflections. The syncline resembles the open symmetrical folds of many unmetamorphosed terrains and contrasts with the small, tight, asymmetrical folds found in country rocks peripheral to large intrusive granite plutons (*e.g.*, Compton, 1955, p. 14). Examples of later folding of country rocks in which large granite plutons have been

TABLE 6.—TRACE-ELEMENT DATA FOR AMPHIBOLITES AND MIGMATITES

Sample number	Ga	Ba	Co	Ni	Cr	Zr
Amphibolites, group 1						
33/53	f	f	f	g	c	f
37/53	f	d	f	f	c	g
59/53	f	d	d	f	c	g
106/53	f	g	d	c	a	f
146/53	f	f	f	d	c	g
232/53	f	g	f	d	c	g
255/53	f	f	f	d	c	g
Amphibolites, group 2						
41/53*	f	d	f	f	f	f
288/53	f	g	f	d	d	g
299/53	f	g	g	f	d	g
Amphibolites, group 3						
5/53	f	d	g	d	c	g
71/53	f	d	f	f	d	g
94/53	f	d	g	f	f	e
96/53	d	d	g	f	f	f
120/53	d	g	g	d	a	h
134/53	d	d	g	g	f	f
151/53	f	d	g	g	f	e
152/53	f	c	g	g	f	e
183/53	f	f	e	f	f	f
210/53	f	c	g	g	g	e
243/53	f	d	f	d	d	f
280/53	f	d	g	f	f	f
291/53	f	d	g	d	d	e
297/53	f	d	g	f	d	f
Migmatites, group 4						
195/53*	f	d	g	f	f	f
281/53*	f	d	h	f	f	e
286/53	f	d	h	g	f	f
Migmatites, group 5						
136/53	f	c	g	g	f	f
192/53	f	f	g	f	f	f
205/53	f	c	h	g	f	e
214/53	f	e	g	f	f	f
215/53	f	d	g	f	f	f
253/53	f	d	g	g	g	f
324/53	f	c	h	g	f	e

* Chemically analyzed samples (Table 1)

emplaced invariably show deflections or even abrupt termination of folds at the granite boundaries, as shown in the Cape Folded Belt of southern Africa (Scholtz, 1947, p. 66–68).

(2) Wherever comparisons can be made in individual outcrops, such structural elements of granitic gneisses and migmatites as foliation, banding, and attitudes of skialiths are parallel to bedding in associated metasediments. This is especially striking in gradations of quartzite into granitic gneiss (Pl. 2, Fig. 1), which show feldspathization along bedding planes, and in gradations of banded migmatite into granitic gneiss (Pl. 2, Fig. 2), which exhibit all signs of passive replacement without disturbance of even the thinnest bands and lamellae. Plate 5 shows that this is also true for the area as a whole. Particularly significant are swarms of skialiths of amphibolite, biotite schist, and biotite gneiss in granitic gneiss. The skialiths are lenticular, and their attitudes conform with the foliation of the surrounding gneiss; both are consistent with the over-all structure of the locality. Thus here, as in so many plutonic terrains (Read, 1948, p. 187), foliation in migmatites and granitic gneisses is the metamorphic expression of original bedding.

(3) Interdigitating tongues of granitic gneiss and migmatite in the boundary zone are parallel to the synclinal trend, and the two rock types grade into one another both across and along strike. Tongues of granitic gneiss pinch out toward the north-northeast, and beyond their terminations small "islands" of granitic gneiss in migmatite are common. Tongues of migmatites pinch out toward the south-southwest, and swarms of skialiths in granitic gneiss are common beyond the terminations of the migmatite tongues. Within tongues of migmatites thin lenses of granitic gneiss occur within tongues of migmatites, just as there are migmatite skialiths within tongues of granitic gneiss. The migmatitic tongues and their extensions of migmatite skialiths in granitic gneiss represent relict stratigraphic horizons more resistant to granitization. Yet all these small and large individual bodies maintain attitudes conformable to the synclinal structure.

These features are observed in individual outcrops and are expressed in the map pattern. Similar field relations can be studied equally well in other parts of the project area. Additional field evidence comes from other areas—*e.g.*, the Lonesome Mountain area (Fig. 2). Here sills and dikes of metagabbro, though emplaced in granitic gneiss, are intruded by the granitic gneiss. Poldervaart (1953, p. 260–261) has discussed these relations; they can be interpreted to mean only that the intrusives were emplaced in granite that was subsequently mobilized, or that the bodies were emplaced in sediments that were later granitized. The structural conformity of skialiths of metasediments (quartzites, banded ironstones, and para-amphibolites) with foliation of granitic gneiss throughout the project area indicates that the second alternative applies to the Beartooth Mountains.

Laboratory evidence yielded by zircon concentrates is as convincing as the field evidence. The high percentages of rounded zircons in all the rocks favor their sedimentary origin. Growth of new mantles on rounded zircons, with the shells eventually acquiring euhedral outlines, also provides strong evidence that the granitic gneiss formed *in situ* from original sediments. Further work in other areas in the Beartooth core may result in recognition of parautochthonous members of Read's Granite Series (1952, p. 20–23), which may have zircon concentrates further advanced in the transformation series than zircons of the two granitic gneisses listed in Table 2.

This is the first time that transformation of zircons has been shown to accompany reconstitution of sediments by granitization. Probably the manner of zircon transformation is not unique but dependent on the type of granitization—*e.g.*, by partial melting or by imbibition of rocks by migrating hot aqueous fluids. In the Quad Creek area new material has grown on rounded zircons present in the pre-existing sediments. The new material is probably derived in large part from solution of smaller zircons, but some may have been introduced.

Pegmatites

Read's Granite Series (1952, p. 20–23) may well be extended to include pegmatites, since in metamorphic terrains examples of autochthonous, parauthchthonous, and intrusive pegmatites are common. Autochthonous pegmatites show in their field relations that they represent metamorphic-metasomatic segregates of country rocks: they are conformable, have gradational borders, are associated with small lenses and stringers of pegmatitic material and individual large feldspar eyes, and show close mineralogical correspondence with the surrounding rocks; some show relict foliation. Parautochthonous pegmatites are crosscutting

but preserve mineralogical affinities with the country rocks. Ramberg (1956) described excellent examples of these members of the Pegmatite Series. In the Quad Creek area field relations (Pl. 2, fig. 3) indicate that the majority of the pegmatites are autochthonous, and the relatively few crosscutting pegmatites are parautochthonous.

Ages of pegmatites are generally equated with the age of the nearest granite pluton or with that of the metamorphic cycle that deformed and recrystallized the country rocks. Without detailed field studies this inference is unwarranted and may lead to correlations as erroneous as earlier attempts to correlate Precambrian formations on the basis of their lithology (*e.g.*, Knopf, 1955, p. 688–689). Pegmatites in the Spruce Pine district, North Carolina, have an age of 340 ± 20 m.y., yet the main deformation and recrystallization of the country rocks occurred a minimum of 700 m.y. ago (Kulp and Poldervaart, 1956, p. 400–401). The age of the Orange River pegmatites in South Africa (1.1 b.y.) is generally believed to indicate that the country rocks are of about the same age (Holmes, unpublished ms). Yet in the eastern parts of Namaqualand the pegmatites are the youngest Precambrian rocks exposed and follow the emplacement of charnockitic adamellite phacoliths, earlier orogeny and metamorphism with synkinematic intrusion of tonalite and granodiorite ("gray gneiss"), still earlier emplacement of basaltic sills and dikes, and original deposition of two sedimentary formations (Gariep and Kheis), separated by a major unconformity (Söhnge and de Villiers, 1947; Poldervaart and von Backström, 1949).

Only after detailed field work can there be reasonable certainty that pegmatites of a region belong to one phase of activity and are allied to a particular granite pluton or contemporaneous with a particular metamorphic cycle. Since the Beartooth pegmatites are in large part autochthonous their age is also probably that of the cycle of metamorphism and granitization. In all cases ages obtained for pegmatites should be checked with ages of country rocks. This has been done for Beartooth rocks at the Lamont Geochemical Laboratory, and for both pegmatites and country rocks the same ages have been obtained.

Para-Amphibolites

Several writers have suggested that there are differences between ortho- and para-amphibolites, either in proportions of major elements (Lapadu-Hargues, 1953, p. 162–163) or in trace-element content (Engel and Engel, 1951). Tests have shown that these suggestions cannot be upheld (Wilcox and Poldervaart, in preparation). Field criteria described earlier are at present the only means of distinguishing the two types of amphibolites, but these criteria are subject to severe limitations.

Many para-amphibolites have compositions very close to or identical to those of basaltic rocks; hence the impression is often gained that they represent mafic tuffs rather than chemical or detrital sediments. There are at present no criteria to distinguish thoroughly recrystallized metatuffs from metasediments. The argument for a mafic tuffaceous origin of para-amphibolites is based on the fact that proportions of Al_2O_3, (FeO + Fe_2O_3), MgO, and CaO in para-amphibolites resemble those in basalts. In Table 7 the writers list compositions of various rocks, reduced free of water and carbon dioxide.

Results indicate that it is possible for a para-amphibolite derived from a dolomitic shale to have high proportions of Al_2O_3, (FeO + Fe_2O_3), MgO, and CaO. However, the $K_2O/(Na_2O + K_2O)$ ratio of dolomitic shales is higher than that of para-amphibolites or basalts. This factor seems more serious, but possibly the alkali ratio has been influenced by metasomatic changes accompanying recrystallization and migration of H_2O and CO_2, through emigration of K, immigration of Na, or both. Early members of the series quartzite-granitic gneiss in the Quad Creek area are quartz-oligoclase rocks with little or no microcline; this indicates that Na advanced ahead of K. Thus para-amphibolites of near-basaltic compositions may represent metamorphosed dolomitic shales.

Siliceous Biotite-Cordierite-Bronzite-Anthophyllite Rocks

Although siliceous biotite-cordierite-bronzite-anthophyllite rocks are rare in the Quad Creek area, their occurrence is of interest. Since Eskola's (1914) classic study of the Orijärvi region in southwest Finland a considerable literature has accumulated on the occurrence, composition, and origin of cordierite-anthophyllite rocks. Tilley (1937, p. 308–309) remarked: "The growing recognition of the importance of metasomatic processes in metamorphism is nowhere more clearly exemplified than in the studies carried out on the

natural history of the anthophyllite-cordierite rocks during the last twenty-five years". Most writers agree with this general statement on the origin of these rocks, but many different views have been expressed regarding the type of metasomatism involved.

Cordierite-anthophyllite rocks may be found in association with mafic igneous rocks or amphibolites. In these cases it has been suggested that metasomatism involved removal of alkalis and Ca and addition of Si, with or without internal migration of Mg and Fe (Brögger, 1934; Prider, 1940; Kuroda, 1956; Tilley, 1937). The Orijärvi rocks are associated with silicic rocks. Eskola (1914, p. 253–263) suggested metasomatic introduction of Mg and Fe and removal of Ca and alkalis; he believed that the Orijärvi granodiorite was a possible source for the metasomatizing solutions. Wegmann and Kranck (1931, p. 62) and others believe that Mg-Fe metasomatism is linked to migmatization and do not consider residual fluids emanating from granodioritic or granitic intrusions necessary or even likely sources for Mg and Fe. Tuominen and Mikkola (1950) presented an interesting kinematic theory to account for the Orijärvi rocks, but their interpretations have been vigorously criticized by Eskola (1950).

The Quad Creek rocks are intimately associated with quartzites, and small lenses of para-amphibolite are also found near by. The analyzed sample has more silica than published analyses of cordierite-anthophyllite rocks (Table 8), but the amount of quartz varies considerably in different samples. The rocks also differ in containing both bronzite and anthophyllite; bronzite is of earlier formation and in part replaced by anthophyllite. The writers find it difficult to reconcile the composition of the analyzed sample with that of a

TABLE 7.—COMPOSITIONS OF BASALTS, PARA-AMPHIBOLITES, AND DOLOMITIC SHALES

Index	SiO_2	TiO_2	Al_2O_3	Fe_2O_3	FeO	MnO	MgO	CaO	Na_2O	K_2O	P_2O_5	$K_2O/(Na_2O + K_2O)$
A	47.0	3.0	15.1	3.7	8.1	.2	7.9	10.9	2.7	1.0	.3	.27
B	51.0	1.4	15.6	1.1	9.8	.2	7.0	10.5	2.2	1.0	.2	.31
C	51.2	.6	15.0	2.0	9.3	.2	8.8	9.8	2.2	.8	.1	.27
D	50.3	1.6	15.7	3.6	7.8	.2	7.0	9.5	2.9	1.1	.3	.28
I	56.3	.8	16.9	6.5		—	6.7	8.5	.4	3.8	.1	.90
II	57.3	—	15.2	6.6		—	4.9	11.3	1.3	3.2	.2	.71
III	53.9	.7	16.5	3.6	6.0	.1	4.9	9.3	1.1	3.7	.2	.77

A—average olivine basalt (Green and Poldervaart, 1955, p. 185)
B—average tholeiitic basalt (Green and Poldervaart, 1955, p. 185)
C—average of 5 analyses of Quad Creek para-amphibolites
D—average of 200 amphibolites (Poldervaart, 1955b, p. 136)
I—Florena dolomitic shale (Permian), Kansas (Imbrie, in preparation)
II—average shale (Clarke, 1924, p. 30) plus 20 per cent Precambrian limestone (Daly, 1909, p. 165)
III—average Precambrian slate (Nanz, 1953, p. 57) plus 20 per cent Precambrian limestone (Daly, 1909, p. 165)

TABLE 8.—SILICEOUS CORDIERITE-ANTHOPHYLLITE ROCKS*

Index	SiO_2	TiO_2	Al_2O_3	Fe_2O_3	FeO	MnO	MgO	CaO	Na_2O	K_2O	P_2O_5	H_2O	Total
14/55	76.19	.24	7.36	.16	4.71	.02	8.00	.18	.22	.94	.06	1.91	99.99
1	67.53	.15	11.45	1.72	9.37	.08	7.96	.19	.22	.22	.02	1.08	99.99
2	65.61	.94	14.22	1.51	6.36	.09	4.88	1.96	.27	.27	.17	1.60	100.00
3	63.74	.73	15.07	4.71	1.99	.13	9.57	.82	.13	.52	.09	2.50	100.00

* Recalculated to 100 per cent
14/55 Siliceous biotite-cordierite-bronzite-anthophyllite rock, Quad Creek area
1 Anthophyllite-cordierite rock, Falun Mine, Sweden (Larsson, 1932, p. 118, no. 606)
2 Anthophyllite-cordierite rock (Tilley, 1937, p. 304)
3 Anthophyllite-cordierite-biotite rock (Kuroda, 1956, p. 65)

sediment and thus accept a metasomatic origin for the Quad Creek rocks. Field relations (Fig. 14) suggest they were probably formed by migration of Mg, Fe, and perhaps Al from bedding. They are associated and interbedded with other metasediments (banded ironstones, biotite schists, and para-amphibolites). Thus in the present area the quartzites are of sedi-

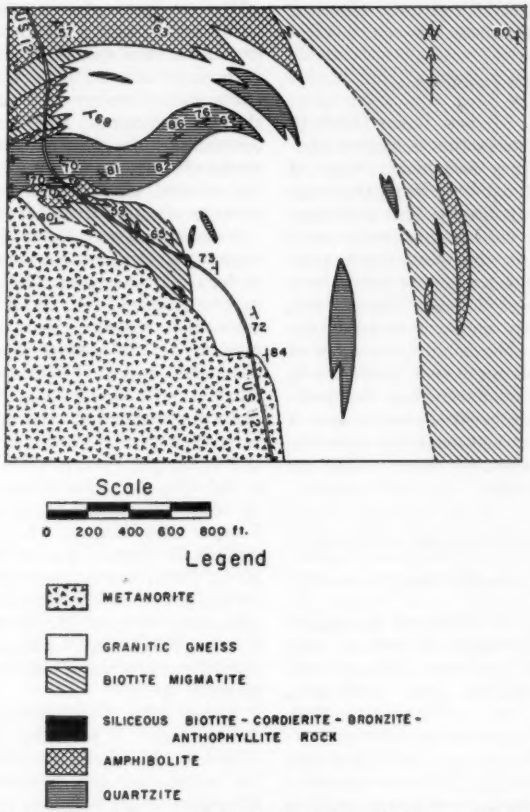

FIGURE 14.—FIELD SKETCH OF SILICEOUS BIOTITE—CORDIERITE—BRONZITE—ANTHOPHYLLITE ROCK

associated para-amphibolites into quartzites. Thus the rocks may demonstrate on a small scale Wegmann and Kranck's (1931) ideas of Mg-Fe metasomatism accompanying migmatization.

Quartzites

In many metamorphic terrains lenses of thoroughly recrystallized quartz are found in gneiss, schist, or granulite. Quartzites of the Quad Creek area show sedimentary structures, such as delicate bedding and even some cross-mentary origin. In the core of the Beartooth range and in other regions these sedimentary features may have been partly or wholly destroyed by metamorphism. Such quartz lenses may represent: (1) segregations from pegmatitic fluids, (2) recrystallized cherts, or (3) metamorphosed sandstones. Where field studies did not determine their origin, the writers found it useful to examine heavy residues of the rocks. Quartz "blows" of pegmatitic derivation contain a few euhedral or rounded zircons. Cherts have no zircons (*c.f.*, Maxwell, 1953). Sandstones have rich zircon crops in which the

majority of the grains are well rounded. Thus the amount of heavy residue and the shape of zircons obtained will generally enable one to determine the origin of these quartz lenses. Field relations and heavy residues indicate that quartzites of the Quad Creek area represent metamorphosed sandstones.

Banded Ironstones

Gruner (1946, p. 73) and James (1955, p. 1476) believe that magnetite of banded ironstones in intermediate and higher zones of metamorphism may represent magnetite originally present in the sediment. This also seems to be indicated by the few small outcrops of banded ironstones in the Quad Creek area. Oölitic structures, well preserved in rocks from the Iron Formation of Michigan (James, 1955, Pl. 5, p. 1469), have not been found in the Quad Creek rocks. The banded ironstones of the Quad Creek area form small lenses associated with para-amphibolites. Thus they probably represent thinly bedded intercalations of quartz (chert or silt) and magnetite with (Fe, Mg)-rich clay in dolomitic lutites, which are also rich in Fe and Mg.

Granitization in Beartooth Mountains

Type of Granitization

The case for *in situ* formation of granitic gneisses in the Beartooth Mountains rests squarely on the field evidence. Although this report concerns only the Quad Creek area, detailed mapping and reconnaissance work under the Beartooth project has advanced sufficiently to establish that the Quad Creek area is representative; the syncline is one of a series of folds, the migmatites are of a type found in the migmatite mantle east and west of the Beartooth core and also as skialiths in the core, and the granitic gneisses are the same as those found throughout the core of the Beartooth block. Field evidence of granitization is not restricted to the Quad Creek area but recurs throughout the project area. The writers find the field evidence wholly convincing and conclude that the Quad Creek area and the whole Beartooth block are a clear example of regional granitization.

Petrographic observations must be combined with field records to determine the process of granitization responsible for the transformation of pre-existing rocks: (1) Residual metasediments in the migmatite mantle show metamorphism in the sillimanite-almandine subfacies of amphibolite facies, which indicates temperatures of 500°–600°. (2) Metasediments and migmatites show seemingly regressive mineral changes which in series of samples prove to be related to degree of feldspathization and distance from tongues and islands of granitic gneiss. The same mineral changes are continued in the series migmatite-granitic gneiss. (3) The relationship between the apparent mineralogical regressions and granitization phenomena excludes the possibility of subsequent retrograde metamorphism but indicates that the mineral changes are due to increased amounts of water accompanying granitization.

Some writers (*e.g.*, Tuttle and Bowen, 1956) suggest that granitization in many regions may be due to partial melting. The minimum melting curve of granite (Tuttle and Bowen, 1953, p. 50) shows that temperatures of *ca.* 650° C. are necessary for the production of granitic partial melts from rocks. This temperature is in the range of the granulite facies of metamorphism. Apart from typical mineral assemblages (Ramberg, 1949, p. 35–47; 1952, p. 156–162; Turner and Verhoogen, 1951, p. 473–477; Eskola, 1952, p. 162–168), the granulite facies is characterized by sodic, cryptoperthitic to microperthitic K feldspar (Buddington, Metamorphism Symposium, Geophysical Laboratory Wash., March 20–22, 1956), and common clouding of minerals such as quartz, feldspars, pyroxenes, and apatite (Ramberg, 1949, p. 35, 44; Poldervaart and Gilkey, 1954). Thus metamorphism in the Quad Creek area was of amphibolite rather than granulite facies.

Yoder (1955, p. 506–509) believes that the water content of sediments at depths of *ca.* 20,000 feet has been diminished considerably by compaction and recrystallization. Metamorphism would result in further decreasing the water content of the rocks. Ramberg (1952, p. 244–245) gave arguments against the idea that hydrous granitic melts may form in quantity in the amphibolite facies at temperatures of 500°–600° C. The writers cannot reconcile these aspects of granitization by partial melting with their observations on the Quad Creek rocks. The observations also do not agree with ideas of granitization by solid diffusion, which are championed by Perrin (1954; 1956) and others.

Field and laboratory evidence in the Quad Creek area does agree with theories of granitization by migrating aqueous solution—the "wet granitization" of Bowen (1948, p. 85). The evidence shows that temperatures increased

first and resulted in metamorphism of the rocks. While temperatures remained high, aqueous solutions ascended, migrated through the rocks, produced mineral changes reflecting the increase in amounts of water, and metasomatized the rocks which were eventually transformed into gneisses of granitic composition. As shown below, high temperatures could have been maintained for some time after migration of solutions ceased. Temperatures and water concentrations were high enough to produce a limited degree of mobility of leucogranitic gneisses in parts of the Beartooth core which may show characters of parautochthonous granites (Read, 1952, p. 21). However, this mobility is the culmination of plutonism, and field relations show that the rocks were granitized before they became mobile. The core of the Beartooth block is also the focus of plutonism, and along this zone the solutions ascended and spread outward into the adjacent rocks. Thus field and laboratory studies have established time-space relations in the transformation of the Beartooth rocks which allow better understanding of the process of granitization.

Chemical Variation

In tracing chemical variation during granitization, the assumption is usually made that samples collected are members of a continuous series. Rocks analyzed were not collected with this in mind—*i.e.*, they are not samples of one metasedimentary bed which grades into granitic gneiss along strike. However, the rocks have been selected after careful evaluation of field notes and thin sections as representative of the main rock types encountered. Although the original sediments probably varied in composition and were not exclusively the equivalents of para-amphibolites, petrographic studies show that imbibition and granitization resulted in chemical convergence of all the rocks in migmatites and granitic gneisses. Thus it is not unreasonable to compare the chemical analyses, although conclusions must remain tentative until more data are available. With these reservations, chemical variation during granitization can be discussed on the basis of 14 analyses of para-amphibolites, migmatites, and granitic gneisses.

Fractionation in magmas is generally directed toward "petrogeny's residua system" (Bowen, 1937, p. 11)—the low-temperature trough in the system SiO_2-$NaAlSiO_4$-$KAlSiO_4$ (Schairer and Bowen, 1935). In granitization there is the same tendency toward an end product consisting of quartz and alkali feldspars. In Figure 15 oxide weight percentages for the 14 analyses have been plotted against the differentiation index suggested by Thornton and Tuttle (1956) as a means for tracing differentiation in magmatic rocks. In the case of the Quad Creek rocks the differentiation index serves as a convenient measure of progress toward a final granitic composition in a series of rocks affected by granitization.

The analyses are well spaced over this diagram; the two minor gaps can probably be covered in future work. The points are remarkably regular in their distribution, and little smoothing is required to draw curves through them. The curve for SiO_2 rises continuously (but not linearly) in the series. Al_2O_3 increases gradually from para-amphibolites to migmatites but decreases in more silicic migmatites and granitic gneisses. The variation of $(FeO+Fe_2O_3)$ is of particular interest. Iron decreases gradually from para-amphibolites to migmatites and from migmatites to granitic gneisses, but the two curves are displaced relative to one another, which indicates a steep decrease within the migmatite group. MgO either remains the same or increases slightly in para-amphibolites and decreases continuously through migmatites and granitic gneisses. CaO shows a sustained decrease. The curve for Na_2O rises gently from para-amphibolites through migmatites but declines slightly in granitic gneisses. K_2O increases progressively in the series and shows an accelerated rise in the progression from tonalitic to leucogranitic gneisses.

The present study leaves unanswered many problems pertaining to granitization by aqueous solutions. A better understanding of the many problems involved can come only from a combination of field and laboratory studies of natural examples of wet granitization and parallel experimental investigations.

Geologic Chronology

General Statement

Reconstruction of the sequence of geologic events is one of the most difficult yet most important tasks facing the student of Archean geology. Its importance derives from the addition of "draughts of time" (Read, 1951, p. 297) to the structural and petrogenetic picture assembled during the investigation. It also provides insight into exactly which events have

been dated by radiochemical methods, if any absolute ages have been determined. The geologic record of earlier events is usually blurred or eradicated by later happenings, so that the folding because: (1) the rocks are thoroughly recrystallized and have local development of foliation; (2) contacts of the body are irregular, particularly along the well-exposed

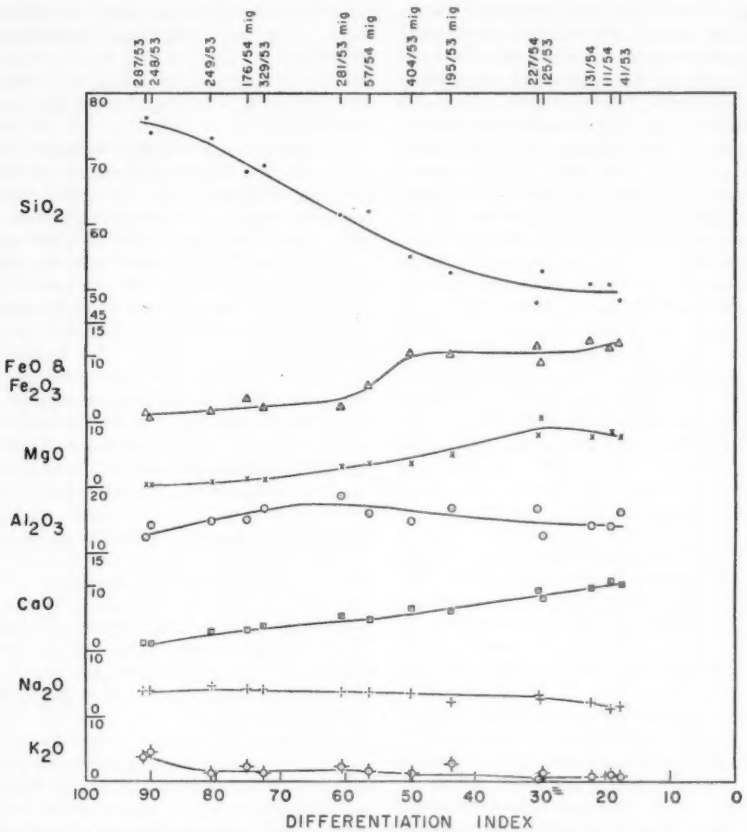

FIGURE 15.—DIFFERENTIATION-INDEX DIAGRAM FOR PARA-AMPHIBOLITES, MIGMATITES, AND GRANITIC GNEISSES

much of the evidence may seem contradictory. Statements of such reconstructions of geologic chronology are often more definite than warranted and are decided in part by the evidence and in part by the judgment and experience of the investigator.

The writers have presented their preferred scheme of the sequence of events for the Quad Creek area in Table 9. Reasons for these conclusions are given below.

Mae West Metagabbro

The Mae West intrusive is regarded as older than both the metamorphism-granitization and northern side (Pl. 5); (3) pegmatite dikes in the metagabbro are related in dip directions to the west limb of the synclinal structure. These relations indicate that the metagabbro is older than the metamorphism-granitization, and that before this cycle planes of weakness, related to the synclinal structure, had developed in the intrusive. In the Quad Creek and Gardner Lake areas metagabbro bodies of Mae West type are relatively scarce and small. Fold structures in these areas have steep (60°–80°) limbs. In the Lonesome Mountain area there are many thick metagabbro sheets of this type. The folds here are gentle (10°–40°). Thus it seems reason-

able to conclude that the intrusions were emplaced before the folding.

Ultramafic Rocks

Field evidence indicates that folding preceded metamorphism and granitization and that these two events were probably separate in time. All fold axes mapped strike north-northeast and plunge south-southwest. The plutonic cycle resulted in the present division of the Beartooth Mountains into a granitic-gneiss core and mantle of migmatites and metasediments, with boundary zones directed northwest. Thus the granitization initiated the northwest trend that is common in the Precambrian dike swarms and in the Laramide structures.

Probably the strongest evidence for the conclusion that folding preceded granitization comes from macro- and microstructures in the Lonesome Mountain and Long Lake areas, which are in the core of the Beartooth block. In the first area a number of northwest zones have flow foliation which disturbed the bedding foliation adjacent to the zones. Field studies indicate that flow foliation is later than bedding foliation. Fabric studies by Dr. S. Sen in the Long Lake area (Fig. 2) show that granitization with northwest trend is superimposed on the older fold structures. The map pattern of the Quad Creek area and the relations of various mafic intrusions also indicate that the plutonic cycle came after the folding.

It may seem strange that the older folds are so well preserved, and that the later metamorphism and reconstitution of the rocks have not been accompanied by equally conspicuous deformation. (*C.f.*, Bucher, 1956, p. 1305.) The writers have been unable to ascertain whether the main folding was accompanied by an older cycle of metamorphism. The relatively slight deformation that attended the main plutonic cycle may have been more severe at higher levels in the crust or may have found its main expression in uplifting, which apparently followed granitization. The problem of the relationship between deformation and plutonism cannot be solved by study of one particular region but must be analyzed on the basis of exhaustive investigations of many regions.

TABLE 9.—GEOLOGIC CHRONOLOGY OF QUAD CREEK AREA

Laramide Revolution	Thrusting Uplift	Emplacement of felsic porphyry dikes
Deposition	of Paleozoic	and younger sediments
	Peneplanation	
	Uplift	Emplacement of younger dolerite dikes
Metamorphism	Granitization	Emplacement of norite and iron-rich dolerite dikes Emplacement of pegmatites Emplacement of older norites of Quad Creek type Tectonic movement of ultramafics
Folding		Emplacement of ultramafic rocks (?) Emplacement of older gabbros of Mae West type
Deposition of Archean sediments (arenites, lutites, and calcilutites)		

Metamorphism and Granitization

Metamorphism results from temperature elevations maintained for a sufficient duration to allow partial or complete recrystallization of the rocks. Granitization in the Beartooth Mountains required migrating aqueous solutions, as well as elevated temperatures. High temperatures prevailed before solutions started to migrate through the rocks and may have continued beyond the time span of granitization. Possibly the start and termination of granitization may fall within a prolonged cycle of thermal activity. This appears to have been

the case in the Beartooth block, although the evidence is not conclusive.

Petrographic studies show that the rocks were metamorphosed before they were granitized. Thus the effects of metasomatism and high water pressures have been superimposed upon earlier mineral assemblages stable in the high-amphibolite facies of metamorphism. Many of these changes are seemingly regressive, but in this case they reflect higher amounts of water rather than lower temperatures. Field relations also indicate that metamorphism preceded granitization. For instance, some granitic patches in amphibolite enclose skialiths of foliated amphibolite which in some cases have moved so that the foliation has different attitudes in different skialiths and differs from that of the surrounding amphibolite.

The writers believe that the autochthonous to parautochthonous pegmatites of the Beartooth block formed during or just after the peak of granitization. These pegmatites play a crucial role in determining whether or not high temperatures prevailed after granitization.

Quad Creek Metanorite

The Quad Creek metanorite is intruded by pegmatites and along its upper contact by a few dikes of mobilized granitic gneiss. This places an upper age limit on the emplacement of the metanorite and might be regarded as proof that the intrusive is pre-granitization. Several considerations must be weighed against this view: (1) contacts of the body are sharp; (2) only the margins have recrystallized to plagioclase-hornblende rocks, over distances of a foot or less, whereas interior portions show remarkably little change; (3) chemical, mineralogical, and petrological affinities are very close between the Quad Creek metanorite and the metanorite dikes that usually cut the pegmatites and must therefore be later. The writers regard the emplacement of the Quad Creek body as having occurred just before the pegmatite phase but after the main granitization of the country rocks.

Metabasaltic Dikes

The mafic-dike criterion has been used by many investigators as one of the most important means of distinguishing time in metamorphic terrains (Poldervaart, 1953, p. 260–261). In the Beartooth block, the presence of metabasaltic dikes which cut the pegmatites, granitic gneisses, migmatites, and metasediments, yet are themselves metamorphosed, indicates a second cycle of metamorphism superimposed upon the main plutonic event. However, an alternative explanation might be that the dikes were emplaced after granitization and pegmatite formation but while high temperatures prevailed in the region—*i.e.*, within the time span of a prolonged plutonic cycle. According to the first interpretation there were two major plutonic events, and age determinations by radiochemical methods would probably provide the age of the younger cycle. According to the second interpretation there was only one major plutonic event, and age determinations would yield its age. Two considerations cause the writers to favor the second view: (1) the remarkably close correspondence between the Quad Creek metanorite and the later metanorite dikes which would be strange if they represented two separate periods of intrusion of basaltic magma, and (2) two metanorite dikes found outside the Quad Creek area cut several pegmatites, but each is also intruded by a pegmatite. Neither of these considerations is conclusive, and the writers' interpretation must therefore be considered tentative.

Precambrian Dolerite Dikes

Several dolerite dikes in the Quad Creek area and many other dikes throughout the project area are unmetamorphosed. Around Beartooth Butte the dolerite dikes are unconformably overlain by Middle Cambrian Flathead Sandstone. Thus the dikes are Precambrian but younger than the Archean cycle of metamorphism and granitization. Several of these younger dikes also cut the Stillwater complex.

In the field there is a marked contrast between the younger dikes and the metabasaltic dikes. The dolerite dikes have many small offshoots which follow directions shown by prominent joint planes in the country rocks. The metabasaltic dikes do not have these features. The writers assume that the younger dikes were emplaced when the region was at a high crustal level and open fractures existed in the country rocks. Thus the dikes may be late Precambrian, emplaced just before peneplanation and subsequent deposition of Paleozoic sediments.

Laramide Revolution

During the Laramide Revolution occurred the uplift and tilting of the Beartooth block, emplacement of felsic porphyry intrusives, and

thrusting of the block, accompanied by major faulting as shown in the Gardner Lake and Lonesome Mountain areas. Laramide movements followed zones of weakness established in the Precambrian, as shown in over-all pattern by the directions of thrusting and faulting and in detail by the fact that joint planes in Paleozoic sediments at Beartooth Butte correspond with joint planes in crystalline basement rocks (Scheufler, 1954, M.S. thesis, Wayne Univ.) and directions of Precambrian dolerite dikes and their offshoots. The northwest Laramide trend appears to have been established during the Archean plutonic cycle.

Absolute Ages and Correlations

Lane (1938, p. 63–64) gives a helium age of 1300–1900 m.y. for the Quad Creek metanorite, 1130 ± 100 m.y. for the center of a 25-foot dike with location given as 44° 58′ N., 109° 29′ W., and 220 ± 15 m.y. (center) and 85 ± 5 m.y. (contact) for a metanorite dike near Long Lake. The 25-foot dike has not been located by the writers, but new samples have been obtained from the metanorite dike near Long Lake. The dike represents a plane of weakness used in Laramide movements and perhaps younger movements, and the metanorite is granulitized, especially along contacts with country rocks. The quarry from which Lane obtained samples for age determinations is also an unknown distance (maximum 2000 feet) above an exceptionally thick intrusive of felsic porphyry, exposed in the cirque facing Rock Creek.

Age determinations of Beartooth rocks have been made at the Lamont Geochemical Laboratory. Ages have been obtained by the potassium-argon and rubidium-strontium methods, using muscovite, biotite, and microcline. Results will be reported in detail elsewhere and are consistent with an age of 2.7 ± 0.1 b.y. for the pegmatites and the granitization. Davis (1954, p. 105) gives a rubidium-strontium age of 3.0 ± 0.3 b.y. for lepidolite from Bridger Mountain, Bonneville, Wyoming. This result is in reasonable agreement with the preliminary age of the Christmas Lake muscovite.

Correlations are uncertain. The Stillwater complex is older than the dolerite dike swarm, and the writers correlate the complex tentatively with the metabasaltic dike swarm. Archean metasediments in the Boulder River area (quartzites and banded ironstones), intruded by the Stillwater complex, are correlated by K. P. Wilson (*in* Schafer, 1937, p. 23) with metasediments in the project area. Similar tentative correlations of Beartooth metasediments have been made with the Yankee Jim and Cherry Creek formations (E. W. Heinrich, 1956, personal communication). Heinrich regards all these metasediments as older than the Belt Formation for which recent determinations give uranium-lead ages of 1030 ± 290 m.y. (Eckelmann and Kulp, in press).

References Cited

Bowen, N. L., 1937, Recent high-temperature research on silicates and its significance in igneous geology: Am. Jour. Sci., 5th ser., v. 33, p. 1–21

—— 1948, The granite problem and the method of multiple prejudices: Geol. Soc. America Mem. 28, p. 79–90

Bowen, N. L., and Tuttle, O. F., 1949, The system MgO-SiO_2-H_2O: Geol. Soc. America Bull., v. 60, p. 439–460

Brögger, W. C., 1934, On several Archean rocks from the south coast of Norway. 2. The south Norwegian hyperites and their metamorphism: Norske Vidensk. Akad. Oslo, Skr., Mat.-naturv. Kl., v. 1, 421 p.

Bucher, W. H., 1956, Role of gravity in orogenesis: Geol. Soc. America Bull., v. 67, p. 1295–1318

Bucher, W. H., Chamberlin, R. T., and Thom, W. T., Jr., 1933, Results of structural research work in Beartooth-Bighorn region, Montana and Wyoming: Am. Assoc. Petroleum Geologists, Bull., v. 17, p. 680–693

Bucher, W. H., Thom, W. T., Jr., and Chamberlin, R. T., 1934, Geologic problems of the Beartooth-Bighorn region: Geol. Soc. America Bull., v. 45, p. 167–188

Chayes, Felix, 1956, Petrographic modal analysis: N. Y., John Wiley & Sons, Inc., 113 p.

Clarke, F. W., 1924, The data of geochemistry: U. S. Geol. Survey Bull. 770, 841 p.

Cloos, Ernst, and Cloos, Hans, 1934, Pre-Cambrian structure of the Beartooth, the Big Horn, and the Black Hills uplifts and its coincidence with Tertiary uplifting (Abstract): Geol. Soc. America Proc., 1933, p. 56

Compton, R. R., 1955, Trondhjemite batholith near Bidwell Bar, California: Geol. Soc. America Bull., v. 66, p. 9–44

Daly, R. A., 1909, First calcareous fossils and the evolution of the limestones: Geol. Soc. America Bull., v. 20, p. 153–170

Davis, G. L., 1954, Age of rocks, p. 104–106 *in* Abelson, P. H., Annual Report of the Director, Geophysical Laboratory; Carnegie Inst. Wash. Year Book 53, 50 p.

Eckelmann, F. D., and Kulp, J. L., 1956, The sedimentary origin and stratigraphic equivalence of the so-called Cranberry and Henderson granites in western North Carolina: Am. Jour. Sci., v. 254, p. 288–315

Eckelmann, W. R., and Kulp, J. L., 1957, The uranium-lead method of age determination. Part II: North American localities: Geol. Soc. America Bull., v. 68, p. 1117–1140

Engle, A. E. J., and Engel, C. G., 1951, Origin and evolution of hornblende-andesine amphibolites

and kindred facies (Abstract): Geol. Soc. America Bull., v. 62, p. 1435

Eskola, Pentti, 1914, On the petrology of the Orijärvi region in southwestern Finland: Comm. géol. Finlande Bull., no. 40, 277 p.

—— 1950, Orijärvi re-interpreted: Comm. géol. Finlande Bull., no. 150, p. 93–102

—— 1952, On the granulites of Lapland: Am. Jour. Sci., Bowen Volume, pt. 1, p. 133–171

Goodspeed, G. E., 1948, Xenoliths and skialiths: Am. Jour. Sci., v. 246, p. 515–525

Green, Jack, and Poldervaart, Arie, 1955, Some basaltic provinces: Geochim. Cosmochim. Acta, v. 7, p. 177–188

Gruner, J. W., 1946, The mineralogy and geology of the taconites and iron ores of the Mesabi Range, Minnesota: St. Paul, Minn., Iron Range Res. and Rehabilitation Comm., 127 p.

Hess, H. H., 1952, Orthopyroxenes of the Bushveld type, ion substitutions and changes in unit cell dimensions: Am. Jour. Sci., Bowen Volume, pt. 1, p. 173–187

James, H. L., 1955, Zones of regional metamorphism in the Precambrian of northern Michigan: Geol. Soc. America Bull., v. 66, p. 1455–1488

Knopf, Adolph, 1955, Bathyliths in time, p. 685–702 *in* Poldervaart, Arie, *Editor*, Crust of the earth: Geol. Soc. America Special Paper 62, 762 p.

Kulp, K. L., and Poldervaart, Arie, 1956, The metamorphic history of the Spruce Pine district: Am. Jour. Sci., v. 254, p. 393–403

Kuroda, Yoshimasu, 1956, On the Mg-Fe metasomatism in the Hitachi district, southern Abukuma plateau, northeastern Japan: Tokyo Kyoiku Daigaku Sci. Repts., sec. C, no. 44, p. 57–80

Lane, A. C., 1938, Report of the committee on the measurement of geologic time, 1937–1938: Wash., D. C., Natl. Res. Council, 123 p.

Lapadu-Hargues, Pierre, 1953, Sur la composition chimique moyenne des amphibolites: Soc. géol. France Bull., sér. 6, v. 3, p. 153–173

Larsson, Walter, 1932, Chemical analyses of Swedish rocks: Geol. Inst. Upsala Bull., v. 24, p. 47–196

Lovering, T. S., 1929, The New World or Cooke City mining district, Park County, Montana: U. S. Geol. Survey Bull. 811-A, 87 p.

Maxwell, J. A., 1953, Geochemical study of chert and related deposits (Abstract): Geol. Soc. America Bull., v. 64, p. 1452

Nanz, R. H., Jr., 1953, Chemical composition of pre-Cambrian slates with notes on the geochemical evolution of lutites: Jour. Geology, v. 61, p. 51–64

Perrin, René, 1954, Granitization, metamorphism and volcanism: Am. Jour. Sci., v. 252, p. 449–465

—— 1956, Granite again: Am. Jour. Sci., v. 254, p. 1–18

Poldervaart, Arie, 1950, Correlation of physical properties and chemical composition in the plagioclase, olivine, and orthopyroxene series: Am. Mineralogist, v. 35, p. 1067–1079

—— 1953, Metamorphism of basaltic rocks: A review: Geol. Soc. America Bull., v. 64, p. 259–274

—— 1955a, Zircons in rocks. 1. Sedimentary rocks: Am. Jour. Sci., v. 253, p. 433–461

—— 1955b, Chemistry of the earth's crust, p. 119–144 *in* Poldervaart, Arie, *Editor*, Crust of the earth: Geol. Soc. America, Special Paper 62, 762 p.

—— 1956, Zircon in rocks. 2. Igneous rocks: Am. Jour. Sci., v. 254, p. 521–554

Poldervaart, Arie, and Backström, J. W. von, 1949, A study of an area at Kakamas (Cape Province): Geol. Soc. South Africa Trans., v. 52, p. 433–495

Poldervaart, Arie, and Eckelmann, F. D., 1955, Growth phenomena in zircon of autochthonous granites: Geol. Soc. America Bull., v. 66, p. 947–948

Poldervaart, Arie, and Gilkey, A. K., 1954, On clouded plagioclase: Am. Mineralogist, v. 39, p. 75–91

Prider, R. T., 1940, Cordierite-anthophyllite rocks associated with spinel hypersthenites from Toodyay, Western Australia: Geol. Mag., v. 77, p. 364–382

Ramberg, Hans, 1949, The facies classification of rocks: A clue to the origin of quartzofeldspathic massifs and veins: Jour. Geology, v. 57, p. 18–54

—— 1952, The origin of metamorphic and metasomatic rocks: Chicago, Univ. Chicago Press, 317 p.

—— 1956, Pegmatites in West Greenland: Geol. Soc. America Bull., v. 67, p. 185–214

Read, H. H., 1948, A commentary on place in plutonism: Geol. Soc. London Quart. Jour., v. 104, p. 155–205

—— 1951, p. 297–298, Discussion of paper by Sutton, John, and Watson, Janet: The pre-Torridonian metamorphic history of the Loch Torridon and Scourie areas in the north-west Highlands, and its bearing on the chronological classification of the Lewisian: Geol. Soc. London Quart. Jour., v. 106, p. 241–296

—— 1952, Metamorphism and granitization: Geol. Soc. South Africa, A. L. du Toit Mem. Lecture no. 2, Annex. v. 54, 27 p.

Rouse, J. T., Hess, H. H., Foote, Freeman, Vhay, J. S., andWilson, K. P., 1937, Petrology, structure, and relation to tectonics of porphyry intrusions in the Beartooth Mountains, Montana: Jour. Geology, v. 45, p. 717–740

Schafer, P. A., 1937, Chromite deposits of Montana: Mont. Bur. Mines and Geology Mem. 18, 35 p.

Schairer, J. F., and Bowen, N. L., 1935, Preliminary report on equilibrium relations between feldspathoids, alkali feldspars, and silica: Am. Geophys. Union Trans., 16th ann. mtg., pt. 1, p. 325–328

Scholtz, D. L., 1947, On the younger pre-Cambrian granite plutons of the Cape Province: Geol. Soc. South Africa Proc., v. 49, p. 35–82

Sederholm, J. J., 1926, On migmatites and associated pre-Cambrian rocks of southwestern Finland. Part 2: Comm. géol. Finlande Bull., no. 77, 143 p.

Shaw, D. M., and Harrison, W. D., 1955, Determination of the mode of a metamorphic rock: Am. Mineralogist, v. 40, p. 614–623

Söhnge, P. G., and de Villiers, John, 1947, Resumé of the geology of the Richtersveld and the eastern Sperrgebiet: Geol. Soc. South Africa Trans., v. 49, p. 263–276

Stobbe, Helen, 1952, Porphyry intrusions in the Beartooth Range near Red Lodge, Montana

(Abstract): Geol. Soc. America Bull., v. 63, p. 1300

Thom, W. T., Jr., 1952, Tectonic team-research, key to social progress and world peace: N. Y. Acad. Sci. Trans., ser. 2, v. 14, p. 146–151

—— 1955, Wedge uplifts and their tectonic significance, p. 369–376 *in* Poldervaart, Arie, *Editor*, Crust of the earth: Geol. Soc. America Special Paper 62, 762 p.

Thornton, C. P., and Tuttle, O. F., 1956, Applications of the differentiation index to petrologic problems (Abstract): Geol. Soc. America Bull., v. 67, p. 1738–1739

Tilley, C. E., 1937, Anthophyllite-cordierite granulites of the Lizard: Geol. Mag., v. 74, p. 300–309

Tuominen, H. V., and Mikkola, Toivo, 1950, Metamorphic Mg-Fe enrichment in the Orijärvi region as related to folding: Comm. géol. Finlande Bull., no. 150, p. 67–92

Turekian, K. K., and Kulp, J. L., 1956, The geochemistry of strontium: Geochim. Cosmochim. Acta, v. 10, p. 245–296

Turner, F. J., and Verhoogen, Jean, 1951, Igneous and metamorphic petrology: N. Y., McGraw-Hill Book Co., Inc., 602 p.

Tuttle, O. F., and Bowen, N. L., 1953, Beginning of melting of some natural granites, p. 50, *in* Morey, G. W., Annual Report of the Director, Geophysical Laboratory: Carnegie Inst. Wash. Year Book 52, 57 p.

Tuttle, O. F., and Bowen, N. L., 1956, Some laboratory experiments bearing on the origin of granite (Abstract): 20th. Internat. Geol. Congress, Mexico, Resumé, p. 203

Vaasjoki, Oke, 1953, On migmatites and ore mineralizations in the Pernaja district, southern Finland: Comm. géol. Finlande Bull., no. 163, 62 p.

Wegmann, C. E., and Kranck, E. H., 1931, Beiträge zur Kenntnis der Svecofenniden in Finnland: Comm. géol. Finlande Bull., no. 89, 107 p.

Yoder, H. S., Jr., 1952, The MgO-Al_2O_3-SiO_2-H_2O system and the related metamorphic facies: Am. Jour. Sci., Bowen volume, pt. 1, p. 569–627

—— 1955, Role of water in metamorphism, p. 505–524 *in* Poldervaart, Arie, *Editor*, Crust of the earth: Geol. Soc. America Special Paper 62, 762 p.

Yoder, H. S., Jr., and Eugster, H. P., 1955, Synthetic and natural muscovites: Geochim. Cosmochim. Acta, v. 8, p, 225–280

Department of Geology, Columbia University, New York 27, N. Y.

Manuscript Received by the Secretary of the Society, January 15, 1957

BULLETIN OF THE GEOLOGICAL SOCIETY OF AMERICA
VOL. 68, PP. 1263–1292, 15 FIGS., 1 PL. OCTOBER 1957

WEATHERING OF GRANITE AND ASSOCIATED EROSIONAL FEATURES IN HONG KONG

BY BRYAN P. RUXTON AND LEONARD BERRY

ABSTRACT

The granite in Hong Kong is frequently weathered to a depth of more than 60 m (200 feet). The soil (or A and B horizons of pedology) is only a few feet thick. The very thick C horizon is considered as the weathering profile and is divided into four zones roughly parallel to the surface. Division is based on the percentage of solid rock and the character of the residual debris.

Local variations in the weathering profiles are due to conditions of slope, subsurface water, vegetation, structure, and type of granite. Widespread modifications are the result of a varied climatic and geomorphological history.

At Lai Chi Kok a wave-cut platform truncates a complete weathering profile. A Han tomb, discovered in the terrace, provides evidence of considerable subsurface eluviation in the upper weathering zone. Eluviation is shown to be important in the differentiation of local weathering debris and may give rise to a well-sorted residue.

Studies in three areas show that thick, complete profiles were formed on gently sloping surfaces and are now variably dissected. Adjustment to structure has taken place within the weathering profiles in a small vertical range of denudation. Large pockets of core stones in residual debris of the upper zones are explained as abandoned portions of the weathering profile.

Most gullying in Hong Kong occurs on slopes from 10°–40° in the region of deep weathering. It is due to instabilities in the upper weathering zones after partial dissection and deforestation. Surface erosion bares the subsoil to drying winds, which with partial eluviacion from available free faces causes a contraction of the debris. Deep cracks are formed, and accelerated eluviation aided by storm runoff develops these into gullies.

CONTENTS

TEXT

	Page
Introduction	1264
Study of weathering	1264
Geological background	1264
Topography	1266
Acknowledgments	1267
Granite weathering profiles in Hong Kong	1267
Soil and weathering profiles	1267
Typical vertical section	1267
Breakdown of granite	1267
Details of profile	1268
Bedrock	1268
Zone IV	1268
Zone III	1269
Zone II	1269
Zone I	1269
Core stones	1269
Discussion	1270
Confirmation from previous work	1270
Effect of eluviation and leaching	1270
Mass movement as a factor in depth of profiles	1272
Form of profiles	1272
Development sequence	1272
Lateral variations—the slope profile	1273
Lateral variations—resistance to weathering	1273
Subsurface water and structure	1274
Climate and vegetation	1275
Geomorphic history	1276
Studies at Lai Chi Kok	1276
Description of terrace	1276
Weathering profile on terrace	1276
Terrace sediments	1277
Eluviation and the tomb	1280
Surface lowering due to eluviation	1281
Three contrasted areas	1281
Choice of areas	1281
Tai Lam area	1282
Description of area	1282
Northwest of Tai Lam valley	1282
East of Tai Lam Chung	1282
Northwest of Castle Peak	1282
Harbor area	1283
Past climates and age of weathering	1285
Climatic considerations	1285
Age of weathering	1285
Erosion features associated with weathering profiles	1286

Erosion processes 1286
Older dissection of profiles 1286
Deforestation 1286
Effects of deforestation 1286
Removal of topsoil 1286
Gullying: characteristics of Hong Kong gullies 1287
Mechanism of gully formation 1287
Importance of eluviation 1287
Further development 1288
Aggradation 1289
Discussion 1289
Conclusion 1290
References cited 1290

ILLUSTRATIONS

Figure Page
1. Location map showing the granite cupolas and drainage in the area 1265
2. Zones of a mature profile of weathering on granite 1266
3. Radially concentric profile of weathering about a core stone 1269
4. Main variations of weathering in core stones 1270
5. Cumulative percentage curves of weathering products 1271
6. Development sequence of weathering profiles on gentle slopes on granite in Hong Kong 1272
7. Types of weathering profile on slopes on granite in Hong Kong 1273
8. Weathering profile on a concave slope on granite in Hong Kong 1274
9. Weathering profile on a concave-convex slope on granite in Hong Kong 1274
10. Sections of terrace in Lai Chi Kok bay 1277
11. Perspective sketch of the tomb at Li Cheng Uk showing the distribution of the sandy clay within 1281
12. Section northeastward about 200 m northwest of the main through valley at Tai Lam 1283
13. Location of land bores on the Kowloon Peninsula 1284
14. Log of land bores on Kowloon Peninsula 1285
15. Sketch section drawn to natural proportions southeastward across the low hills around Tai Lam 1289

Plate Facing Page
1. Erosional features on weathered granite 1286

TABLES

Table Page
1. Summary of the properties of rocks of the terrace 1278
2. Grade size distribution of weathering products 1281

INTRODUCTION

Study of Weathering

Hong Kong lies just within the tropics and has a South China monsoonal climate with a cool dry winter and a hot humid summer; the annual rainfall is about 84 inches. These conditions are favorable for the development of thick weathering profiles and local granitic rocks are particularly susceptible. As Kingsmill (1862, p. 2) noted:

> "This granite wherever it occurs, has been deeply disintegrated, sometimes to a depth of one or two hundred feet; whilst everywhere, imbedded in the soft yielding matrix, there occur nodules of a more quartzose character, which have resisted the effects of time and chemical change. These masses are usually of a lozenge shape, and vary in size from a few feet to several hundred .... In the higher ground the soft yielding matrix has generally been removed by denudation, leaving these pseudo boulders perched all over the granitic hills, ..."

Between 1923 and 1933 Dr. Brock collected a wide range of weathered samples for study, but unfortunately he died in 1935 before the completion of his work. Some of his results were published (1943), and these show that the changes of chemical weathering operating in this district are similar to those noted elsewhere though the mineral changes were not readily diagnosed.

The present paper represents a field study of the local weathering of granite and its erosional features. No local facilities have been available for carrying out X-ray work, differential thermal analysis, or detailed mineralogical work. Ruxton has concentrated on the weathering profiles and Berry on the erosional features, but both authors have co-operated closely on the whole paper.

In field work during the last 2 years the authors were able to inspect abundant sections in gullies, rejuvenated stream courses, and coastal cliffs. Also the tremendous amount of excavation which is necessary in an area of about 18 square miles containing more than 2 million people provides numerous exposures. On the Kowloon peninsula, a great lane is being cut through the hills to provide an air approach, and the residual debris of the upper weathering zones is being used to reclaim land for a runway 2500 m into the harbor. Hills are removed; the residual debris is used for reclamation and the core stones for facing.

Geological Background

The large granite batholith on the southeast coast of China stretches southwestward for

FIGURE 1.—LOCATION MAP SHOWING THE GRANITE CUPOLAS AND DRAINAGE IN THE AREA

Contours are at 250, 500, and 750 m. Barbs on boundaries point to granite areas. For clarity grid lines are drawn for every five grid units only. Four figure references are given in the text.

more than 800 miles from Ningpo to Hainan. It apparently forms a belt of hills 12–30 miles wide, which range in height from 100 to 1000 m. Deep weathering and gullying are common phenomena over much of this region, and the occurrence in Hong Kong is in many ways representative.

granite batholith, and discontinuous patches have been left sandwiched between the exposed cupolas. In some places these form central depressions ringed by mountains of which the Hong Kong harbor is the best example. In the extreme northeast is a series of red breccia beds that appear to be typical

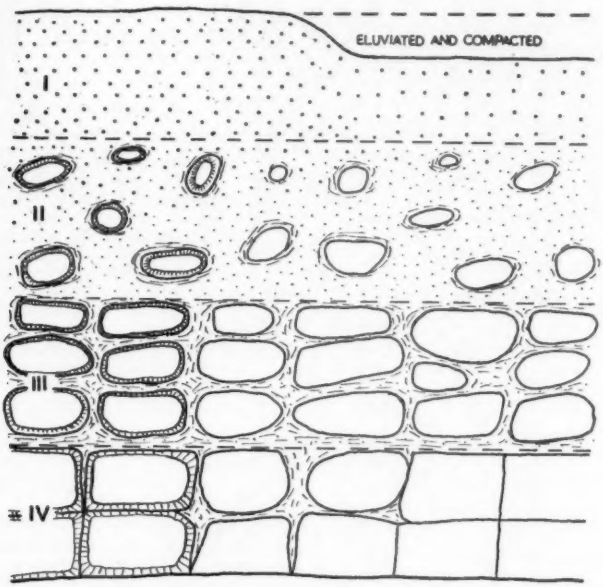

FIGURE 2.—ZONES OF A MATURE PROFILE OF WEATHERING ON GRANITE
The iron staining inside the core stones is shown only on the left-hand side.

A recent paper (Ruxton, 1956) shows that in Hong Kong upper Paleozoic and Lower Jurassic marine and deltaic sediments and Upper Jurassic acid volcanic rocks were intruded by quartz porphyry sheets. These rocks were then injected by a large granite batholith, cupolas of which form about one-third of the area of the Colony (Fig. 1). The intrusion of this granite, believed to be Cretaceous, was followed by acid and basic dike swarms. Later continental red beds, full of derived volcanic fragments, were laid down in the northeast of the Colony and are affected by thrusting, folding, and faulting, probably of mid-Teritary age. These movements laid the foundation of the present geomorphic framework. Since this time most of the "Red Beds" and much of the acid volcanic and older sedimentary rocks have been eroded from the fanglomerates. Owing to their undisturbed state and position they are thought to be a product of a land form similar in outline to that of today and have been placed tentatively as late Tertiary.

Topography

The Hong Kong region consists of a drowned, submaturely dissected landscape, with numerous rias, and a profusion of offshore islands. The earlier stages of the development of the local land form have not yet been worked out. Some accordance of summit heights points to possible earlier uncompleted cycles, though these cannot be readily related to erosion cycles of other areas in South China. W. Schofield (1942, p. 102) pointed out that hard felsite summits are generally in accordance at about 700 m,

whereas the upper granitic surfaces reach to just over 400 m (All heights refer to principal datum H. K.). At lower levels a well-marked surface of low relief between 200 and 250 m appears to mark a subaerial stage. Recent studies have shown that the topography below 70 m shows a marked stepped pattern which is probably related to marine erosion at various levels in the Pleistocene Epoch (Berry and Ruxton, 1957).

Acknowledgments

Acknowledgments are gratefully made to the Research Grants Committee of the University of Hong Kong for financial assistance; to Mr. P. Lumb for mechanical analyses of seven samples of debris; to Scott and Wilson, Kirkpatrick and Partners for allowing free access to all their valuable information on the excavations in the Kowloon hills; and to Prof. F. S. Drake for allowing use of the information on the Li Cheng Uk tomb and for advice on archeological matters.

Granite Weathering Profiles in Hong Kong

Soil and Weathering Profiles

Much of the granite in Hong Kong is weathered to depths of more than 30 m. Under these conditions the A and B soil horizons are only a superficial feature, and practically all the residual mantle would be considered as the C horizon by pedologists. Since local weathering profiles are so thick it is necessary to set up a classification based on numerous sections seen in the field (Leighton and MacClintock, 1930).

The weathering profile is the expression of the sequence of changes necessary to bring the fresh bedrock into equilibrium with the near-surface environment. A soil profile, however, is considered as a modification of any part of the weathering profile which occurs near, or at, the ground surface.

Typical Vertical Section

Some of the excavations in the weathered granite in Hong Kong reveal a typical vertical section, somewhat generalized in Figure 2. The most striking feature of these sections is the mixture of solid rock and residual debris throughout most of their vertical range. The solid rock is in the form of core stones (Linton, 1955, p. 472, after core boulders of Scrivenor, 1931, p. 136–138) and the ratio of solid rock to residual debris gradually decreases from the base upward. There is thus a complete gradation from unweathered massive rock at the base to the residual debris at the top.

For the purpose of field description the sections are arbitrarily divided into four zones based on the percentage of solid rock, as follows:

Field occurrence	Character	Percentage of solid rock	Zone
Soil	dark-colored; up to a few feet thick; upper layer sandy and lower layer clayey		A and B horizons of pedologists
Residual debris	structureless sand clay or clayey sand	usually 0 per cent	I
Residual debris with core stones	core stones subordinate, rounded and free	less than 50 per cent	II
Core stones with residual debris	core stones dominant rectangular and locked	50–90 per cent	III
Partially weathered rock	minor residual debris along major structural planes, but may be considerably iron-stained	greater than 90 per cent	IV

Zone numbers are given in Roman numerals because no correlation with letters used by pedologists or Arabic numerals used by some geologists is intended.

Before describing each zone in detail it is first necessary to consider the changes that take place during the weathering of granite.

Breakdown of Granite

The granite, owing to its coarse grain and four main minerals, undergoes changes during weathering the effects of which can be readily observed in the field. Thus biotite commences to decompose first in the solid rock and is followed by plagioclase. When part of the plagioclase has decomposed and the orthoclase is beginning to be attacked, the rock breaks down to platy fragments of decomposed granite called gruss. Plagioclase completes its decomposition first, and when most of the ortho-

clase has been rotted to kaolin, the gruss crumbles into a silty sand. Greasy yellow flakes of mica persist in this residual debris and may outlast the orthoclase. Apart from some disaggregation the quartz appears to remain unchanged.

The most striking type of rock breakdown noted in local sections is that due to spheroidal weathering. Chemical action penetrating inward from the structural surfaces results in the formation of core stones which recline in a matrix of residual debris. Since there is every gradation from fresh rock inside the core stone to completely decomposed granite outside, zones of change become radially concentric about loci of unweathered granite. These changes can be readily summarized in two sets of four roughly parallel stages as follows:

Chemico-mineralogical change	Effect	Symbol
Reddening and argillization[1]	Formation of reddish-brown silt and clay	D
Complete decomposition of feldspars and biotite	Formation of light-colored kaolinitic debris	C
Partial decomposition of feldspars and biotite	Formation of gruss	B
Partial decomposition of biotite	Formation of brown margin to joint blocks and core stones	A
State of physical disintegration	**Cause**	**Symbol**
Differentiated debris	Further disaggregation, illuviation or eluviation	Z
Residual debris	Disintegration and disaggregation	Y
Gruss	Spheroidal scaling	X
Core stones	Penetration of weathering agents inward normal to the open structural surfaces	W

The relation of these stages to the radial weathering profile about a fresh core stone and to one another is shown in Figure 3, and two intermediate stages are inserted.

Each core stone in a weathering section has a radial weathering profile around it. Near the base of the section this profile is only partially developed, and it becomes more complete upward. Thus there is a gradual vertical change in the character of the residual debris.

The four zones of weathering are distinguishable not only by the percentage of solid rock in the debris but also by the relative development of the different stages of the radial weathering profile. The properties of these four zones, excluding soil and fresh bedrock, are summarized as follows:

Zone	Weathering stages present	Characteristics
I	D, (c, b, a); Z, (y, x, w)	D–Z, core stones generally absent
II	C, B, A (d); Y, X, W, z	C–Y, core stones generally common
III	B, A, c; X, W, y(z)	B–X, dominant core stones
IV	A, b, or a, b; x	Partially weathered massive jointed rock

Capitals indicate normal presence, small letters minor amounts only, and parentheses are used to emphasise rarity of occurrence.

Details of Profile

Bedrock.—The fresh unweathered granite is normally a medium-grained (1–5 mm) *very light-gray*[2] hololeucocratic rock with a xenomorphic granular texture. It is typically a calc-alkali biotite granite (for analyses *see* Brock, 1943, p. 720), though in places its mode shows it to be an adamellite. Masses of coarse-grained and porphyritic types occur locally, and near contacts the rock is typically fine-grained and often muscovitic. Two sets of vertical joints, roughly at right angles to one another, are almost universally present, and a variably developed sheet jointing subparallel to the surface is often observed. The joint spacing ranges from 0.5 to 12 m (1–40 feet). The granite is also affected in places by shear and shatter belts, more common in the west, and by local dike intrusion.

Zone IV.—Zone IV varies in thickness from only 3 m in places to more than 30 m in others. Any residual debris is negligible (less than 10 per cent), but the rock may nevertheless be much affected. In some instances more than 50 per cent of it is iron-stained and indicates that some of the biotite has been partly altered. Thus significant chemical decomposition is

[1] Argillization here refers to a marked increase of the clay-size fraction; it is uncertain what mineralogical and chemical changes are involved.

[2] Colors given in italics have been checked against the Rock Color Chart (National Research Council, 1948)

effected before the rock breaks down from its massive state. This partly weathered bedrock is often seen in its natural setting on actively developing sea cliffs, in deeply incised rejuvenated stream valleys, and on some steep derivation slopes.

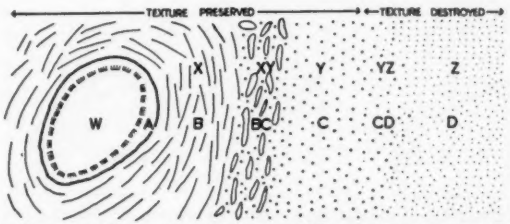

FIGURE 3.—RADIALLY CONCENTRIC PROFILE OF WEATHERING ABOUT A CORE STONE

As seen at Li Cheng Uk. The thickness of each stage is diagrammatic. This sequence may be almost completely developed in any direction around the core stone.

Zone III.—This zone ranges in thickness from about 7 to 17 m and is easily recognized by the dominance of core stones and their rectangular or angular shape. Most of the comminuted material is gruss and subordinate residual debris; the later in most places retains some visible orthoclase and biotite. This zone is commonly seen on some boulder-strewn slopes and near the oversteepened coasts, and exerts a prominent influence on the erosional development.

Zone II.—Zone II is the most variable part of the weathering profile. It often contains roughly equal amounts of core stones, gruss, and residual debris; occasionally core stones and gruss are rare or absent. Apart from the disappearance of orthoclase and biotite, the zone may in places lose its granitic texture. It attains great thicknesses in some places more than 60 m (200 feet) and covers large areas at the surface, mostly associated with moderate-angled, boulder-strewn or sheet-eroded slopes.

The most characteristic feature of Zone II, apart from its light color and preservation of texture, is the paucity of clay-size grains, (seldom more than 5 per cent) yet the material contains abundant clay minerals; these are dominantly sericite and kaolin. It is often useful to subdivide this zone into two parts. Where core stones are rare (less than 10 per cent) it is named Zone IIa. This subzone is in some places highly kaolinitic and forms a useful economic deposit. Where core stones are between 10 and 50 per cent it is called Zone IIb.

Zone I.—Zone I ranges in thickness from 1 to 25 m. It is in most places a structureless mass of reddish-brown clayey sand and is notable for its variability in grade-size distribution which is due both to the nature of the parent granite and to eluviation (the washing out of fine particles by circulating water). It can contain as much as 30 per cent clay-size material (less than 0.005 mm) and consists dominantly of quartz and kaolin. In general the color seems to vary in relation to the amount of clay present. Thus when very clayey it is a *moderate reddish brown*, and changes to a *light brown* or *pale yellowish orange* as the clay content decreases.

The base of Zone I bears a closer relationship to the ground surface than any other part of the profile. In many places in the Colony it represents the upper portion of a polygenetic profile.

A notable mottled area often occurs between Zones I and II, and is considered to be a lower subdivision of Zone I (Ib). It may be as much as 10 m thick and consists of a continuum of *reddish-brown* clayey sand (I) enclosing and penetrating (and presumably replacing) a lighter-colored silty sand (II). This mottled zone corresponds to the "piebald" "patchy" lithomarge described from Malabar and Kanara (Fox, 1935–1936, p. 398) and was there termed lithomargic laterite. The latter was found overlying normal lithomarge (a quartziferous kaolin) with the texture preserved, and underlying a more completely reddened horizon (Fox, 1935–1936, Pl. 31, fig. 2). Unfortunately, we cannot use the same terminology in our occurrences because the few analyses we have (Brock, 1943) are very different from those quoted by Fox.

Core stones.—The core stones occurring in these zones are of three main types (Fig. 4). The commonest are those with a margin of iron-stained granite bordering a fresh interior. Sometimes specimens with more than one such zone of staining occur, and in some instances

there is a succession of four or five concentric units affecting almost the whole core stone. Only the outer zone is accompanied by a marked mechanical breakdown of minerals in the granite.

An abnormal type from the Kowloon hills is of interest. The outer rim of the core stone shows normal iron staining and attendant breakdown of minerals. Next to this is a thin concentric zone of unstained granite whereas the interior is completely, though faintly, iron-stained a *very pale yellowish orange* which increases in intensity to a maximum against the unstained granite.

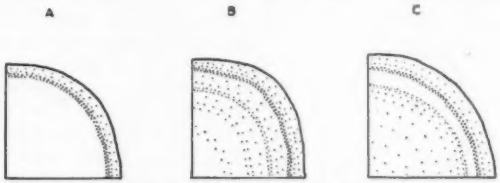

FIGURE 4.—MAIN VARIATIONS OF WEATHERING IN CORE STONES
Intensity of dots indicates the intensity of staining; blank areas are unstained. A. Commonest and simplest type B. Fairly common rhythmically stained rock C. Abnormal type from Kowloon Hills.

A specimen of biotite granite taken from the center of a core stone of type A (Fig. 4) showed the biotite completely altered to chlorite with some epidote and iron ore. Also apparently unweathered specimens of granite collected from other core stones often show a bleaching of the brown biotite to rich green tones with release of iron ore and the formation of chlorite.

Owing to the virtual absence of iron ore in this hololeucocratic rock the iron staining has been derived almost entirely from the biotite. In many core stones the greenish-black biotite is margined by a *moderate-brown* rim .5–1 mm thick.

The abnormal core stones from Kowloon are confined to within about 17 m of the surface and occur in an abandoned portion of the weathering profile where active weathering has become a somewhat intermittent process. Some abnormal core stones are 2.5 m in diameter. At about 1 m in diameter all core stones break up throughout by granular disintegration. Few are less than this size.

Discussion

Confirmation from previous work.—Henry and Grace (1948) in a study of decomposed granite near Ping Shan, New Territories, classified the residual debris into type A and type B on the basis of their content of fine material. Type A had as much as 25 per cent passing B. S. Sieve No. 200, and type B 30–40 per cent (Fig. 5C). Type A was a pink, gritty, friable material, in which texture was preserved, and corresponded to our Zone II. Type B was made up of quartz grains and clay and was harder and less friable. It corresponds to our Zone I.

Index tests on 16 samples showed that: ". . . The liquid limit varied between 33 and 500 and the plastic limit between 18 and 33. The upper limits for both of these were astonishingly high for comparatively friable material of this type." The high readings on type B may have been due to the presence of colloidal material. Type A was suitable for stabilization work, whereas type B could be used only in the lower base courses.

Effect of eluviation and leaching.—In the early stages of weathering expansion due to partial decomposition of the feldspars and biotite, causes spheroidal scaling. Leaching, however, which is active in the solid rock, becomes more important in the gruss and residual debris and is responsible for the removal of large quantities of material. In the later stages leaching and eluviation may be so strong that either the material becomes highly porous or it contracts and loses its granitic texture. A measure of this loss may be obtained by studying the percentage of quartz. During mechanical analysis, it was noticed that the gravel and sand grades of Zone I represent approximately the quartz content. In the non-eluviated sandy clay from Li Cheng Uk (Fig. 5) quartz makes up 53 per cent by weight of the residual debris. The original rock contained about 36 per cent quartz, so that at least one-third of the original granite appears to have been leached out. This fraction may for the most part represent the plagioclase which is the first mineral to decompose completely.

The average Zone I material in the Colony

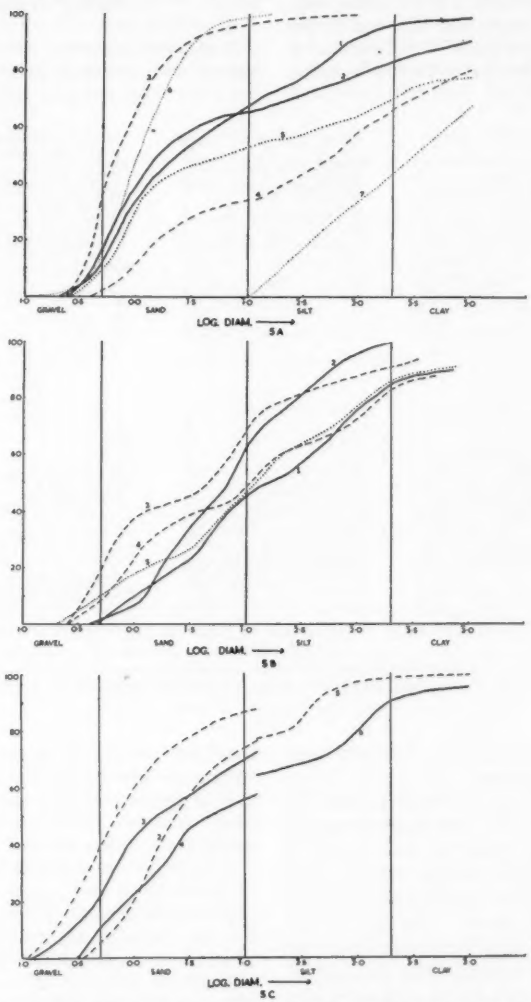

FIGURE 5.—CUMULATIVE PERCENTAGE CURVES OF WEATHERING PRODUCTS

A. Li Cheng Uk. 1. ×× 16, Zone II; 2. ×× 5, plus ×× 8 divided by 2; 3. ×× 5, Zone I outside the tomb; 4. ×× 8, Zone I inside the tomb; 5. ×× 18, Zone I probably non-eluviated; 6. ×× 25, well-stratified sediment from between clay layers; 7. Red silty clay washed out from Zone I.

B. Northwest of Castle Peak. 1. ×× 35, Zone I; 2. ×× 36, Zone II 5 yards from sample ×× 35; Tai Lam 3;. Zone I from intensely gullied area; 4. Slope wash from Zone I near sample 3; 5. Typical sample of Zone I used in earth dams.

C. Near Ping Shan (Modified from Henry and Grace, 1948). 1. Limit of coarse grading (Zone II). Nine samples from six different localities; 2. Limit of fine grading (Zone II). Nine samples from six different localities; 3. Limit of coarse grading (Zone I). Eight samples from four different localities; 4. Limit of fine grading (Zone I). Eight samples from four different localities; 5. Hydrometer analysis (Zone II). average of two tests; 6. Hydrometer analysis (Zone I). average of two tests.

(13 samples) contains about 15 per cent gravel, 45 per cent sand, 28 per cent silt, and 12 per cent clay; nearly two-thirds of the material is quartz. Thus a further loss of 10–15 per cent of the original granite has occurred for the most part owing to eluviation.

With a fresh specimen of granite it should be possible to predict the approximate grade size distribution of the resulting Zone I and II material and also to indicate the probable limits of variation due to eluviation. In both cases the important factor is the amount and grain size of the quartz in the rock. Figure 5*A* illustrates the differentiation from the weathering of granite at Li Cheng Uk, compared with further changes produced by local erosion and transportation (Table 2).

Mass movement as a factor in depth of profiles.—A regular and consistent arrangement of core stones in Zone III indicates little, if any, mass movement. In Zone II mass movements are more likely but have not yet been detected, whereas in Zone I diagnosis is not possible because of lack of texture. Any surface addition by slope wash is, however, easily recognizable by its clear stratification.

Form of Profiles

Development sequence.—Whereas geomorphic history and erosional position are over-all modifying and guiding factors in the development of weathering profiles, the specific controls in any one locality are time, degree of slope, subsurface water regime, climate, vegetation, and the structure and type of rock.

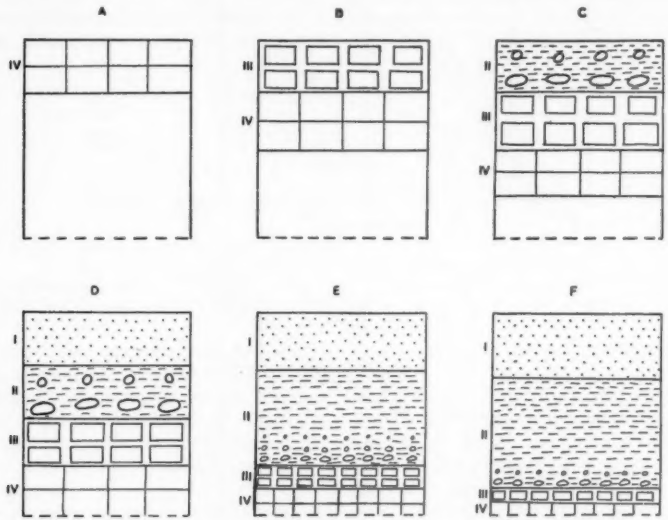

FIGURE 6.—DEVELOPMENT SEQUENCE OF WEATHERING PROFILES ON GENTLE SLOPES ON GRANITE IN HONG KONG

The stages depicted are a function of time. *A* and *B*—youthful; *C*—early maturity; *D*—maturity; *E*—late maturity; *F*—old age. The dashed line at the bottom of the figures indicates the limit of normal weathering.

With time there is a successive development of all four zones and a concomitant deepening of the profile (Fig. 6). The early stages of this sequence may be designated youthful, and when all zones are present and under active development maturity has been reached (Fig. 6*D*). At this stage the base of the profile is probably nearing the maximum depth attainable by active weathering and is limited either by the water table, by the lack of open structural surfaces, or by the ineffectiveness of agents to penetrate further. Thus a mature profile is one which has become relatively stabilized in form in relation time (Jenny, 1950, p. 45).

Further development will be slower and will merely increase the proportion of highly weathered material in the profile (Penck, 1953,

p. 51). Zones I and II will continue to develop at the expense of III and IV until the latter pair are very thin. Zone II normally becomes very thick. The core stones become smaller and sometimes disappear from the upper parts and core stones which sometimes migrate to form rock streams. During migration they break up into angular boulders with one curved face.

On concave slopes complete profiles are found near the base, whereas upslope succes-

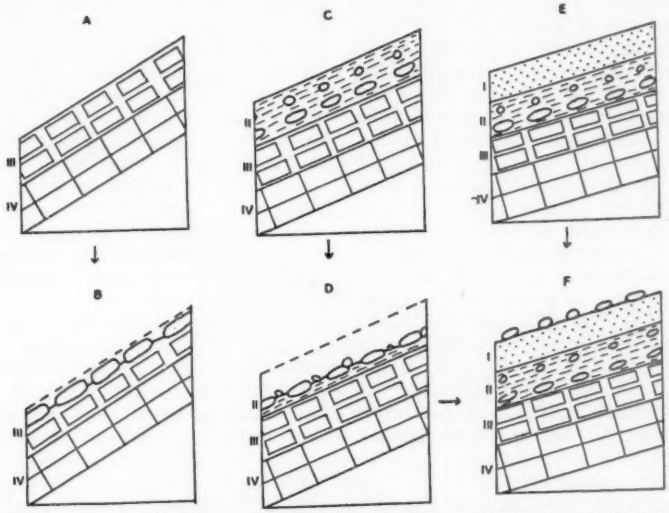

FIGURE 7.—TYPES OF WEATHERING PROFILE SEEN ON SLOPES ON GRANITE IN HONG KONG
Arrows indicate possible developmental stages. *A* and *B* slope at 30°; *C* and *D* at 22.5°; and *E* and *F* at 15°. *F* may be developed from *E* by migration of core stones from gravity slopes above, or from *D* by renewed intensity of weathering and the abandonment of the upper portions of the profile.

eventually from the greater part of it. These later stages may be called old age. From maturity onward the profile is complete and all four zones are present.

An incomplete profile is one in which one or more of the upper zones is missing. There are three types of incomplete profile: profiles truncated by erosion, partially developed profiles, and complex profiles. For example, on a steep slope, soil and an immature Zone I may rest on Zone III or IV.

Lateral variations—the slope profile.—The development outlined above normally occurs on slopes less than about 15°. On steeper slopes the effects of creep, slump, and slope wash become important, and downhill migration of the surface material may occur at the inception of any of the upper three zones depending mainly on the angle of slope and vegetation covering (Fig. 7). On a steep slope mass sliding or removal of debris from Zone III results in a surface littered with rectangular core stones. On lower gradients Zone II produces rounded sively lower zones reach the surface (Fig. 8; Penck, 1953, p. 71). In many cases the decreasing thickness of the upper zones on steeper slopes is compensated by an increase in the thickness of the lower part of the profile. This is also illustrated on some hills with a concavo-convex form; thickest profiles often occur beneath the hilltops (Fig. 9). If erosion proceeds more rapidly than weathering, core stones are released from Zone II and may migrate downslope onto Zone I (Fig. 7*F*).

Lateral variations—resistance to weathering.—The different types of granite have a varying resistance to weathering and erosion, and the sequence from least to most resistant is as follows: coarse porphyritic granite, coarse-grained granite, medium-grained granite, fine-grained granite, granite porphyry dykes.

On northern and central Lantau Island, where abundant and large granite porphyry dikes transect the medium-grained and porphyritic granite, the high zones of weathered granite are closely juxtaposed against lower

zones of weathered granite porphyry. In many places differential erosion and migration of the finer material has resulted in a related ridge and valley topography.

directly related both to the lateral variations in the weathering profiles and to the relative resistance to weathering of the bedrock. Superficial adjustment to structure, so well developed

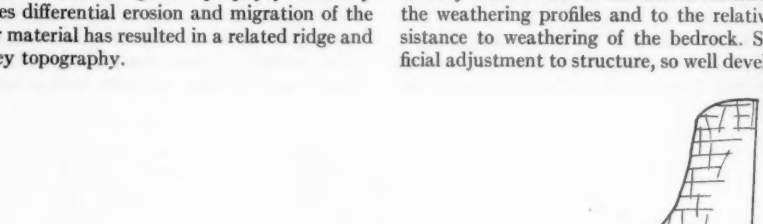

FIGURE 8.—WEATHERING PROFILE ON A CONCAVE SLOPE ON GRANITE IN HONG KONG

FIGURE 9.—WEATHERING PROFILE ON A CONCAVE-CONVEX SLOPE ON GRANITE IN HONG KONG

Generally the spacing of joints increases with the coarseness of the granite, but the post-granite earth movements have in places partly offset these original differences. The porosity also increases with grain size, and this is a very important factor in the rate of weathering. In the granite porphyry dikes the extent and amount of spheroidal weathering is related to the grain size of the groundmass and is greatest in the coarsest central portion of the dikes, despite the fact that the joint spacing increases markedly toward their centers.

An important feature of thick weathering profiles is the loss of material from them by subsurface erosion. If leaching and eluviation removes more than 30 per cent of the material from the upper zones the surface may become locally depressed and uneven. Deep weathering profiles on a flat or gently sloping surface may develop surface and near-surface irregularities in this Colony, has to a great extent originated within the weathering mantle.

Subsurface water and structure.—In any rock mass of given susceptibility weathering is most intense and most rapid where its agents are most concentrated for the longest time. This is a fundamental principle which is of the greatest importance in the study of our local profiles.

The agents of chemical weathering are gas (carbon dioxide and oxygen) and water (often with organic and other acids), and they act effectively only together. Subsurface water containing, or in association with, atmospheric gases is then the prime cause of chemical weathering.

Since the gases originate from near and above the ground surface the weathering processes in most places commence near the surface and work inward, generally normal to the surface. At the commencement of the development of a

weathering profile the rate and intensity of weathering processes decreases with depth below the surface as the gases are gradually exhausted.

In the youthful stages of the weathering of granite the complex of joint and fracture planes (inner surface of Penck) form interconnecting or isolated networks and so produce a host of local water levels. Irregularities in the water circulation at this stage possibly cause certain masses of rock to remain relatively untouched well into the later stages of development. In some localities pockets of large core stones can be found abandoned in the upper parts of Zone II in an old-age profile.

Once the inner surface becomes an integrated network of channels the relative concentration of inner surfaces and the porosity of the rock will to a large extent control the rate of weathering. Variations in these properties will cause further lateral variations in the profiles (Linton, 1955, joint spacing and tors).

When a complete profile is developed a water table can be recognized, and weathering assumes a definite pattern. Core stones on the surface are moist for only short periods, whereas those in the zone of aeration are moist for a much longer time particularly in Zone I where a thick vegetation cover is present. Thus core stones on the surface are only slightly attacked, whereas those below are intensely attacked. On the crest of some hilltops and spurs granite core stones are resting on Zone I debris containing no core stones (Fig. 7 *F*) and to explain this the principle outlined above was invoked. A partially developed weathering profile has undergone slight erosion exposing core stones on the surface. Renewed weathering has partially abandoned the ground surface and is rapidly developing the subsurface portion of the profile.

The most active weathering is believed to take place within the vadose zone where gas and moisture mix most freely. As the water table fluctuates throughout the year the vadose zone is restricted or expands accordingly, and very active weathering takes place from near the surface down to the lowest level attained by the water table.

Weathering is thought to be slight below the lowest level of the water table in complete granite profiles, partly because most of the gas supply will have been exhausted before it reaches this depth. Further, at this depth interconnections for circulation will be few and, unless there is vigorous circulation, any gas present would soon be used up. Finally, the water table is only at this low level for very limited periods, and at other times weathering below the higher water tables would probably be inside the seasonal limits of the vadose zone.

The lowest level of the water table acts as a base level in the normal processes of weathering (Penck, 1953, p. 61; Linton, 1955, p. 574). Linton recognizes a basal platform at this level, and many local sections indicate a definite lower limit to active weathering which is sometimes marked by a rapid change to fresh bedrock.

There are at least three explanations to account for the presence of weathered material below the lowest water table which do not alter the general rule. In the first place irregularities in the youthful stage may have caused deep weathering before an integrated water circulation was established. Secondly, any prominent fracture lines and shatter belts will attract a rapid flow of water which may retain considerable quantities of gas when it reaches the zone of saturation and so cause a local deepening of the profile. Thirdly, the level of the water table may have altered since the original development of the profile.

The average depth of the water table will also affect the rate of development of the profile. If there is a thick vadose zone then a long time may be needed to produce a mature profile. A thin vadose zone however, would cause a concentration of weathering activity, and a mature profile would be expected to develop rapidly perhaps with a well-marked basal surface.

Climate and vegetation.—Apart from their effects on the rate of weathering the factors of humidity, rainfall, and vegetation may determine the type of profile particularly on slopes. An increase in humidity, rainfall, and temperature which tends to thicken the vegetational cover, causes a stabilization of the lower-angled gravity slope, and converts it into wash slopes thus allowing a fuller development of the upper zones; moreover, the water table tends to be fairly high and regular, and the weathering agents work at a rapid rate in a highly concentrated area.

On the other hand, a decrease of humidity, rainfall, and vegetation causes a fluctuating water table whose lowest level is much lower than before, and weathering agents work more slowly in a more dispersed vadose zone. The upper weathering zone particularly on the hilltops is partially abandoned in the dry periods, and when excessive rainfall temporarily

raises the water table to a high level, marked eluviation of the finer particles occur and differentiates the debris.

Geomorphic history.—Apart from the alterations to the weathering profiles considered above more drastic changes can occur. Thus an almost complete arrest of development is assumed to take place if the profile is submerged beneath the sea or below the permanent water table. Again the profile may be truncated by erosion. Later, owing to a return of favorable conditions a revival of these primary profiles takes place, and secondary profiles develop. If these are merely an extension of an earlier profile their secondary nature would be obscured. If they transect the primary profile obliquely then their secondary nature becomes apparent. Nearly all the changes outlined above affect the upper weathering zones first, and these are the most sensitive to small changes.

Considerable changes of land form, sea level, and climate are thought to have occurred during late Tertiary to Recent times, and it is apparent that any particular profile may be the result of a complex series of events. The characteristics of the profile may be an aid in elucidating this history as illustrated by detailed studies of selected localities which also provide a basis for the principles outlined above.

Studies at Lai Chi Kok

Description of Terrace

Considerable excavations for resettlement building sites at Li Cheng Uk in Lai Chi Kok Bay (Fig. 1) provided a rapidly changing series of sections. These cut across a well-marked granite weathering profile as well as stream and slope-wash sediments derived from the decomposed granite. Detailed studies revealed that the weathering profile in some areas had originally developed in relation to a sloping surface which was later truncated, and the profile was now being adapted to the new topographic conditions. Considerable eluviation had occurred in the upper weathering zones, and the sediments and the infilling of a Han tomb (discovered during the excavation) provided evidence of the processes involved.

The Han tomb was discovered in a dissected terrace which lies at the foot of hills rising with 20°–30° slopes to 300 m. The terrace remnants can be traced around 750–800 m of the coast at a height of about 21 m, and the maximum width of more than 120 m occurs near the tomb. The terrace is believed to be a relatively raised, wave-cut platform (F. S. Drake, in preparation).

In this area fresh rock is a *very light-gray*, medium-grained adamellite, and its mode is approximately: quartz 36 per cent, orthoclase 33 per cent, oligoclase 26.5 per cent, and biotite 4.5 per cent. It is xenomorphic equigranular, and the quartz tends to occur as irregular aggregates of interlocking crystals which may be as much as 15 mm long and 5 mm wide, whereas the individual grains average about 2.0 mm in diameter.

The granite is well-jointed in three planes nearly at right angles; two vertical sets trend northward and eastward, and later sheet jointing dips at a low angle southwestward. The spacing of the joints is variable, ranges from 1 to 5 m, and averages about 3 m.

The deforested hillslope behind the terrace shows Zone II material at the surface, and this extends downward in most places to at least 12 m, and quarries show Zone III at depths of 10–25 m (Fig. 10*A*). Abundant core stones 2–5 m in diameter mantle the hillslopes, and small accumulations occur in the steeply incised stream valleys at the head of the terrace. The debris of Zone II often retains some pink orthoclase and black biotite, and in depressions superficial patches of *reddish-brown* silty sand may also contain these minerals. It is clear that erosion is rapidly stripping off the upper weathering zones on these hills and that some low zone features are being retained in the higher zones; this phenemenon is called immaturity. The development of Zone I is proceeding prematurely in the small depressions.

Weathering Profile on Terrace

Toward the northeast of the terrace core stones of granite up to 2.7 m in diameter occur in a mass of residual debris, whereas to the southwest there is a mass of *reddish-brown* clayey sand with no core stones. The contact between the two zones is quite well defined. It dips at about 7° southwestward near the surface of the terrace and increases to 15° in the southwest where the contact is last seen 10–12 m below the terrace surface. There is thus a lower zone (II) more than 14 m thick and a higher zone (I) as much as 12 m thick (Fig. 10*B*).

The debris in Zone II shows the texture of granite in fine detail, but it is friable and open-textured and disintegrates rapidly into sand and silt at the slightest disturbance. Its color ranges from *very pale orange*, *grayish orange* to *light brown*, and its grade size distribution shows

about two-thirds gravel and one-third silt and clay. The clay size fraction is only 4 per cent (Fig. 4*A*). The core stones in Zone II are of the simple type.

The surface of the terrace transects these upper zones of weathering obliquely, and it therefore represents a surface of erosion post-dating the formation of the weathering profile.

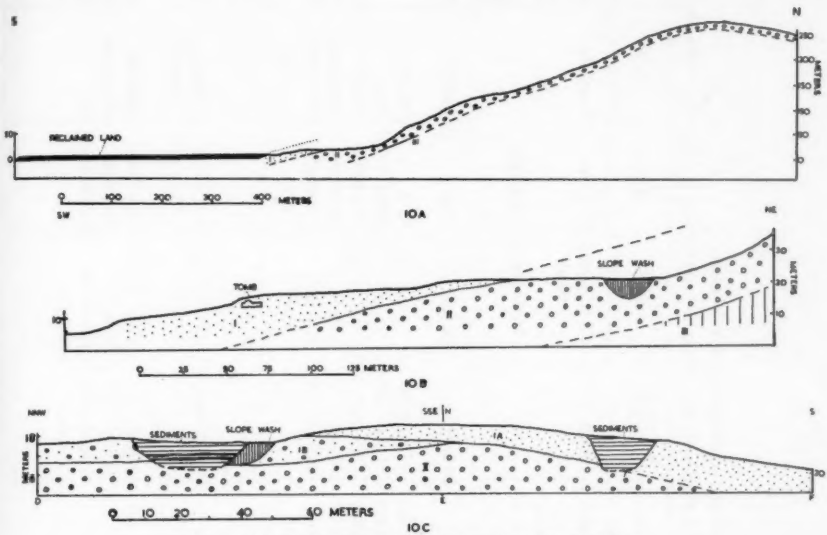

FIGURE 10.—SECTIONS OF TERRACE IN LAI CHI KOK BAY

A. Section across terrace at Li Cheng Uk southward showing the weathering profiles observed in the field. B. Section southwestward showing weathering profile in the excavations at Li Cheng Uk. Close vertical ruling indicates tongue of poorly stratified sediments at the head of the terrace. C. Transverse section across terrace. Close vertical ruling indicates poorly stratified sediment to the northwest of the terrace.

The clayey sand of Zone I has no core stones and is notable for its moderate-to *pale-reddish-brown* color and its high content of clay—about 30 per cent when non-eluviated. It shows no residual textures of granite and is soft, friable, and variably porous and permeable depending on the amount of eluviation.

On the northwest side of the main terrace spur, excavation revealed an intermediate zone between the two types described above. It appears about half way across the terrace, thickens northwestward, and attains a maximum thickness of about 8 m. Its main character is a remarkable mottling caused by the dual presence of *reddish-brown* clayey sand and *grayish-orange* silty sand. In detail the reddish-brown patches are normally confluent and surround disconnected masses of grayish orange. There is a marked increase in the clay content with attendant changes in physical properties between the differently colored patches. The material has core stones in it and is clearly an intermediate zone between I and II. Post-terrace weathering is thought to be responsible for the low-angle Zone I–II surface where it transects the terrace surface.

Terrace Sediments

Two masses of stratified sediments were exposed during the excavations, one on the southeast and one on the northwest of the main terrace spur (Fig. 10*C*). The southerly mass running southwestward is a poorly stratified, *moderate-orange-pink* silty sand. It contains no core stones or coarse fragments and is soft, friable, very porous, and highly permeable.

On the northwest of the main terrace spur excellent sections of well-stratified sediments were exposed. The beds are well differentiated into thin discontinuous lenses of gravel sand and silt and two bands of clay. The details of these sediments are given in Table 1.

The coarse clastic types (XX 25 and XX 26) from below and between the clay bands show slight rounding of the larger grains, and the

TABLE 1.—SUMMARY OF THE PROPERTIES OF ROCKS OF THE TERRACE

Bi—Biotite; C—Compound Grains; K—Kaolin; L—Long Diameter of Largest Grain; M—Mica; Or—Orthoclase; Q—Quartz; S—Simple Grains

	××16	××5 and ××17	××8	××28	××19	××18	××25 ××26	××24	××20A	××20B	××33
NATURE	Silty arkosic sand	Clayey sand		Silty arkosic sand	Arkosic silty sand	Sandy clay	Arkosic sand	Clayey arkosic sand	Silty clay	Gray clay	Silty gravel
TYPE	Zone II	Zone I		Intermediate Zone Ib	Poorly stratified sediment	Non-eluviated Zone I	Well-stratified sediment				Slump and slope wash. Poorly stratified
BOULDERS	Common	Absent		Fairly common	Absent	Absent	Absent	Absent	Absent	Absent	Absent
GRAVEL	12 per cent	17 per cent		—	—	10 per cent	15 per cent	—	Rare	Absent	—
SAND	55 per cent	48 per cent		—	—	43 per cent	84 per cent	—	Minor	Rare	—
SILT	29 per cent	18 per cent		—	—	17 per cent	1 per cent	—	Abundant	Minor	—
CLAY	4 per cent	17 per cent		—	—	30 per cent	0 per cent	—	Abundant	Dominant	—
COLOR	Grayish orange to light brown	Pale reddish brown to light brown		Dark yellowish orange to moderate reddish brown	Moderate orange pink	Moderate reddish brown	Light brown	Moderate brown	Yellowish grey	Very pale orange	Moderate brown
PHYSICAL PROPERTIES	Granitic soft friable	Gritty soft friable		Partly granitic hard compact	Soft friable	Compact plastic	Soft friable	Soft slightly plastic	Soft floury fairly plastic	Compact plastic	Compact slightly plastic
POROSITY	High	High		Moderate	High	Low	High	Low	Very low	Very low	Moderate
PERMEABILITY	High	High		Moderate	High	Low	High	Low	Very low	Negligible	Moderate
RATE OF DISAGGREGATION IN WATER	Very rapid	Very rapid almost complete		Very slow incomplete	Very rapid	Rapid	Already disaggregated	Slow	Fairly rapid	Nil	Rapid but incomplete
DECANTED											

WATER										

DECANTED RESIDUE DESCRIPTION	S and C L—7 mm Angular Q Compact white K. Greasy yellow M minor iron oxide grains	S and C L—7 mm Angular Q Some red clay adheres to grains	S and C L—10 mm Angular Q Minor compact white K. Red clay lumps	S and C L—10 mm Angular Q Compact white K pink Or yellow M	Mostly S L—7 mm Angular Q Some red clay adheres to grains	Mostly S L—7 mm Angular Q Compact white K pink Or, Bi and iron ore	S and C L—10 mm Similar to XX25 and XX26 but grains have pellicle of red clay	S L—5 mm Angular Q Compact white K	S L—2 mm Very minor Angular Q and compact white K	Large C L—13 mm Angular Q Compact white K, L—6 mm lumps of clay. Minor pink Or and bleached Bi
REMARKS	No pink Or No dark M	No pink Or No M Rare compact white K	No pink Or No M	No dark M	No pink Or No compact white K No M	Slight rounding of coarser grains. Ratio compact K, pink Or about 4:1	Similar to XX25 and XX26	No M. Very rare pink Or	No M. No pink Or	Minor pink Or and minor bleached Bi

compact kaolin lumps in the decanted residue outnumber the pink orthoclase grains by about 4 to 1. Samples from near the top of the sediments (XX 24 at 20 m above principal datum 1.3 m from the surface) show very similar mineralogical characters but have a notable content of silt and clay which causes them to be slightly plastic and poorly permeable. Their *moderate-brown* color is in contrast with the *light-brown* shade of the lower members, and it seems that the top 1 m has had clayey material washed in from the top soil.

Moreover, between the surface clayey layer and the lower clay bands kaolin lumps are rare though remnants can be seen adhering to the re-entrants of some of the larger grains. This may be due to vigorous eluviation of the soft kaolin by the rapid flow of subsurface water confined between the impermeable clay layers. During excavation strong flow did occur here, and this band was highly charged with pungent residues derived from the waste waters of a squatter settlement situated around the head of the terrace a short distance up this small valley.

A mechanical analysis of the sand between the two lower clay bands and thus sheltered from the marked effects of illuviation and eluviation, shows a very well-sorted sediment (XX 25, Fig. 5*A*). The length of the stream from this deposit to its source (near the top of Crow's Nest Hill) is only about 350 m and it has a fall of 125 m. The state of sorting and stratification shows that only a very short distance is needed to accomplish such differentiation particularly with debris of this type.

The lower clay band has no visible pink feldspar or mica, but contains grains of quartz and compact white kaolin. The upper clay band is similar though a few grains of pink orthoclase were observed. The paucity of orthoclase in these clays is an example of differential weathering, in this case due to the presence of the acid clay (pH 5.7; Graham, 1941). The hydrogen-ion concentration of all the terrace materials was fairly constantly acidic and ranged from 5.6 to 5.9 (20 samples).

A tongue-shaped mass of poorly stratified material extends in a southeasterly direction nearly across the head of the terrace. This is a poorly sorted arkosic silty gravel notable for the abundance of large compound grains of aggregated quartz and compact white kaolin set in a *light-brown* mass of silt and clay. It probably represents slope-wash material filling in an old depression or cut.

Eluviation and the Tomb

The partial infilling of the tomb by subsoil, similar in character to that outside it revealed conclusive evidence of eluviation.

The tomb was situated toward the southwest end of the terrace in Zone I material at a height of 13–16 m and was originally excavated from the surface. The clayey sand was replaced around it, and today the contact between the original and disturbed Zone I material is extremely hard to distinguish. The tomb was constructed between 100 B. C. and 300 A. D.; the early date is favored by Professor F. S. Drake, Director, Institute of Oriental Studies, the University of Hong Kong.

About 664 cubic feet of light-brown sandy clay found inside the old tomb (Fig. 11) represents about 45 per cent of the total volume (about 1500 cubic feet). The lower layers were a clayey sand and the upper layers a silty clay. The material outside the tomb was a *reddish-brown* silty sand (Table 2).

The tomb, when constructed, was an almost empty space contained by loosely fitting bricks. At first the cracks between the bricks allowed a mixture of coarse and fine material to filter through, and later as the larger grains become wedged in the cracks only fine material was washed in. The distribution of the deposit (Fig. 11) shows that most of it came through the end walls, and minor amounts entered through the side walls.

The material inside and outside the tomb represents two differentiated fractions, the illuviated and eluviated, of one original subsoil of the Zone I type. This may have been similar to the mean of the sum of the two grade distributions, (*i.e.* XX 5 plus XX 8, divided by 2). If the mean curve is compared with that of the typical Zone II material (XX 16, Fig. 5*A*) it will be noted that there is an increase in the clay content and decrease in the silt content which represents the disaggregation of the kaolin lumps into finer clay particles.

The mean mechanical analysis curve has not been compared with the sample of non-eluviated Zone I material, because eluviation could have occurred before excavation of the tomb.

If the mean curve represents the approximate nature of the original material then for every 2 tons of original Zone I debris 1 ton is now external eluviated residue and the other ton was found illuviated into the tomb. The volume contraction in the material outside the tomb was not necessarily 50 per cent, as much of the

fine material washed out may have simply increased the void-to-volume ratio of the subsoil. These conditions represent a high rate of eluviation, and the process in this instance is almost at the limit of change, as the material outside the tomb is now a gravelly sand with thin pellicles of red clay around the grains.

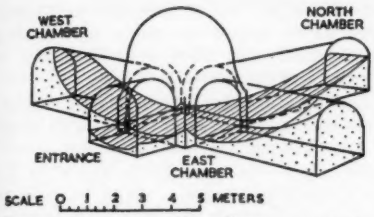

FIGURE 11.—PERSPECTIVE SKETCH OF THE TOMB AT LI CHENG UK SHOWING THE DISTRIBUTION OF THE SANDY CLAY WITHIN

The rate of illuviation may have been more rapid at first because of the admittance of coarser material, and as time went on only the finer grades would gain entrance. At the same time the area of effective seive would be reduced as the tomb began filling up. These retarding factors would be partially balanced by the fact that, as eluviation proceeded outside, the porosity and permeability of Zone I material would increase, and eluviation would tend to be accelerated.

Surface Lowering Due to Eluviation

From Figure 10*B* it will be seen that the terrace has two dominant levels at about 21 m and 18 m (67 and 57 feet) respectively, above the principal datum. This may mean two terraces or a lowering of the southwestern half of the terrace after it was formed. The latter postulate is preferred since the presence of eluviated material is not confined to the immediate neighborhood of the tomb. The upper 7 m of the southern and southeastern side of the main terrace spur is mantled by well-eluviated sandy and silty zones (I and possibly II in its upper parts). The thickness of material affected in this way becomes gradually less toward the northwest.

Two conditions favoring eluviation are a free face to provide an exit for eluviated material which would then travel dominantly subhorizontally and good drainage allowing a fairly free passage for subsurface water. The former would be present after the elevation of the terrace well above sea level, and the latter would either develop slowly as the zone of eluviation grew larger or be hastened by a marked decrease in the vegetation cover. It is thought that the easterward-facing spur and perhaps the steep-sided valley running west-southwestward across the southern end of the terrace provided free faces from which eluviation could work back northwestward into the terrace.

TABLE 2.—GRADE SIZE DISTRIBUTION OF WEATHERING PRODUCTS

	Gravel	Sand	Silt	Clay
LI CHENG UK				
×× 16, Zone II	12	55	29	4
×× 5, plus ×× 8, Zone I	17	48	18	17
×× 5, Zone I outside the tomb	36	60	4	0
×× 8, Zone I inside the tomb	2	32	32	34
×× 18, non-eluviated Zone I	10	43	17	30
×× 25, well stratified arkosic sand	15	84	1	0
TAI LAM AREA				
Zone I in gullied area	19	49	23	9
Slope wash from Zone I	8	40	34	18
Zone I used in earth dams	10	36	40	14
NORTHWEST OF CASTLE PEAK				
×× 36, Zone II, 5 yards apart	2	60	38	0
×× 35, Zone I, 5 yards apart	1	44	40	15
NEAR PING SHAN				
Type A, Zone II, average of 9	22	58	18	2
Type B, Zone I, average of 8	16	46	28	10

THREE CONTRASTED AREAS

Choice of Areas

Deep weathering profiles have been noted over much of the Colony, but only limited areas have been specifically studied. Localities situated on three separate cupolas were chosen after general traverses. In each case work was aided by good exposures resulting from deforestation, gullying, and human activities.

Tai Lam Area

Description of area.—Between the Castle Peak valley (near 3313, Fig. 1) and the Tai Mo Shan area lies one of the largest continuous granite outcrops in the Colony. The region has an extremely variable topography including an upland surface of low relief, a high granite mass, smaller areas of accordant spurs, and undulating topography at lower levels. A distinctive rectangular drainage pattern (southeastward and southwestward) over most of the area, bears a direct relationship to the direction of joints, faults, and dikes in the granite. The Tai Lam Valley is the main through depression following a dominant southwestward-trending line of structural weakness. Successive rejuvenation heads appear to have moved rapidly along this line, and extensive river capture has taken place in the headwater region. Two parts of this area have been studied in detail.

Northwest of Tai Lam Valley.—Over an area of about 3 square miles to the extreme northwest of the Tai Lam Valley a series of undulating hills with a relief of less than 100 m have summit heights between 150 and 200 m. They have been considerably dissected by stream action, and gullies more than 25 m deep are also found. Many gully sections show that the boundary between Zone I and II tends to be convex upward on the low hills, whereas the lower weathering zones have much smaller undulations. This is probably due mainly to the beginning of an adjustment of the upper weathering zones to the post-dissection topography. The profile noted in the district is about 80 m (250 feet) thick and is composed of the following (complete beneath the hills, Fig. 12).

Zone	Thickness	Color	Gravel	Sand	Silt	Clay
I	0–25 m	*pale-yellowish orange*	19	49	23	9[3]
			10	36	40	14[4]
IIa	19–21 m	*very pale orange*	Not analyzed			
IIb	12–15 m	*very pale orange*				
III	about 8 m					
IV	about 8 m					

This has the characteristics of an old-age profile probably formed on a gently rolling, forested land surface which has since been partially dissected. At the present most of the topsoil has been removed, and the upper zones are being actively degraded. Much of the gullying is occurring in Zone I material. The close small-scale adjustment to structure has taken place in a vertical downcutting of less than 100 m almost all within the weathering profile. The lateral variations in the profile may have been expressed as surface, or near-surface, irregularities which helped to guide the drainage development. The thick residual mantle has allowed very rapid adjustment.

East of Tai Lam Chung.—Quite different features occur lower down the Tai Lam stream. A tunnel about 4½ miles along has recently linked the Tai Lam and Tsun Wan areas (Fig. 1). It is generally within a mile of the coast, and most of it is between 30 m and 240 m below the surface. One 200 m section at 4509 (Fig. 1) between 15 and 80 m below the surface, showed over half of the closely jointed granite to be iron-stained, and on the margin of the joint planes the plagioclase was as soft as putty. In this area Zone III is seldom far from the surface, and Zone IV must be at least 30 m thick. The coastal strip is thus in a youthful stage in the present cycle of weathering, and considerable irregularities in weathering are encountered. The new cycle was probably initiated by the downcutting which produced the steep coastal slopes and is being aided by the rejuvenated streams now cutting deep valleys into the upland.

The Tai Lam Valley provides an illustration of the importance of knowledge of the weathering profile to engineering schemes. A dam has been constructed across a narrow part of the main valley (Fig. 1, 3909) where it transects the lower part of the weathering profile. The valley bottom was thought to be sound rock when the excavations commenced, but later a clay band 1 m wide and following one of the flat-lying shear joints, was found to pass right under the main dam. As the valley is in an area of active rejuvenation, active weathering can be expected along lines of structural weakness. Also the preliminary bores did not penetrate sufficiently to reveal the Zone III and IV character of the lower valley sides. Later no continuous solid rock could be found on the eastern slope, and the dam had to be curved round to the north.

Northwest of Castle Peak

Castle Peak (585 m) is one of the highest granite summits and forms the culminating

[3] Spot sample of much eluviated material from an intensely gullied area

[4] Average sample of material used in the construction of earth dams

point of a northward-trending ridge. On the west the steep upper slopes grade into a series of long spurs many of which show a marked stepped profile. Slopes on the sides and ends of these spurs are generally 30°–35°. The streams follow a rectangular pattern though this is less well developed than in the Tai Lam area. Their long profiles have a series of breaks in slope which may indicate progressive rejuvenation of the region.

In many localities the granite is fine-grained, and shear and shatter belts trending northeastward are common. The shattered bands are frequently intensely weathered 10–15m below the surrounding levels. In general the Zone I–II boundary shows a correlation with the present spur form though with more subdued oscillations.

On many of the spurs the vegetation and top soil have been removed and in places all of Zone I as well, so that eluviation and gullying are developing in Zone II. The only reliable figures of thickness for this area are for the upper zones in the area northeast of Nim Wan.

Zone	Thickness	Color	Gravel	Sand	Silt	Clay[5]
I	0–7 m	*Pale yellowish orange*	1	44	40	15
IIa	16–20 m	*very pale orange*	2	60	38	0

There seems to have been complex interaction of weathering and erosion in this region. The series of stepped spurs may represent remains of former flat surfaces on which the weathering developed. As these flats began to be dissected by streams the weathering profiles tended to adapt themselves to the new form though they lagged somewhat behind. With deforestation the general seaward slope probably accelerated the breakdown of the upper zones. The gullying now mostly in Zone II is much further advanced than in the Tai Lam area. Unfortunately little information on the lower zones is available from this area.

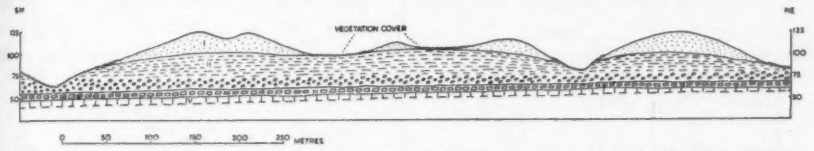

FIGURE 12.—SECTION NORTHEASTWARD ABOUT 200 M. NORTHWEST OF THE MAIN THROUGH VALLEY AT TAI LAM

Shows form of weathering profile, level of the main valley is shown as the basal dashed line. Drawn to natural scale.

[5] Two spot samples taken from 3016 (Fig. 1) within 2 m of each other. Zone I was about 3 m thick, and only remnants remained: Zone II had texture of a fine-grained granite preserved.

Harbor Area

The partly drowned lowland which forms the harbor area is the deeply denuded center of a granite cupola, and it is in this region that the greatest weathering thicknesses have been recorded.

North of the harbor the more resistant rim of the cupola has been left relatively upstanding to form an escarpment like feature which rises to just over 600 m. The steep southern slope of this escarpment descends abruptly to the line of dissected foothills at about 120–130 m, and these are continued as low scattered hills on the Kowloon peninsula (Fig. 13). Lower ridges and summits are common between 50 and 60 m. It seems likely that these accordances represent the remains of former gently sloping surfaces on which deep weathering occurred and which have now been dissected to a mature stage. Borings in Kowloon Bay show an old weathered surface below present sea level, and stream dissection associated with such lowered base levels must have played a large part in the erosion of the area.

Considerable data is available for this area. To the north of Kowloon peninsula in the foothill area borings put down between 84 and 33 m (273 and 108 feet) have revealed only 12 per cent solid rock in the debris of Zone II. Zone III was met with at a height of 35 m (117 feet). The new air approach being cut through these hills down to 43 m (140 feet), shows excellent sections of 37–44 m of Zone IIa (with few core stones) overlying about 10–15 m of Zone IIb (with abundant core stones). Near-by quarries show Zones III and IV each to be about 10 m wide, and fresh unweathered bedrock does not appear to occur above a level of 30 m above principal datum.

Vertical boreholes sited between large core stones at the surface may travel down near

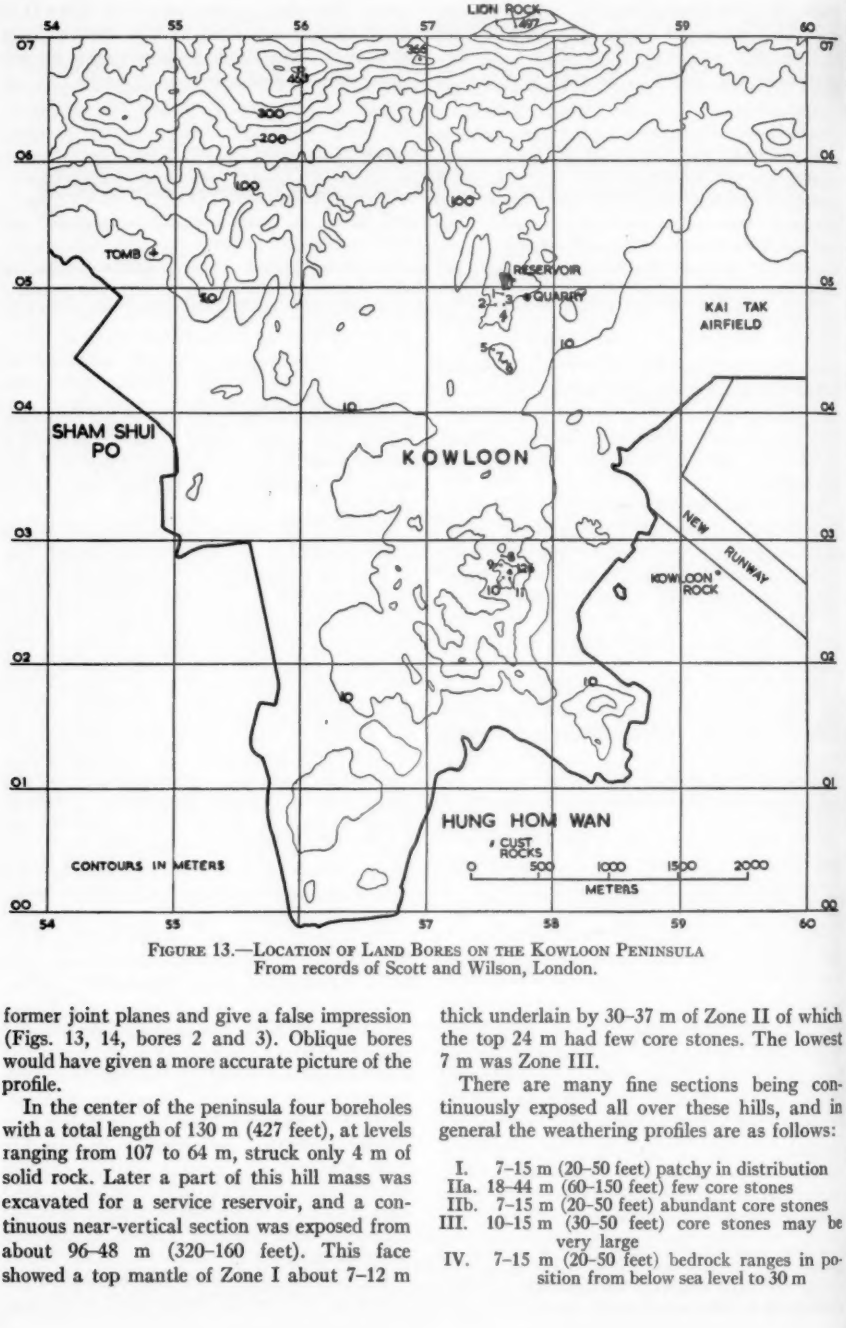

FIGURE 13.—LOCATION OF LAND BORES ON THE KOWLOON PENINSULA
From records of Scott and Wilson, London.

former joint planes and give a false impression (Figs. 13, 14, bores 2 and 3). Oblique bores would have given a more accurate picture of the profile.

In the center of the peninsula four boreholes with a total length of 130 m (427 feet), at levels ranging from 107 to 64 m, struck only 4 m of solid rock. Later a part of this hill mass was excavated for a service reservoir, and a continuous near-vertical section was exposed from about 96–48 m (320–160 feet). This face showed a top mantle of Zone I about 7–12 m thick underlain by 30–37 m of Zone II of which the top 24 m had few core stones. The lowest 7 m was Zone III.

There are many fine sections being continuously exposed all over these hills, and in general the weathering profiles are as follows:

I. 7–15 m (20–50 feet) patchy in distribution
IIa. 18–44 m (60–150 feet) few core stones
IIb. 7–15 m (20–50 feet) abundant core stones
III. 10–15 m (30–50 feet) core stones may be very large
IV. 7–15 m (20–50 feet) bedrock ranges in position from below sea level to 30 m

The highest summit (Fig. 1, 5705) rises to 100 m and is capped by a pocket of core stones up to 10 m long in Zone IIa. This capping by large core stones is a common feature of these hills and the pockets appear to be remnants

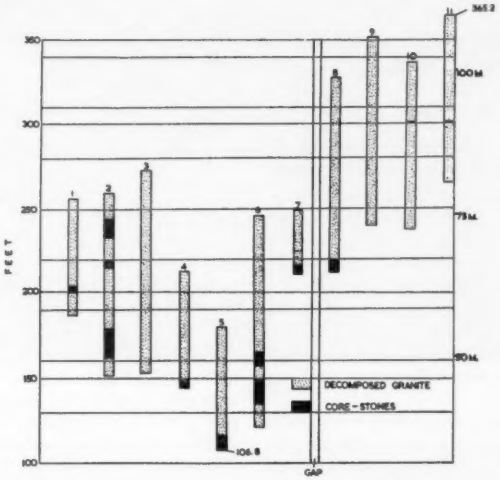

FIGURE 14.—LOG OF LAND BORES ON KOWLOON PENINSULA
From records of Scott and Wilson, London

from youthful irregularities in the profile. The upper 15 m of many of these small hills often contains core stones of the abnormal type and these, with the pockets of core stones, represent partially abandoned portions of the weathering profile.

Thus in many ways the three areas illustrate the progressive breakdown of continuous, complete, and very thick weathering profiles. The dissection in the Tai Lam area is comparatively slight; there is instability and gullying in Zone I. Northwest of Castle Peak the dissection is moderate, and most of Zone I is stripped off many of the spurs. The present instability and gullying is now affecting Zone IIa, whereas on the Kowloon peninsula deep dissection has removed most of Zone I and parts of IIa, and the instability and gullying now occur on Zone IIa and IIb.

PAST CLIMATES AND AGE OF WEATHERING

Climatic Considerations

No detailed assessment of the climate of South China in Pliocene and Pleistocene times has yet been made. Hellmut de Terra (1939) suggests that his four climatic 'pessima' may be an over-all feature in southern Asia, but as yet no evidence of alternation of pluvial and interpluvial conditions as he suggests has been found. His period of laterite formation, however, may be contemporaneous with a period of most active weathering in Hong Kong.

Considering the general climatic background and the supposed fluctuations of the climatic belts it seems improbable that the coastal regions underwent a period of acute aridity during Pleistocene or later Pliocene times. If fluctuations occurred they would probably be between a longer or shorter wet season.

Age of Weathering

It is probable that conditions throughout much of Pleistocene time and earlier have been conductive to deep weathering. Thus the depth of weathering after a certain time would be more a function of its erosional position than of time.

Local deep weathering occurs in many topographic situations, and usually it seems impossible to relate its depth and character with the time involved. Decomposed granite when non-eluviated is fairly compact, however, and in some localities terraces which have been cut across it by stream and marine attack are a possible dating factor.

The terrace at Lai Chi Kok can be linked with Tester's 21-m sea level for the Pacific region (1948) dated as main Monastirian by Zeuner (1952, p. 145). The original profile in this area must have formed in the earlier parts of Pleistocene or late Pliocene times.

Erosion Features Associated with Weathering Profiles

Erosion Processes

Most of the gullied and sheet-eroded areas in the Colony are found in regions of granitic rocks. In these areas two main processes of regrading are found. Over wide stretches and particularly on spurs the surface soil and weathered material are being removed by sheet erosion, and hard barren slopes are left. Associated with some of these bare areas are considerable gullies cutting deeply into the hillside. The gullies are almost invariable found in areas with thick layers of the upper weathering zones.

Skertchly (1893) first noted that a two-stage process must be invoked to explain the present breakdown of the weathering profiles: a period when chemical weathering was dominant and a more recent episode of erosion. He attributed the changeover to the removal of the vegetation resulting from the misuse of the uplands and the deforestation of the area.

Older Dissection of Profiles

In the areas studied the gullying is frequently associated with an older dissection of the profile due to stream rejuvenation. The rejuvenation of the streams was probably a result of Pliocene and Pleistocene changes of level. The variations in height and distance from the sea of the regions considered make it probable that the dissection cannot always be related to the same wave of rejuvenation. In our three selected areas it seems likely that a similar series of changes has affected all the profiles.

In these areas the valleys cutting across the profile are V-shaped in form and are graded with the main stream system; their floors are generally cut into one of the lower weathering zones (III or IV). An examination of the zones indicated that the dissection is subsequent to the major episode of weathering. Later weathering, creep, and slump have brought about varying degrees of adaptation to the valley form (Fig. 12).

In most cases it seems that dissection took place before deforestation; the upper zones were left stable, and little gullying took place. These conditions of dissection are similar to those described by Krynine (1936, p. 301).

Deforestation

Fenzel (1929) concluded that the natural vegetation of South China would probably be a thick rain forest. He thought that the movement of Chinese culture and agriculture into the area resulted in application of farming methods of the plainlands to the less suitable basin topography of the south. The hillsides were burnt and cut, partly for timber, and partly to keep bandits and wild animals away. With the continuing increase in population the procedure was intensified.

The present hillside cover is generally a sparse grass, and thicker scrub is mainly restricted to the stream valleys. On the granite in the Hong Kong region this deforestation has gone a stage further, and many low granite hills have lost even their grass cover; the friable subsoil allows the roots to be pulled out by the blunt hooks of the grass cutters.

The date at which Chinese agricultural settlement, as distinct from political control, became dominant locally is somewhat uncertain. The Li Cheng Uk tomb indicates that control even of this remote area was in the hands of the Chinese in Han Times. Thus progressively intensive deforestation has probably occurred over the last 2000 or more years.

Effects of Deforestation

Removal of the topsoil.—A common feature on many rock groups is the presence of arcuate

PLATE 1.—EROSIONAL FEATURES ON WEATHERED GRANITE

FIGURE 1.—Arcuate slips in colluvial material on moderate angled slopes of weathered granite. The biggest scarp is about 3 m (10 feet) high.

FIGURE 2.—Deeply gullied hills northwest of the main Tai Lam valley after reforestation, taken in 1956. Note the large hollows gouged out of the upper slopes and the abandoned earthpillars and triangular-shaped masses.

FIGURE 3.—A side valley northwest of Tai Lam. Upper slopes are bare pale-yellowish-orange eluviated Zone I material, and lateral cracks are developing into gullies. Intermediate slopes are covered with vegetation and veneered by slope wash. The center of the valley is being aggraded by moderate reddish-brown silty clay derived mainly by eluviation from Zone I and bearing marshy vegetation.

FIGURE 1

FIGURE 2

FIGURE 3

EROSIONAL FEATURES ON WEATHERED GRANITE

slips on the hillslopes. They are often found just below the ridge crests on the eastward- and southeastward-facing slopes, though they can occur on slopes with any orientation (Pl. 1, fig. 1). The scar at the head of the slope is generally between 0.5 and 3 m high and exposes most of the topsoil profile.

When the stabilizing root system was destroyed, the clayey and humic upper layers dried out in the winter, particularly on slopes exposed to steady easterly winds. The resulting compaction and hardening of the upper layers and the corresponding swelling with the summer rain tended to produce differential movement downslope (Penck, 1953, p. 86–87). The upper layers moved over the lower material along a surface which appears in some cases to be a hardpan layer and in others the base of the humic layer. Many scars show that this process is still going on, and in many places it may be in the second or third generation. Also the *B* horizon of the soil profile is often more compact than the lower decomposed granite of the *C* horizon. As erosion proceeds the illuviated zone acts as minor scarp former. Thus on some slopes tufts of grass still remain on tiny mesas 1 m high, whereas all the surrounding area is completely bare and often covered with a layer of quartz grains derived from the eroding *C* horizon. In contrast, the slopes where the *B* horizon is still present may also be clear of vegetation and yet remain compact and firm underfoot. Sheet wash is naturally much more effective on the *C* horizon particularly when this is Zone II material, whereas slip and creep appear more important in the illuviated zone.

After the removal of vegetation unstable slopes often tend to be degraded by landslipping (Wood, 1942, p. 135). Yet here the removal of the soil layers is only a partial expression of regrading. The remaining slope appears to be relatively stable except for some sheet erosion. The main regrading is being carried out by gullying.

Gullying: Characteristics of Hong Kong gullies.—In the Castle Peak district the gullies are generally found on the spurs often cutting longitudinally up the crest though more numerous lateral gullies are found on the valley sides.[6] The lower slopes near the sea show few gullies, but from 70 m to above 230 m these features are common; few occur on higher slopes.

In the Tai Lam area gullies are found mainly in the lower land near the mouth of the Tai Lam valley and in the hills to the northwest of the main stream. In the Kowloon hills they occur frequently on the spurs sweeping toward the peninsula and are also well developed in the foothills to the northeast of Kowloon Bay.

The gullies do not show the same slope preference as the arcuate slips described above. Generally U-shaped in cross section they are often fanshaped in plan and extend in a widening arc as they retreat into the spur. The head and sides are characteristically vertical and sometimes overhanging; a little talus covers the foot of the slope, and in the well-developed gullies there is scant evidence of water flowing over the lip. Normally these features are not graded to the main stream system and present discontinuous gashes on the spur slopes. The depth is variable but usually between 2 and 30 m, whereas some of the larger ones are between 150 and 200 m long.

Kingsmill's description of the gullying in 1862 must long postdate the start of the general dissection. Trees, about 3–5 years old, are seen growing in some of the gullies at Tai Lam, and little cutting or extension has occurred since that time. In some gullies an unbroken manganese coating also indicates that erosion of the face has not occurred within the 3–4 years which this coat takes to form. In periods of intense rainfall it is probable that extensive retreat will occur, though some gullies are nearing the end of their most active period of expansion. Rainfall totals as much 22 inches have occurred within 24 hours.

Mechanism of Gully Formation

Importance of eluviation.—Many slope forms have a convex profile near the summit tops, and a concave (waning slope) near the valley floor. There is an intermediate steeper zone which corresponds to Wood's "free face" (Wood, 1942). Regrading by landslipping and slump affects the upper weathering zones only where the free face becomes almost vertical as on the coast and the outside of river bends. Local regrading is accomplished principally by eluviation followed by gullying. Eluviation removes the fine particles from the upper weathering zones, lessens their cohesion and causes increasing instability, and thus promotes gullying.

Eluviation presumably begins to be of greater importance after deforestation owing to the more rapid fluctuations of the water table and more rapid underground flow. For eluviation to

[6] Longitudinal gully occupies the crest of a spur. Lateral gully is at right angles to the main spur direction.

start there must be some sort of free face from which material can be washed out onto the surface. In many places this face may have been present when dissection occurred, but eluviation was retarded because the dense root network obstructed large-scale washing out. If the process did not start locally the vegetation cover would not be of overruling importance, as the eluviation and the gullying would be able to work at levels below the root system.

During deforestation and the removal of the topsoil eluviation would develop more rapidly, as washing out would then become very active. This stage is now in progress on some stream valley sides on the uplands of the Tai Lam area, and patches of *moderate-reddish-brown* clay supporting a marshlike vegetation are found in local depressions.

This washing out tends to occur where the wet-weather water table intersects the valley side. It may be more prominent at the beginning of the wet season when the water is moving rapidly through the dried-up weathering zones. If the free face is a steep valley side eluviation will start in a small zone behind the seepage outlet and will work backward from that position. Drying out in winter will become more effective after commencement of eluviation, and large cracks may occur on the slopes. These generally run downslope, so they cannot be confused with slip features. Once a crack is formed the sides form a free face which is much more effective than the valley side, and eluviation can now develop more rapidly. Although these cracks are small they are rapidly widened by storm water, and a gully is started.

If a larger area, such as a hill ridge, becomes affected by eluviation, the settling will be greatest under the greater thickness of eluviated material which is often the crest of the spur. This results in a zone of weakness along the spur which is frequently tapped by a gully originally working back laterally from the valley side. A number of gullies have a right-angle bend resulting from this rapid retreat up the spur crest. Some spurs show minor depressions running along the crest and give an expression of this line of weakness even before gullying affects the locality.

Further development.—Once any small area is well-eluviated local sinking may occur and even without the help of a crack a vertical face may form through slipping. The further development will be of the same pattern as that where cracks are found. Eluviated material will be washed into the void, and as the scarp becomes overhanging it will retreat by landslipping. Storm water will keep the floor free of material and enable the vertical face to retreat rapidly. With active development the area of the free face increases rapidly in size and allows a more intense eluviation on all sides; further retreat seems to follow very closely the scheme outlined by Rubey (1929, quoted in Buckham and Cockfield, 1950, p. 138).

> "Miniature tunnels would form below the temporary ground water of the rainy season and once started the effects would be cumulative . . . subsidence of the roofs over the tunnels would develop surface depressions which would concentrate rainwash . . . . Loose wet soil would gradually move in from both sides to fill the tunnels and the ground would sink, perhaps as a flat gully floor."

As Rubey indicated, the arcuate head of the gully and the vertical walls are explained by this process, and some gullies at Castle Peak illustrate this point. They form discontinuous features with some of the upper segments eroded below their surface outlet, and more depressions occupy the same line further downslope. In this instance eluviation is so strong that natural underground channels have been formed, and the ground has sunk over them to form these discontinuous features.

An accelerating effect is noted in Hong Kong where the retreat takes place in all directions on the upslope side and works back radially from the initial crack or free face; the free face increases in height as it retreats. On the comparatively narrow spurs the gully shape is often controlled by the amount and distribution of weathered material available. At first, as the gully retreats, it taps more and more of the percolating ground water of the spur, and accelerates the processes involved. But as the radius increases it reaches a stage when further retreat means a diminution in the amount of water available for each unit of the gully face and wall, and development becomes much slower.

The typical form developed in lateral gullies is thus fan-shaped, whereas the longitudinal gullies tend to be elongate as radial expansion is limited. The lateral gullies tend to have a lower floor gradient than the longitudinal ones. They are often seen cut back into the middle of the spur. At times considerable bodies of water flow through them. The flat floor owes its form to this action. The longitudinal gullies tap a much smaller part of the underground water, and the steeper gradient (up to 20°) is probably a reflection of the smaller erosion by running

water. The original outlet of the gully is related to the main zone of washing out, but later erosion may deepen it well below this level.

If retreat continues until a gully nears either the crest of the spur or the wall of another gully gullies may be traced to recent human activity. Footpaths on spurs have developed potholes which may in time develop into considerable gullies, though the weakness of the spur crests is also a factor in this development. Mining

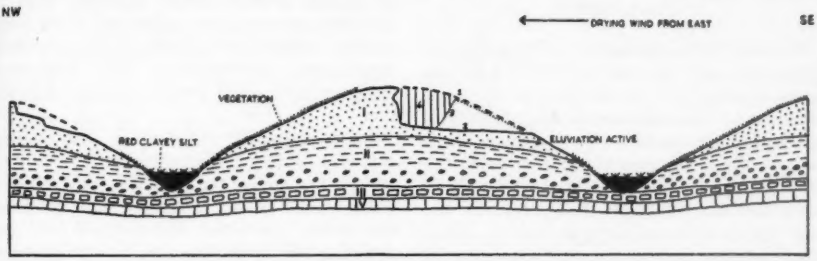

FIGURE 15.—SKETCH SECTION DRAWN TO NATURAL PROPORTIONS SOUTHEASTWARD ACROSS THE LOW HILLS AROUND TAI LAM

Shows gullying on the upper slopes and aggradation in the side vallyes. 1. Original surface; 2. Surface after extensive gullying; 3. Section oblique to main gully course; 4. The area most extensively eroded.

the amount of ground water available becomes almost negligible, and pinnacles of material are left upstanding. These are mainly removed by the undercutting of water flowing through the gully. The different processes involved are reflected in the difference between the vertical face of the normal gully head and the rounded top and steeper lower slopes of the pinnacles. (Figs. 2, 15; Pl. 1).

Aggradation.—In the Tai Lam area where the development of some gullies has reached an advanced stage, the washing out of the finer particles results in local deposition.

The main valleys and through streams are deeply incised into the lower weathering zones and carry stream water for much of the year. The smaller side valleys in contrast, appear to have been little influenced by the erosion of running water in their recent history. Their floors show few traces of stream courses and the tend to hang slightly at the junction with the main stream. This may be explained by the diversion of the water by the gullies and by the general lowering of the water table by gullying on the spurs. They are now the repository of part of the eluviated fraction (Pl. 1, fig. 3), and a cross profile shows that the normal V-shaped valley has been modified and partly infilled. The deposit is a *moderate-reddish-brown* clay in marked contrast to the *pale-yellowish-orange* color of the upper zones nearby. It is a few feet thick and is characterized by a marsh vegetation which adds to its distinction from any other deposits seen in the locality.

In the densely populated parts of the Colony areas have produced considerable waste which has led to gullying, and site excavations and road cuts have had similar effects.

Discussion.—The processes of drying out and eluviation have been considered a number of times in relation to gullying. Lyell (1849, p. 22–23), noted the large cracks in the dried-up earth and saw their connection with the development of gullying. Penck (1953, p. 103–104) showed that slumping was often found near spring heads and was also related to the general water table though he did not describe the process. Rubey (1928) outlined the process in more detail, and his deductions, which were mainly theoretical, were later confirmed in part by Buckham and Cockfield (1950) who noted features which were caused by eluviation in silts in British Columbia. Grave-Morris (1937) studied the formation of gullies in the southeastern United States and suggested that an important factor was the throwing out of water by the sandy layer of the soil profile undercutting an indurated layer and causing retreat by sapping. Also Anderson (1934, after Fuller, 1922) explained the formation of gullies in the loess of North China as being due to the saturation of the lower layers which then flowed out like gruel, and the top collapsed as large blocks. Thus in various localities movement of water underground has played a large part in gully formation.

On the weathered granite in Hong Kong conditions are favorable for differential eluviation as the grade sizes of the residual debris show a wide range. There must be many areas

outside Hong Kong where differentiating eluviation is an important factor both in active erosion and also in the degradation of gently sloping surfaces.

Conclusion

The selective and progressive decomposition of the three main unstable minerals in a granite causes a progressive breakdown of the rock substance by spheroidal weathering, disintegration, and disaggregation. These changes occur most readily in the zone of aeration under the influence of vadose water and atmospheric gases, and are guided in their action by the nature of the inner surface in the bedrock. Their rate of progress is at least in part related to the porosity of the rock.

With time, and under suitable conditions, this reaction zone passes through a series of developmental stages until its upper parts attain equilibrium with the near-surface environment, and a complete weathering profile is formed. This profile can be arbitrarily divided into four zones, IV–I from base upward, which will be roughly subparallel with the surface of the ground. The top Zone I represents the end stage of the reaction, and in this climate and topography is a reddish-brown sandy clay, consisting of quartz and ferruginous kaolin. This material represents only about two-thirds of the parent rock; the remainder was leached away by subsurface processes. If this product occurs near a free face, rapid flow of subsurface water will remove the finer clay particles from it, and considerable differentiation may ensue; sometimes a well-sorted deposit remains.

In Hong Kong complete profiles are fairly common on gentle slopes, but elsewhere profiles tend to develop to an extent determined by the rate of production, mobility of weathered material, and the rate and intensity of denudation. Most complete profiles are thought to have been formed on fairly level surfaces which were stable for a long period of time. The restless geomorphological history of the area has been partly reflected in the modifications and alterations in the present weathering mantle. In recent times the almost complete removal of the vegetation over large areas has rendered the superficial weathering zones unstable, and erosion is proceeding more rapidly than profile development. The chemical and mineralogical changes occurring in the weathering profiles are not yet well known, and this paper has concentrated on the macroscopic changes observed in the field.

Irregularities in the subsurface water regime in the youthful stages of development and differential resistances to weathering of the parent rock cause considerable lateral variations in the profile. These may be expressed by an uneven ground surface and may help to guide the surface agents of erosion. With thick profiles, adjustment of landform to bedrock is considerably accelerated and takes place in a comparatively small vertial range of denudation.

Partial dissection followed by deforestation causes instability in the upper weathering zones, and the first step in the regrading is the removal of the topsoil by slip, creep, and slope wash and concomitant eluviation of the subsoil from any available free faces. The subsoil, now bared of topsoil and perhaps partially eluviated tends to dry out more thoroughly in the dry season, and deep cracks develop. At the onset of the wet season rapid eluviation occurs from the free faces of the cracks, and water channeled in them rapidly forms a gully. Gullies here occur on slopes ranging from 10°–40°. In many instances the valleys are aggrading by the addition of *reddish-brown* silty clay and have a thick often marshy vegetation cover, whereas the bare spurs are undergoing very active erosion.

References Cited

Andersson, J. G., 1934, Children of the yellow earth: London, Kegan Paul, 345 p.

Berry, L., and Ruxton, B. P., 1957, Structure and form on Cheung Chau Island: Geol. Mag., v. 94, p. 249–260

Brock, R. W., 1943, Weathering of igneous rocks near Hong Kong: Geol. Soc. America Bull. v. 54, p. 717–738

Buckham, A. F., and Cockfield, W. E., 1950, Gullies formed by the sinking of the ground: Am. Jour. Sci., v. 248, p. 137–141

De Terra, H., 1939, The Quaternary terrace system of southern Asia and the age of man: Geog. Rev., v. XXIX, p. 101–118

Fenzel, G., 1929, On the natural conditions affecting the introduction of forestry as a branch of rural economy in the province of Kwangtung, especially north Kwangtung: Lingnan Sci. Jour., v. 7, p. 37–99

Fox, C. S., 1935–1936, Buchanan's laterite of Malabar and Kanara: Rec. Ind. Geol. Survey, v. LXIX, p. 389–422

Fuller, M. L., 1922, Some unusual erosion features in the loess of China: Geog. Rev., v. 12, p. 570–584

Graham, E. R., 1941, Acid clay, an agent in chemical weathering: Jour. Geology v. 49, p. 392–401

Grave-Morris, F., 1937, Soil erosion in South-Eastern United States: Geog. Jour., v. XC, p. 363–370

Henry, J. K. M., and Grace, H., 1948, The investigation of decomposed granite in Hong Kong for use as a stabilised base course material:

2d. Internat. Conf. Soil Mech. and Found. Eng. Proc., Rotterdam, p. 187–192
Krynine, P. D., 1936, Geomorphology and sedimentation in the humid tropics: Am. Jour. Sci., v. 232, p. 297–306
Jenny, H., 1950, The origin of soils: *in* P. D. Trask, *Editor*, Applied sedimentation: John Wiley & Sons, N. Y., 707 p.
Kingsmill, T. W., 1862, Notes on the geology of the east coast of China: Geol. Soc. Dublin, v. X, p. 1–6
Leighton, M. M., and MacClintock, P., 1930, Weathered zones of the drift-sheets of Illinois: Jour. Geology, v. 38, p. 28–53
Linton, D. L., 1955, The problem of tors: Geog. Jour., v. CXXI, p. 470–486
Lyell, C., 1849, A second visit to the United States: London, v. 2, p. 22–23
Penck, W. (Translated by Czech and Boswell), 1953, Morphological analysis of landforms: Macmillan and Co., London, 429 p.
Rubey, W. W., 1928, Gullies in the Great Plains formed by sinking of the ground: Am. Jour. Sci., 5th ser., v. 12, p. 417–422
Ruxton, B. P., 1956, The foundation of a new succession in Hong Kong: XXth Internat. Geol. Cong. (Mexico) Proc.
Schofield, W., 1942, Recent changes of sea level on the coast of east Asia: Proc. Liv. Geol. Soc., v. XVIII., Pt. 4, p. 101–112
Scrivenor, J. B., 1931, The geology of Malaya: London, p. 136–138
Skertchly, S. B. J., 1893, Our island. A naturalists's description of Hong Kong: Hong Kong, Kelly and Walsh, 56 p.
Tester, A. C., 1948, Marine terraces of the Pacific Ocean area (Abstract): 18th Internat. Geol. Cong. (England) Proc., p. 57
Wood, A., 1942, The development of hillside slopes: Proc. Geol. Assoc., p. 128–140
Zeuner, F. E., 1950, Dating the past: London Meuthen and Co., 2d. ed., 496 p.

Department of Geography and Geology, University of Hong Kong, Hong Kong
Manuscript Received by the Secretary of the Society, July 5, 1956

BULLETIN OF THE GEOLOGICAL SOCIETY OF AMERICA
VOL. 68, PP. 1293-1304, 3 FIGS., 4 PLS. OCTOBER 1957

ANTHRACITIC COAL FROM PRECAMBRIAN UPPER HURONIAN BLACK SHALE OF THE IRON RIVER DISTRICT, NORTHERN MICHIGAN

BY S. A. TYLER, E. S. BARGHOORN, AND L. P. BARRETT

ABSTRACT

An anthracitic carbonaceous sedimentary rock interbedded in the upper Huronian, Michigamme shales of the Iron River District, Michigan, has been subjected to intensive petrographic and chemical analysis as well as x-ray diffraction study. Field studies were aided by small-scale stripping and trenching operations. The coal occurs as lenticular bodies concordantly bedded with the Michigamme black shale. Similar relations between anthracitic coal and black shale have been observed in drill cores taken at a depth of 1000 feet several miles distant. The associated black shales exhibit numerous graphitic elliptical bodies of varying size but relatively constant form. These are interpreted as being of organic origin. Numerous small elliptical structures may also be observed in flame-etched polished surfaces of the anthracitic coal. X-ray diffraction patterns demonstrate that the coally sedimentary rock is partially graphitized, but less so than that of Rhode Island meta-anthracite of Pennsylvanian age. Use of various extractive and chromatographic techniques demonstrates the presence of strongly pigmented organic compounds. The organic extractives show strong fluroescence in ultraviolet light, solubility in both acid and base solutions, color change with pH change, relatively featureless absorption spectra in the visible and ultraviolet light, and high thermal stability. Oxidative treatment increases the yield of organic extractives. Concatenation of the evidence on the origin and composition of the Michigamme anthracitic carbon suggests probable derivation from algal remains. The sedimentary rock is, hence, of much interest in connection with the problem of the antiquity of Precambrian life.

CONTENTS

TEXT

	Page
Introduction	1294
Acknowledgments	1295
Glacial drift	1296
Iron formation	1296
Carbonaceous shale	1296
Description	1296
Structure	1297
Chemical composition	1298
Anthracitic carbon	1298
Description	1298
Polished surface studies	1301
Chemical analyses	1302
X-ray diffraction patterns and interpretation	1302
Organic extractives	1302
Evidence for the biogenic origin of the graphic coal	1303
Summary and conclusions	1304
References cited	1304

ILLUSTRATIONS

Figures	Page
1. Index map of south shore of Lake Superior	1294
2. Map showing location of test pits and outcrops at the Morrison Creek exploration	1295
3. Map of bulldozer excavation	1297

Plate	Following page
1. Graphitic imprints of organisms on the black shale and suggested modern source equivalent	1300
2. Lump and core samples of the coal and associated black shale	
3. Micro-structure of the coal observed in polarized and non-polarized reflected light	
4. X-ray diffraction diagrams showing oriented molecular structure of the Morrison Creek coal, associated shales and demineralized Pennsylvanian anthracite as compared to graphitized Michigamme coal and graphitized Pennsylvanian anthracite	

TABLES

Table	Page
1. Chemical analyses of shales	1298
2. Proximate analysis of the Morrison Creek anthracitic coal in comparison with other carbonaceous sediments	1298
3. Analysis of Morrison Creek anthracitic coal from fresh sample collected from exposure in 1954	1299
4. Ash analysis of Morrison Creek anthracitic coal	1299
5. Spectrographic analysis of Morrison Creek coal	1300
6. Analysis of anthracitic coal from core taken at 1000 feet in Wauseca mine, Mineral Hills area, Iron River, Michigan	1302

Introduction

Upper Huronian rocks of the Lake Superior region consist predominantly of argillites; black, gray, and green shales; argillaceous quartzites; graywackes; and cherty ferruginous sedimentary rocks. Pyrite-bearing carbonaceous argillites and shales, or their metamorphic equivalent graphitic slates, are commonly associated with iron-bearing sedimentary rocks. The carbon content ranges from 5 to 25 per cent and is normally disseminated throughout the shale as fine-grained particles with or without graphitic properties. More highly enriched members of the black shales were described by Van Hise, Bayley, and Smyth (1897, p. 446) who noted that "A portion of the carbon appears to be in the form of anthracitic coaly substance . . ." in the Marquette district of Michigan. Berry (1927, p. 120) reported the occurrence of ". . . thin seams of metamorphosed coal . . . underlying the Gogebic in Wisconsin." Unfortunately Berry gave neither exact location, physical description, nor chemical analysis of the material. Inasmuch as the Gogebic range in Wisconsin is underlain by granites, greenstones, and other igneous rocks interpretation of this reported occurrence of a coal-like substance is not possible. It is probable that Berry had observed fissure-filling anthraxolite such as the authors have noted at the base of the Gunflint Iron Formation along the White Fish River in the Port Arthur region of Ontario.

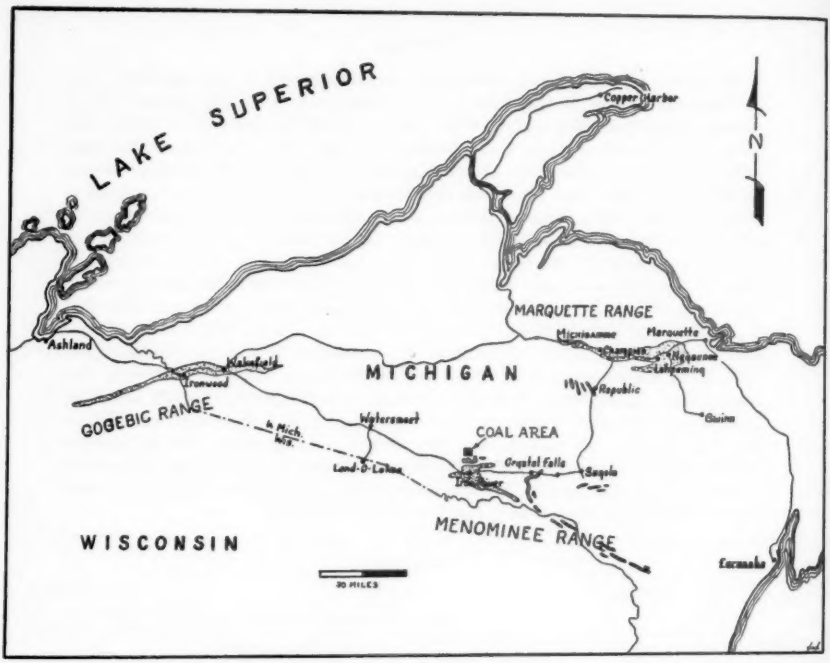

FIGURE 1.—INDEX MAP OF SOUTH SHORE OF LAKE SUPERIOR
Showing location of coal area.

A rock resembling anthracite coal was discovered in the summer of 1949 on the dump of a test pit located (SE ¼ of SE ¼ sec. 21, T. 44 N., R. 35 W.) at the old Morrison Creek exploration about 6½ miles due north and 1 mile east of the city of Iron River, Michigan (Figs. 1, 2). Several hundred pounds of the material, occurring as chunks up to a foot or more in diameter were found on the test pit dump in association with several tons of black pyritic carbonaceous shale. Preliminary physical, chemical, and x-ray analyses indicated that the high carbon rock was not ordinary

bituminous coal or anthracite such as might be utilized in connection with test pitting or diamond drilling operations, but rather some form of anthracitic coal or anthraxolite. The association of carbon rock with black pyritic shales suggested that the material represented a portion of the bed rock encountered in sinking the test pit. The bed rock is the Precambrian Michigamme Formation of upper Huronian age. The rocks comprising the Michigamme Formation in this area consist of arkoses, graywackes, argillites, and pyritic carbonaceous black shales. Lenses of cherty iron formation occur interbedded with the carbonaceous shales. About 1800 feet to the west of the test pits at the Morrison Creek exploration, steeply dipping iron formation crops out on the banks of de Mongo Creek. The iron formation here is interbedded with and underlain to the south by black shale and overlain to the north by a succession of sericitic phyllites, graywackes, and arkoses. The iron formation horizon is outlined by a series of test pits dating from about the turn of the century when test pitting was the favored prospecting method utilized in the search for iron ores.

A bulldozer was used in the late summer of 1954 to excavate a north-south and two east-west trenches at the Morrison Creek locality in order to learn more regarding the occurrence of the anthracitic coal. There was considerable question as to whether bed rock could be reached by bulldozer operation, for little was known regarding the thickness of the glacial drift other than the fact that many of the early test pits had reached ledge. Some pits were cribbed, and the prospectors were known to have been persistent in their efforts even though bed rock lay 50 feet or more below the surface.

FIGURE 2.—MAP SHOWING LOCATION OF TEST PITS AND OUTCROPS AT THE MORRISON CREEK EXPLORATION S. ½ of SE. ¼ sec. 21, T. 44 N., R 35 W., Michigan. MS—Mica schist, IF—Iron formation, SH—Black shale, NL—No ledge, ■—Test pit, ✱—Rock ledge.

ACKNOWLEDGMENTS

The authors are grateful for a generous grant from the Geological Society of America, which made the excavation at the Morrison Creek exploration possible. The authors further wish to express their gratitude to T. E. Stephenson for bringing the occurrence to their attention; to C. E. Dutton, Wm. Holway, E. Hendrickson, D. H. Hase, and E. A. Beutner for assistance in the field; to A. E. Walker and the geological staff of the M. A. Hanna Co. for specimens and information concerning the Wauseca Mine occurrence; to J. Eddy of the Michigan State Conservation Commission for permission to excavate trenches; to Wm. Pasich, Jones and Laughlin Steel Corporation Research Laboratory, C. L. Potter, Jones and Laughlin Steel Corporation, Coal and Coke Research Division, Robert M. Kosanke, Coal Division, Illinois State Geological Survey for securing chemical analyses; and D. B. McLaughlin for references on Precambrian carbon. The authors are grateful to Kalervo Rankama of the University of Helsinki and to the Geological Survey of Finland for the gift of specimens of shungite. The authors are indebted to the late J. W. Gartland of the National Carbon Research Laboratories for the x-ray diffraction studies. To Irving Breger of the U. S. Geological Survey thanks are extended for data on trace elements. John Ohlson of the Inland Steel Corporation made the bed-moisture determination at Iron River.

Glacial Drift

The bulldozer excavations revealed that the glacial drift in the trench area ranges from 12 to more than 20 feet in thickness. The upper 5 feet consists of yellowish sandy till containing occasional boulders. This is underlain by 6–8 feet of dense clayey gray till containing numerous boulders up to 18 inches or more in diameter. At a depth of 11–13 feet a red to yellow, very dense, well-cemented, sandy clay hardpan was encountered. The hardpan contains abundant fragments of black shale, numerous chunks of graphitic carbon, and locally a rather large amount of cherty iron formation. The hardpan, which proved very difficult to penetrate with a bulldozer blade, grades downward into broken ledge of the Michigamme formation. About 600 square feet of relatively solid shale ledge was exposed, but the high degree of induration of the hardpan and the uneven and broken character of the ledge surface made it impossible to reach undisturbed ledge throughout the trench area. The rather complex character of the drift cover is suggestive of a record of two ice advances and an intervening period of weathering.

Iron Formation

The anthracitic coal locality lies near the center of a belt of magnetic disturbances known as the Morrison Creek magnetic anomaly. This magnetic anomaly extends for a distance of 6 miles in an east-west direction and is apparently associated with a rather narrow belt of iron formation.

A large quantity of angular blocks of iron formation was encountered in the northeastern portion of the north-south bulldozer trench. The iron formation rubble has the appearance of disturbed and broken ledge. The iron formation consists of rather lean, oxidized ferruginous cherts and a few layers and lenses of black carbonaceous shale. The chert is massively bedded and ranges in color from yellowish brown through gray to black, depending on the relative quantity of hematite, goethite, and fine-grained carbonaceous material present. The chert has a rather even-grained sugary texture suggestive of recrystallization. Rhombic negative pseudomorphs in the chert indicate that a carbonate, perhaps siderite was once present.

Carbonaceous Shale

Description

A fairly extensive exposure of black shale was developed by the trenching operations (Fig. 3). The rock consists of a thinly bedded carbonaceous shale which grades into a more massively bedded carbonaceous argillite. A few lenses of cherty iron formation up to 6 inches in thickness are interbedded with the shale. The shale splits readily parallel to the bedding, whereas the argillite tends to break with a conchoidal fracture. Examination of thin sections with the microscope reveals that much of the shale and argillite is a microbreccia consisting of angular blocks of opaque material, separated by a network of cherty quartz veins. Some sections suggest the incipient development of a secondary cleavage at an angle to the bedding. Fine-grained pyrite occurs either in the form of cubes, pyritohedrons, or as small ellipsoidal bodies oriented parallel to the bedding. The presence of the pyrite causes the rock to decrepitate with explosive violence when heated and normally induces even the more massively bedded argillites to split parallel to the bedding.

The occurrence of an extraordinarily large quantity of graphitic bodies upon the bedding surfaces is a very interesting feature of the carbonaceous argillites (Pl. 1, figs. 1, 5, 6). These bodies are thin graphitic films which stand out distinctly because they reflect light more effectively than the dull-sooty-black carbonaceous matrix (Pl. 1, figs. 2, 5). On one specimen of shale a structure identical in form with the graphitic bodies was, however, found to consist of a three-dimensional pyrite bleb with thickness approaching 15 per cent of the long axis. The concavity in the shale left by removal of this pyrite filling is shown in Plate 1, figure 3.

The shape of the graphitic bodies upon the bedding surface shows considerable variation, ranging from angular and irregular forms to circular, egg-shaped, and elliptical outlines. The long axis of the elliptical forms often shows a rude to good parallel orientation, but adjacent forms with the maximum axis of elongation at 90° are not uncommon. The long axis of the elliptical forms ranges from a fraction of a millimeter to an observed maximum of 12 mm; the maximum for the intermediate axis oriented parallel to the bedding is 4.75 mm. The axial ratio, in general, averages about 2.0–2.5 and is relatively constant. The surface of the graphitic

bodies when examined with the microscope shows a checked, or micro-faulted appearance (Pl. 1, figs. 5, 6). The black shale in general resembles the "speckled gray" breccia described by James (1951, p. 254) as a basal member of

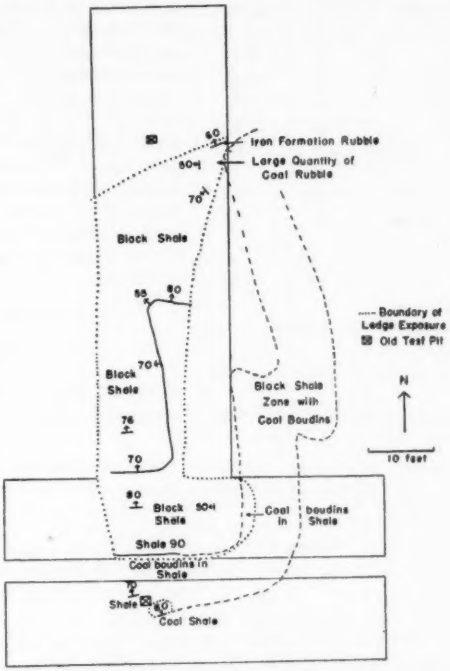

FIGURE 3.—MAP OF BULLDOZER EXCAVATION
Showing exposed ledge and inferred zone of coal boudins in black shale.

otherwise identical in form, is likewise strong presumptive evidence of organic origin. It is possible that the proposed organisms, responsible for the ellipsoidal bodies, may have had somewhat the character and growth habit found today among the primitive free-floating colonial blue-green algae such as certain forms of the genus *Nostoc* (Pl. 1, fig. 4). The organic origin of the ellipsoidal bodies in the black shale is also strongly supported by the existence in the graphitic anthracite of extractable organic compounds.

the iron-rich suite and a marker horizon throughout the Iron River district. The ellipsoidal bodies which are abundant in the Morrison Creek shales, however, appear to be rare or lacking in the typical "speckled gray" breccia. Although the Morrison Creek shales show distinct evidence of brecciation on a micro-scale, it seems unlikely that the ellipsoidal bodies are due to brecciation. It seems more probable that they represent the remains of colonial organisms such as free-floating algae which have been preserved in a manner similar to that of graptolites and algae in Paleozoic black shales. The relative constancy of form of the ellipsoidal bodies, in conjunction with the occurrence of a three-dimensional pyrite filling,

Structure

The black shales and argillites exposed in the bulldozer trench are folded into a series of rather small northwestward-pitching anticlines and synclines. The structures pitch 50°–60° N. 50° W. The pitch of individual folds was observed to flatten or steepen markedly over a

TABLE 1.—CHEMICAL ANALYSES OF SHALES

	A	B	C	D
SiO_2	59.06	55.58	36.67	58.38
Al_2O_3	9.78	9.64	6.90	15.47
FeO	1.58	4.32	2.35	6.07
FeS_2	.....	.....	38.70	.....
CaO	tr	.....	.13	3.12
MgO	1.04	.....	.65	2.45
Na_2O	.....	.....	.26	1.31
K_2O	.....	.....	1.81	3.25
TiO_2	.56	.68	.39	.65
P_2O_5	.007	.....	.20	.17
SO_3	2.25	.12	2.60	.65
C	22.87	19.28	7.60	.81
N	1.00	.....	.....	.....
H_2O-	.....	.....	.55	1.34
H_2O-	.....	.....	1.25	3.68

A and B—Black shale Morrison Creek Exploration, Wm. Pasich, Chemist
C—Graphitic slate Iron River District (James, 1951, p. 255)
D—Composite analysis of 78 shales (Clarke, 1924)

Chemical Composition

The chemical analyses in Tables 1, 4, and 5 indicate that the black shale from the Morrison Creek locality is markedly siliceous and rich in carbon. The silica-alumina ratio is about 6 as compared to 5.3 for the graphitic slate from the Iron River district and 3.77 for Clarke's composite of 78 shales. The microscopic evidence indicates that the relatively high silica content is due to the abundance of cherty quartz in the Morrison Creek shale. The relatively high nitrogen content of the shale, in conjunction with high carbon content, is of much interest with reference to the proposed biogenic origin of the carbon. In this connection also it is of interest to compare the nitrogen content of the shale with that of the anthracitic coal (Table 3).

ANTHRACITIC CARBON

Description

Several tons of the anthracitic coally substance were uncovered by the trenching operations. Much of the material consisted of blocks up to a foot or more in diameter occurring as rubble in the hardpan zone overlying the shale ledge. A few fragments were encountered in the gray glacial till. Lenticular bodies of anthracitic carbon were observed within the black shales in the two east-west-trending trenches. The long axis of each body was oriented parallel to

TABLE 2.—PROXIMATE ANALYSIS OF THE MORRISON CREEK ANTHRACITIC COAL IN COMPARISON WITH OTHER CARBONACEOUS SEDIMENTARY ROCKS

	1 Michigan coal	2 Rhode Island meta-anthracite*	3 Sudbury anthraxolite	4 Pennsylvania anthracite
Volatile matter	3.80	1.82–5.04	1.35–1.88	1.72–10.75
Fixed carbon	79.90	55.0–83.0	77.0–94.0	74.0–91.0†
Ash	16.30	19.0–40.0	4.0–21.0	3.0–30.0
Ash fusion temperature	2850°F.	.....	.....	.....
Sp. G.	2.03	1.65–2.45	1.90	1.46–1.70
Ignition temperature	755°F.	.....	.....	.....
B. T. U.	11,480	7830–11,268	13,482	9230–13,298

1. Analysis by Charles Potter, Jones and Laughlin Steel Corporation, Coal Research Laboratory, Pittsburgh, Pennsylvania.
2. Ashley, G. H. (1915, p. 26–28).
3. Ellis, W. H. (1896, p. 162).
4. Moore, E. S. (1940, p. 105).

* Additional and extensive coal analyses of this sediment may be found in Toenges *et al.* (1948).
† Higher values, up to 96 per cent carbon may be found in Pennsylvania anthracites.

short distance along the axial line. Slickensides are common upon bedding surfaces. They are oriented perpendicular to the axial line and indicate movement of the beds toward the crest of the fold. The intensity of the folding indicates that the shales and argillites behaved as a rather weak incompetent zone during deformation.

TABLE 3.—ANALYSIS OF MORRISON CREEK ANTHRACITIC COAL FROM FRESH SAMPLE COLLECTED FROM EXPOSURE IN 1954

Air-Dry loss 0.7 per cent	Air dried	As received	Moist free	Moist and ash free	Unit dry	Coal moist
Proximate analysis						
Moisture	0.8	1.5	.....	.....	.....	1.9
Volatile matter*	4.0	4.0	4.0	4.9	3.0	3.1
Fixed Carbon	77.0	76.4	77.7	95.1	97.0	95.0
Ash	18.2	18.1	18.3	.....	.....	.....
Total	100.0	100.0	100.0	100.0	100.0	100.0
Ultimate analysis						
Hydrogen	0.71	0.78	0.63	0.78	Moisture for ultimate	
Carbon	76.24	75.73	76.82	94.04	calculations = 0.76	
Nitrogen	0.97	0.96	0.98	1.20	per cent air-dry	
Oxygen	3.65	4.22	3.00	3.66	loss = 0.67 per cent	
Sulfur	0.26	0.26	0.26	0.32		
Ash	18.17	18.05	18.31	.....	.....	
Total	100.00	100.80	100.00	100.00	.....	.....
Total sulfur	0.26	0.26	0.26	0.32		
Calorific value determined						
Cal./g	6127	6084	6176	7564	7702	7567
B.T.U./lb.	11,028	10,951	11,117	13,615	13,863	13,620

Analysis by Illinois State Geological Survey, Analytical Division.
* Little or no carbonate was detected.

the bedding of the shale. The shale-graphitic coal contact was observed to be concordant with the shale and tended to wrap around the lenticular bodies of graphitic carbon. Thin seams of shale occur parallel to the contact in a few places within the graphitic carbon mass. Nowhere was the graphitic carbon seen to bear discordant relationships to the shale or to occur as cavity or fracture filling within the shales, argillites, and cherts. The largest graphitic coal lens was uncovered in the southernmost trench. It measured 5 feet in length and 3 feet in thickness from the upper to the lower shale contact. At the lower contact there appeared to be a gradual transition from shale, through a high carbon argillite into graphitic coal.

The coally matrix within the lenticular masses ranges in color from gleaming bluish-gray to dull sooty black. The material is extensively brecciated throughout, with fragments ranging in size from several centimeters to a fraction of a millimeter. The fragments are angular in shape and are cemented by an intricate network of thin chert veinlets. The chert ranges in color from white to black depending upon the amount of included carbon. The

TABLE 4.—ASH ANALYSIS OF MORRISON CREEK ANTHRACITIC COAL

Ash = 16.30 per cent of sample as received
Analysis by C. L. Potter, Jones and Laughlin Steel Corp.

Fe_2O_3	1.85
SiO_2	96.98
Al_2O_3	.65
CaO	.02
MgO	.12
Phos	trace
MnO	.03
SO_3	.....
$Na_2O \cdot K_2O$	...
TiO_2	2.0

graphitic coal adjacent to a shale contact is in most places pulverized into a fine breccia, and the fragments increase in size toward the interior of the mass. In the more coarsely brecciated phases the coal matrix exhibits a platy or blocky appearance. Individual fragments of the breccia show a well-developed conchoidal fracture. The surface of freshly developed fractures are often marked by numerous concentric rings which show a convex surface. At right angles to the concentric rings on the fracture are fine structures appearing as striations to the naked eye. These oval or eyelike forms produced on fresh fractures closely resemble the "birds-eye" structures occurring in many true anthracite coals. The extremely brecciated character of the graphitic coal indicates that during deformation the material behaved as a competent but brittle substance within the enclosing more plastic shales. The lens-shaped

TABLE 5.—SPECTROGRAPHIC ANALYSIS OF MORRISON CREEK ANTHRACITIC COAL
Two Samples

	Sample 1	Sample 2
10 per cent	Si	Si
5.0–10.0 per cent	..	..
1.0–5.0 per cent	Ca Fe	Fe
.5–1.0 per cent	Al K	Ca
.1–.5 per cent	Ni Mg	K Al
.05–.1 per cent	V Na Cu B	Mg
.01–.05 per cent	Ba Mn	Ni B V Cu Na Mn
.005–.01 per cent	Ti Mo	..
.001–.005 per cent	Y Cr La Sr Pb Ga	Ba Sr Cr
.0005–.001 per cent	Zr	Zr Ti
.0001–.0005 per cent	Yb	Yb
(germanium not detected)		

Analysis by Mona Frank, Geochemistry and Petrology Branch, U. S. Geological Survey, Washington, D. C.

PLATE 1.—GRAPHITIC IMPRINTS OF ORGANISMS ON THE BLACK SHALE AND SUGGESTED MODERN SOURCE EQUIVALENT

FIGURE 1.—Slab of Michigamme black shale, showing numerous graphitic imprints. Note prevailing oval to rounded form. × 6.7.

FIGURE 2.—Michigamme black shale showing graphitic imprint. × 3.8.

FIGURE 3.—Michigamme black shale showing a three-dimensional imprint. The cavity was filled with an ovoidal pyrite bleb. × 3.8.

FIGURE 4.—Group of living colonies of the blue-green alga, *Nostoc*. The colonies are illustrated as a possible analogous biogenic source for the rounded imprints of the highly carbonaceous Michigamme shale. It is not suggested that the Michigamme "Fossils" are those of *Nostoc*. Photograph courtesy of the General Biological Supply House. × .28.

FIGURE 5.—Elongated graphitic imprint of Michigamme shale. Note adjacent small round imprints. × 3.45.

FIGURE 6.—Same as Figure 5. Note highly reflective graphite films as in Figure 5. × 3.8.

PLATE 2.—LUMP AND CORE SAMPLES OF THE COAL AND ASSOCIATED BLACK SHALE

FIGURE 1.—Block of Michigamme graphitic coal showing conchoidal fracture and highly reflective quartz-filled fracture planes. × .4.

FIGURE 2.—Contact of the black shale and the brecciated coal. Two shale laminae within the coal parallel the shale-coal contact. × .62.

FIGURE 3.—Black shale "coal" contact, Wauseca mine, Mineral Hills area, Iron River district. Natural size.

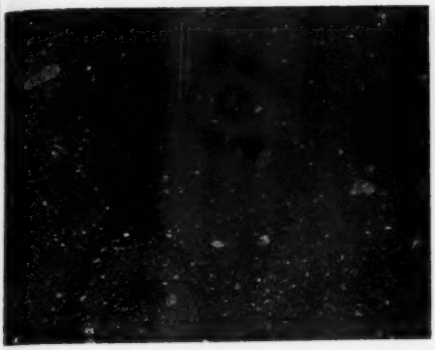

FIGURE 1

FIGURE 2

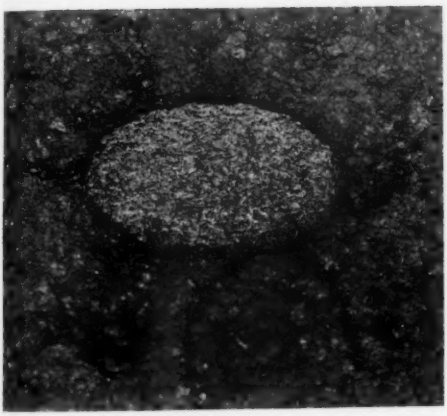

FIGURE 3

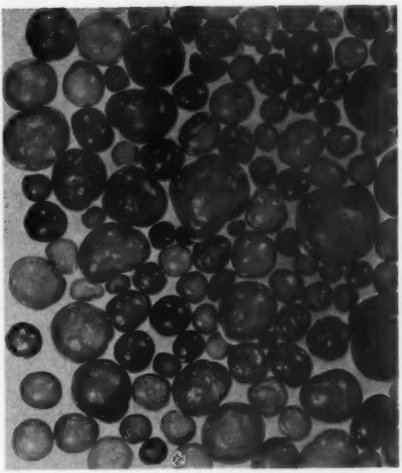

FIGURE 4

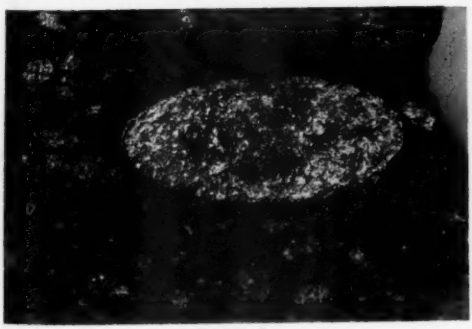

FIGURE 5

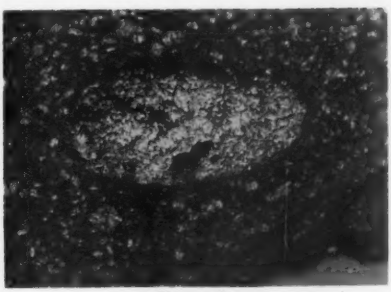

FIGURE 6

GRAPHITIC IMPRINTS OF ORGANISMS ON THE BLACK SHALE AND SUGGESTED MODERN SOURCE EQUIVALENT

FIGURE 1

FIGURE 2

FIGURE 3

LUMP AND CORE SAMPLES OF THE COAL AND ASSOCIATED BLACK SHALE

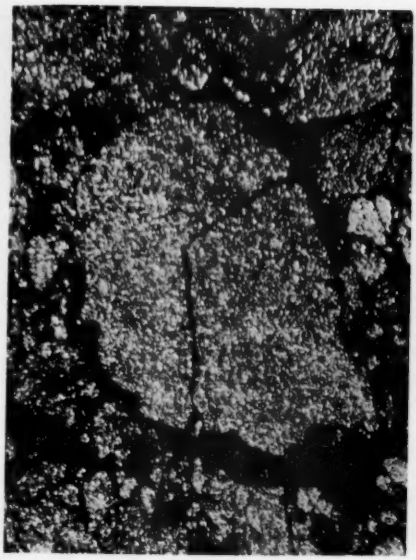

FIGURE 1

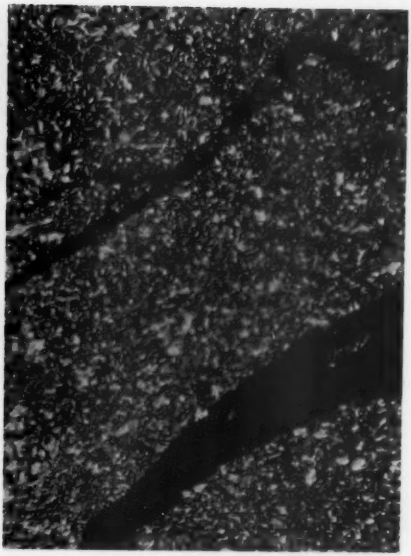

FIGURE 2

FIGURE 3

FIGURE 4

MICROSTRUCTURE OF THE COAL OBSERVED IN POLARIZED AND NONPOLARIZED REFLECTED LIGHT

FIGURE 1

FIGURE 2

FIGURE 3

FIGURE 4

FIGURE 5

FIGURE 6

X-RAY DIFFRACTION DIAGRAMS SHOWING ORIENTED MOLECULAR STRUCTURE OF THE MORRISON CREEK COAL, ASSOCIATED SHALES, AND DEMINERALIZED PENNSYLVANIAN ANTHRACITE AS COMPARED TO GRAPHITIZED MICHIGAMME COAL AND GRAPHITIZED PENNSYLVANIAN ANTHRACITE

graphitic carbon masses are best interpreted as boudins or remnants of a once more continuous body.

The external surfaces of the fragments of graphitic coal embedded in the drift are covered with a soft sooty layer up to several millimeters in thickness. This sooty layer consists of extremely fine carbon particles freed from the cherty cementing veins through desilication by ground water. Desilication and resulting sooty texture can be induced in the laboratory by treatment with hydrofluoric acid. The highly brecciated phases of the coal yield, by acid treatment, carbon particles ranging from colloidal size to several microns. When washed and dried the pulverulent carbon resembles soot in texture and shows none of the gross properties of the mineral graphite. The graphitic coal, therefore, seems intermediate between a true anthracite and sedimentary graphite, a conclusion corroborated by x-ray diffraction studies. (Pl. 4).

During the progress of the excavation at the Morrison Creek locality geologists of the M. A. Hanna Iron Company called the authors' attention to a material resembling coal which was encountered in a diamond drill hole at the Wauseca Mine in the Mineral Hills area of the Iron River district (Pl. 2, fig. 3). About 18 inches of core was recovered from the footwall slates at a depth of 1000 feet. This material proved to be very similar in appearance and composition to the Morrison Creek graphitic coal (Tables 3, 6). It is highly brecciated, and the cherty quartz matrix is somewhat more abundant than in the Morrison Creek sediment (*cf.* Pl. 2, fig. 1; Pl. 2, fig. 3). The black shale "coal" contact in the core appears to be concordant, and the shale shows evidence of plastic deformation, whereas the "coal" behaved as a more competent but brittle body (Pl. 2, fig. 1).

Polished Surface Studies

Polished surfaces of the graphitic coal when etched with an oxidizing flame reveal rather closely packed steel-gray elongated bodies set in a sooty black matrix (Pl. 3, fig. 4). The bodies show a rude to good parallel arrangement within a single breccia fragment, and the maximum axis of elongation is oriented parallel to the bedding of the shale. The bodies range in length from several hundred microns to a maximum of about 1 mm, and the ratio of the longer diameter to the shorter ranges from 2:1 to 4:1. The flame-etched surfaces of the Morrison Creek graphitic coal resemble cross sections of

---

PLATE 3.—MICRO-STRUCTURE OF THE COAL OBSERVED IN POLARIZED AND NON-POLARIZED REFLECTED LIGHT

FIGURE 1.—Polished surface of Morrison Creek anthracitic coal photographed in polarized reflected light. The larger dark areas are quartz fillings in the brecciated matrix of carbon. × 35.

FIGURE 2.—Same as Plate 3, figure 1, except more highly magnified. Note the rounded anisotropic granules of the carbon matrix, interspersed with elongated bodies more clearly shown in figure 3. × 130.

FIGURE 3.—Polished surface of Morrison Creek coal highly magnified. Note the threadlike elongated structures interspersed through the matrix. Polarized reflected light, oil immersion. × 530.

FIGURE 4.—Flame-etched surface of another specimen of the graphitic coal, showing rounded elliptical bodies resembling in shape and orientation the graphitic imprints illustrated in Plate 2, figures 1, 2, 5, and 6.

PLATE 4.—X-RAY DIFFRACTION DIAGRAMS SHOWING ORIENTED MOLECULAR STRUCTURE OF THE MORRISON CREEK COAL, ASSOCIATED SHALES, AND DEMINERALIZED PENNSYLVANIAN ANTHRACITE AS COMPARED TO GRAPHITIZED MICHIGAMME COAL AND GRAPHITIZED PENNSYLVANIAN ANTHRACITE

Note the sharpness of the 200 and 201 diffraction lines in figure 3 immediately to the right of the central halation, also the partial resolution of the line in the 0.22 plane. This is strongly developed in graphite (see Pl. 5, figs. 2, 3). The suggestion of the .022 plane in the purified (demineralized) Michigamme coal indicates a relatively high alteration of the original organic carbon.

FIGURE 1.—Michigamme shale.

FIGURE 2.—Precambrian coal as received.

FIGURE 3.—Purified Precambrian coal.

FIGURE 4.—Purified Pennsylvanian anthracite.

FIGURE 5.—Graphitized Precambrian coal.

FIGURE 6.—Graphitized Pennsylvanian anthracite.

typical boghead coals such as those illustrated by Thiessen (1925, Pl. 38-B).

Polished surfaces of shungite (Metzger, 1924) from Shunga, Karelo-Finnish S.S.R. and anthraxolite from three Canadian localities, Nolalu, Ontario (from the Gunflint Iron Formation), Lake Albanel, Quebec (Albanel Formation), and near Sudbury, Ontario (Whitewater Series) were prepared and exposed to an oxidizing flame. Oxidation of the polished surfaces of the shungite and the anthraxolites proceeds in a uniform manner without differential etching of the carbon and without revealing structures such as occur in the Morrison Creek graphitic anthracite.

TABLE 6.—ANALYSIS OF ANTHRACITIC COAL FROM CORE TAKEN AT 1000 FEET IN WAUSECA MINE, MINERAL HILLS AREA, IRON RIVER, MICHIGAN

Michigamme Formation

Analyses by Illinois State Geological Survey, Analytical Division.

	As received	Moist free	Moist and ash free	Unit dry	Coal moist
Moisture	.9	....	....	.....	
Volatile matter	2.6	2.6	4.2	.....	
Fixed carbon	59.5	60.1	95.8	.....	
Ash	37.0	37.3	....	.....	
Total	100.0	100.0	100.0		
Hydrogen	.73	.64	1.02	Moisture	
Carbon	58.36	58.91	94.05	for ultimate	
Nitrogen	.76	.77	1.22	calculations	
Oxygen	2.16	1.33	2.15	= .93	
Sulfur	.97	0.98	1.56	per cent	
Ash	37.02	37.37	....		
Total	100.0	100.0	100.0	.....	
Calorific value determined					
Cal./g	4882	4926	7862	.....	
B.T.U./lb.	8788	8868	14151	.....	

Chemical Analyses

Samples of the coal were analysed at several laboratories for routine coal analysis. Trace element analysis was made of the ashed coal. The authors are greatly indebted to the several laboratories for these data since the analyses have been invaluable in adequate interpretation of the sediment.

X-Ray Diffraction Patterns and Interpretation

Through the courtesy of the late Dr. J. W. Gartland of the National Carbon Research Laboratories, data were secured on the x-ray diffraction patterns of the Morrison Creek anthracitic coal and associated Michigamme shale (Pl. 4). These studies indicate that graphitization of the coal has proceeded further than that in metamorphism of Pennsylvania anthracite. In the pattern for the purified (desilicated) Morrison Creek anthracitic coal (Pl. 4, fig. 3) there is a diffraction line at the right of the pattern which corresponds well with the lines in the graphitized anthracite (Pl. 4, fig. 6). By comparison with the purified Pennsylvania anthracite (Jeddo Mine) (Pl. 4, fig. 4) it will be noted that partial graphitization of the Michigan coal (Pl. 4, fig. 5) is evidenced in the .022 plane, which is strongly developed in artificially graphitized anthracite (Pl. 4, fig. 6).

Although in the course of geologic time the alteration processes leading to coalification and increase in rank of coal may be the result as well of time, heat, and pressure, it should be noted that the degree of graphitization exhibited by the Michigan coal is on the order of that produced by temperatures of 1250°C. in the graphitization of petroleum coke (Gartland, 1951, personal communication). There is no geologic evidence that the Michigamme formation has been subjected to high temperatures, although it has been extensively and intensively folded and faulted.

From the available petrographic and chemical evidence, supported by the presence of organic extractives in the Michigamme coal it seems most reasonable to conclude that coalification and partial graphitization of the sediment has been primarily the result of pressure and time, rather than thermal alteration.

ORGANIC EXTRACTIVES

The existence of complex organic molecules in sedimentary rocks has long been known as the result of studies on the chemistry of coal and oil. Discrete complex groups such as the porphyrins and their derivative products have been reported from both coal and shales of considerable geologic age (Treibs, 1934; 1935). The

ultimate persistence of recognizable or identifiable organic compounds in ancient sedimentary rocks has, however, been little explored. Recently, Ableson has reported the presence of amino acids in fossil shells of Devonian and more recent ages (Abelson, 1953–1954).

Because of potential significance in establishing the biogenic or organic nature of Precambrian sediments by the use of chemical criteria, an extensive study was made of the extractable constituents of the Michigamme anthracitic coal. It has been found possible to secure, by various techniques, a pigmented substance or substances of as yet unknown composition. Evidence that the extractable material is organic may be deduced from its behavior with various reagents and solvents. The pigmented compound is strongly fluorescent in ultraviolet light and fluctuates from orange yellow or ocher brown to yellow green, depending upon solvent and pH. By extracting the powdered coal through continuous solvent extraction in a Soxhlet apparatus a yellow to reddish-brown pigment was obtained with the following reagents: acetone, ethyl alcohol (100 per cent), diethyl ether. By use of a separatory funnel extraction of this aqueous solution with chloroform and ethyl ether yields a solution exhibiting yellow fluorescence. Extraction of the powdered coal with glacial acetic acid yielded a heavily pigmented solution consisting of ferric acetate and the unknown substance. Precipitation of the iron from this extract with NH_4OH resulted in a pale-yellow strongly fluorescent solution.

The highest yields by the various techniques tried are secured by the following procedure: desilication of the powdered coal in cold hydrofluoric acid followed by (after repeated washing and centrifuging) 20 per cent aqueous KOH at room temperature. The KOH solution is deep reddish brown and becomes light brown at pH 8.2 upon acidification with HCl. The acidified KOH extract, upon cooling, precipitates a small quantity of a gelatinous precipitate. The filtered solution is passed through a chromatographic column containing acid-washed iron-free talc. The pigmented substance or substances are strongly held in the upper few millimeters of the talc column. Upon extrusion of the talc the pigment is readily eluted in either acetone or ethyl alcohol. The pigment may be brought into aqueous solution by evaporation of the acetone or alcohol in aqueous dilutions. Although the bulk of the pigment carries over into the water phase, a slight turbidity results upon complete removal of acetone or alcohol.

Various techniques have been employed in efforts to identify or characterize the pigments extractable from the Morrison Creek coal, and a wide range of reactions has been observed. The possibility that the colored substance is an inorganic complex has been rather thoroughly explored. Its solubility in organic solvents, change in color with pH, inability to diffuse through a dialyzing membrane and its strongly developed fluorescence in ultraviolet light, however, indicates an organic complex. Certain of these reactions indeed would be indicative of porphyrins or metallo-porphyrin complexes. Absorption spectrophotometric measurements in both the visible and ultraviolet light indicate porphyrin groups. The absorption spectra curves show no defined peaks but rather a featureless steady rise in the ultraviolet range. Further studies are now in progress to determine the chemical affinity of this pigment or pigments. It should be noted that substances exhibiting similar properties to those shown by the Morrison Creek coal extractives have also been secured, though in smaller amounts, from anthraxolite and algal cherts of the Huronian Gunflint Formation north of Lake Superior (Tyler and Barghoorn, 1954) as well as from Carboniferous coals.

Evidence for the Biogenic Origin of the Graphitic Coal

That the Morrison Creek graphitic coal is of biological origin and, hence, the result of organic sedimentation may be deduced from various lines of evidence discussed in this paper. It is desirable to summarize these as follows:

(1) Lithologic evidence. The coal occurs as boudins within highly carbonaceous shales and hence is interpreted to constitute a higher carbon facies change in a sedimentary sequence featured by high carbon content. In addition to its concordant relations with the black shale it is also significant to note that between the true coal and the fissile shale there occurs intermediate or transitional facies. The higher organic content appears to be the result of a greater concentration of initial organic content in the sedimentary sequence.

(2) Paleontological and petrographic evidence. The occurrence in the shale of oval graphitic imprints of relatively constant shape but varying size seems most reasonably to represent graphitized compressions of organisms. Among existing primitive plants certain free-floating colonial members of the blue-green algae comprise source for analogous sedimen-

tary relations as obtained in Michigamme time. Flame-etched surfaces of the coally sediment likewise show the presence of structures comparable to the graphitic imprints in the shale.

Petrographic study of polished surfaces of the coal demonstrate a texture and pattern which seem most logically to be interpreted as the result of coalification of algal cells.

(3) Biochemical evidence. The presence in the coal of small amounts of a pigmented compound extractable in organic solvents seems capable of explanation only on the grounds that the sediment represents coalified organic remains. The organic nature of the extractable pigment is indicated by fluorescence, inability to pass through dialysis membranes, characteristic adsorptive properties in chromatographic columns, and changes during pyrolysis. Its chemical composition is unknown and is being further investigated.

Summary and Conclusions

Although coal-like carbonaceous sediments have long been known from Precambrian rocks in several areas of the world, little coordinated study has been made of their geochemistry, petrography, and possible biogenic origin. The discovery of a graphitic coal in the Iron River district of Michigan presented an opportunity to examine this unusual occurrence both by field and laboratory procedures. This study summarizes the results of a rather intensive investigation of the coally lenses or boudins occurring within the black shales of the upper Huronian Michigamme Formation.

Exposure of the coal by small-scale stripping operations revealed a folded and faulted series of carbonaceous sediments of rather low degree of metamorphism. The relation of the coal to the shale suggests an original graded facies change featured by varying amounts of carbon to argillaceous clastics. Structures occurring in the shale appear to represent compressed remains of organisms. Comparable structures on flame-etched polished surfaces may be observed in the coally facies. The biogenic origin of the graphitic coal is indicated by several lines of coordinated evidence among which one of the most significant is the presence of organic compounds extractable from the coal.

The Michigamme graphitic coal is of much interest in connection with the general problem of the antiquity and extent of Precambrian life. Its age, however, is probably less than that of the structurally preserved plant forms occurring in the black cherts of the Gunflint Iron Formation north of Lake Superior. The Gunflint chert has recently yielded consistent ages of about 1700 million years by the potassium-argon technique of age determination (Patrick Hurley, May 1957, personal communication).

References Cited

Abelson, P., 1953–1954, Annual Report: Director Geophysical Laboratory, Carnegie Institution of Washington Year Book No. 53, p. 95–145

Ashley, G. H., 1915, Rhode Island coal: U. S. Geol. Survey Bull. 615, p. 1–62

Berry, E. W., 1927, Devonian floras: Am. Jour. Sci., v. 214, p. 109–120

Blumer, M., 1950, Porphyrinfarbstoffe und Porphyrin-Metallkomplexe in schweizerischen Bitumina: Geochemische Untersuchungen V. Helvetica Chimica Acta 33, p. 1627–1637

Clarke, F. W., 1924, Data of Geochemistry: U. S. Geol. Survey Bull. 770, p. 1–841

Coleman, A. P., 1896, Anthraxolite or anthracitic carbon: Ontario Bur. Mines, v. 6, p. 159–161

Ellis, W. H., 1896, Chemical Composition of the Anthraxolite: Ontario Bur. Mines, v. 6, p. 162–166

James, H. L., 1951, Iron Formation and associated rocks in the Iron River District, Michigan: Geol. Soc. America Bull., v. 62, p. 251–266

Metzger, A. A., 1924, Die Jatulischen Bildungen von Suojarvi in Ostfinnland: Comm. Geol Finlands Bull. 11, No. 64, p. 1–86, 1923–24

Moore, E. S., 1940, Coal: London, John Wiley & Sons, Inc., p. 1–473

Rankama, K., 1948, New Evidence of the Origin of Pre-Cambrian Carbon: Geol. Soc. America Bull., v. 59, p. 389–416

Thiessen, R., 1925, Origin of the Boghead Coals: U. S. Geol. Survey Prof. Paper 132-I, p. 121–135

Toenges, A. L., *et al.*, 1948, Investigation of metaanthracite in Newport and Providence Counties, R. I.: Petrography, Chemical Characteristics and Geology of Deposits: U. S. Bur. Mines Rept. of Inv. 4276, p. 1–37

Treibs, A., 1934, Ueber das Vorkommen von Chlorophyllderivaten in einem Oelschifer aus der oberen Trias: Annalem der Chemie, 509, p. 103–114

—— 1935, Chlorophyll- und Haemin Derivate in bituminosen Gesteinen, Erdölen, Kohlen, Phosphoriten: Annalen der Chemie, 517, p. 172–196

Tyler, S. A., and Barghoorn, E. S., 1954, Occurrence of structurally preserved plants in pre-cambrian rocks of the Canadian Shield: Science, v. 119, p. 606–608

Van Hise, C. R., Bayley, W. S., and Smyth, H. L., 1897, The Marquette iron-bearing district of Michigan: U. S. Geol. Survey Mon. 28, p. 1–580

Department of Geology, University of Wisconsin, Madison, Wisconsin; Botanical Museum and Biological Laboratories, Harvard University, Cambridge, Mass.; Box 119, Ispeming Michigan

Manuscript Received by the Secretary of the Society, February 2, 1957

BULLETIN OF THE GEOLOGICAL SOCIETY OF AMERICA
VOL. 68, PP. 1305-1314, 1 PL. OCTOBER 1957

MINERALOGY, PETROGRAPHY, AND RADIOACTIVITY OF REPRESENTATIVE SAMPLES OF CHATTANOOGA SHALE

BY THOMAS F. BATES AND ERWIN O. STRAHL

ABSTRACT

Qualitative and quantitative mineralogical studies of the Chattanooga Shale are in progress. Problems of separation and analysis of mineral and organic components are difficult because the rock is fine-grained. However, the application of light and electron microscopy, X-ray diffraction, nuclear-track study, and other methods has provided data of interest.

Megascopically, the shale is a massive chocolate-brown sediment which displays faint indications of lamination. Some pyrite lenses, nodules, and crystals and a few mica flakes are large enough to be seen with a hand lens.

In thin section the rock is seen to consist of grains of quartz and feldspar in a matrix of yellow to red-brown organic material, which incorporates shreds of mica and probably clay particles and is dotted by small clusters of pyrite. Larger organic fragments with associated pyrite are common and take various forms. Individual mineral particles range from pyrite cubes less than 0.15 micron on a side to quartz and feldspar grains as large as 0.10 mm.

X-ray studies show the clay minerals to be illite, kaolinite, and chlorite in decreasing order of abundance. Tourmaline, zircon, and apatite are the characteristic heavy minerals of the sediment.

Quantitative studies, accomplished by a combination of chemical and mineralogical methods, have shown the composition of a batch sample of this rock to be approximately: 22% quartz, 9% feldspar, 31% illite and kaolinite, 22% organic matter, 11% pyrite and marcasite, 2% chlorite, 2% iron oxides, and 1% tourmaline, zircon, and apatite.

Alpha-track studies of emulsion-covered thin sections indicate that no uranium mineral is present. Approximately 70% of the uranium atoms is randomly distributed throughout the fine-grained matrix of the rock, whereas another 25% is concentrated in organic-pyrite-clay complexes such as pyrite nodules and discrete organic bodies. In unweathered samples there is no relationship between uranium distribution and textural features such as bedding.

The data indicate that the uranium was precipitated from sea water under reducing conditions and has not been redistributed following compaction of the sediment.

CONTENTS

TEXT

	Page
Introduction	1306
Acknowledgments	1306
Megascopic description	1306
Microscopic description	1307
Composition	1307
Quartz and feldspar	1307
Pyrite	1307
Nonopaque heavy minerals	1308
Clay minerals	1308
Other minerals	1308
Organic material	1309
Uranium content and distribution	1309
General	1309
Autoradiographic study	1310
Interpretation of autoradiographic data	1311
Summary	1312
References cited	1313

ILLUSTRATIONS

Plate	Facing page
1. Microscopic features of the Chattanooga Shale	1312

TABLE

Table	Page
1. Relationship of alpha tracks to microscopic constituents	1311

Introduction

The purpose of the research described in part in this paper was to make a detailed qualitative and quantitative mineralogical and petrographic study of certain uraniferous black shales in an effort to increase understanding of the nature of these fine-grained rocks and to determine the nature, location, and specific associations of the uranium. The research program was devoloped along the following lines:

(1) Qualitative investigation of material representative of the more uraniferous portion of the Chattanooga Shale in Tennessee.

(2) Qualitative and quantitative chemical, mineralogical, and petrographic analysis of:
   (a) the vertical variation in the Chattanooga Shale as revealed in 60 samples from a 30-foot drill core;
   (b) the lateral variation of the Chattanooga as represented by samples from two drill cores 5 miles apart;
   (c) the regional variation of the upper, more uraniferous portion of the Chattanooga as found in 165 samples from 11 drill cores representing the area from northern Tennessee to central Alabama;
   (d) the relationship of the Chattanooga samples to approximately 1000 samples from 17 drill cores representing black shales in New Mexico, Pennsylvania, Ohio, Kansas, France, and Sweden.

This paper deals with the first aspect of the program and describes the results of qualitative study based largely on typical uraniferous Chattanooga Shale material obtained from an adit driven into the formation in the vicinity of the Sligo Bridge over Caney Fork, 5.5 miles east of Smithville, Tennessee. The adit penetrated the top unit of the formation which is referred to as the "E" unit by geologists of the University of Tennessee (Klepser, 1953) and as the "Top Black" by the U. S. Geological Survey group (Haas, 1956, p. 12). The location within the adit from which each sample came is not known, since the material had been mined and placed in storage before the present investigation was initiated.

Concurrent work on the geology and uranium content of the Chattanooga Shale has been done in the Department of Geology of the University of Tennessee (Klepser, 1953; Maher, 1956), the Mineral Beneficiation Laboratories of Columbia University, the U. S. Bureau of Mines, and the U. S. Geological Survey (Swanson, 1953, 1956; Breger and Schopf, 1955; Brown, 1956; Conant, 1956; Haas, 1956).

Acknowledgments

This research program and a similar study of uraniferous lignites have been supported by funds provided by the U. S. Atomic Energy Commission on contract AT(30-1)-1202 with The Pennsylvania State University. Dr. Daniel R. Miller of the Chemical Branch of the Division of Research of the A.E.C. has been extremely helpful with many of the technical as well as administrative problems that have been encountered.

Under the supervision of the senior author the research has been carried out by Research and Graduate Assistants of the Department of Mineralogy of the Mineral Industries College of The Pennsylvania State University. Personnel who contributed to the work described herein are: Charles E. Weaver, Bruce W. Nelson, Lois W. Luedemann, Eugene N. Silverman, Nicholas M. Short, Elena C. Shafer, and Eugene White.

Harold D. Wright, Assistant Professor of Mineralogy, assisted with many of the radiometric aspects of the work, and John C. Griffiths, Professor of Petrography, gave unsparingly of his time in advising on the statistical design of experiments, control of techniques and analysis of data.

The facilities of the Mineral Constitution Laboratories of the College of Mineral Industries have been used extensively, and the advice and assistance of Joseph Comer, electron microscopist, Harold Lovell, spectroscopist, and H. A. McKinstry, X-ray crystallographer, are sincerely appreciated.

Excellent co-operation has been given by Louis C. Conant, Vernon Swanson, and Tom Kehn of the U. S. Geological Survey; by Paris B. Stockdale, Harry B. Klepser, and their coworkers at the University of Tennessee; and by Frank Grimaldi and other members of the staff of the Trace Elements Laboratory of the U. S. Geological Survey.

Megascopic Description

The material from the Top Black or E member of the formation as exposed in the Sligo adit is a massive, blocky shale of uniform color and texture containing a few thin streaks and lenses

of pyrite and quartz and a few patches of organic material. Secondary gypsum has in places crystallized along fractures and partings. The shale breaks with a conchoidal fracture except along joints or parallel to the faint horizontal laminations referred to as bedding. A fresh surface is dark chocolate, but after prolonged exposure the color darkens. The rock takes a high polish and appears black except where concentrations of pyrite give it a faint bronze metallic luster. With the exception of pyrite crystals and aggregates, a few "large" flakes of mica, and the lenses and streaks referred to above, no mineral particles are large enough to be distinguished with a hand lens. Sandstone layers such as those in the lower portions of the formation described by Maher (1956) have not been found in the Top Black unit.

Microscopic Description

Figure 1 of Plate 1 is a photomicrograph of a typical portion of a thin section of the Top Black member of the formation. The section was cut perpendicular to the bedding and shows something of the mineral composition and texture as observed at the high magnification necessitated by the fine-grained character of the rock. The various components that can be recognized are labelled in the photograph. Grains of zircon, rutile, tourmaline, calcite, and apatite are sometimes observed. Organic particles of various types are common and will be discussed in more detail. The discrete entities labelled in the photograph are surrounded by a matrix which consists of smaller particles of the minerals already mentioned and illite, kaolinite, chlorite, and sufficient organic matter to make the mass red to orange brown in transmitted light.

Composition

Quartz and Feldspar

Chemical determinations indicate that approximately 31 per cent of the Sligo sample is quartz and feldspar. Quantitative X-ray studies of a preliminary nature indicate that the feldspar makes up about a quarter of this amount.

In thin section the clear grains of these two components account for most of the discrete mineral particles seen. The largest are approximately 100 microns in diameter. From this as a maximum the size decreases until individual particles can no longer be resolved in the light microscope and become part of the matrix. X-ray studies of fine fractions show that quartz persists in appreciable amounts in the <0.4-micron fraction but is not abundant enough to cause recognizable peaks in the X-ray pattern of the <0.3-micron material. Most of the large quartz grains have straight extinction and contain relatively few bubble inclusions. A few metaquartzite rock fragments are seen, as well as subrounded aggregates of quartz grains held together by the clay-organic matrix. The clear grains are penetrated to varying degree by shreddy material (Pl. 1, fig. 1).

Only a few of the feldspar grains visible in thin section are twinned and can be distinguished optically from the quartz. Several varieties of feldspar have been recognized in grain mounts by application of staining, universal stage, and X-ray techniques.

Orthoclase is the most abundant feldspar in the shale. It is clear to mottled, rarely twinned, and commonly shows distinct crystal outlines suggesting authigenic origin. Microcline is commonly observed in grain mounts but is rarely visible in thin sections. A few grains of sanidine have been found. Plagioclase feldspar is common, as recognized by the polysynthetic twinning. Numerous grains have authigenic overgrowths.

Pyrite

Pyrite is a major constituent of the Chattanooga Shale. Chemical determinations based on analysis of iron and sulfide sulfur give values for the Sligo adit sample that indicate 10–11 per cent of this mineral. The pyrite occurs in framboidal masses and as cubes, octahedrons, and pyritohedrons either in single crystals or aggregates. The size range observed is from crystals half an inch on an edge to those as small as 0.15 micron in diameter seen in the electron microscope. These are commonly surrounded by an amorphous-appearing material which sometimes volatilizes in the electron beam and is believed to be organic in nature. Pyrite aggregates seen in thin sections and polished surfaces are irregular to round in cross section and commonly show structures suggestive of those observed in organic particles in the shale; this suggests replacement of the latter by the sulfide. Hand-picked nodules are very impure; they contain appreciable amounts of kaolinite, illite, mixed-layer clay, quartz, siderotil ($FeSO_4 \cdot 4H_2O$), and gypsum. When viewed in polished section the pyrite can be seen to contain many pits and inclusions of

organic and claylike material. The sulfide lines and replaces the walls of small cavities and also occurs as cavity fillings and as lenses and sheets which are micro- to megascopic in thickness and may extend for many feet parallel to the bedding.

Nonopaque Heavy Minerals

In the heavy-mineral concentrate the most abundant nonopaque minerals are tourmaline and zircon. The former occurs in the form of hypidiomorphic, subangular grains which average 30–50 microns in length and are colorless to blue, olive, and light brown. Fluid inclusions are commonly present. The zircon grains are subangular and up to 20 microns in length. They are colorless but contain dark inclusions. Apatite constitutes approximately 1 per cent of the total heavy minerals in fractions studied under the microscope. Most of the grains are isotropic and are colorless to gray and light yellow brown. The particles average 50 microns but range up to 300 microns in diameter. Crystals of prismatic, birefringent apatite and grains of garnet and rutile have also been observed.

Xenomorphic to hypidiomorphic, colorless apatite grains averaging 50 microns in length make up 95 per cent of the nonopaque heavy minerals in a persistent thin layer of clay and mica known as the Chattanooga bentonite. It is located not in the "Top Black" but approximately 1 foot below the contact between the Dowelltown and Gassaway units of the formation (Campbell, 1946). Most of the remaining 5 per cent of the nonopaque heavy minerals in this layer is zircon in the form of idiomorphic colorless grains averaging 25 microns in length. Similarities in heavy-mineral content between this layer and the Ordovician K-bentonites of central Pennsylvania (Weaver, 1953) indicate that the Chattanooga material is probably also of volcanic origin.

Clay Minerals

Approximately one-third of the material in the rock from the Sligo adit is the clay mineral, illite. It makes up most of the shreddy material in the matrix. In spite of the large amount present, it is difficult to obtain relatively pure concentrates of the clay because of the intimate association with organic material, very fine quartz, and pyrite. However, X-ray studies show that this clay mineral is of the 2:1 dioctahedral variety and has a 10 Å (001) spacing which does not change with ethylene glycol treatment. Electron micrographs show irregular flakes with discrete outlines typical of illite.

Chlorite is present in amounts approximating 2 or 3 per cent, as evidenced in X-ray and differential thermal-analysis patterns. The chemical composition of the mineral has not been ascertained.

One of the most interesting results of the qualitative mineralogical study was the discovery that some of the clay minerals intimately associated with the pyrite are different from those characteristic of the sample as a whole. The complexity of the clay mineralogy increases with increasing intimacy of association with the sulfide. The clay mineral released by grinding hand-picked pyrite nodules to <140 mesh and separation in bromoform is the same 10 Å illite as that found in the bulk shale. However, in the light minerals concentrated after additional grinding of the pyrite to <325 mesh, the clay consists largely of kaolinite, a small amount of halloysite, and a 2:1 variety with a (001) diffraction effect extending from 10.0 to 11.8 Å with a maximum intensity at 10.6 Å. Calcium treatment of this 2:1 material produces a sharp line at 10.0 and a very weak line at 13.1 Å. These data indicate that this clay is of the mixed-layer type and contains some expanded and some nonexpanded layers.

Pyrite from another source (Woodbury outcrop, U. S. Geological Survey locality RC-2) also contains 10.0 Å illite and 10.6 Å mixed-layered material but differs noticeably from the Sligo samples in the mineral associations of the kaolinite. There is no evidence of this mineral in the light fraction, but a weak X-ray diffraction effect indicates its presence with the <325-mesh heavy fraction. A still more intimate association of kaolinite and pyrite in this sample may explain the presence of the former in the heavy fraction.

Other Minerals

Flakes of mica are obvious in thin sections. Particles large enough to be studied in the light microscope have the optical properties of muscovite. Flakes of biotite and chlorite have been observed in heavy-mineral separates.

Marcasite commonly constitutes less than 2 per cent of the total iron sulfide present in the Top Black samples studied. The mineral occurs in discrete subhedral and anhedral grains and as a fracture filling.

Very little carbonate has been observed in

the Sligo adit material. A few of the thin sections contain idiomorphic rhombs of calcite either scattered through the matrix or concentrated in thin lenses and "pockets."

Organic Material

The organic material is another very important constituent of the Chattanooga Shale. A duplicate determination yielded values of 13.63 and 13.62 per cent organic carbon in a batch sample of Sligo material. Since the composition of the organic matter has not been determined, the percentage of this constituent cannot be accurately calculated. On the basis of suggested conversion factors which range from 1.2 to 1.6, the amount of organic matter in this sample would be between 16.4 and 21.8 per cent.

The organic material occurs megascopically, in lenses parallel to the bedding, and microscopically (1) as round to elongated bodies which have markings and structures presumably derived from the original organism, (2) as irregular thin shreds and flakes, and (3) as very fine material which cannot be resolved in the light microscope but makes the matrix yellow to reddish when observed in thin section. Breger and Schopf (1955) report that microscopic study of several of the thin lenses reveals "coalified woody plant tissue identical with that observed in vitrain." They also found that the material has an unusually high germanium content.

The writers made no attempt to determine the botanical identities of the more discrete bodies of microscopic size but characterized them by their morphology and optical properties. In thin sections cut perpendicular to the bedding these units range in shape from round to elongate with a maximum length/width ratio of 14/1. The smallest discrete units of group 1 above approximate 15 microns in diameter, whereas the largest that has been seen is 415 microns long. The units range from yellow through orange red or red brown to nearly black; some fragments are uniform, others mottled. The birefringence is zero in some particles to marked in others, but the value cannot be obtained in the latter cases because of the masking effect of the color. Figure 2 of Plate 1 illustrates one of these discrete organic particles. The light organic material marked "O" was dodged slightly during enlargement of the photograph in order to accentuate the border between the organic entity and the surrounding pyrite (P) and matrix material (M). In the thin section the diaphaneity of these components is more nearly the same, but the red-brown of the organic particle sets it off from the associated black to gray material.

Like all the other components of the shale, the organic matter does not occur in a pure state. Even the ¼ to ½-inch lenses of black, highly lustrous organic material give X-ray patterns with peaks for quartz, pyrite, and clay. Clean particles hand-picked from thin sections, ground, and placed in the electron microscope show flakes of clay, cubes of pyrite, and angular opaque particles which may be quartz.

Pyrite is commonly associated with the organic entities either as a complete or partial rim around the outer edge or as irregular bodies within. Occasionally a rim of organic matter surrounds an area of quartz, of carbonate, or of material resembling the matrix.

Uranium Content and Distribution

General

The search for 0.001 to 0.012 per cent uranium in this fine-grained rock involves (1) attempts to correlate variations in uranium content with variations in the amount and kind of each organic and inorganic constituent, and (2) efforts to trace the uranium to its location in the rock by the use of alpha and fission-fragment autoradiography.

The first approach is made difficult by the complexity of the rock and the consequent problem of concentrating fractions of sufficient purity to provide conclusive evidence that the uranium is associated with a single constituent or even a group of constituents. The relationship of uranium to such elements as sulfur, phosphorous, and carbon has been pointed out by several authors (Beers and Goodman, 1944; Beers, 1945; McKelvey and Nelson, 1950; Swanson, 1953; 1956). McKelvey and Nelson (1950, p. 39) and Swanson (1956, p. 453) noted that uranium decreases markedly with an increase in calcium and magnesium carbonates. From data such as these it has been inferred that the uranium is associated with and is genetically related to the pyrite and organic material. This belief is supported by the fact that lenses rich in bitumen commonly possess more uranium than the bulk shale (Swanson, 1953; Breger and Schopf, 1955, p. 290). A bentonite layer and natural concentrations of quartz or carbonate have less uranium than the adjacent shale.

Pyrite lenses, crystals, and nodules vary

significantly in uranium content. The most interesting results obtained thus far relate to the light and heavy fractions of ground pyrite nodules from the Sligo material which have been described in the previous section of this paper. The light fractions in which the clay is concentrated contain more uranium than the heavy fractions, which consist largely of pyrite. The difference in radioactivity between light and heavy fractions increases with decreasing size of the particles liberated by grinding; this again suggests an intimate association of uranium with the light material. Base exchange experiments designed to remove uranium that might be absorbed on the clay have not been successful.

Similar experiments performed on pyrite obtained from another locality (Woodbury outcrop, U. S. Geological Survey locality RC-2) did not yield analogous results. The pyrite concentrates were found to be low in radioactivity, and no significant increase was produced by the fractionation experiments. The only mineralogical difference found between the Sligo and Woodbury material is the presence of more kaolinite in the finest fractions of the former.

Autoradiographic Study

Autoradiography provides a more direct means of seeking the source of the radioactivity. Ross (1952) described some of the problems of technique and made effective use of the method in studying the distribution of alpha tracks emitted from certain marine shales. In the present research the method described by Stieff and Stern (1952) was used. A thin film of nuclear emulsion is mounted in permanent direct contact on the surface of the polished section or uncovered thin section to be studied. Because of the low radioactivity of the shale, the film is "exposed" for a period of 3 months before it is developed and fixed, still on the section[1].

Alpha tracks emitted from sources in the section are thus registered in the overlying emulsion where they can be studied and related to the rock beneath them. Although the color and opacity of thin sections of black shale make track study difficult, the method is more direct and effective than any other yet found in relating alpha radioactivity to its source in the rock. In the thin sections of the Sligo samples the tracks associated with the matrix do not point to particles that can be resolved under the light microscope. This, and the fact that the tracks commonly occur singly rather than in "star clusters," suggest that the uranium is not present in a "uranium mineral." Concentrations of tracks, up to 45 in number, have been found originating from discrete organic bodies. In many cases like this, pyrite, enclosed by or surrounding the organic matter is abundant. The tracks do not come from any single point within the organic-pyrite complex but appear to be distributed randomly; some apparently come from the pyrite, and others from the organic material. During a 2-month exposure five tracks originated from the organic body pictured in Figure 2 of Plate 1.

X-ray and electron microscope studies reveal the presence of clay minerals and very fine pyrite not only in the matrix but also within organic particles such as that pictured, which in thin section do not appear to contain mineral matter. Thus, although an alpha track may point to the center of an organic particle, it may have as its source a radioactive atom in or on a mineral particle that cannot be resolved at the magnification of 2000 times that is being used for these studies. To get around the problem of insufficient resolution in the light microscope, electron microscope and diffraction work has been initiated on micromanipulated organic and organic-pyritic specks removed from the thin sections. To aid in these studies Comer and Skipper (1954) devised and perfected a method of studying alpha tracks and their source in the electron microscope.

The relationship of alpha-track concentration and distribution to the composition of the shale has been evaluated by a high-magnification (2000 times) study of 13 emulsion-covered thin sections from a drill core through the formation.[2] The mean values for all sections are presented in Table 1. The composition was first determined by point counting the recognizable constituents grouped as follows: quartz and feldspar; matrix (all material that cannot be

[1] The long exposure time has subsequently been reduced to a matter of hours by use of a method involving photographic registration of fission fragment tracks produced by thermal neutron bombardment of U^{235} atoms in the thin sections (Bates *et. al.*, in press). A comparison of fission and alpha radiographs from identical thin sections has also corroborated other evidence indicating that most Chattanooga Shale samples are in radioactive equilibrium. Fission fragment studies are being continued to determine whether or not equilibrium exists in each of the microscopic components.

[2] U. S. Bureau of Mines core YB-4, Youngs Bend Area near Smithville, Tennessee

placed in other groups including fine-grained quartz, feldspar, and all clay minerals); opaque material (pyrite and opaque organic matter); organic bodies; calcite, mica, and miscellaneous mineral particles. The relationship of alpha

TABLE 1.—RELATIONSHIP OF ALPHA TRACKS TO MICROSCOPIC CONSTITUENTS

Constituent	Per cent*	Per cent tracks	Concentration coefficient
Quartz and Feldspar	10.9	2.9	0.27
Matrix	76.0	68.5	0.90
Opaque material	10.5	26.7	2.54
Organic bodies	0.9	0.6	.67
Calcite	1.7	1.3	.76

* By volume

tracks to constituents was determined by recording the apparent source of each of 100 tracks in each thin section. A "concentration coefficient" (degree of association of tracks with constituent) is obtained by dividing the percentage of tracks associated with the constituent by the percentage of the constituent in the sample. A value of 1 would indicate that the constituent contains the amount of uranium to be expected if the element were randomly distributed throughout the rock. A value greater than 1 indicates a "concentration" above that expected for random uranium distribution, whereas a value of less than 1 indicates that there are fewer associated tracks than would be expected from random distribution.

Column 2 of Table 1 indicates that most of the uranium (mean value 0.0045 per cent) is in the material referred to as matrix. On a volumetric basis the opaque material shows a significant "concentration" of tracks, but because of its relatively low percentage this constituent accounts for only a quarter of the radioactivity. Nevertheless, this association and concentration is highly significant in the light of previously discussed evidence for the concentration of uranium in the "light fractions" of some pyrite nodules. Organic bodies, some of which show high track concentrations, are not significant in the sections studied, largely because for every one with associated tracks there are many without them. Because there is some degree of uncertainty in relating tracks to their ultimate source in the thin section beneath, it is questionable how much significance can be attached to the association of tracks with "identifiable" grains of quartz, feldspar, and calcite.

A microscopic investigation to establish whether track distribution is related to the direction of the bedding involved the use of nuclear emulsions on glass slides which were kept in contact with polished sections (cut perpendicular to the bedding) for a period of 4 months and then removed for processing and study. A 1/16-inch grating was ruled on both the polished sections and the emulsions, and a similar grating, plotted to scale on graph paper, was used to portray any megascopic feature seen on the polished section such as pyrite areas and trace of the bedding planes. The number of tracks per field was recorded for each of the 1/16-inch squares, and the data were analyzed following a random block design (Snedecor, 1953, p. 253). In the sections studied the track distribution was not significantly different from random and thus showed no relationship to the bedding.

Interpretation of Autoradiographic Data

The data from nuclear-track studies suggest certain interpretations concerning the source, manner of emplacement, and subsequent history of the uranium in the samples of Chattanooga Shale investigated. The homogeneous distribution of the element, as evidenced by single alpha tracks scattered throughout the matrix of the rock, and the lack of apparent association of any appreciable amount of the element with detrital mineral matter suggest that the uranium was precipitated from sea water under reducing conditions. No evidence of a uranium mineral, even of "electron microscopic" dimensions, has been observed, and the manner in which the uranium atoms are tied to other components in the rock has not been determined. There is no evidence that uranium atoms occupy positions within pyrite crystals. With the exception of a few megascopic lenses of organic matter, certain microscopic organic–pyrite–clay complexes appear to be the only hosts for concentrations of the uranium. These aggregates commonly have the external form of pyrite nodules, organic entities, or irregular blobs of material opaque in 10-micron thin sections.

The quantitative studies described above show that two-thirds or more of the uranium is held in interstitial positions in the fine-grained matrix, whereas roughly one-fourth is intimately associated with the organic–pyrite-clay

complexes. This microscopic evidence is corroborated by leaching studies made in the Mineral Beneficiation Laboratory of Columbia University under the direction of Prof. M. D. Hassialis, who found that approximately 66 per cent of the uranium is easily removed at room temperature from −400-mesh shale with dilute sulfuric acid, whereas release of the remainder requires a significant increase of temperature and acid concentration.

The random distribution of alpha tracks is evidence that the uranium atoms probably lie where they were originally located after deposition and compaction of the sediment. Because of the ease with which uranium is removed from crushed material by solution, the lack of movement of the element in the samples investigated is attributed to the impermeability of the shale rather than to strength of bonds with shale components or chemical resistance of the element to release and transport from original positions in the rock.

Summary

The Chattanooga Shale samples obtained from the Sligo adit have a composition estimated to be within plus or minus 10 per cent of the figures given below. Although this sample is considered representative, analysis of many Top Black samples indicates considerable variability in composition. These data and their significance will be discussed in a subsequent paper.

	Per cent
Quartz and feldspar	31
Clay minerals and muscovite	31
Organic matter	16–22
Pyrite and marcasite	11
Chlorite	2
Iron oxides	2
Accessory minerals: tourmaline, zircon, apatite	1

X-ray data indicate that the first figure given above may be broken down into approximately 22 per cent quartz and 9 per cent feldspar. Most of the material included in the second figure is illite, but small amounts of kaolinite associated with pyrite may be of particular significance.

The range in the amount of organic matter results from the fact that commonly used factors for converting from the carbon percentage range from 1.2 to 1.6. The determined percentage of carbon, in this case 13.62 per cent, is more useful in comparing samples.

In microscopic study of thin and polished sections, approximately 45 per cent of this sample must be designated as "matrix," because no constituent mineral particle can be identified at the magnification of 2000 times. All the clay and iron oxides and much of the quartz, feldspar, pyrite, and organic matter are in this category.

The nature of the uranium-bearing component has not yet been discovered, but there is no evidence of the presence of any uranium mineral. Investigation of pyrite nodules by gravity-separation techniques has shown that the enclosed, very fine-grained light minerals (largely kaolin clay minerals) contain uranium, but the pyrite does not.

Quantitative evaluation of microscopic components and associated alpha tracks seen in emulsion-covered thin sections of drill-core samples representing the total thickness of the Chattanooga Shale has demonstrated that nearly 70 per cent of the uranium is held in material designated as "matrix," whereas another 25 per cent is concentrated in organic-pyrite-clay complexes which take the form of pyrite nodules, discrete organic bodies, and irregular opaque aggregates. There is no relationship between track distribution and bedding direction.

On the basis of the data obtained thus far the following interpretations are suggested:

(1) Most of the uranium was precipitated from sea water in a reducing environment.
(2) Alpha tracks are not sufficiently concentrated at any spot to indicate the presence of a uranium mineral in the material studied.

PLATE 1.—MICROSCOPIC FEATURES OF THE CHATTANOOGA SHALE

FIGURE 1.—Typical field showing the textural relationship of discrete mineral grains and matrix. Q, quartz or feldspar; M, mica; P, pyrite. The matrix is red brown because of organic matter in the form of very fine fragments and apparently as a coating on mineral grains. Magnification: 1375 ×.

FIGURE 2.—Organic particle (O) surrounded by matrix (M) and some pyrite (P). In the thin section the organic matter is red brown and contrasts with the surrounding material in color more than diaphaneity. In making the photograph the area marked "O" was dodged to bring out the boundary between organic and mineral matter. Magnification: 1375 ×.

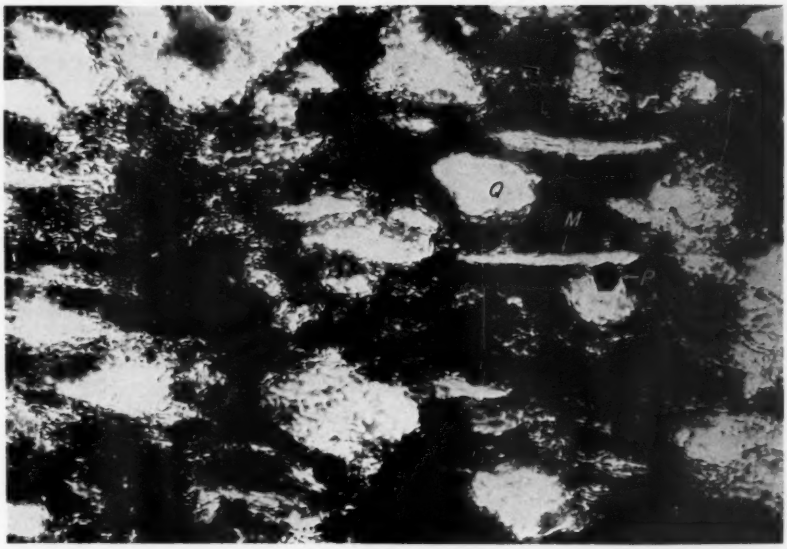

FIGURE 1

FIGURE 2

MICROSCOPIC FEATURES OF THE CHATTANOOGA SHALE

(3) Except along joint planes and weathered surfaces there has been no movement of uranium following final compaction of the sediment.

References Cited

Bates, T. F., Wright, H. D., and Skipper, S. J., in press, Geological studies of uraniferous minerals and rocks by fission fragment radiography: XX International Geol. Cong. Proc.

Beers, R. F., 1945, Radioactivity and organic content of some Paleozic shales: Am. Assoc. Petroleum Geologists Bull., v. 29, p. 1–22

Beers, R. F., and Goodman, C., 1944, Distribution of radioactivity in ancient sediments: Geol. Soc. America Bull., v. 55, p. 1229–1253

Breger, I. A., and Schopf, J., 1955, Germanium and uranium in coalified wood from Upper Devonian black shale: Geochim. Cosochim. Acta 7, p. 287–293

Brown, Andrew, 1956, Uranium in the Chattanooga Shale of Eastern Tennessee: U. S. Geol. Survey Prof. Paper 300, p. 457–462

Campbell, Guy, 1946, New Albany Shale: Geol. Soc. America Bull., v. 57, p. 829–908

Comer, J. J., and Skipper, S. J., 1954, Nuclear emulsions for electron microscopy: Science, v. 119, p. 441–442

Conant, L. C., 1956, Environment of accumulation of the Chattanooga Shale: U. S. Geol. Survey Prof. Paper 300, p. 463–467

Haas, W. H., 1956, Age of the Chattanooga Shale and Maury Formation: U. S. Geol. Survey Prof. Paper 286, 47 p.

Klepser, Harry J., 1953, Stratigraphy of the Chattanooga Shale (Abstract): Geol. Soc. America Bull., v. 64, p. 1933

Maher, S. W., 1956, Sandy zones in the Chattanooga of the Eastern Highland Rim, Tennessee: Jour. Sed. Petrology, v. 26, p. 338–342

McKelvey, V. E., and Nelson, J. W., 1950, Characteristics of marine uranium-bearing sedimentary rocks: Econ. Geology, v. 45, p. 35–53

Ross, V., 1952, Autoradiographic study of marine shales: Econ. Geology, v. 47, p. 783–793

Snedecor, G. W., 1953, Statistical methods: 4th ed., Ames, Iowa, Iowa State College Press, 485 p.

Stieff, L. R., and Stern, T. W., 1952, Preparation of nuclear-track plates and stripping films for the study of radioactive minerals: Am. Mineralogist, v. 37, p. 184–196

Swanson, V. E., 1953, Uranium in the Chattanooga Shale (Abstract): Geol. Soc. America Bull., v. 64, p. 1481

Swanson, V. E., 1956, Uranium in marine black shales of the United States: U. S. Geol. Survey Prof. Paper 300, p. 451–456

Weaver, C. E., 1953, Mineralogy and petrology of some Ordovician K-bentonites and related limestones: Geol. Soc. America Bull., v. 64, p. 921–924

College of Mineral Industries, The Pennsylvania State University, University Park, Pa.

Manuscript Received by tne Secretary of the Society, April 18, 1955

Contribution No. 56-70, College of Mineral Industries, The Pennsylvania State University

BULLETIN OF THE GEOLOGICAL SOCIETY OF AMERICA
VOL. 68, PP. 1315-1342, 3 FIGS., 3 PLS. OCTOBER 1957

GEOLOGY OF THE COCHISE HEAD AND WESTERN PART OF THE VANAR QUADRANGLES, ARIZONA

By Floyd F. Sabins, Jr.

Abstract

The area of this report includes parts of the Chiricahua and the Dos Cabezas Mountains which together constitute a typical range in the Mexican Highland section of the Basin and Range province. The Precambrian basement complex consists of the Pinal Schist, with a massive quartzite member, and two granite intrusives: the foliated Sheep Canyon Granite which is a small synkinematic stock, and the nonfoliated Rattlesnake Point Granite which is a large postkinematic intrusive. All these units are cut by Precambrian aplite dikes.

The Paleozoic strata have an aggregate thickness in excess of 7600 feet and consist of the following units, in ascending order: Bolsa Quartzite (Middle(?) and Upper Cambrian), El Paso Formation (Upper Cambrian and Lower Ordovician), Portal Formation (Upper Devonian), Escabrosa Limestone (Lower Mississippian), Paradise Formation (Upper Mississippian), and the Naco Group (Pennsylvanian and Permian). The Naco Group is subdivided into the following formations, in ascending order: Horquilla Limestone, Earp Formation, Colina Limestone, Scherrer Formation, and Concha Limestone.

The Bisbee Group (Lower Cretaceous) is about 2600 feet thick and includes the Glance Conglomerate at its base. It unconformably overlies the older rocks. The Nipper Formation is here named for mafic volcanic rocks and associated sediments that unconformably overlie the older rocks. The rhyolitic flows of the succeeding Faraway Ranch Formation overlie the Nipper and Bisbee units, and are overlain by the welded tuffs of the Rhyolite Canyon Formation. These volcanic units were formed during the late Cretaceous to late Tertiary interval. All the pre-Rhyolite Canyon formations are cut by Tertiary intrusions of two major types: a light-colored quartz monzonite group and a dark-colored diorite and basalt group.

There is evidence for at least five periods of tectonic activity within the area. The Precambrian orogeny, which pre-dated the intrusion of the Rattlesnake Point Granite and the aplite dikes, caused the regional metamorphism and folding of the Pinal Schist. An epeirogenic uplift that began late in early Ordovician time resulted in the disconformity between the Lower Ordovician strata and the Upper Devonian strata. Uplift and erosion occurred in the late Permian-early Cretaceous interval and supplied the clastic sediments for the Glance Conglomerate.

During the major post-Comanche to pre-Pliocene orogeny, strong southerly to southwesterly horizontal compression caused the following tectonic sequence. The autochthonous rocks along the northeast front of the range were overridden from the southwest by the first thrust sheet. Strike-slip displacement along the Emigrant fault cut the autochthonous block and the overlying thrust sheet, which was separated into the Fort Bowie plate and the Wood Mountain plate. The Fort Bowie plate was later folded to form the Marble Quarry syncline and was truncated by the younger Fort Apache reverse fault. Finally, the Whitetail plate overrode the Fort Apache fault block.

During the Basin and Range orogeny (Pliocene?) vertical displacement along high-angle faults adjacent to the range uplifted the mountains relative to the valleys on either side.

CONTENTS

TEXT

	Page
Introduction	1316
Location and Accessibility	1316
Previous work	1317
Scope of work	1318
Acknowledgments	1318
Geography	1318
Regional setting	1318
Local features	1319
Drainage	1319
Climate, vegetation, and culture	1319
Precambrian rocks	1320
Introduction	1320
Pinal Schist	1320
General	1320
Quartzite member	1321
Origin of the Pinal Schist	1321
Igneous rocks	1321
General	1321
Sheep Canyon Granite	1321
Rattlesnake Point Granite	1322
Aplite dikes	1323
Paleozoic and Mesozoic stratigraphy	1323
Cenozoic rocks	1323
Nipper Formation	1323
Type locality	1323
Petrology	1325
Age	1325
Faraway Ranch Formation	1325
General	1325
Volcanic rocks	1325
Sedimentary rocks	1326
Age	1327
Rhyolite Canyon Formation	1327
General	1327
Petrography	1327
Age	1328
Intrusions	1328
General	1328
Diorite assemblage	1328
Quartz monzonite assemblage	1328
Alluvial deposits and associated geomorphic features	1329
Precambrian orogeny	1329
Introduction	1329
Regional metamorphism	1330
Folding	1330
Age of the orogeny	1330
Mid-Paleozoic epeirogeny	1330
Post-Paleozoic to pre-Cretaceous disturbance	1331
Post-Comanche to pre-Pliocene orogeny	1331
Introduction	1331
Autochthonous block	1332
General	1332
Structure west of Emigrant Canyon	1332
Maverick fault	1332
Structure east of Emigrant Canyon	1332
Blue Mountain	1334
Strike-Slip faults within autochthonous block	1334
Wood Mountain thrust and thrust plate	1334
Fort Bowie thrust and thrust plate	1335
Marble quarry syncline	1335
Emigrant strike-slip fault	1336
Apache Pass reverse fault	1336
General	1336
Northwestern segment	1336
Anderson Canyon to Buckhorn Basin segment	1337
Timber Mountain segment	1337
Southeastern segment	1337
Whitetail thrust and thrust plate	1338
Age of the orogeny	1338
Basin and Range orogeny	1339
General	1339
Border faults	1339
Age of the orogeny	1340
Summary and geologic history	1340
References cited	1341

ILLUSTRATIONS

Figure	Page
1. Index map of Southeast Arizona	1317
2. Diagram of Precambrian relationships	1322
3. Tectonic map	1333

Plate	Facing page
1. Geologic map and structure sections of Cochise Head and western part of Vanar quadrangles, Arizona	1315
2. Photomicrographs	1326
3. Bowie Mountain and vicinity	1327

TABLES

Table	Page
1. Paleozoic and Mesozoic formations of the Chiricahua and Dos Cabezas Mountains	1324
2. Hypothetical sequence of post-Paleozoic events	1328

INTRODUCTION

Location and Accessibility

The Cochise Head quadrangle is in southeast Arizona in the northeast part of Cochise County (Fig. 1). The quadrangle is bounded by lat. 32° 00′ and 32° 15′ and by long. 109° 15′ and 109° 30′. In order to study all the Chiricahua Mountains north of lat. 32° 00′, the western part of the Vanar quadrangle which joins the Cochise Head quadrangle on the east was also mapped. Thus, the area of this report includes the southern part of the Dos Cabezas Mountains and the northern part of the Chiricahua Mountains. Approximately 325 square miles are included in this area.

Arizona Highway 86 and the Southern Pacific Railroad pass a few miles north of the

area. The nearest towns, Bowie and San Simon, are on this highway. A gravel road from Bowie extends through Apache Pass, which is the only pass through the range in this vicinity

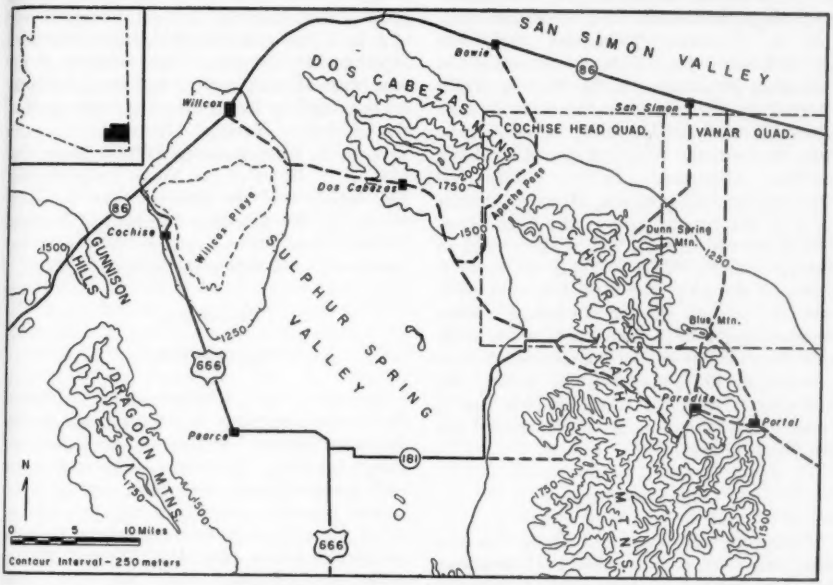

FIGURE 1.—INDEX MAP OF SOUTHEAST ARIZONA
Showing location of Cochise Head and Vanar 15-minute quadrangles.

that can be traveled by vehicles. A gravel road from San Simon to Wood Canyon is connected, along the northeast range front, to the Apache Pass road by a poor dirt road, which can be traveled only by truck or Jeep. Branches from this road extend short distances up some of the northward-trending canyons. A good gravel road extends southward from the Checking Station 3 miles east of San Simon and provides access to the eastern part of the Chiricahuas.

The southwest front of the range is accessible from Arizona Highway 181 which connects the Chiricahua National Monument with U. S Highway 666 about 23 miles to the south. A gravel road connects Highway 181 with the towns of Dos Cabezas and Willcox, both west of the Cochise Head quadrangle. Dirt roads branching to the north provide access to the southwest range front. Few roads extend very far into the range, and much of the area can be reached only on foot.

Previous Work

Very little has been published regarding the area of this report, but the Dos Cabezas-Chiricahua Mountains are mentioned briefly in the reports of several reconnaissance surveys. The earliest of these was by G. K. Gilbert (1875, p. 510–513), who measured stratigraphic sections near Dos Cabezas and Fort Bowie, while with the Wheeler Survey. He also published some structural cross sections showing the major faults between Dos Cabezas and Fort Bowie. During a brief trip through Cochise County, E. T. Dumble (1902) noted the Carboniferous limestones in the southern Chiricahuas. He mentioned the granite and the sedimentary beds at Wood Canyon and Apache Pass and noted a large fault at Fort Bowie. Sidney Paige (1909) described the marble prospects near Apache Pass and along lower Whitetail Creek. His brief report has several acute geologic observations regarding the faulting and folding of the Carboniferous strata in the vicinity of Fort Bowie.

In a short abstract, C. J. Sarle (1922, p. 544) outlined the general features of the Dos

Cabazas Mountains and mentioned some of the rock units present. N. H. Darton (1925, p. 296) briefly redescribed Gilbert's section at Dos Cabezas. The Geologic Map of Arizona shows the general features of the Chiricahua-Dos Cabezas Mountains on a 1/500,000 scale.

A. A. Stoyanow (1926 and 1936) has described some of the Paleozoic strata of the Chiricahua Mountains. R. M. Hernon (1935) reported on the fauna of the Paradise formation. Enlows (1951, 1955) described the Cenozoic volcanic rocks of the Chiricahua National Monument. Sabins (1957) has described the Paleozoic and Mesozoic stratigraphy of the central part of the Chiricahua-Dos Cabezas Mountains and has presented an abstract (Sabins, 1955) outlining the tectonic history of the area. The 1953 field trip guide book of the New Mexico Geological Society contains some brief geologic notes and a small-scale map of part of the mountains. Meinzer and Kelton (1913) described the geology and groundwater resources of the Sulphur Spring Valley, and Schwennesen (1917) studied the San Simon Valley.

Scope of Work

Field work for the present study extended from June 1953, to September 1953, and from June 1954, to mid-September 1954. Two weeks in the spring of 1957 were spent checking the geologic map. Mapping was done on aerial photographs (scale 1/39,230) purchased from the U. S. Geological Survey, and data were transferred with the aid of a stereoscope to the topographic base map enlarged to a scale of 1/31,250. Dips were measured to the nearest 5°. Color nomenclature follows the Rock-color chart of the National Research Council (1948).

Acknowledgments

The author is indebted to numerous organizations and individuals for assistance and encouragement during the course of this study. E. D. McKee aided in selection of the problem, and the Humble Oil and Refining Company generously financed the two seasons of field work. E. F. Hollyday ably assisted in the second season's work. Laboratory and living expenses were defrayed by the H. G. Ferguson and the Sterling Fellowships at Yale. C. O. Dunbar and C. R. Longwell gave generously of their time in supervising the dissertation, and John Rodgers offered numerous helpful suggestions. C. A. Anderson and E. D. Wilson reviewed the manuscript. James Gilluly and J. R. Cooper of the U. S. Geological Survey supplied useful information on the Dragoon and Little Dragoon Mountains. In the field, the author profited from the visits of C. R. Longwell, and of J. L. Wilson and Otto Majewski of the Shell Development Company. The residents of the area were all cooperative, and special thanks are extended to R. L. Barrel and the staff of the Chiricahua National Monument, Mr. and Mrs. R. L. Brittain of the Hilltop Mine, and Mrs. E. F. Bates of the Yucca Lodge, Bowie. The facilities of the Southwestern Research Station of the American Museum of Natural History were made available to the writer during a 2-week trip in the spring of 1957.

Geography

Regional Setting

Together, the Chiricahua-Dos Cabezas Mountains constitute a typical range in the Mexican Highland section of the Basin and Range province. The ranges in this section are well-dissected block mountains separated by broad, aggraded, semi-desert valleys, some of which have through drainage whereas others are closed basins. The Dos Cabezas Mountains are separated from the Chiricahua Mountains by the divide called Apache Pass. This separation is one of nomenclature only, for the mountains on the two sides of the Pass are similar physiographically and geologically. It is convenient to refer to the entire mountain block as "the range."

North of Lat. 32° 00′, the range trends northwestward and is 35 miles long by 10 miles wide. South of this latitude, it trends northward and is 25 miles long by 20 miles wide. The Dos Cabezas Mountains reach their maximum altitude of 8369 feet at the Dos Cabezas Peaks northwest of the area shown on Plate 1. The Chiricahuas reach their maximum elevation of 9795 feet at Flys Peak and Chiricahua Peak, south of the area shown on Plate 1. To the south, the Chiricahuas join the Pedregosa and the Perilla Mountains. The Dos Cabezas Mountains are separated from the Graham Mountains to the north by Railroad Pass, a broad divide between the Sulphur Spring Valley to the west and the San Simon Valley to the east.

The San Simon Valley on the east side of the range separates it from the Peloncillo Mountains in New Mexico which trend parallel

to the range. The valley is drained by the intermittent San Simon Creek which drains northward to the Gila River. The range is separated from the Dragoon, the Little Dragoon, and the Winchester Mountains to the west by Sulphur Spring Valley (Fig. 1). The northern half of this valley has no exterior drainage and is the site of the Willcox Playa. The southern half drains south into Mexico through the intermittent Whitewater Draw.

Local Features

The area of this report includes the southern part of the Dos Cabezas Mountains and the northern part of the Chiricahua Mountains. This area includes the largest and best-exposed outcrops of Paleozoic strata in the entire range. The mountainous belt within the area is about 22 miles long from the northwest corner of the Cochise Head quadrangle southeast to Blue Mountain. The mountains are only 2½ miles wide at Apache Pass, but along the south border of the area they are 9 miles wide. Viewed from either side, the mountains are an impressive array of rugged ridges and peaks rising abruptly from the surrounding valleys. The ridges are cut by narrow canyons that give a somewhat serrated profile to the range.

The highest elevations are in the southern part of the area where many peaks and ridges are higher than 7000 feet and Cochise Head, the highest point (elevation 8109 feet), dominates the landscape and provides a name for the quadrangle. The height of the range decreases toward Apache Pass, which is the narrowest and lowest part. Northwest from the Pass, the ridges become higher and reach elevations in excess of 6000 feet. The lowest point is in the northeast corner of the area where the elevation of the San Simon Valley is 3640 feet. The maximum relief is 4470 feet, but the local relief is less; near Wood Mountain it is 2500 feet, but elsewhere it is generally less than 2000 feet.

Drainage

There are no permanent streams within the area, as the numerous water courses flow for only a few days each year during the short but often heavy rainstorms of July and August. Usually all the runoff sinks into the bolson deposits of the valleys within a few miles of the range front. There are only seven permanent springs, all utilized by the inhabitants for domestic water supplies.

The range is a high drainage divide between the adjacent valleys. Stream piracy seems imminent at several points along the narrow divide, for the canyons draining into the San Simon Valley have steeper gradients because that valley is almost a thousand feet lower than the Sulphur Spring Valley.

Within the mountains, the streams are well adjusted to structure. In the areas of stratified rocks the streams trend northwestward or southeastward, parallel to the strike. The cross-axial streams commonly follow fault zones.

Climate, Vegetation, and Culture

The climate of southeast Arizona is semi-arid, for even the driest parts of the valleys receive more than 10 inches of precipitation annually. The mountains receive more precipitation; data kindly supplied by Acting Superintendent J. A. Randall show that for the period from 1940 to 1954, the average annual precipitation at the weather station of the Chiricahua National Monument (elevation 5380 feet) has been 18.24 inches. During this period, the wettest year was 1948, in which rainfall was 25.24 inches, and the driest was 1953, in which rainfall was 12.07 inches. July and August are the wettest months and have an average rainfall of 3.29 and 4.42 inches, respectively. This summer precipitation maximum is due to short, but frequently heavy, local rain storms that usually occur in the afternoon after a morning buildup of clouds over the mountains.

Data from the Chiricahua National Monument weather station covering the period from 1948 through 1954 show that January is the coldest month and has an average mean temperature of 42.1° F., and July is the hottest and has an average mean temperature of 74.0°. The lowest recorded temperature is −1° and the highest is 102°. The diurnal temperature range is high and averages about 30°. Temperatures in the valleys are several degrees higher than those in the mountains and also have a higher diurnal range.

The low lying San Simon Valley is covered with greasewood or creosote bush. The part of the Sulphur Spring Valley within the area of this report has a cover of sod and grass that provides excellent pasturage for cattle. The lower, rocky slopes of the mountains support a growth of ocotillo, Spanish dagger, yucca, mescal, sotol, cactus, and scrub oak. Along the canyon floors are cottonwood, walnut, hackberry, and other trees that require more

water. The higher parts of the Chiricahuas have large stands of pine and oak and an undergrowth of manzanita and other shrubs.

The area of this report is sparsely populated. Except for the staff of the Chiricahua National Monument and an occasional prospector, all the residents are cattle ranchers. In the valleys beyond the area of this report, irrigated farming is the major occupation.

Precambrian Rocks

Introduction

The Precambrian rocks of Arizona belong to two major systems which Butler and Wilson (1938, p. 11) have termed the younger and older Precambrian. The older Precambrian includes the Pinal Schist of southeast Arizona, the Yavapai Schist of central Arizona, and the Vishnu Schist of the Grand Canyon. Also included are large intrusions of granitic rocks. The younger Precambrian includes the Apache Group of central and southeast Arizona and the Grand Canyon "Series." These are sedimentary rocks unconformably overlying the older Precambrian and postdating the intense Precambrian orogenies which deformed and metamorphosed the older rocks. Only the older Precambrian rocks occur in the Chiricahua-Dos Cabezas Mountains, but younger Precambrian strata occur in the Little Dragoon Mountains 30 miles to the west.

Pinal Schist

General.—The name Pinal Schist was given by Ransome (1903, p. 23) in the Pinal Mountains near Globe to rocks ranging from cryptocrystalline slaty sericite schists to crystalline muscovite schists. In the Chiricahua-Dos Cabezas Mountains, the Pinal Schist crops out along the northeast front of the range where it forms slopes beneath the ledges of overlying Bolsa Quartzite (Cambrian). North of the main range front, the Pinal forms low ridges and hills, some of which are isolated from the main range front by alluvial fan deposits. It also forms part of a large fault block on the southwest side of the range near Helens Dome and Bowie Mountain. Timber Mountain in the S ½ sec. 1, T. 16 S., R. 29½ E., is part of another large block of Pinal Schist faulted against the Naco Group (Pennsylvanian and Permian) and the Faraway Ranch Formation (Tertiary). Everywhere in the area the Bolsa Quartzite unconformably overlies the Pinal Schist, and the younger Precambrian Apache Group is absent.

Typical Pinal hand specimens are aphanitic to fine-grained, dark greenish gray, and commonly color-banded. No minerals are identifiable megascopically. Foliation is not strongly developed, but the schist splits fairly readily along planes that have a satiny sheen and undulatory surfaces. The foliation is parallel to the color and grain-size banding that indicates the stratification of the original sedimentary rocks from which the Pinal was formed. In the numerous small folds in the Pinal, the foliation bends around the crests of the folds. The outcrops at the NE ¼ SE ¼ sec. 24, T. 15 S., R. 28 E., include many very thin, lenticular beds of white quartzite that are tightly folded. Along the northeast front of the range the strike of the foliation ranges from westward to northwestward, and there are some southwestward-striking foliations in the vicinity of Long Canyon. These outcrops are in the autochthonous part of the range, which has not been strongly affected by the post-Comanche to pre-Pliocene thrusting. At Timber Mountain the foliation trends N. 50° W., but these outcrops are in a fault block so the original orientation of this foliation cannot be determined.

Petrographic study of a thin section cut normal to the foliation of a Pinal specimen from the SW ¼ sec. 8, T. 15 S., R. 29 E., showed that quartz and sericite in about equal proportions are the major constituents. The quartz occurs as extremely fine interlocking grains. The sericite occurs as birefringent, extremely fine-grained flakes aligned parallel to the schistosity. The preferred orientation of the flakes is such that nearly all undergo optic extinction simultaneously when the stage is rotated. The lamellae of the schist are deformed by numerous small "crinkles" or flexures. The only other mineral observed was magnetite, which occurs as small euhedral grains cutting across the schistosity and indicates that it was formed by replacement after the schist was formed.

Several different rock types are included in the Pinal. At the outcrops immediately below the Bolsa Quartzite on the north face of the ridge southwest of the Lawhon Ranch (SW ¼ SW ¼ sec. 36, T. 14 S., R. 28 E.) there is a conspicuous boulder bed about 4 feet thick. The foliation wraps around the rounded cobbles and small boulders of pink quartzite. Originally this bed was a quartzite conglomer-

ate in a silty matrix that was metamorphosed to Pinal Schist. Dark-colored quartzose metadiorite occurs in secs. 26, 27, and 28, T. 14 S., R. 28 E., where the contacts are parallel to the foliation of the schist. All these rocks are foliated, except in the NE ¼ sec. 26, T. 14 S., R. 28 E., where they are massive. In mapping, all these rocks were included in the Pinal.

Quartzite member.—A quartzite member is the most conspicuous unit of the Pinal Schist for it forms the rugged precipice of Bowie Mountain and the ridge southwest of Helens Dome. It was mapped as a separate unit in order to show the Precambrian structure more clearly. The medium- to coarse-grained quartzite is light pink to light gray and has some black laminae. There is much cross-stratification, which aids in determining the top and bottom of the sequence. On weathering, the very resistant, massive quartzite forms cliffs with large talus accumulations at the base. The talus covers much of the quartzite-schist contacts, which are rather sharp at the few exposures. Along the west side of Bowie Mountain the quartzite is intruded by the Rattlesnake Point Granite (Precambrian). Near Helens Dome the basal part of the member is a conglomerate of variable thickness composed of rounded cobbles and boulders of quartzite and mafic igneous rocks.

The quartzite member was originally a pure quartz sandstone interbedded with the strata which were metamorphosed to form the Pinal Schist. During the Precambrian orogeny, the competent quartzite was folded into a northward-trending syncline which is now tilted so that it plunges vertically to form the horseshoe-shaped outcrop at Bowie Mountain. The foliation of the Pinal Schist stratigraphically above and below the quartzite trends parallel to the syncline. The schist within the trough of the syncline has been tightly folded on a small scale.

Origin of the Pinal Schist.—The original sedimentary strata of the Pinal Schist constituted a very thick, entirely clastic sequence with some mafic igneous rocks. In the Little Dragoon Mountains, Cooper and Silver (1954, p. 38) have concluded that the Pinal is a eugeosynclinal accumulation of sedimentary and volcanic rocks deposited in a trough of unknown extent. This trough was the site of Wilson's (1939, p. 1161) early Precambrian Mazatzal revolution. None of the field evidence from the Chiricahua-Dos Cabezas Mountains is contradictory to this interpretation.

Igneous Rocks

General.—Within the area of this report are three distinct types of Precambrian igneous rocks, which were intruded in a definite sequence. The oldest is the small Sheep Canyon stock of gneissose granite, which was deformed contemporaneously with the Pinal Schist. The large pluton of Rattlesnake Point Granite was emplaced after the Precambrian orogeny. The youngest Precambrian intrusives are aplite dikes that cut all the other Precambrian rocks. The Precambrian relationships are shown on Figure 2.

Sheep Canyon Granite.—The Sheep Canyon Granite crops out in the northwest corner of Plate 1 over an area of about 4 square miles. It is bounded on the west by a Tertiary stock of quartz monzonite, and on the south by the Pinal Schist. On the north and east it is overlapped by the alluvium of the San Simon Valley; hence the original extent of the granite in those directions cannot be determined. The granite is fairly resistant to weathering and forms a group of large knobs and hills cut by the steep-sided gorge of Sheep Canyon.

The Sheep Canyon Granite has a rather sharp, almost vertically dipping intrusive contact with the Pinal Schist. No chill border occurs at this contact. Some small tabular masses of granite that are completely enclosed by the schist near the contact are apophyses connected at depth with the main Sheep Canyon stock. Both the schist and the granite are cut by thin pegmatitic stringers consisting of quartz, white feldspar, and small muscovite books The schist is somewhat coarser-grained at the contact and contains some medium-sized muscovite flakes; this is the only evidence of contact metamorphism at the periphery of the stock. Typical hand specimens of the granite are very pale orange on fresh surfaces and weather light brown. There are numerous limonite-stained joints. In outcrops, the most striking characteristic of the Sheep Canyon Granite is its gneissose texture which trends approximately parallel to the N. 50° W. strike of the foliation in the adjacent Pinal Schist. The gneissose texture is formed by bands of quartz grains separating large feldspar grains which have a maximum length of seven mm. Under the microscope this texture is very pronounced, for the quartz bands consist of small interlocking anhedral grains that show undulose extinction and are elongated parallel to the gneissose bands. The large feldspar grains are altered perthite with small euhedral inclu-

sions of strongly altered plagioclase. There are a few small bent flakes of almost uniaxial colorless mica, which contain very small zircon inclusions.

The gneissose texture, bent mica flakes, and quartz grains with undulose extinction clearly show that the Sheep Canyon stock has been strongly deformed. The gneissose structure of the granite trends approximately parallel to the schistosity of the Pinal, so both these rock units must have been deformed by the same Precambrian orogeny, and the Sheep Canyon stock is a synkinematic intrustion. Both the schist and granite are cut by post-kinematic aplite dikes.

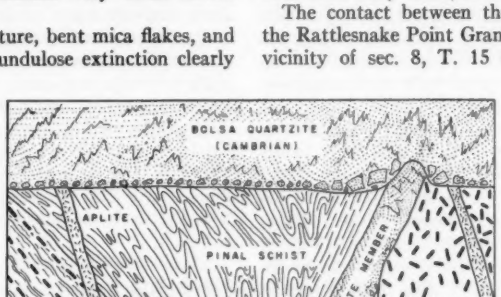

FIGURE 2.—DIAGRAM OF PRECAMBRIAN RELATIONSHIPS
(Not to scale)

Rattlesnake Point Granite.—The nonfoliated Rattlesnake Point Granite forms most of the Precambrian outcrops in the area of this report. It crops out along the northeast front of the range from the vicinity of the Emigrant Hills and Little Emigrant Canyon east to Rattlesnake Point from which the granite takes its name (Pl. 1). It also crops out along the north flank of Blue Mountain and in the large fault block at Timber Mountain. The other main occurrence is on the southwest side of the range in the vicinity of Apache Pass where the granite forms the major part of a large fault block. The topographic expression of the granite varies with the distribution of the joints that cut it. Along the northeast front of the range, the jointing is not very intense, and the granite forms rugged outcrops cut by numerous steep-walled canyons. The more strongly jointed granite of the fault block at Apache Pass forms a low, well-dissected terrane with many small, rounded hills.

The contact between the Pinal Schist and the Rattlesnake Point Granite crops out in the vicinity of sec. 8, T. 15 S., R. 29 E. This steeply dipping contact is sharp and truncates the folds and schistosity of the Pinal. The granite at the contact is fine- to medium-grained and has no mafic chill border. Within 10–20 feet of the contact, the fine-grained border rock grades into the typical coarse-grained granite. A few narrow granite apophyses extend a few tens of feet into the Pinal. The Rattlesnake Point-Pinal contact at Timber Mountain is similar to that just described. At the west side of Bowie Mountain the granite cuts the quartzite member of the Pinal Schist, but no visible contact metamorphism occurs in the quartzite.

The granite is coarse-grained with a granitic-porphyritic texture. Fresh surfaces are greenish gray and weather light brown. The most conspicuous feature is the abundant large light-colored euhedral feldspar phenocrysts which have maximum dimensions of 15 by 25 mm and commonly show carlsbad twinning. At Rattlesnake Point and other outcrops, there is a pronounced flow-type preferred orientation of the feldspar phenocrysts. Other minerals visible to the naked eye are milky quartz and dark-greenish-gray ferromagnesian grains. Microscopic study of a typical specimen from the SE ¼ SE ¼ sec. 16, T. 15 S., R. 29. E showed

that the phenocrysts consist of well-altered perthite with numerous unaltered plagioclase inclusions. Other plagioclase occurs as discrete, medium-sized, highly altered euhedral grains that were originally albite. Large clear interlocking anhedral grains of quartz fill the interstices between the feldspar grains. The estimated proportions are: quartz—20 per cent, perthite—60 per cent, albite—10 per cent, ferromagnesian minerals—10 per cent.

The Precambrian age of the Rattlesnake Point Granite is clearly established where the Bolsa Quartzite (Cambrian) unconformably overlies it. The quartzite is not metamorphosed and locally contains cobbles of the granite in its basal conglomerate. The granite is post-kinematic, for it was emplaced after the deformation of the Pinal as shown by the sharp intrusive contact cutting the Pinal schistosity and by the undeformed texture of the granite. The granite is cut by the Precambrian aplite dikes.

Aplite dikes.—In the northwest corner of the Cochise Head quadrangle, a swarm of northeastward-trending silicic dikes cuts the Pinal Schist and the Sheep Canyon Granite. These dikes are clearly Precambrian, for at several localities along the range front they are truncated by the Bolsa Quartzite. West of the area of this report, similar dikes that occur within the Rattlesnake Point Granite are also truncated by the Bolsa. The dikes are several feet wide and generally are less than a mile in length. No attempt was made to plot all of the dikes on the geologic map, but the major ones are shown. They are very conspicuous in the field where they form light-colored outcrops in contrast to the darker colors of the surrounding schist and granite.

A typical hand specimen from the SE ¼ sec. 28, T. 14 S., R. 28 E. is yellowish gray, weathering to dark-yellowish orange. The rock is holocrystalline, has a sugary appearance, and is so fine-grained that no minerals are identifiable megascopically. Under the microscope the rock shows an aplitic texture formed by equigranular interlocking anhedral grains of orthoclase and quartz. The orthoclase exhibits some carlsbad twinning and comprises about 60 per cent of the rock. Less than 5 per cent consists of accessory minerals, mainly light-green flakes of biotite that have a very low 2V and high birefringence. The texture, mineralogy, and mode of occurrence of these dikes indicates that they are aplites developed from residual solutions formed late in the solidification of the Rattlesnake Point pluton, for they cut the pluton as well as older rocks.

Paleozoic and Mesozoic Stratigraphy

The stratigraphy of the central part of the Chiricahua and Dos Cabezas Range has already been described (Sabins, 1957), so only the general features will be given here. The general lithology, thickness, and age of the formations are given in Table 1. The pre-Pennsylvanian strata were deposited on a slowly subsiding shelf that underwent epeirogenic uplift from Middle Ordovician through Middle Devonian time. The rate of subsidence accelerated during the Pennsylvanian and Permian, for the strata deposited during these periods are much thicker than the older ones. The total thickness of the Paleozoic section exceeds 7600 feet.

The Lower Cretaceous strata, which rest with angular discordance on the Paleozoic beds, were deposited in a tectonic setting that was very different from that of the Paleozoic (McKee, 1951, p. 495). Southeast Arizona was the site of a trough that subsided fairly rapidly and was filled with predominantly clastic sediments. In the area of this report, the Lower Cretaceous beds exceed 2500 feet in thickness and are referred to the Bisbee Group. At the type area in the Mule Mountains, the Bisbee Group is divided into four formations, but in the Chiricahua-Dos Cabezas Mountains the group was divided into two map units; the Glance Conglomerate at the base, and the "middle and upper Bisbee strata" for the remainder of the group.

Except for the Paradise Formation, all the units on Table 1 are fairly widely distributed throughout the area of this report. The Paradise Formation is restricted to the southern Chiricahua Mountains and adjacent parts of southwest New Mexico. The outcrop at Blue Mountain is the northwesternmost extension of the Paradise Formation. Its absence from the rest of the map area is due to nondeposition or to pre-Pennsylvanian erosion.

Cenozoic Rocks

Nipper Formation

Type locality.—The Nipper Formation is here named for mafic volcanic conglomerates, flows, and associated sedimentary rocks that make up the Nippers and other hills south of Blue Mountain in the southwest corner of the

TABLE 1.—PALEOZOIC AND MESOZOIC FORMATIONS OF THE CHIRICAHUA AND DOS CABEZAS MOUNTAINS

System	Series	Group and Formation	Thickness (feet)	Lithology
Cretaceous	Lower Cretaceous (Comanche)	Bisbee Group: "Middle and upper Bisbee strata"	2500±	Quartzite and siltstone member Limestone member Reddish-purple siltstone member
		Glance Conglomerate	0–1000±	Rounded cobbles and boulders of limestone, quartzite, and volcanic rocks
		Major Angular Unconformity		
Permian	Guadalupe (?) to Leonard	Naco Group: Concha Limestone	245–730	Light- to dark-gray limestone with abundant chert and silicified fossils
	Leonard	Scherrer Formation	120–150	Quartzitic sandstone with basal red-bed member
	Leonard to Wolfcamp	Colina Limestone	473–535	Black aphanitic limestone with locally abundant silicified fossils
	Wolfcamp to Virgil	Earp Formation	2700±	Alternating limestone, shale, and sandstone beds; large fusulinids common
Pennsylvanian	Virgil to Morrow	Horquilla Limestone	1605	Pure limestone with abundant chert and Pennsylvanian fossils—fusulinids, corals, and brachiopods
		Disconformity		
Mississippian	Upper Mississippian	Paradise Formation	0–150	Brown shaly limestone, alternating with shale and sandstone; abundant *Archimedes*
	Lower Mississippian	Escabrosa Limestone	630–730	Massive, light-gray, pure limestone; crinoidal; chert nodules common
		Disconformity		
Devonian	Upper Devonian	Portal Formation	200–342	Thick-bedded shale and limestone member Thin-bedded shale and limestone member Black, fissile, siliceous shale member Thin-bedded shale and limestone member
		Disconformity		
Ordovician and Cambrian	Canadian to Croixian	El Paso Formation	340–715	Thin- to medium-bedded limestone and dolomite; some chert
Cambrian	Croixian to Albertan (?)	Bolsa Quartzite	320–600	Cross-stratified quartzite, shaly toward top Basal conglomerate
		Major Unconformity Precambrian Basement		

Vanar quadrangle[1]. The Nipper Formation holds up the ridge between Whitetail and Indian creeks in sec. 20, T. 16 S., R. 30 E. It forms a large fault slice southwest of Cochise Head, which is the northern and westernmost exposure of the formation within the area of this report. The unit forms dark hills and ridges, in contrast to the light-colored peaks and cliffs formed by the overlying volcanic rocks of the Faraway Ranch Formation.

At the ridge between Whitetail and Indian creeks, the Nipper Formation unconformably overlies upper Paleozoic strata that dip steeply southwestward. Although the contact is poorly exposed, its unconformable nature is demonstrated in the SW ¼ sec. 20, T. 16 S., R. 30 E., where erosional inliers of Colina Limestone are surrounded by Nipper rocks. The overlapped Paleozoic strata reappear farther northwestward along their strike, and here the poorly exposed Nipper rocks rest on Glance Conglomerate and higher members of the Bisbee Group (Lower Cretaceous). Southeast of Portal (Fig. 1) the Nipper Formation overlies the Bisbee Group. The upper contact of the Nipper Formation is widely exposed and marked by the change from mafic volcanic rocks and dark sediments to the pink rhyolite and rhyodacite of the Faraway Ranch Formation. The massive and poorly stratified nature of much of the Nipper Formation makes it difficult to determine accurately its structural relationships to the units above and below it. Only in the Whitetail Creek locality is there evidence for angular discordance at the lower contact. There is no pronounced angular discordance at the upper contact.

Petrology.—The lower half of the Nipper Formation is a thick conglomerate of mafic volcanic rocks. The poorly sorted, well-rounded cobbles and boulders range up to several feet in diameter, with a maximum size of 12 feet for one boulder on the east side of the Nippers. These clasts consist of aphanitic to porphyritic altered andesite and possibly basalt, tightly cemented in a matrix of graywacke sandstone. Very dark purple and green are the dominant colors. There are some rare cobbles of Paleozoic limestone.

Similar conglomerates occur higher in the formation, but are interstratified with dark-green augite basalt flows and graywacke sandstones. South of the Nippers, a 20-foot bed of Paleozoic limestone conglomerate is interstratified with this sequence. Light-weathering aphanitic andesite flows comprise much of the upper part of the formation, and are conspicuous along Whitetail Creek where they crop out as high ledges. In thin section this rock consists of andesine microlites in parallel flow arrangement, set in a glassy matrix that is locally devitrified to a microcrystalline aggregate.

Age.—The Nipper Formation is unfossiliferous, but is clearly post-Comanchean for it overlies the Bisbee Group. The succeeding volcanic units are also unfossiliferous, however, and the Nipper Formation can only be dated as late Cretaceous to Tertiary. It was involved in the major post-Comanche to pre-Pliocene orogeny.

Faraway Ranch Formation

General.—The Faraway Ranch Formation was named by Enlows (1951) for exposures near the Faraway Ranch, a short distance west of the Chiricahua National Monument. The unit consists of a complex of volcanic flows and agglomerates and some stream-deposited tuff and lacustrine deposits. In the southeast part of the area of this report, the Faraway Ranch Formation overlies the Nipper Formation, but to the north and west, the Nipper Formation is absent and the Faraway Ranch rocks unconformably overlie the Bisbee Group. The Faraway Ranch Formation is overlain by the Rhyolite Canyon Formation.

The Faraway Ranch Formation crops out in the vicinity of the Chiricahua National Monument and also covers much of the eastern part of the area of this report where it forms very rugged topography with numerous peaks and cliffs. To the south, the Chiricahua Mountains consist largely of volcanic rocks very similar to this formation and the Rhyolite Canyon Formation.

Volcanic rocks.—All but a minor part of the formation consists of volcanic flows and agglomerate. The pale-reddish-brown-weathering porphyritic flows that constitute the major part of the formation are typically banded, and thin, pale red layers alternate with pinkish-gray layers. The color layers are parallel and at many localities there are well-developed flow structures. Petrographic study of a specimen from the SW ¼ SW ¼ sec. 5, T. 16 S., R. 30 E., showed that the rock consists of

[1] In a letter of April 10, 1957, George V. Cohee, Chairman of the Geologic Names Committee of the U. S. Geological Survey, stated that the name Nipper Formation was not pre-empted and would be reserved for the writer's use.

euhedral phenocrysts (20 per cent) of andesine, sanidine, quartz, and a few brown biotite flakes in a cryptocrystalline, somewhat glassy matrix that has a faint flow texture. A specimen from the NE ¼ sec. 27, T. 16 S., R. 29 E., consists of euhedral phenocrysts (35 per cent) of sanidine, zoned andesine, and brown biotite, in a glassy matrix with pronounced flow texture. The mineralogy of these flows indicates that they are rhyodacites and rhyolites. At least 2000 feet of these rocks are exposed at Cochise Head.

The layering of the flows dips southward to southwestward at angles ranging from 15° to 35° and becoming steeper in the vicinity of the major faults along Whitetail and Indian creeks. No vents were found within the area of this report; therefore the source of the flows must have been in the central or southern part of the Chiricahua Mountains where the volcanic rocks are very thick.

The agglomeratic phase of the formation is well exposed in the road cut just north of the Ranger Station at the Chiricahua National Monument. It consists of angular fragments of dark basaltic rock up to a foot in diameter enclosed in a tuffaceous matrix.

Two basalt flows in the formation are exposed in the road cut in the NW ¼ NE ¼ sec. 19, T. 16 S., R. 30 E. The lower flow is purplish black and is separated from the overlying greenish-black flow by an irregular surface marked by a thin layer of red clay. Both flows are vesicular and contain some amygdules. The upper flow is overlain by lacustrine red beds.

Sedimentary rocks.—Lenses of lacustrine deposits and stream-deposited tuff constitute a minor part of the formation. The two distinct types of lacustrine deposits are a red clastic sequence and a light-colored sequence containing fresh-water limestone. The red sequence is well exposed at the road cuts near Bonita Park, where it consists of medium- to thin-bedded, dark-red sandstones and shale with numerous pebbles and granules of volcanic rocks. This is probably the "Bonita Park formation" mentioned by Enlows (1955, Table 1), but the unit is here considered a member of the Faraway Ranch Formation because it is of insufficient size and continuity to be a mappable formation. The beds are cut by numerous white gypsum veinlets. The red beds are overlain by medium- to thin-bedded white sandstone, derived from silicic volcanic rocks. The Faraway Ranch Formation contains lenses of red sediments at other localities within the area of this report.

A typical exposure of the light-colored lacustrine sequence along the north side of Keating Canyon consists of about 30 feet of very fine-grained, soft, brown tuff overlain by about 25 feet of laminated flaggy aphanitic limestone with some beds of fine-grained sandstone. The yellowish-gray limestone weathers grayish orange, has a fetid odor, and is cut by numerous stylolite seams parallel to the stratification. Some of these unfossiliferous limestone beds contain abundant small gray chert nodules. The lacustrine origin of the red beds and the limestone sequence is suggested by their very even stratification and lenticular distribution. The lakes in which these sediments were deposited probably formed where volcanic flows blocked stream channels.

Lenses of stream-deposited tuff are exposed along Little Picket Canyon in the SE ¼ NW ¼ sec. 26, T. 16 S., R. 29 E., and along Picket Canyon. The soft, white tuff is thin- to medium-bedded, and commonly is cross-stratified.

PLATE 2.—PHOTOMICROGRAPHS

FIGURE 1.—Welded tuff. Rhyolite Canyon Formation (Tertiary) from N ½ SE ¼ sec. 26, T. 16 S., R. 29 E.; crystal fragments of sanidine (with carlsbad twinning) and quartz, set in matrix of devitrified glass; (X-nicols, × 10).

FIGURE 2.—Welded tuff. Same as Figure 1, in plain light. Note outlines of glass shards that impart the vitroclastic texture typical of welded tuffs; (Plain light, × 10).

FIGURE 3.—Quartz monzonite. From Tertiary stock in sec. 13, T. 15 S., R. 29 E. Embayed quartz and fresh oligoclase are the major constituents; (X-nicols, × 10).

FIGURE 4.—Quartz monzonite porphyry. From Tertiary sill in sec. 17, T. 16 S., R. 30 E.; phenocrysts of cloudy, altered feldspar and embayed quartz in finely crystalline altered matrix; (plain light, × 10).

FIGURE 5.—Granite. Rattlesnake Point Granite (Precambrian) from SE ¼ SE ¼ sec. 16, T. 15 S., R. 29 E.; quartz and strongly altered feldspar; (nicols X-60°, × 10).

FIGURE 6.—Gneissose granite. Sheep Canyon Granite (Precambrian) from synkinematic stock in SW ¼ sec. 23, T. 14 S., R. 28 E.; stretched quartz with undulose extinction, strongly altered feldspar; outside this field are large muscovite flakes with zircon inclusions; (X-nicols, × 10).

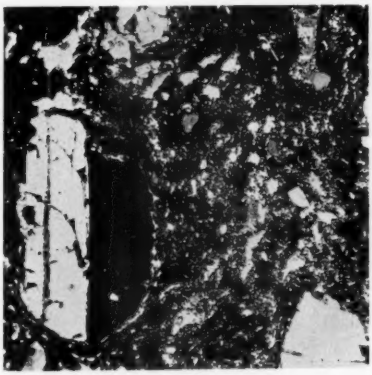

FIGURE 1

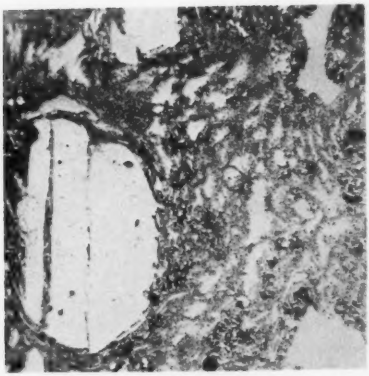

FIGURE 2

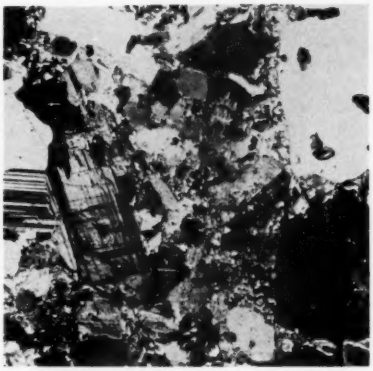

FIGURE 3

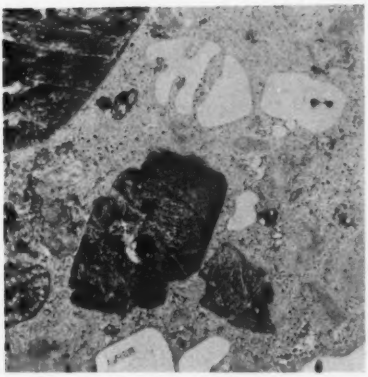

FIGURE 4

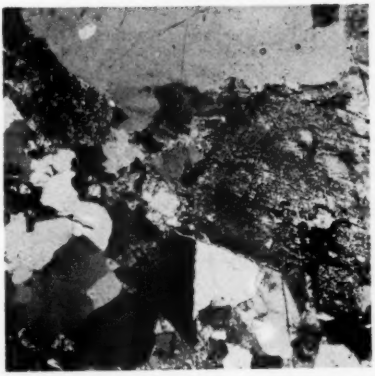

FIGURE 5

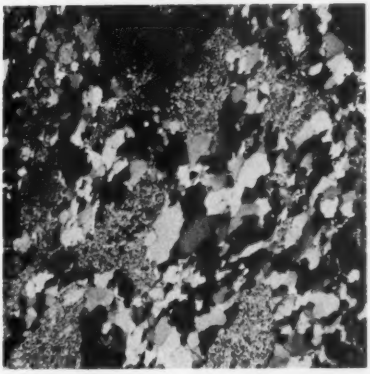

FIGURE 6

PHOTOMICROGRAPHS

BOWIE MOUNTAIN AND VICINITY

Graded beds of small fragments of mafic volcanic rocks in a tuffaceous matrix are common in the lenses.

Age.—No fossils have been identified from the Faraway Ranch Formation, but a study of its sparse pollen flora is being undertaken. Without fossils, the unit can be dated only as late Cretaceous to late Tertiary. The formation was not found to be involved in the earliest thrust faulting of the post-Comanche—pre-Pliocene orogeny, but it is involved in the later faulting. It is cut by small intrusions that are younger than the post-Comanche orogeny, and was affected by the normal faults of the Basin and Range orogeny (Pliocene?).

Rhyolite Canyon Formation

General.—The Rhyolite Canyon Formation was named by Enlows (1951) for exposures along Rhyolite Canyon in the Chiricahua National Monument. In the original description the volcanic rocks of Sugarloaf Peak were put in a separate formation, but later Enlows (1955, Table 2) included all the volcanic rocks above the top of the Faraway Ranch Formation in the Rhyolite Canyon Formation. Within the area of this report, the Rhyolite Canyon Formation occurs only in the vicinity of the Chiricahua National Monument, but great thicknesses of similar rocks occur farther south in the Chiricahua Mountains. The massive units of the formation crop out in cliffs more than a hundred feet high. The rocks exposed in these cliffs are strongly jointed and weather to form columns and balanced rocks.

The formation consists of several volcanic members ranging in thickness from a few feet to almost a thousand feet; the thickest is the unit which Enlows (1955, p. 1229) called member six and which forms the most spectacular columns and balanced rocks. All the members become thinner and pinch out toward the west. Most of them are similar to member six, which is composed of massive, pale red-purple welded rhyolite tuff that weathers light brownish gray. The bulk of the member is hard and compact, and rings when struck by a hammer. The upper few feet consists of unconsolidated light-gray tuff. There are numerous flattened inclusions of white pumice that give a pseudostratified (eutaxitic) appearance to the outcrops. At the south side of hill 5425 in the SW ¼ sec. 22, T. 16 S., R. 29 E., the basal 4 feet contain numerous spherical inclusions up to 3 inches in diameter that consist of structureless dark-reddish-brown rhyolite. The base of the member here overlies a thin flow of black porphyritic obsidian that rests with angular discordance on the Faraway Ranch Formation. Elsewhere, member six is underlain by other welded rhyolite tuff members of the Rhyolite Canyon Formation.

Petrography.—Petrographic examination of a typical specimen from the base of member six just north of the Silver Spur Ranch shows that crystals and crystal fragments of quartz and opalescent sanidine constitute 30 per cent of the rock. The anhedral quartz crystals are shattered and broken and are commonly strongly embayed. The euhedral to subhedral sanidine crystals show carlsbad twinning and are also shattered and broken. There are a few small flakes of reddish-brown biotite. The matrix has a pronounced vitroclastic texture formed by curved glass shards that surround the crystal fragments (Pl. 2, figs. 1, 2). Many of these shards are flattened and squeezed between adjacent crystal fragments. The shards are devitrified to microcrystalline aggregates. Numerous specks of opaque minerals give the matrix a dusty appearance.

The dominance of the alkali feldspar sanidine and the presence of quartz show that this rock is of rhyolitic composition. The vitroclastic texture of the ground mass, and the presence of crystal fragments, the flattened pumice inclusions, and other features show that the rock is a welded tuff. The welded tuff of the Rhyolite Canyon Formation is lithologically similar to the Bishop welded tuff of eastern California, which Gilbert (1938, p. 1852) showed to be a deposit formed by *nuées ardentes*. This is probably the origin of the massive rhyolite members of the Rhyolite Canyon Formation as pointed out by Enlows (1955). As the members become thinner to the west and thicker to the south, the vents from which the *nuées ardentes* originated were probably located to the south of the area of this report.

The top member of the formation is the dark vesicular rhyodacite flow, about 200 feet thick,

PLATE 3.—BOWIE MOUNTAIN AND VICINITY

Note the nearly vertically plunging syncline of Precambrian quartzite forming the horseshoe-shaped ridge of Bowie Mountain. The Marble Quarry syncline lies in the high ridges north of Bowie Mountain. For structural details see Plate 1. Vertical air photo No. GS-EP 3-60, U. S. Geological Survey.

that caps Sugarloaf Peak. Some small lenses of cross-stratified, unconsolidated tuff crop out on the peak below the flow.

The base of the formation is the base of the lowest welded tuff member. The Rhyolite Canyon Formation is thus lithologically distinct from the underlying Faraway Ranch Formation. Locally, as along Picket Canyon, there is a pronounced angular discordance in the attitudes of the two formations, probably as a result of pre-Rhyolite Canyon faulting related to the extrusive igneous activity. Elsewhere, the contact is a disconformity marked by a weathered surface.

TABLE 2.—HYPOTHETICAL SEQUENCE OF POST-PALEOZOIC EVENTS

Pliocene (?) to Recent	Basin and Range Faults
Post-Comanche to Pre-Pliocene	Rhyolite Canyon welded tuffs Silicic intrusive rocks Mafic intrusive rocks Apache Pass reverse fault Faraway Ranch volcanic rocks Nipper volcanic and sedimentary rocks Wood Mountain and Apache Pass thrusts
Early Cretaceous (Comanche)	Bisbee Group
Post-Paleozoic to Pre-Comanche	Uplift and erosion

Age.—The unfossiliferous Rhyolite Canyon Formation is probably not much younger than the Faraway Ranch Formation, for it too is cut by faults of the Basin and Range orogeny. Therefore, the Rhyolite Canyon Formation is also tentatively dated as Tertiary.

Intrusions

General.—The numerous stocks, sills, and dikes shown on the geologic map (Pl. 1) consist of intermediate rocks of two distinct types: a dark-colored assemblage of diorites, and a light-colored assemblage of quartz monzonites and related rocks. At several places the diorite stocks are cut by light-colored dikes, showing that the diorites antedate at least some of the quartz monzonite group of intrusions. Possibly the diorites antedate all the light-colored intrusives, for at no place were they observed cutting the quartz monzonites. Many of the igneous bodies cut structures formed by the post-Comanche to pre-Pliocene orogeny, and none of the intrusive rocks were found to be deformed by that orogeny. Therefore, the intrusions must be younger than the orogeny. Several intrusives cut the Nipper and Faraway Ranch formations, but none were seen cutting the Rhyolite Canyon Formation. Therefore, the intrusives are all referred to the Tertiary, with the understanding that there was probably more than one period of intrusive igneous activity during that interval. In addition to the exposed intrusives, it is inferred that there are some concealed stocks in the vicinity of Apache Pass, for there the shales of the Bisbee Group have been converted to chiastolite hornfelses, and the Paleozoic limestones have been strongly recrystallized.

Diorite assemblage.—A group of dark-colored intrusives occurs mainly as small plugs and less commonly as dikes and sills. The intrusive in the NW ¼ sec. 15, T. 15 S., R. 30 E. may be a small laccolith, for the Cretaceous strata below the lowest igneous outcrop are almost horizontal. This intrusion is cut by a northward-trending light-colored dike. The plug in the NW ¼ sec. 29, T. 15 S., R. 29 E. cuts the Apache Pass fault block. The intrusions in the SE ¼ sec. 33, T. 15 S., R. 29 E. and in the vicinity of Buckhorn Basin cut the Bisbee strata. The Buckhorn Basin intrusive is cut by a rhyolite plug. Most of the dark-colored rocks are resistant and form prominent hills, except for the western part of the Buckhorn Basin intrusive, which forms a topographic depression.

All the dark-colored rocks are medium-grained, greenish black, and weather to various shades of brown. Petrographic study of two typical specimens shows that they have a granitic texture and are strongly altered, which makes it difficult to identify the original mineral constituents. Plagioclase, probably andesine, constitutes at least half of the rock, and hornblende is the dominant mafic constituent. Orthoclase and opaque grains and a few small anhedral garnets are the chief accessory minerals. Quartz is present in some of the rocks and absent in others, so the rock type ranges from diorite to granodiorite. A few small basalt plugs are included in this map unit.

Quartz monzonite assemblage.—The majority of the Tertiary intrusive rocks are light-colored

and occur as dikes, sills, and small stocks. The larger bodies are fairly uniform in texture and composition, but these characters are variable in the smaller intrusions. Some of the intrusions are resistant to weathering, and others are nonresistant, so there is no characteristic topographic expression.

Specimens from the stocks are typically porphyritic and have phenocrysts of quartz and white and pink feldspar in a medium-gray matrix. Petrographic study shows the quartz phenocrysts to be anhedral and strongly embayed. The euhedral andesine and perthitic phenocrysts are commonly altered to clay minerals. Hornblende, biotite, and pyrite grains are the chief accessory minerals. The fine-grained matrix consists of interlocking quartz and feldspar grains. The approximately equal proportions of plagioclase and orthoclase, plus the presence of quartz shows that these rocks are quartz monzonite porphyries. Some of the stocks of similar composition are holocrystalline and medium-grained, so they are classified as quartz monzonites.

Alluvial Deposits and Associated Geomorphic Features

The youngest rocks within the area of this report are the stream gravels and valley fill deposits which were mapped together as a single unit. The stream gravels consist of poorly sorted, rounded to subrounded rock fragments of local derivation that cover the floors of the canyons and stream channels. The valley fill consists of detritus eroded from the mountains and deposited in the adjacent valleys. At the foot of the mountains the fill consists of angular cobbles and boulders intermingled with finer-grained sediments. The maximum grain-size decreases rapidly away from the mountains, and a few miles from the bedrock outcrops the surficial deposits are fine-grained sand and silt. Only the uppermost layers of the valley fill deposits are exposed, so the structural relationships cannot be determined. All the surficial deposits are shown as Quaternary alluvium on the geologic map.

The unsuccessful oil well of the Arizona Oil and Gas Corporation, about 2 miles north of Dunn Springs Mountain (sec. 36, T. 14 S., R. 30 E.), penetrated 7568 feet of valley fill (Baldwin, 1956, Table 5) that was mainly rhyolite gravel. Deep-water wells drilled in the center of the San Simon Valley near Bowie and San Simon have penetrated 300–400 feet of impermeable homogeneous blue clay that occurs within 150 feet of the surface and is underlain by more than a thousand feet of gray, yellow, or reddish clay interbedded with sand or fine gravel and thin layers of hard sandstone, according to Schwennesen (1917, p. 8). Meinzer and Kelton (1913, p. 57) reported similar deposits in the Sulphur Spring Valley. Knechtel (1936, p. 83) presented paleontologic and stratigraphic evidence to confirm earlier suggestions that these fine-grained sediments were lacustrine deposits. Knechtel suggested that the lacustrine deposits interfinger with the coarser deposits along the margins of the valleys. His fossil collections from the valley fill in the Gila Valley and the northwestern part of the San Simon Valley established a Pliocene age for part of the deposits.

Alluvial fans built out from the canyon mouths into the valleys are the most striking geomorphic features associated with the alluvial deposits. Where the canyons are closely spaced, the fans have coalesced. The fans are dissected to varying degrees by the distributary drainage channels radiating from the canyon mouths.

The well data showing great thicknesses of valley fill within a short distance from the range front prove that pediments are poorly developed. All the low terrane at the foot of the mountains is covered with detritus, which makes it very difficult to recognize any pediments that might be present. Under these conditions, the only reliable evidence for the presence of pediments is the occurrence of bedrock outcrops in the low terrane. Judged by this criterion the area between the Emigrant Hills and the range front is a pediment veneered with a thin gravel cover. The large indentation in the northeast front of the range at the junction of the Chiricahua and the Dos Cabezas Mountains is a covered pediment formed on the Pinal Schist which here is nonresistant to weathering. The presence of bedrock within a short distance of the surface is established by the isolated schist outcrop in the SE ¼ sec. 25, T. 14 S., R. 28 E., and by bed-rock exposures in several arroyos.

Precambrian Orogeny

Introduction

The earliest orogeny which can be deciphered in the Chiricahua-Dos Cabezas Mountains is the one that caused the metamorphism and deformation of the Precambrian Pinal Schist and its quartzite member. This orogeny

was accompanied by the emplacement of a minor synkinematic granite stock, but the major Precambrian pluton was emplaced after the orogeny (Fig. 2).

Regional Metamorphism

The original sedimentary sequence that was metamorphosed to form the Pinal was a thick geosynclinal accumulation of volcanic and clastic rocks. The intensity of the metamorphism in the area of this report was fairly low, for only low-grade metamorphic facies occur in the Pinal. Strong compressional forces accompanied the metamorphism and caused the folding and foliation of the Pinal and the gneissose texture of the Sheep Canyon granite stock. The metamorphism was truly on a regional scale for its effects are present at all the Pinal outcrops over a wide area in southeast Arizona.

Folding

The folds in the Pinal Schist range in magnitude from the small tight folds along the northeast front of the mountains to the large open folds at Bowie Mountain. The axial trend of the small folds along the mountain front ranges from N. 50° W. to N. 30° W., and some are overturned.

The major folds involve the quartzite member of the Pinal at Bowie Mountain and Helens Dome, which are separate, vertically plunging synclines. These synclines were originally connected by an anticline in sec. 23, T. 15 S., R. 28 E., which has been obliterated by erosion and talus deposits. The amplitude from trough to trough of the synclines is about 1.2 miles, and their original depth is estimated at .5 mile. The center of the Bowie Mountain syncline is occupied by strongly contorted Pinal Schist. Less contorted schist crops out stratigraphically below the west limb of the Helens Dome syncline and the east limb of the Bowie Mountain syncline. The west limb of the Bowie Mountain syncline is cut by a fault and is in contact with typical nonfoliated Precambrian Rattlesnake Point Granite. The intrusion of this granite and later normal and thrust faulting was probably responsible for the large outcrops of Precambrian quartzite north of Bowie Mountain which show no clear structural relationship to the syncline. All these Precambrian rocks are now part of a post-Comanche fault block.

The synclines now plunge almost vertically and are overlapped by Paleozoic strata dipping southward at approximately 65°. Restoration of these strata to their original horizontal position shows that the synclines plunged southward at about 25° during the Paleozoic. The southerly trend of these major folds diverges somewhat from the northwesterly trend of the minor Pinal folds along the northeast range front. This divergence is probably due to the post-Comanche to pre-Pliocene thrusting which shifted the axial trend of the two synclines.

The compression which formed the north- to northwestward-trending Precambrian folds must have acted in a generally westerly direction. This is in accord with Anderson's (1951, p. 1345) summary of Precambrian structure in south-central Arizona in which he shows that this structure is characterized by folds trending northwestward to northeastward, indicating westward compression during the orogeny.

Age of the Orogeny

In the Chiricahua-Dos Cabezas Mountains the Precambrian orogeny preceded the emplacement of the nonfoliated Rattlesnake Point Granite. Both the granite and Pinal Schist are unconformably overlain by the Bolsa Quartzite (Cambrian). In the Little Dragoon Mountains, however, Anderson (1951, p. 1334) reported that the schist and granite are overlain unconformably by the unmetamorphosed Apache Group of younger Precambrian age. This shows that the deformation of the Pinal Schist is an older Precambrian event and probably correlates with the Mazatzal revolution of Wilson (1939, p. 1161), although such correlations are, of course, quite tentative.

Mid-Paleozoic Epeirogeny

The disconformity between the El Paso Formation (Upper Cambrian-Lower Ordovician) and the Portal Formation (Upper Devonian) in the Chiricahua-Dos Cabezas Mountains is the result of epeirogenic uplift that caused no angular discordance between the strata above and below the disconformity. South and west of the Chiricahua region this disconformity is somewhat more pronounced, for the Ordovician strata are absent and the Martin Formation (Upper Devonian) rests disconformably on the Cambrian. In central Arizona, Huddle and Dobrovolny (1950, p. 76) have shown that the Devonian strata rest unconformably on Cambrian and Precambrian rocks. Toward the east in New Mexico the disconformity is represented by several stratigraphic breaks of smaller mag-

nitude. Thus, the mid-Paleozoic epeirogeny affected a rather large area.

Post-Paleozoic to Pre-Cretaceous Disturbance

The massive Glance Conglomerate (Lower Cretaceous) reaches considerable thickness in the Chiricahua-Dos Cabezas Mountains. It is also reported by McKee (1951, p. 496) and other authors from most of the Basin Ranges of southeast Arizona where it unconformably overlies the older rocks with varying degrees of angular discordance. These older rocks, which were the source of the conglomerate, must have been elevated in a series of uplifts throughout southeast Arizona to provide detritus for such a widespread sheet of coarse clastic material. Although these uplifts are now largely concealed beneath post-Glance sedimentary and volcanic rocks, their former existence can be proved by a study of pre-Glance structures. In the Cochise Head quadrangle, two distinct types of erosion surfaces underlie the Lower Cretaceous strata: a planar erosion surface of low relief, and an irregular surface of high relief. These two types of unconformity were originally developed in areas an undetermined distance apart that have since been brought into closer proximity within the quadrangle as a result of post-Comanche–pre-Pliocene thrusting.

The planar surface occurs along the northeast front of the range where the Glance Conglomerate is 20–30 feet thick and consists of well-rounded quartzite pebbles and boulders. It overlaps the Paleozoic formations at a low angle of discordance. The youngest formation bevelled by this surface is the Horquilla Limestone near Silverstrike Spring, and the oldest is the Bolsa Quartzite at Marble Canyon. East and west from Marble Canyon, progressively younger Paleozoic formations are exposed at the erosion surface (Pl. 1). This indicates that the vicinity of Marble Canyon was the site of a pre-Cretaceous upwarp, the crest of which was truncated by erosion to expose the oldest beds at its center. The upwarp and the planar erosion surface occur only in the autochthonous part of the range which presumably was not involved in the post-Comanche–pre-Pliocene thrusting.

The other type of unconformity at the base of the Lower Cretaceous is an erosion surface of strong relief cutting the upper Paleozoic strata. This surface, which occurs only in the post-Comanche thrust plates of the area, cuts down onto no formations older than the Horquilla Limestone. This irregular surface occurs just south of Wood Mountain and Dunn Springs Mountain (Pl. 1) where formations ranging from the Concha Limestone to the Horquilla Limestone crop out next below the base of the Bisbee Group. There is no regular distribution of these formations below the Bisbee Group; rather their presence or absence appears to have been controlled by pre-Cretaceous topography. Other examples of this irregular surface occur along Timber Mountain ridge where the Glance Conglomerate fills old stream channels eroded in the underlying Naco Group. This irregular erosion surface developed as a result of pre-Cretaceous uplift that caused stream dissection of the underlying Paleozoic terrane. The Glance Conglomerate overlying this surface consists of upper Paleozoic limestone clasts and attains a maximum thickness of about 1000 feet at Dug Road Mountain.

Ransome (1904, p. 62) reported similar pre-Cretaceous erosion surfaces from the Bisbee quadrangle, where displacement along the Dividend fault caused uplift of the northeastern half of the quadrangle during pre-Cretaceous time. The Paleozoic strata of the upthrown block were eroded so that there the Glance Conglomerate rests on a surface of low relief formed on the Precambrian rocks. In the southwest half of the Bisbee quadrangle, however, the pre-Glance terrane has as much as 600 feet of relief and is formed on the Paleozoic strata. Ransome (1904, p. 106) inferred that the uplift occurred in late Paleozoic-early Mesozoic time, and that the erosion took place during the Triassic and Jurassic Periods.

In the Dragoon Mountains, Tombstone Hills, and northern Mule Mountains southwest of the area of this report (Fig. 1), Gilluly (1956, p. 53–70) has described a post-Paleozoic–pre-Cretaceous history of deformation and intrusive and extrusive igneous activity. No igneous rocks of this age occur in the Cochise Head and western Vanar quadrangles, and the absence of Triassic and Jurassic strata in southeast Arizona makes it impossible to date the pre-Glance disturbance more closely than post-Paleozoic to pre-Cretaceous.

Post-Comanche to Pre-Pliocene Orogeny

Introduction

In the Chiricahua-Dos Cabezas Mountains and elsewhere in southeast Arizona, a post-Comanche to pre-Pliocene orogeny caused thrusting, folding, and strike-slip faulting. In

the following discussion of the thrust faults, which are the most important structures, it is recognized that no criteria exist within this area for discriminating overthrusts from underthrusts. In other words, identical structures could be formed in several ways; by an active block moving northeastward over a passive block, or by an active block moving in the opposite direction beneath a passive block, or by a combination of movements of the two blocks in opposite directions. The displacement on all the thrusts within the area of this report indicates that the relative movement of the upper plates was from the southwest toward the northeast. In the following discussion, it is assumed that the upper plates were thrust from the southwest over passive blocks.

Before presenting the details of the various structures formed by the post-Cretaceous to pre-Pliocene orogeny, a brief summary of the more important conclusions may facilitate an understanding of the structures to be described. The rocks along the northeast front of the range constitute an autochthonous block that was overridden from the southwest by the first thrust sheet (Fig. 3). Strike-slip displacement along the Emigrant fault cut the authochthonous block and the overlying thrust sheet, which was thus separated into the Fort Bowie plate to the west and the Wood Mountain plate to the east. The Fort Bowie plate was later folded to form the Marble Quarry syncline and was truncated by the younger Fort Apache fault block. The Fort Apache reverse fault at the base of this block has a strike length of 35 miles. In the south-central part of the area, the steeply dipping beds of the Fort Apache block are overridden by the gently dipping Whitetail thrust plate. The Wood Mountain thrust, which is the earliest structure, trends westward, whereas the younger structures of the Marble Quarry syncline and the Apache Pass reverse fault trend northwestward. This may indicate a reorientation of compressive stresses during the orogeny.

Autochthonous Block

General.—The autochthonous block constitutes the part of the range that apparently remained *in situ* during the orogeny and was overridden by thrust plates moving northeastward. The block consists of Precambrian rocks and the strata overlying them in depositional contact. The sedimentary sequence is cut by minor bedding plane thrusts. From west to east the block is overridden by the Apache Pass, Fort Bowie, and Wood Mountain faults, which bring older rocks onto the Bisbee Group of the autochthonous block (Fig. 3). To the north, the block is overlapped by the alluvial fan deposits at the margin of San Simon Valley. The block extends from the northwest corner of the Cochise Head quadrangle southeast along the range front to Emigrant Canyon where it is offset to the north along the Emigrant strike-slip fault. The block extends east from Emigrant Canyon to the W ½ sec. 14, T. 15 S., R. 30 E., where it disappears beneath alluvial fan deposits. Blue Mountain in the southeast corner of the area of this report also belongs to the autochthonous block. West of the Cochise Head quadrangle, the block crops out for 16 miles along the northeast front of the Dos Cabezas Mountains. The block is broken by several strike-slip faults and is cut by large Tertiary intrusives in the northwest corner of the area and north of Wood Mountain.

Structure West of Emigrant Canyon.—From the west border of the Cochise Head quadrangle southeast to the vicinity of Marble canyon, the strata of the autochthonous block dip steeply southwestward. Northwest of Marble Canyon, however, the dip steepens, becomes vertical and then overturned so that the Bisbee strata on either side of the canyon dip steeply northeastward. No folds were observed in these overturned strata, which presumably were deformed in response to thrusting of Horquilla Limestone over the Bisbee strata. A small right lateral strike-slip fault in the NE ¼ sec. 20, T. 15 S., R. 29 E. may have been a factor in overturning the Bisbee strata. Eastward toward Maverick Canyon the Bisbee strata resume their normal southwestward-dipping attitude.

Maverick Fault.—A northward-trending fault along the course of Maverick Canyon is confined to the autochthonous block and brings southward-dipping Bisbee strata on the west against Rattlesnake Point Granite and Bolsa Quartzite on the east. This Maverick fault is truncated on the south by the Fort Bowie thrust plate which therefore must be younger than, or contemporaneous with, the Maverick fault. The Maverick fault is truncated on the north by the Emigrant strike-slip fault. The Maverick fault is believed to be a strike-slip fault developed in response to the thrusting of the Fort Bowie thrust plate. There are some small igneous intrusions along the Maverick fault.

Structure East of Emigrant Canyon.—East of the major strike-slip fault along Emigrant

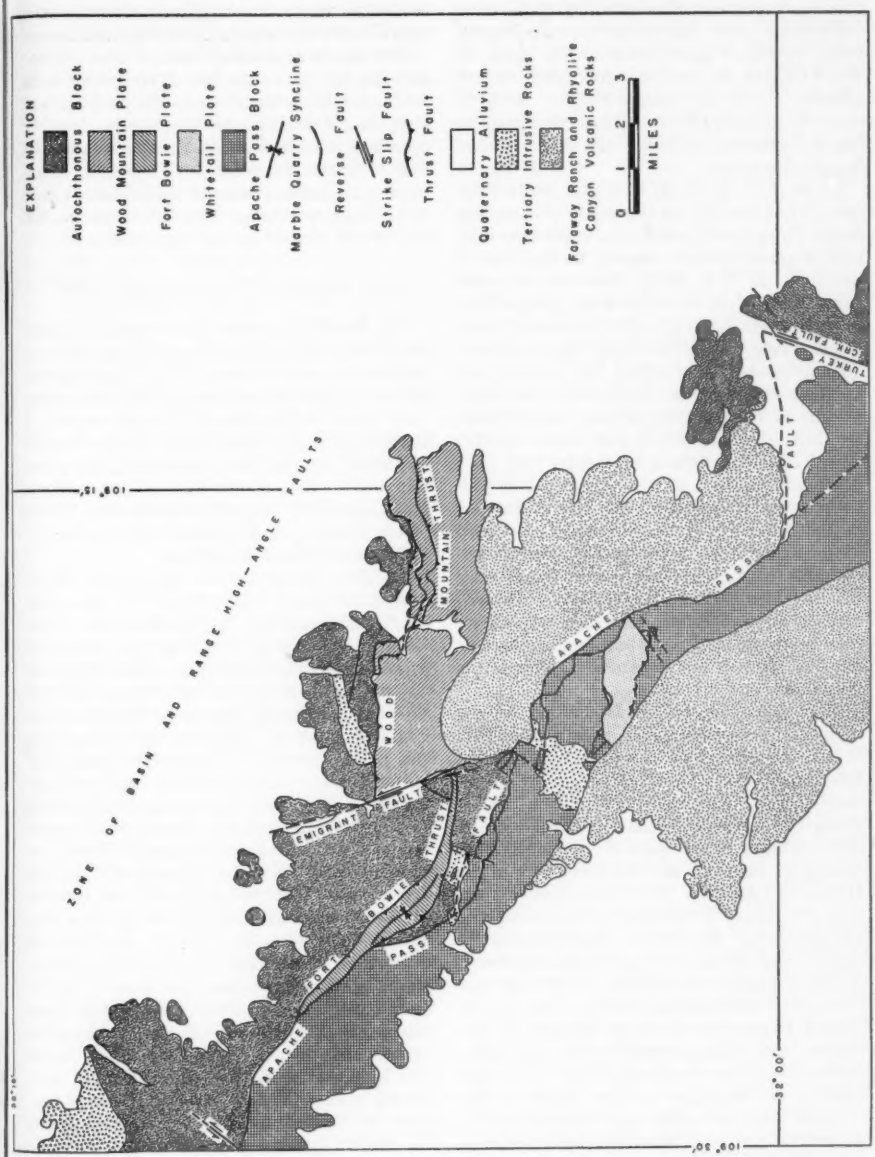

FIGURE 3.—TECTONIC MAP COCHISE HEAD AND WESTERN PART OF VANAR QUADRANGLES

Canyon (to be discussed later) the autochthonous block consists of Rattlesnake Point Granite overlain by south- and southwestward-dipping lower Paleozoic and Bisbee strata. East of Wood Canyon the granite is concealed beneath alluvium, and the autochthonous block is represented by Bisbee strata that also disappear beneath alluvium near the east end of Dunn Springs Mountain.

In sec. 7, T. 15 S., R. 30 E., the lower Paleozoic strata are cut by two westward-trending faults. These faults, however, are referred to the later Basin and Range orogeny. In the center of sec. 16, T. 15 S., R. 30 E., there is a westward trending anticlinal structure with a core of Portal Formation flanked by the Escabrosa Limestone. These formations have been contact-metamorphosed to hornfels and marble and are contorted. The anticlinal structure is not present in the overlying Bisbee strata, which are somewhat disturbed and have variable dips. These structural relationships may have developed in one of two ways: (1) a pre-Cretaceous anticline unconformably overlapped by the Bisbee Group or (2) a drag fold formed by post-Comanche thrusting along the unconformable contact at the base of the Bisbee Group. The second suggestion is favored because no comparable structures of definite pre-Cretaceous age are present and because the trend of the anticline is parallel to that of the post-Comanche structures.

Blue Mountain.—Blue Mountain, in the southeast corner of the area, is an isolated part of the autochthonous block that consists of Rattlesnake Point Granite overlain by southward-dipping Paleozoic strata. The Bisbee Group and most of the Naco Group that occur a short distance to the south are absent at Blue Mountain, however, and the lower part of the Horquilla Limestone is in concealed contact with the Nipper Formation on the south. The alluvial cover prevents a determination of whether this contact is a fault or unconformity. A fault is suggested, however, by the fact that two northward-trending porphyry dikes in the Nipper Formation terminate abruptly at the contact and do not extend into the Horquilla. However, on cross section *F-F'* of Plate 1, this contact is illustrated as an unconformity.

Strike-Slip faults within autochthonous block.—In addition to the Maverick and Emigrant faults, there are other strike-slip faults within the block. The northwesternmost of these, in sec. 33, T. 14 S., R. 28 E., is a left lateral fault that trends N. 30° E. and has displaced the strata on the west side about 800 feet to the south relative to those on the east. Several smaller northeastward-trending faults offset the strata in the belt southeast of Siphon Canyon.

The Paleozoic outcrops east of Blue Mountain are cut by a right lateral strike-slip fault that brings Bolsa Quartzite on the south against Escabrosa Limestone on the north. Another right lateral fault is inferred at the west end of Blue Mountain, for in sec. 13, T. 16 S., R. 30 E., there is an isolated outcrop of Horquilla Limestone displaced almost 3000 feet to the northeast of the Blue Mountain outcrops.

Wood Mountain Thrust and Thrust Plate

The Wood Mountain thrust crops out along the north sides of Wood and Dunn Springs Mountains where a plate of Naco and Bisbee strata overrides the autochthonous block. The plate ends at the Emigrant fault where it abuts against the Rattlesnake Point Granite that crops out on the west side of Emigrant Canyon. On the east the Wood Mountain plate is overlapped by the alluvial deposits of San Simon Valley, and on the south it is overlain by the Faraway Ranch Formation.

All along its strike the sole of the Wood Mountain thrust occurs at about the same stratigraphic horizon in the Horquilla Limestone, but a variety of stratigraphic units are overridden by the thrust plate. From Emigrant Canyon to about a mile from the east end of Wood Mountain, the plate rests directly on the strata of the autochthonous block. East from this point, however, a series of large slices of various strata forms a thick and complex thrust zone between the base of the Wood Mountain plate and the top of the autochthonous block. The westernmost of these slices consists of Bisbee strata that dip 30° W. and overlie upper Bisbee strata of the autochthonous block that dip 75° S. 20° W. This slice disappears eastward beneath the alluvial deposits of Wood Canyon. At the west end of Dunn Springs Mountain the thrust zone is more complex, for there are several large superposed slices of Naco and Bisbee strata that appear and then pinch out along the strike (Pl. 1, section *D-D'*). One of the slices is overturned so that the sequence from Colina Limestone to Concha Limestone is inverted. Along the eastern part of the north front of Dunn Springs Mountain, the series of thrust slices is replaced by a single plate ranging from Colina Limestone at the base up to the Bisbee Group (Pl. 1, section *E-E'*). The thrust zone is cut at irregular intervals by minor cross faults. This

thrust zone at the base of the Wood Mountain plate seems similar to features in the Dragoon Mountains which Gilluly (1956) has described.

The strata of the Wood Mountain plate dip southward to southwestward at angles ranging from 25° to 70°. A small low anticlinal fold within the Earp Formation occurs on the southward-trending spur at the east end of Wood Mountain. East of the triangulation station on Wood Mountain the Earp strata beneath the Glance Conglomerate are locally overturned and dip steeply northeastward to northwestward. These overturned beds are probably due to local thrusting along the unconformity at the base of the Glance. Along the ridge south of Fox Canyon, the Wood Mountain plate is cut by numerous northward-trending strike-slip faults that dip nearly vertically and have a maximum horizontal displacement of 300 feet. The Willie Rose copper mining claims are located along some of these faults that are mineralized to varying degrees.

The sole of the Wood Mountain plate crops out in the center of sec. 22, T. 15 S., R. 30 E., (unsurveyed), on the north face of Dunn Springs Mountain. The irregular, undulatory surface dips about 15° S. 20° W. at this locality, but elsewhere the dip is steeper. Here the strongly jointed Horquilla Limestone of the thrust plate has an average dip of about 45° S. 30° W., but there are local variations. The contorted sandstone and siltstone beds of the Bisbee Group beneath the plate have an average dip of about 50° S. 20° E. There is some small scale imbricate structure, for slabs of Horquilla Limestone alternate with the Bisbee strata directly below the thrust. At the east end of Wood Mountain (SE ¼ sec. 18, T. 15 S., R. 30 E., unsurveyed) the Horquilla overrides a large slice of the Bisbee strata which is not contorted at the thrust contact. The overlying Horquilla is slightly contorted however. Near the head of Little Wood Canyon (SE ¼ sec. 13, T. 15 S., R. 29 E., unsurveyed) the Horquilla at the base of the plate is contorted and recrystallized.

Fort Bowie Thrust and Thrust Plate

The Fort Bowie thrust brings the Naco Group onto the autochthonous block. The westernmost outcrop of the thrust is just east of Apache Pass where the thrust plate consists of a narrow imbricate zone of slices of the Naco Group overriding the Bisbee Group. A small slice of Glance Conglomerate and upper Bisbee strata is also present in this zone. The Fort Bowie thrust does not crop out west of Apache Pass for it is truncated by the Precambrian granite of the Apache Pass fault block. Southeast of Apache Pass the Fort Bowie thrust follows a somewhat sinuous course cut by two minor strike-slip faults, for 6 miles to the west bank of Emigrant Canyon where it ends at the Emigrant fault.

From the center of sec. 18, T. 15 S., R. 29 E. to the NW ¼ sec. 28, T. 15 S., R. 29 E., the thrust crops out in both limbs of the Marble Quarry syncline (Pl. 1, section *B-B'*). At these outcrops the beds above and below the thrust are generally parallel and show no brecciation. A small anticline with a core of Portal strata flanked by Escabrosa Limestone in the NE ¼ sec. 20, T. 15 S., R. 29 E. is the only drag structure in the thrust plate. Except for this occurrence of Devonian and Mississippian strata, the plate consists entirely of strata of the Naco Group. Two small southwestward trending synclines occur in the Fort Bowie plate in the vicinity of the Knape ranch (SW ¼ sec. 7, T. 15 S., R. 29 E.), but it could not be determined whether these were drag folds formed by the Fort Bowie thrust or were formed by later compression when the Apache Pass block overrode the Fort Bowie plate.

Marble Quarry Syncline

The Marble Quarry syncline, which trends southwestward through secs. 18, 20, and 21, T. 15 S., R. 29 E., is formed of the stratified rocks of the autochthonous block and the overlying Fort Bowie plate (Pl. 1, section *B-B'*). To the northeast the syncline is bounded by the massive Precambrian rocks of the autochthonous block. To the southwest it is bounded by the Apache Pass fault block, which here consists largely of Precambrian rocks.

The northeast limb of the syncline consists of Bolsa Quartzite and El Paso Formation, unconformably overlain by the Bisbee Group which is overridden by the Fort Bowie plate. All these strata dip steeply southwestward except in the disturbed area along Marble Canyon already discussed. The outer part of the southwest limb of the syncline consists of recrystallized Escabrosa Limestone with some Portal beds exposed in the core of a small drag fold. The Escabrosa is unconformably overlain by the Bisbee Group which is overridden by the Fort Bowie plate that forms the center of the syncline. All the strata of the southwest limb dip 55°–70° NE. The

Naco strata in the center of the syncline have been contact-metamorphosed to marble beds that are contorted but generally strike northwestward and dip steeply northeastward or southwestward.

The eastern extremity of the syncline is a narrow belt of contorted Naco Marble, bounded on the north and south by the Bisbee Group, and ending abruptly at the Emigrant fault. No real synclinal structure is visible in this extremity and it is possible that the Bisbee strata on the south are faulted against the Naco rather than overridden by it and folded as inferred in Plate 1, section *C-C'*. At the western end of the syncline, the Apache Pass block overrides the southwest limb in the center of sec. 18, T. 15 S., R. 29 E. and west of that point only strata dipping steeply southwest crop out beneath the Apache Pass block.

The Fort Bowie plate was folded to form the Marble Quarry syncline either before or during the time of Apache Pass faulting, and then the fold was truncated by the Apache Pass block.

Emigrant Strike-Slip Fault

The Emigrant strike-slip fault is a zone of major dislocation that cuts the autochthonous block and offsets the overlying Fort Bowie and Wood Mountain thrust plates (Pl. 1, section *C-C'*). The zone probably consists of several faults, but they are covered by the alluvial deposits on the floor of Emigrant Canyon. The fault trends N. 30° W. and is assumed to extend northward along the course of the large canyon in the W ½ secs. 3 and 10, T. 15 S., R. 29 E. There is no definite evidence of the faulting south of the head of Emigrant Canyon, and it is possible that there the Apache Pass fault block truncated the Emigrant fault. This indicates that the Emigrant dislocation occurred before or during the Apache Pass faulting. The Emigrant fault cuts the Fort Bowie and the Wood Mountain thrust plates (Fig. 3); therefore, it is younger than these structures. These two plates were originally a single large thrust sheet that was offset by the Emigrant fault. A large northward-trending slice of Horquilla Limestone from one of these plates occurs along the fault just south of the intersection of Emigrant and Maverick Canyons. The Maverick fault in the autochthonous block is truncated by the Emigrant fault.

In lower Emigrant Canyon the base of the Bolsa Quartzite has been offset 4000 feet, measured in a direction normal to the strike of the beds. The separation along the trace of the fault is 1.7 miles; the east side was displaced to the northwest relative to the west side. The Emigrant fault is believed to be a strike-slip fault because it was formed during a compressive orogeny and strikes across the trend of the thrust and reverse faults. The relative displacement shows that this is left lateral fault.

Apache Pass Reverse Fault

General.—The Apache Pass reverse fault is the dominant post-Comanche to pre-Pliocene structure within this area, for it has a length of 35 miles and involves all the rocks older than the Rhyolite Canyon Formation. It has a northwesterly trend and extends beyond the western and southern boundaries of the Cochise Head quadrangle. The Apache Pass fault is younger than the Wood Mountain plate and the Fort Bowie plate, which it truncates. It has a steeper dip than the original dip of these older faults and involves Precambrian rocks in the hanging wall block, whereas the older thrust plates include no pre-Devonian rocks. The Apache Pass fault also cuts the Nipper and Faraway Ranch volcanic units which apparently were not involved in the Fort Bowie-Wood Mountain thrusts.

Throughout the Cochise Head quadrangle, the Apache Pass fault dips steeply, but is generally too poorly exposed for accurate dip measurements. At all but one locality, however, the dip was estimated or measured to be south to southwestward. As the rocks of the hanging wall are older than those of the footwall, this is a reverse fault formed by a continuation of the compressive stresses responsible for the older thrust faults. There is no evidence of any appreciable strike-slip displacement along the Apache Pass fault zone within the area of this report.

From northwest to southeast, the Apache Pass fault block may be divided into the following structural subdivisions: northwestern segment, Anderson Canyon to Buckhorn Basin segment, Timber Mountain segment, and southeastern segment.

Northwestern segment.—From the west boundary of the Cochise Head quadrangle southeast to Apache Pass, the Apache Pass fault block consists of Rattlesnake Point Granite overlying the southwestward-dipping Bisbee strata of the autochthonous block. This fault block of Precambrian rocks was traced for about 11 miles west of the quadrangle on aerial photographs and by field reconnaissance. The Apache Pass

fault has pronounced topographic expression in this vicinity for the Precambrian granite of the hanging wall block weathers to rounded hills and knobs in contrast to the Paleozoic and Mesozoic strata north of the fault which form ridges parallel to the strike. West of Apache Pass, the thrust plane dips approximately 60° S. 10°–20° W. and is generally parallel to the stratification of the Bisbee strata in the underlying autochthonous block (Pl. 1, section *A-A'*).

East of Apache Pass, the footwall rocks are southwestward-dipping Horquilla strata of the Fort Bowie thrust plate which has been folded into the Marble Quarry syncline and overridden by the Apache Pass block so that the block is in contact with the northeast limb of the syncline. Farther east in the vicinity of Bear Spring Pass, the southwest limb of the syncline appears beneath the Apache Pass block, which here consists of Pinal schist and quartzite, overlain in depositional sequence by Paleozoic strata (Pl. 1, section *B-B'*). These strata are cut by a bedding plane thrust and several strike-slip faults in sec. 30, T. 15 S., R. 29 E.

At the center of sec. 18, T. 15 S., R. 29 E., the southeasterly trend of the Apache Pass fault swings more toward the south and results in a progressive thinning of the Precambrian rocks of the hanging wall block, which disappear at a mafic intrusive in NW ¼ sec. 29, T. 15 S., R. 29 E. This truncation of the Precambrian rocks results in a fundamental change in structure of the Apache Pass block, for southeast of this point the massive block becomes a series of large and small slices of a variety of rocks (Fig. 3). At one outcrop of the southward-trending part of the fault in the SE ¼ sec. 19, T. 15 S., R. 29 E., the fault plane dips 80°E.

Anderson Canyon to Buckhorn Basin segment.—This part of the Apache Pass block begins where the continuous Precambrian block ends and extends southeastward beyond Buckhorn Basin. The Bisbee strata and underlying Horquilla Limestone of Red Mountain are part of the northwestern segment, but west of Anderson Canyon are a series of major fault slices, cut by Tertiary intrusive rocks. The westernmost slice consists of Bisbee strata overridden on the south by the Horquilla Limestone and cut on the north by silicic and mafic intrusives that mark the main Apache Pass fault plane. Huge xenoliths of Rattlesnake Point Granite in these intrusives indicate the presence of Precambrian rocks along this part of the fault. East of Anderson Canyon the hanging wall block is Rattlesnake Point Granite, overlain in depositional contact by Bolsa Quartzite, and faulted against Bisbee strata of the autochthonous block. This contact is marked by a slice of Horquilla Limestone in the SE ¼ sec. 28, T. 15 S., R. 29 E. In the SW ¼ sec. 27, T. 15 S., R. 29 E. (unsurveyed), the Bisbee strata of the autochthonous block are folded into a pronounced drag syncline with its axis parallel to the northwesterly trend of the Apache Pass fault. The Rattlesnake Point Granite slice is overridden on the south and truncated on the east by the great block of Glance Conglomerate that constitutes Dug Road Mountain (Pl. 1, section *C-C'*). This fault dips 35°S. and is marked by a slice of Horquilla Limestone at the southwest and east flanks of the Precambrian granite block. Farther east the Glance depositionally overlies Horquilla Limestone, which is thrust over Bisbee strata to the north.

Timber Mountain segment.—Most of this segment consists of a very large block of Pinal Schist and Rattlesnake Point Granite, overlain on the west by Bolsa Quartzite, which is intruded by the Buckhorn Basin mafic intrusive. A westward-trending slice of this quartzite is faulted against Horquilla and Earp strata on the north in the NW. ¼ sec. 1, T. 16 S., R. 29 E. (unsurveyed). These strata are faulted against Faraway Ranch volcanic rocks to the north, along the main branch of the Apache Pass fault which is here followed by the course of Bitter Creek. This fault zone is about 20 feet wide and consists of a breccia of rhyolite and silicified limestone in a fine-grained, limonite-stained matrix. Farther east, a much larger slice of Horquilla and Earp strata is faulted between the Precambrian block on the south and Faraway Ranch volcanic rocks on the north. The spur trending southward from Cochise Head is part of a slice of Nipper Formation, faulted against the Faraway Ranch Formation on the east and the Naco Group and Precambrian on the west (pl. 1, section *D-D'*).

At the southwest part of the Timber Mountain block is a northwestward-trending syncline with El Paso Formation in the trough flanked by Bolsa Quartzite. South of this is a slice of recrystallized limestone, probably Escabrosa, that is faulted against Glance Conglomerate. The south boundary of the Timber Mountain block is a westward-trending fault that brings the Precambrian rocks against the Glance Conglomerate and Concha Limestone on the south.

Southeastern segment.—The north boundary of this part of the Apache Pass block is the

westward-trending fault that also marks the south boundary of the Timber Mountain segment. The southeastern segment extends southeastward to the south boundary of the Cochise Head quadrangle and beyond. At the south boundary, the hanging wall block consists of southwestward-dipping Paleozoic strata that are locally overturned and dip northeastward along Whitetail Creek, where they are adjacent to the main fault. The trace of the Apache Pass fault, which is marked by Indian and Whitetail creeks, cuts diagonally across the strike of these beds and brings them against the Faraway Ranch volcanic rocks on the northeast. The southwestward-dipping strata disappear beneath the unconformable cover of Nipper volcanic rocks, but reappear along the strike to the north. In sec. 7, T. 16 S., R. 30 E., these beds of the southeastern segment are cut by strike-slip faults and overridden by the gently dipping Whitetail thrust plate. This plate conceals all the underlying rocks, except for southwestward-dipping Scherrer Formation and Glance Conglomerate in the SW ¼ sec. 7, T. 16 S., R. 30 E (Pl. 1, section *D-D'*).

The Apache Pass fault extends beyond the south boundary of the Cochise Head quadrangle. From the point of departure at the southeast corner of sec. 28, T. 16 S., R. 30 E., the fault extends east for 5 miles, marked by the course of Whitetail Creek, and bringing Paleozoic strata and Rattlesnake Point Granite on the south against Faraway Ranch and Nipper volcanic rocks on the north (Fig. 3). The fault is generally concealed beneath the broad alluvial fill of Whitetail Creek, but directly south of the center of the south line of sec. 26, T. 16 S., R. 30 E., a slice of Colina Limestone and Glance Conglomerate against Nipper volcanic rocks to the north marks the trace of the Apache Pass fault. The Apache Pass fault appears to terminate against the northeastward-trending Turkey Creek strike-slip fault that brings the Rattlesnake Point Granite on the west against Paleozoic and younger rocks to the east. The Turkey Creek fault does not appear to extend north of the concealed Apache Pass fault, for the Blue Mountain outcrops are almost on strike with the equivalent outcrops to the east of the Paradise road (Pl. 1; Fig. 3). Any northward extension of the Turkey Creek fault would have greatly displaced these contacts. Additional field work is planned for the important area south of the Cochise Head and Vanar quadrangles.

Whitetail Thrust and Thrust Plate

The Whitetail plate covers less than two square miles (Fig. 3), and consists of gently dipping beds of the upper part of the Naco Group, with an unconformable cover of Glance Conglomerate. It has overridden the steeply dipping strata of the Timber Mountain segment of the Apache Pass block (Pl. 1, section *D-D'*) and has a shallow synclinal structure. On the north, the plate is bounded by the branch of the Apache Pass fault that brings it into contact with the Precambrian rocks of the Timber Mountain segment. The main east boundary is the northeastward-trending fault at the southeast corner of sec. 7, T. 16 S., R. 30 E. Two small, faulted outliers of the plate occur to the east of this fault.

In the eastern part of the plate, the approximate location of the thrust contact with the underlying Timber Mountain segment was determined by the difference in attitude of the beds above and below the thrust, even where the thrust itself was not exposed. In the SE ¼ sec. 12, T. 16 S., R. 29 ½ E., however, the Glance Conglomerate occurs both above and below the thrust. The massive, nonstratified character of the Glance made it impossible to trace the thrust to the west, although it must extend farther in that direction. The steep dips of the underlying Timber Mountain segment indicate that strong deformation preceded the thrusting of the gently dipping Whitetail plate. The final movement along the Apache Pass fault zone must have followed the Whitetail thrusting.

Age of the Orogeny

Within the area of this report, a definite sequence of tectonic events can be deciphered, based on the reasonable assumption that the thrust plates moved northeastward. The autochthonous block was overridden by a large thrust sheet, and both units were cut by the Emigrant strike-slip fault, either during or after the thrusting. The Fort Bowie thrust plate, west of the Emigrant fault, was folded into the Marble Quarry syncline and overridden by the extensive Apache Pass block. The Timber Mountain segment was strongly deformed and then overridden by the gently dipping Whitetail thrust plate before the final movement along the extensive Apache Pass fault.

The orogeny occurred in post-Comanche

(post-Early Cretaceous) time for the Bisbee Group is involved in all the faults. The oldest thrust faults, (Wood Mountain and Fort Bowie) do not involve the post-Bisbee volcanic units. Although this suggests that these older thrusts were of pre-volcanic age, the evidence is not conclusive for at no place do the volcanic rocks unconformably overlap the thrust faults. The Apache Pass reverse fault is clearly of post-volcanic age for it cuts both the Nipper and Faraway Ranch formations. The nearly horizontal Rhyolite Canyon welded tuffs were not found to be cut by the thrusts or reverse faults, and probably they were erupted after the faulting. The thrusts and reverse faults, and all the pre-Rhyolite Canyon units are cut by the Tertiary intrusive rocks.

The lack of fossils in all the volcanic rocks makes it impossible to date them and to assign an upper age limit to the thrusting. The thrusting did precede the Basin and Range orogeny of Pliocene (?) age, for the thrust faults are cut by Basin and Range high-angle faults. In the Dragoon Mountains, Gilluly (1956, p. 86) reported the same dearth of fossiliferous Tertiary beds and therefore referred the thrust faulting to a "post-Comanche to pre-Pliocene" deformation. In the Dos Cabezas and Chiricahua mountains also, the thrust faulting occurred during the post-Comanche to pre-Pliocene interval.

One is tempted to correlate this deformation with the thrust faulting of the Laramide orogeny which elsewhere has been dated as late Cretaceous to early Tertiary. The possibility, however, that in southeast Arizona the thrusting could be of middle or even late Tertiary age prohibits this unwarranted use of "Laramide"

Basin and Range Orogeny

General

The term Basin and Range orogeny is here used to denote the period of tectonic disturbance that produced the block mountains of the Basin and Range province. In his discussion of the Great Basin, Nolan (1943, p. 178) states: "... most geologists now working in the region seem to agree that at least the greater number of the Basin Ranges are bounded on either one or both sides by a fault or fault zone, that the faults are normal rather than reverse, and that the faulting has occurred from late Oligocene to the present time, although some of the scarps may be fault-line scarps rather than primary faults."

Border Faults

In the Chiricahua-Dos Cabezas Mountains, as in most of the Basin Ranges of southeast Arizona, the normal boundary faults are not exposed, for erosion and alluvial deposition have greatly modified the original configuration of the range front. The Chiricahua-Dos Cabezas Mountains are a large structural block uplifted relative to the topographic and structural depressions of the adjacent Sulphur Spring and San Simon Valleys. The uplift of the mountain block is due to movement along a fault zone bordering the northeast front of the range, and probably also a zone along the southwest front.

The major northeast fault zone is now largely concealed beneath the alluvial deposits at the southwest margin of the San Simon Valley, but some evidence may be seen at the north side of Blue Mountain where the Bolsa Quartzite dips 50° S. 40° W. At the Haystack, however, 1000 feet to the northeast, the quartzite is almost horizontal and is several hundred feet below the projection of the steeply dipping beds. There must be a fault between these two outcrops, but it could not be found in the deeply weathered outcrops of Rattlesnake Point Granite. A small Bolsa outcrop to the northeast has been downthrown 220 feet relative to the Haystack outcrop along a second concealed fault. These are probably strike faults trending parallel to the front of Blue Mountain, and to the major border-fault zone.

Two miles northeast of the bedrock outcrops at Blue Mountain, the Portal Drilling Company well No. 1, drilled in an unsuccessful search for oil, penetrated about 2000 feet of alluvium underlain by rhyolite. The well was still within the rhyolite when it was abandoned at a depth of 5800 feet (Pl. 1, section *F-F'*). Cuttings from this well, supplied by the New Mexico Bureau of Mines and examined by the writer, were of the same rock type as the Rhyolite Canyon Formation. Thus, there must be a zone of much vertical displacement between the well and the Precambrian and Paleozoic bedrock exposures at Blue Mountain. This displacement probably occurred along a series of step faults similar to those at Blue Mountain, which trend northwestward and are downthrown on the northeast side.

There is similar subsurface evidence for the border faulting in the vicinity of Dunn Springs Mountain where the unsuccessful Arizona Oil and Gas Corporation State No. 1 well (sec. 36, T. 14 S., R. 30 E.) was drilled at a location 3 miles northeast of the bedrock outcrops at the

range front. When abandoned at a depth of 7568 feet, this well had encountered only valley-fill deposits of rhyolite gravel, indicating that here too the range front is bordered by a zone of great vertical displacement (Pl. 1, section *E-E'*). It is estimated that this displacement has a throw in excess of 10,000 feet. Several other wells in the Sulphur Spring and San Simon Valleys have also encountered great thicknesses of alluvium and some volcanic rocks, according to the records of the Arizona State Land Department.

In the SW ¼ sec. 8, T. 15 S., R. 29 E., a small strike fault cuts the Bolsa Quartzite and Pinal Schist along the range front. On the southwest side of this steep fault, the strata of the autochthonous block all dip steeply southwestward, but the Bolsa strata on the northeast side dip 75° N. 60° E. This fault is probably part of the border fault zone, and the northeast dip of the Bolsa may represent drag effects. The vertical displacement along the border fault zone appears to be progressively greater to the northwest along the range front, for the elevation of the Precambrian rocks of the range front is progressively higher in that direction. The absence of any evidence of compressive deformation of the Quaternary alluvium suggests that the border faults are normal faults rather than reverse faults.

Age of the Orogeny

Within the area of this report much of the Basin and Range border faulting must have postdated the extrusion of the youngest volcanic rocks, which are uplifted relative to the adjacent valleys and are cut by several normal faults. Erosion of the volcanic rocks during and after the faulting produced the great thickness of rhyolite gravel encountered by the wells in the San Simon Valley. These gravels are probably correlative with the Gila Conglomerate named by Gilbert (1875, p. 540–541) in the Gila River Valley about 45 miles north of the area of this report.

The oldest known fossils from these detrital sediments, reported by Knechtel (1936) from the northwestern San Simon Valley are Pliocene. The major border faulting must have terminated by late Pliocene or early Pleistocene time, for the orogeny has been followed by a long period of relative stability during which erosion obliterated the fault scarps. Some mild tectonism still occurs, for in the northwest part of the Vanar quadrangle the writer observed a graben in the unconsolidated surficial deposits of the San Simon Valley. This feature had a southerly trend and was approximately 30 feet long by 2 feet wide. The narrow central block was downdropped about a foot. This feature was only slightly weathered when it was observed in August 1954, and had obviously formed later than a heavy rainstorm earlier in the month. The night watchman at the nearby drilling rig of the Arizona Oil and Gas Corporation reported feeling a strong tremor a few days before the graben was discovered. Similar features are not uncommon in the San Simon Valley, according to local residents.

Summary and Geologic History

A long and complex history is recorded in the rocks of the Cochise Head and western part of the Vanar quadrangles. Precambrian clastic sediments accumulated in a geosynclinal trough and were folded and regionally metamorphosed, probably during the Mazatzal revolution, to form the Pinal Schist. The synkinematic stock of foliated Sheep Canyon Granite was emplaced during this orogeny. The postkinematic Rattlesnake Point granite pluton, which was emplaced after the orogeny, and all the older units were cut by Precambrian aplite dikes. All these Precambrian units were eroded to a peneplain, with some monadnocks of resistant quartzite, across which the Cambrian sea transgressed in an easterly direction and deposited the Bolsa Quartzite. Following the deposition of the Upper Cambrian to Lower Ordovician carbonate strata of the overlying El Paso Formation, there was an epeirogenic uplift that caused the absence of Middle Ordovician through Middle Devonian strata. Marine sedimentation resumed from late Devonian through middle Permian time, although interrupted by minor disconformities.

Uplift and erosion from late Permian to early Cretaceous time had at least two major effects: (1) development of a planar erosion surface truncating strata of Pennsylvanian through Cambrian age, (2) in other areas strong uplift followed by erosion resulted in canyon topography incised in the upper Paleozoic strata. The Glance Conglomerate (Lower Cretaceous), derived from uplifted Paleozoic rocks, was spread over the planar erosion surfaces and also filled the rugged canyon topography. The predominantly clastic strata of the middle and upper parts of the Bisbee Group were deposited upon this basal conglomerate.

The post-Comanche to pre-Pliocene orogeny was characterized by strong lateral compression

that resulted in large thrust faults with a relative displacement of the thrust plates toward the northeast. The earliest of the plates was folded into a large drag syncline and truncated by the Precambrian rocks of a younger reverse fault block. Large strike-slip faults developed approximately parallel to the direction of displacement of the thrust plates.

The volcanic rocks of the Nipper and Faraway Ranch formations may have been extruded after the oldest thrust faulting, but are cut by the younger reverse faults. The Faraway Ranch Formation and the older rocks, as well as the post-Comanche to pre-Pliocene structures, are cut by igneous intrusions that range in composition from quartz monzonite to diorite and basalt. The Basin and Range orogeny of Pliocene (?) age uplifted the Chiricahua-Dos Cabezas Mountain block relative to the adjacent structural valleys, which have been filled with detritus eroded from the rising mountains. Subsurface information from the San Simon Valley indicates that the vertical displacement occurred along a high-angle fault zone with a throw in excess of 10,000 feet.

References Cited

Anderson, C. A., 1951, Older Precambrian structure in Arizona: Geol. Soc. America Bull., v. 62, p. 1331–1346

Baldwin, B. F., 1956, Developments in Arizona and western New Mexico in 1955: Am. Assoc. Petroleum Geologists Bull., v. 40, p. 1330–1338

Butler, B. S., and Wilson, E. D., 1938, General features of some Arizona ore deposits: Ariz. Bur. Mines Bull. 145, p. 9–25

Cooper, J. R., and Silver, L. T., 1954, Older Precambrian rocks of the Dragoon quadrangle, Cochise County, Arizona (Abstract): Geol. Soc. America Bull., v. 65, p. 1242

Darton, N. H., 1925, A resumé of Arizona geology: Ariz. Bur. Mines Bull. 119, 298 p.

Dumble, E. T., 1902, Notes on the geology of southeastern Arizona: Am. Inst. Min. Engineers Trans., v. 31, p. 696–715

Enlows, H. E., 1951, The igneous geology of Chiricahua National Monument, Arizona: Tulsa Geol. Soc. Digest, v. XIX, p. 105–107

—— 1955, Welded tuffs of the Chiricahua National Monument, Arizona: Geol. Soc. America Bull., v. 66, p. 1215–1246

Gilbert, C. M., 1938, Welded tuff in eastern California: Geol. Soc. America Bull., v. 49, p. 1829–1862

Gilbert, G. K., 1875, Report on the geology of portions of New Mexico and Arizona: U. S. Geog. and Geol. Survey W. of 100th Meridian (Wheeler), v. 3, pt. 5, p. 507–567

Gilluly, James, 1956, General geology of central Cochise County, Arizona: U. S. Geol. Survey Prof. Paper 281, 169 p.

Hernon, R. M., 1935, The Paradise Formation and its fauna: Jour. Paleontology, v. 9, p. 653–696

Huddle, J. W., and Dobrovolny, Ernest, 1950, Devonian and Mississippian rocks of central Arizona: U. S. Geol. Survey Prof. Paper 233-D, p. 67–112

Knechtel, M. M., 1936, Geologic relations of the Gila conglomerate in southeastern Arizona: Am. Jour. Sci., 5th. ser., v. 31, p. 81–92

McKee, E. D., 1951, Sedimentary basins of Arizona and adjoining areas: Geol. Soc. America Bull., v. 62, p. 481–505

Meinzer, O. E., and Kelton, F. C., 1913, Geology and water resources of Sulphur Spring Valley, Arizona: U. S. Geol. Survey Water-Supply Paper 320, p. 9–213

National Research Council, 1948, Rock-color chart, Washington, D. C.

Nolan, T. B., 1943, The Basin and Range Province in Utah, Nevada, and California: U. S. Geol. Survey Prof. Paper 197-D, p. 141–196

Paige, Sidney, 1909, Marble prospects in the Chiricahua Mountains, Arizona: U. S. Geol. Survey Bull. 380, p. 299–311

Ransome, F. L., 1904, Geology and ore deposits of the Bisbee quadrangle, Arizona: U. S. Geol. Survey Prof. Paper 21, 167 p.

Sarle, C. J., 1922, Sketch of the geology of the Dos Cabezas Mountains of southeastern Arizona (Abstract): Science, new ser., v. 55, p. 544

Sabins, F. F., 1955, Tectonic history of part of the Dos Cabezas and Chiricahua Mountains, Arizona (Abstract): Geol. Soc. America Bull., v. 66, p. 1610

—— 1957, Stratigraphic relations in Chiricahua and Dos Cabezas Mountains, Arizona: Am. Assoc. Petroleum Geologists Bull., v. 41, p. 466–510

Schwennesen, A. T., 1917, Ground water in San Simon Valley, Arizona and New Mexico: U. S. Geol. Survey Water-Supply Paper 425-A, p. 1–35

Stoyanow, A. A., 1926, Notes on recent stratigraphic work in Arizona: Am. Jour. Sci., 5th ser., v. 12, p. 311–324

—— 1936, Correlation of Arizona Paleozoic formations: Geol. Soc. America Bull., v. 47, p. 459–540

Wilson, E. D., 1939, Pre-Cambrian Mazatzal revolution in central Arizona: Geol. Soc. America Bull., v. 50, p. 1113–1164

California Research Corporation, Box 446, La Habra, Calif.

Manuscript Received by the Secretary of the Society, October 29, 1956

BULLETIN OF THE GEOLOGICAL SOCIETY OF AMERICA
VOL. 68, PP. 1343–1370, 11 FIGS., 1 PL. OCTOBER 1957

GEOLOGICAL AND GEOPHYSICAL SYNTHESIS OF THE TECTONICS OF PORTIONS OF BRITISH COLUMBIA, THE YUKON TERRITORY, AND ALASKA

BY PIERRE ST. AMAND

ABSTRACT

The seismic activity of Alaska is associated with the Aleutian Island arc and with a line of faulting in southeastern Alaska that appears to be the northward extension of the San Andreas fault system. The activity in western Alaska is enhanced where the Aleutian Range intersects the Alaska Range. It is again enhanced where the Chugach Range intersects the Aleutian Range.

The Denali fault can be traced from the Bering Sea through the Kuskokwim Mountains, past Mt. McKinley, to a point past Lake Dezadeash. Here it is joined by a line of faulting associated with a northern extension of the San Andreas system.

A similar line of faulting runs from Lake Clark past Anthracite Ridge to join the faulting in southeastern Alaska.

It is suggested that the major Yakutat Bay earthquakes took glace on a very long, straight lateral fault running from north of Yakutat Bay to south of the Queen Charlotte Islands.

The Denali fault is thought to be right lateral strike slip in habit, with over 150 miles of movement.

Seismic data and geologic observations indicate that the north Pacific Basin, from Baja California to the Kurile Islands at least, is and has been for a long time, rotating counterclockwise.

CONTENTS

TEXT

	Page
Introduction	1344
Statement of intent	1344
Seismological work	1344
Geological field work	1344
Acknowledgments	1345
Distribution of seismic activity	1345
Epicentral locations	1345
Strain release	1345
Active areas	1345
Quiescent areas	1347
Aleutian Island arc	1347
Configuration	1347
Bowers Bank	1347
Aleutian range	1347
Pacific arc features	1348
Geologic reports	1349
Faulting in the Alaska range	1350
Alaska range	1350
Denali fault	1351
Kuskokwim region	1351
Mt. McKinley to the Nenana glacier	1352
Suspected Lake Clark fault zone	1352
Thrust faulting along the Susitna-Chulitna depression	1352
Nenana glacier to Delta River	1353
Delta River to Canadian border	1353
Canadian border to Lake Kluane	1354
Lake Kluane to Lake Dezadeash	1355
Lake Dezadeash to Lynn Canal	1356
Lynn Canal	1356
Recapitulation	1357
Other possible zones of faulting in southeastern Alaska	1357
Faulting along the Gulf of Alaska	1357
Movements in 1899	1357
Small-scale Tsunamis in Yakutat and Lituya Bays	1358
Other faulting	1359
Faulting south of Dixon Entrance	1359
Inference from seismology	1359
Inference from oceanography	1360
Geodetic information	1360
Contemporary changes in land level	1360
Post Pleistocene uplift	1362
Tectonic speculation	1364
Nature and movement of the Denali fault	1364
Direction of faulting in southeastern Alaska	1365
Connection between Denali fault and faulting in southeastern Alaska	1365
Juncture at Lake Dezadeash	1365
Relation of faulting westward	1365
Present state of activity	1365
Connection with the San Andreas fault system	1365
Hiatus between the San Andreas and Alaskan faults	1365

	Page
Possibility of rotational movement	1365
Is the Pacific Basin being shoved under Alaska?	1365
Is the Pacific Basin rotating?	1366
Do Pacific Arcs undergo lateral motion?	1367
First motion from seismograms	1367
Menard's theory of a convection cell	1367
Is the Alaska Range an inverted Pacific Arc?	1368
Similarities and differences	1368
Tanana Valley	1368
Alternate possibilities	1368
Suggestions for further work	1368
Geologic field work	1368
Geophysical studies	1369
References cited	1369

ILLUSTRATIONS

Figure	Page
1. Map showing seismic activity of the northern Pacific area	1346
2. Generalized submarine topography of the Aleutian Islands	1348
3. Distribution of mountain ranges and other physiographic features in Alaska and northwestern Canada	1350
4. Course of the Denali and Lake Clark faults in western Alaska	1352
5. Index map and course of the Denali and Lake Clark faults in western Alaska	1354
6. Course of Denali fault in central Alaska, Yukon Territory, and British Columbia.	1356
7. Course of Denali fault in southeastern Alaska and British Columbia	1358
8. Sketch of submarine depression on continental shelf in Gulf of Alaska	1360
9. Change of land elevation in parts of Alaska, Yukon Territory, and British Columbia, with respect to sea level	1361
10. Change in sea level at Alaskan ports	1364
11. Speculative consequence of movement on the Denali fault	1366

Plate	Facing page
1. Strain-release map of Alaska	1370

TABLES

Table	Page
1. Changes in land level observed by geodetic means	1362
2. First-motion data for north Pacific earthquakes	1363

Introduction

Statement of Intent

Although about 6 per cent of the world's large, shallow earthquakes occur in the Aleutian Islands and Alaska, little is known in detail of the seismicity or structural geology of this vast region. This paper is an attempt at a synthesis prepared from a study of the published geologic and geophysical literature and from topographic maps. It endeavors to point out the general nature of the problem but probably raises more questions than it answers. It is but an introduction and does not purport to contain either a definitive discussion of the geology and tectonics or a comprehensive bibliography.

Seismological Work

The great earthquakes of 1899 at Yakutat Bay, discussed by Tarr and Martin (1912), were the first Alaskan seisms to have been investigated extensively. These shocks produced displacements along faults in the Yakutat Bay area, on which the vertical component of movement was as great as 47 feet. The earthquake swarms in interior Alaska, studied by Bramhall (1938) and St. Amand (1948) appear to be the only others for which investigations have been published. Descriptions of some of the shocks appear in the U. S. Coast and Geodetic Survey Publications, *United States Earthquakes* by Murphy (1950) and Murphy and others (1951–1953) and in Heck (1938).

There is a great deal of information on epicentral locations and magnitudes in Gutenberg and Richter (1954). A paper by Merrell (1950) deals with the frequency and distribution of earthquakes in the territory on the basis of reports of temblors felt in various places.

There are three seismograph stations in the territory. These are located at College on the University of Alaska Campus near Fairbanks, at Sitka, and at Unalaska.

Geological Field Work

The United States Geological Survey has done most of the geological field work in the territory, and the Canadian Geological Survey has performed most of the investigations in northwestern British Columbia and in southwestern Yukon Territory. Field work in this general region proceeds very slowly because of the great topographic relief, the difficulties in provisioning and transporting the parties, and in keeping alive while the work is being done. The peculiar nature of the vegetation and the extensive overburden add to the difficulties. It is difficult to draw detailed conclusions as to the structural geology because most of the published geological maps are reconnaissance maps.

Acknowledgments

The author is grateful to R. P. Sharp, J. E. Noble, and the late J. P. Buwalda of the Department of Geological Sciences of the California Institute of Technology for helpful discussion and for information pertaining to the Denali Fault. Clyde Wahrhaftig of the U. S. Geological Survey, who has worked on the great fault in the Mt. McKinley region, has been most generous with ideas, suggestions, and critical discussion. R. B. Campbell of the Canadian Geological Survey has also contributed to this study.

B. Gutenberg and C. F. Richter of the Seismological Laboratory have made epicentral determinations available in advance of publication. H. Benioff has discussed the tectonic aspects with the author as has C. H. Dix under whom a portion of this work was done while the author was a graduate student at the California Institute of Technology.

Captain Elliott B. Roberts of the U. S. Coast and Geodetic Survey has made tide-gauge data and other information available and has been very helpful, as has H. Nichols of the same organization. Thanks are due also to E. N. Wolff of the University of Alaska and to H. R. Joesting of the U. S. Geological Survey.

Much of the library work was done while the author was a Fulbright Research scholar in Geophysics at the Institut d'Astrophysique in Paris, France. The excellent libraries of the Ecole de Mines, and the Institut de Geologie and the Institut de Physique du Globe made the work of tracking down endless references simple.

The author is indebted to the U. S. Naval Ordnance Test Station for help with typing and illustrations, especially to Ella M. Kowalsky, Dawn Hayford and Marjorie Caro.

Distribution of Seismic Activity

Epicentral Locations

Figure 1 shows the location of Alaska in the circum-Pacific ring of tectonic activity. The epicenters shown are from Gutenberg and Richter (1954). The map also indicates some structural features to be discussed later.

Plate 1 shows a number of epicentral determinations, in addition to those in Figure 1, given by Murphy (1950), Murphy and Ulrich (1951a; 1951b; 1952) and Murphy and Cloud (1953; 1954). Several locations determined by the present author are also shown. A few shocks, given by Gutenberg (1956), for the year 1899 are included. It is believed that most shocks of magnitude 5¾ or more from 1900 to 1953 are included. The individual locations are given by Gutenberg and Richter (1954, p. 4) to about ¼°. Many small shocks have no doubt gone unreported.

Strain Release

The contours in Plate 1 represent the strain released by earthquakes since 1900, expressed in equivalent earthquakes of the fourth magnitude per square degree per year. The technique of preparing such a map is discussed by St. Amand (1956, p. 43) and also by Ritsema (1953, p. 41–42). The epicentral data enumerated above were used. Those earthquakes for which magnitudes were not given were arbitrarily assigned magnitude 5. Certain shocks listed in Gutenberg and Richter (1954) as being of magnitude "d" were arbitrarily considered 5¾. The map has been smoothed over a circle with a radius of 1° of latitude. It was arbitrarily assumed that the collection of information was complete for a 50-year period, although the effective time is somewhat less.

In view of the foregoing arbitrary assumptions no great claim is made for the precision of this illustration, except that it shows the relative seismic activity in addition to places where earthquakes are thought to have occurred.

Active Areas

Since 1900 most of the activity has occurred in southwestern Alaska. This activity is doubtless associated with the Aleutian Island Arc and the Aleutian Range, the landward extension of the Arc. The activity is more intense near the northeastern end of the arc, where it is transected by the Alaska Range. A large part of this activity occurs along the northern front of the range between Mt. McKinley and Mt. Kimball. Some of the activity is situated well in front of the range under the Tanana Valley. A number of small earthquakes take place each year at a distance of 15–20 km from the College Seismograph Station. There is another especially active area near the head of Cook Inlet and in the Chugach-Prince William Sound area.

Most of the remainder of the activity is in southeastern Alaska and adjacent parts of British Columbia. It is distributed along the coast, the Queen Charlotte Islands, Baranof

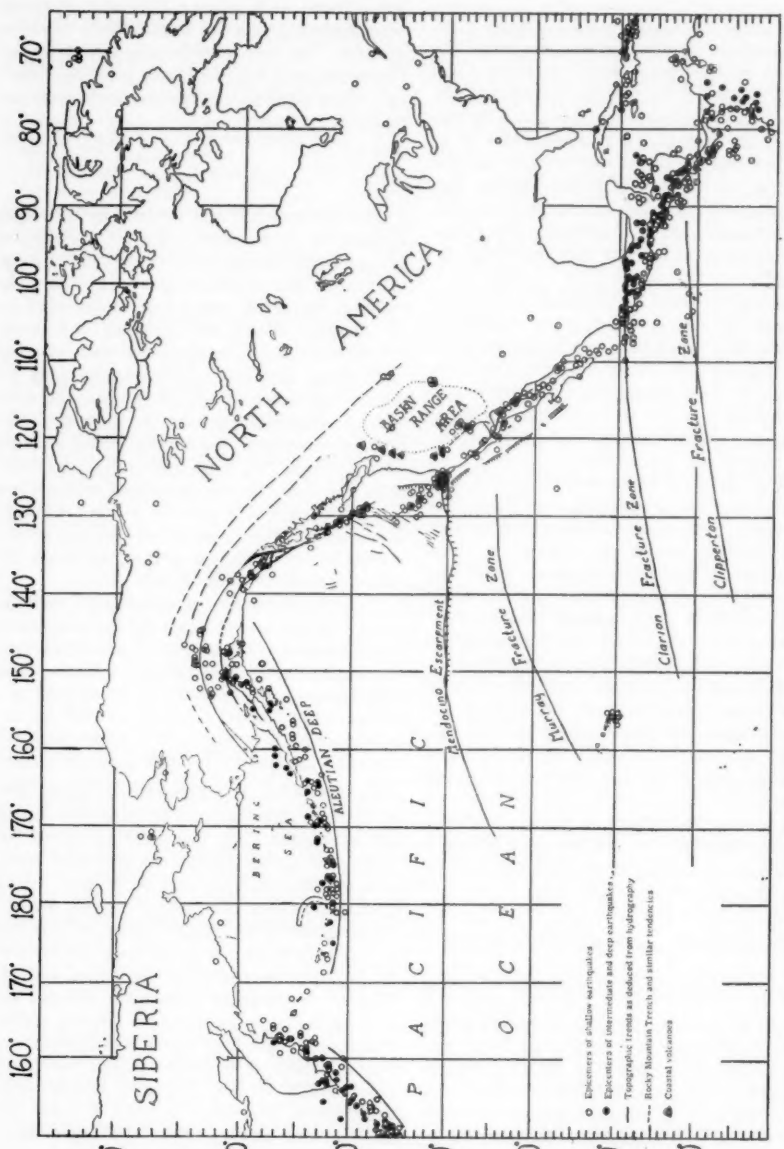
160° 170° 180° 170° 160° 150° 140° 130° 120° 110° 100° 90° 80° 70°
70° 60° 50° 40° 30° 20° 10°
SIBERIA
NORTH AMERICA
PACIFIC OCEAN
BERING SEA
ALEUTIAN DEEP
Mendocino Escarpment
Murray Fracture Zone
Clarion Fracture Zone
Clipperton Fracture Zone
BASIN RANGE AREA
Epicenters of shallow earthquakes
Epicenters of intermediate and deep earthquakes
Topographic trends as deduced from hydrography
Rocky Mountain Trench and similar lineaments
Coastal volcanoes

FIGURE 1.—MAP SHOWING SEISMIC ACTIVITY OF THE NORTHERN PACIFIC AREA
The San Andreas fault is presumed to continue northwestward past the Mendocino Escarpment.

and Chichagof Islands, in the vicinity of Yakutat Bay, in the St. Elias Range, and the neighborhood of Lake Kluane. The present activity in this region is not as great as that in southwestern Alaska, but in view of the Yakutat Bay earthquakes the region is more to be regarded as quiescent than inactive.

There are a few epicenters north of the Tanana and the Yukon Valleys. Some activity occurs in eastern Siberia, on the Seward Peninsula, in the region of the middle Koyukuk River, and in northwestern Canada.

Quiescent Areas

That portion of the Kuskokwim and Yukon Flats between the mountains and the Bering Sea has been free of epicenters since 1900. The Yukon Flats north of the Yukon-Tanana Highlands, in the vicinity of Circle City and Fort Yukon has also been quiescent.

There is a large quiescent area between the Aleutian earthquake region and the active region in southeastern Alaska. If the Denali fault and the Lake Clark-Chugach area are not active, then this region may be reasonably free of earthquakes. The presence of the Denali fault, the suspected fault zone through Lake Clark, and several other eastward-trending features in the south, make it conceivable that large earthquakes can occur in this area. On the basis of the activity since 1900 it appears that earthquakes are absent in this zone, but recently Gutenberg (1956, p. 610) has given the location of one Yakutat Bay shock as 60°N. Lat., 142°W. Long. Should it be subsequently demonstrated by field work and seismological observation that these structures are no longer active, then the zone might be regarded as free of seismic disturbances. Even at this stage in our knowledge of the seismicity of the territory it seems a wise policy to route any future railway and pipeline construction from the coast to the interior through this area rather than along the present route of the Alaska Railroad, one of the more active areas in Alaska.

Aleutian Island Arc

Configuration

The volcanic islands of the Aleutian chain, shown in Figure 2, trace an almost perfect circular arc of 760 statute miles (1220 km) radius, with a pole at 62° 40′ N. Lat. and 178° 20′ W. Long. (Murray 1945, p. 759). In the arc as a whole, the curvature is nearly uniform from the Komandorsky Islands to the point where the Alaska Peninsula emerges from the sea; here the arc widens, and the radius of curvature increases. West (1951, p. 81) has noted that it seems to consist of a series of straight lines (great circle arcs) meeting at slight angles. Plate 1 shows concentrations of strain near the ends of these segments and reduced strain between the segments.

To the west of the intersection with the continent, the arc is a volcanic ridge containing 76 major volcanoes (Coats, 1950, p. 37). The ridge is bounded by a deep oceanic trough on the south and backed by a deep, relatively flat-floored basin to the north. This basin, 2000 fathoms deep in places, is bounded as much as 500 miles north by the continental slope, which drops from the shallow floor of the Bering Sea.

Bowers Bank

At about Long. 180°, Bowers Bank forms a semicircular arc, of 125 miles radius (Murray, 1945, p. 779), curved to the north and west away from the main Aleutian Arc. Bowers Bank itself is almost aseismic (Gibson and Nichols, 1953, p. 1187), but the area at the junction with the Aleutian Arc is active. To the south of Bowers Bank, the Aleutian ridge is widened. The Aleutian Arc changes directions abruptly at Long. 180° (West, 1951, p. 81) and again near the intersection with the mainland. It seems likely that the change near 180° is connected in some way with the Bowers Banks structure.

Aleutian Range

From the Alaska Peninsula eastward, the arc joins the continent. The line of volcanoes continues to Mt. Spurr. The deep departs from the line of volcanoes, traverses the Gulf of Alaska, and terminates near a submarine canyon running out of Yakutat Bay. A second trough follows the line of volcanoes and forms Shelikof Strait and Cook Inlet. This trough continues northward through the Yentna-Susitna-Chulitna depression, Broad Pass, and perhaps the south end of the Nenana Valley. This depression marks the eastern boundary of the Aleutian Range. It seems plausible that the portion of the Alaska Range lying south and west of the north face of Mt. McKinley belongs, structurally at least, to the Aleutian Range.

FIGURE 1.—MAP SHOWING SEISMIC ACTIVITY OF THE NORTHERN PACIFIC AREA
The San Andreas fault is presumed to continue northwestward past the Mendocino Escarpment.

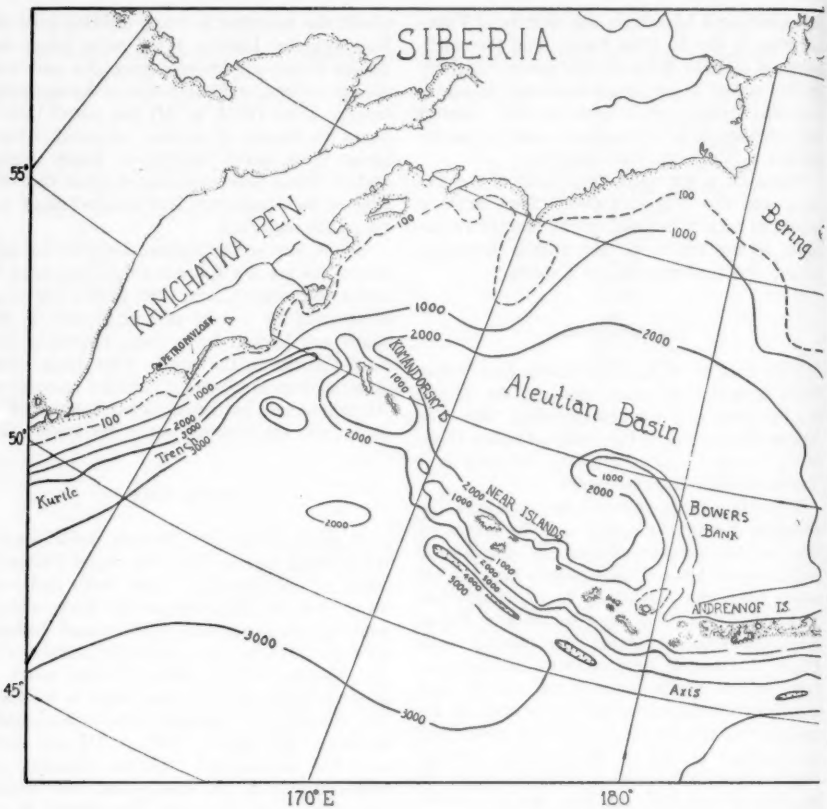

FIGURE 2.—GENERALIZED SUBMARINE

This figure has been adapted from Murray (1941). Note the deep oceanic basin behind the

Pacific Arc Features

The Aleutian chain possesses most of the attributes of a Pacific structural arc: the line of volcanoes, the circular form, the ocean deep, and the earthquakes. It, however, lacks others; there is no well-developed older range of mountains inside the western and central reaches over the locus of intermediate shocks. Indeed, the locus of intermediate shocks is not clearly distinguished from that of the shallow ones. Deep-focus earthquakes are comparatively rare in the Aleutian Arc; the locus of these few deep and intermediate shocks lie west of Prince William Sound and indicate a profound geologic change at that point.

Benioff (1954, p. 390) has discussed the Aleutian Arc and concludes that it represents a thrust, the northern edge rides up and over the Pacific Basin, relatively speaking, on a fault plane dipping under the northern side at an angle of about 28°. The composite fault plane appears to the author to be steeper in the central and western reaches than in the eastern portion and attains an angle of about 45° between 172° and 179° W. Long., but there are too few earthquakes to permit making a firm judgment.

Gibson and Nichols (1953, p. 1184) indicate that the volcanic arc protrudes out of the northern edge of the Aleutian Ridge, and they present arguments that a single fault, serving as a vent for the volcanoes, possibly exists all along the chain. They also point to great variety of step faults and transverse faults with which earthquakes might be correlated and stress the desirability of a network of seismic stations for

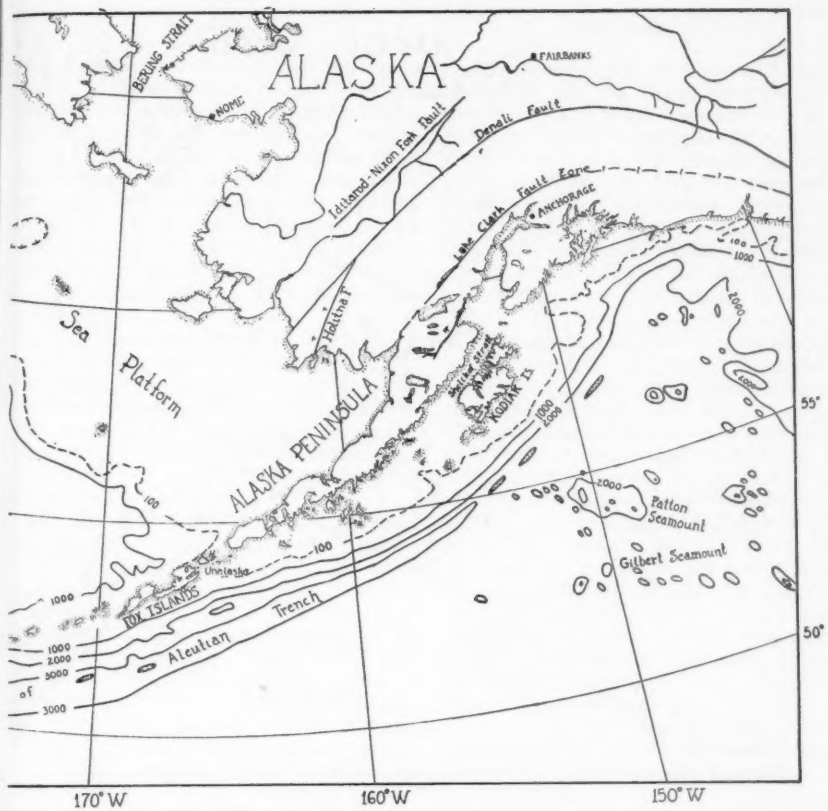

TOPOGRAPHY OF THE ALEUTIAN ISLANDS
Aleutian Island arc and the rather shallow platform of the Bering Sea. Depths are in fathoms.

the purpose of studying the problem more satisfactorily.

The same writers discuss the relation of earthquakes to the arc and indicate that about 12 per cent occur south of the deep, 7 per cent in the deep, 40 per cent on the insular slope beneath 3000 fathoms, 15 per cent on the north insular slope, and 1 per cent on Bowers Bank. The location of the epicenters, as they remark, is such that these ratios could easily be shifted by moving the epicenters about in a circle corresponding to the probable error of location. It may be noted on Plate 1, however, that the clustering of epicenters changes location with respect to the line of volcanoes as it proceeds westward.

Gates and Gibson (1956, p. 128 ff.) present considerable detail as to the geologic history and submarine topography of the Near Islands (Fig. 2). They conclude (p. 144–145) on the basis of geologic studies and hydrography, that the principal structural features of the arc are (1) a normal fault along the north side of the Ridge, (2) northward-dipping reverse faulting and warping on the south insular slope, (3) a possible northward-dipping thrust along the inside edge of the Aleutians Bench, and (4) a zone of thrusting or shearing dipping northward beneath the Aleutian Ridge and delineated by the Aleutian Trench.

Geological Reports

The geology of some of the Aleutian Islands has been discussed by Coats (1950), Robinson (1947), and Sharp (1946). The information presented in Robinson (1947) has been published in a series of separate chapters in U. S. Geo-

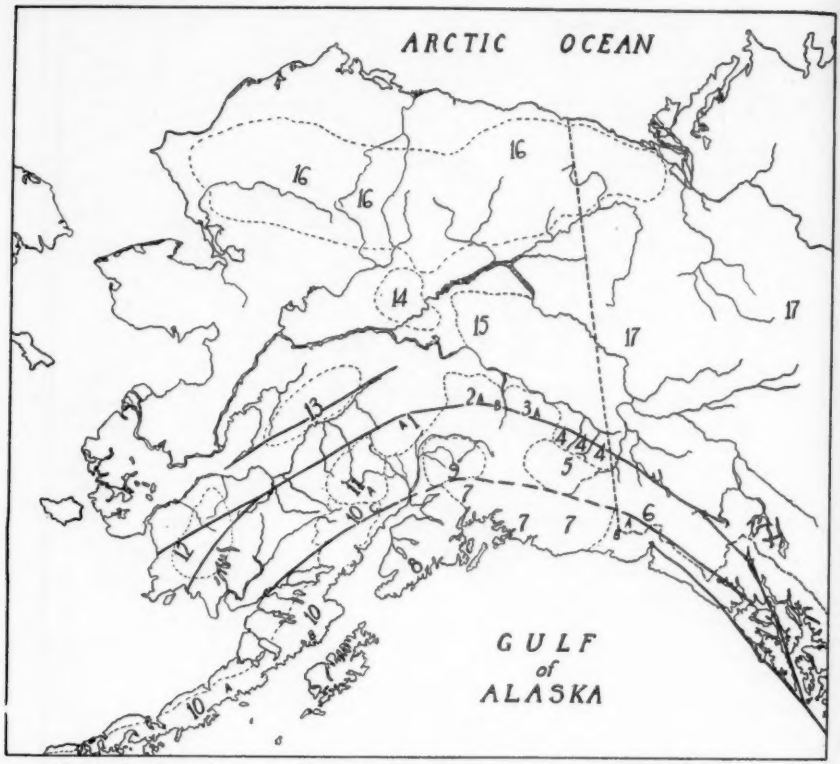

FIGURE 3.—DISTRIBUTION OF MOUNTAIN RANGES AND OTHER PHYSIOGRAPHIC FEATURES IN ALASKA AND NORTHWESTERN CANADA

Alaska Range
1. Mt. McKinley Massif
   A. Mt. McKinley
2. Mt. Hess-Mt. Hayes Massif
   A. Mt. Hess
   B. Mt. Hayes
3. Mt. Kimball Massif
   A. Mt. Kimball
4. Nutzotin Mountains
Volcanic Mountains
5. Wrangell Mountains
Coast Ranges
6. St. Elias Range
   A. Mt. Logan
   B. Mt. St. Elias
7. Chugach Mountains
8. Kenai Mountains
9. Talkeetna Mountains
Aleutian Ranges
10. Aleutian Range
   A. Mt. Aniakchak
   B. Mt. Katmai
   C. Mt. Spurr
Mountains Between Alaska Range and Aleutian Range
11. Skwentna Group
   A. Mt. Gerdine
Other Mountains
12. Kilbuck Mountains
13. Kuskokwim Mountains
14. Ray Mountains
15. Yukon Tanana Upland
16. Brooks Mountains
17. McKenzie Mountains

logical Survey Bulletin 1028. A summary has been published by Gates, Fraser, and Snyder (1954).

FAULTING IN THE ALASKA RANGE

Alaska Range

The Alaska Range extends from the vicinity of Mt. McKinley in a sweeping arc eastward and then southward to the Coast ranges. The range consists of some of the tallest mountains in North America. These mountains are situated on either side of a great fault. The distribution of mountainous masses in Alaska is shown in Figure 3. The Wrangell Mountains are volcanic and are not properly a part of the folded and faulted mountains of the Alaska Range that are composed of sedimentary, metamorphic, and batholithic rocks.

Denali Fault

A gigantic fault runs through the Alaska Range. It probably extends from the Bering Sea, past Mt. McKinley to southeastern Alaska. The fault is described by a number of authors of the U. S. Geological Survey and the Canadian Geologic Survey. It has been discussed by St. Amand (1954) and by Sainsbury and Twenhofel (1954). In many places the fault was unrecognized, for the most part because of its size and the fact that along much of its length it forms a trough occupied by glaciers and other overburden.

The fault has been active for a long time and in places shows signs of very recent activity. The epicenters of Alaska Range earthquakes are distributed on either side of this feature as they are about other major faults; they are, however, lacking for at least the last 50 years along the portion of the fault between the Delta River and Lake Kluane.

The author has taken the liberty of calling this the Denali fault (St. Amand, 1954, p. 1350). This name is suggested, because no other seems to have been applied to the whole structure. The fault has been referred to as the Great fault, a very fitting name, by Wahrhaftig (1948, personal communication) while speaking of the portion in the Mt. McKinley region. It has in that region also been called the Anderson Pass fault. Mendenhall and Schrader (1903, p. 51) referred to it as the great fault but did not indicate it as a proper name. In his paper Bostock (1952, p. 8) has not named the feature but heads a paragraph the Shakwak Valley fault. Cady *et al.* (1956, p. 90–93) have referred to faulting in the Denali fault zone by a number of names, most particularly the Boss Creek fault and the Farewell fault zone. The feature is so fragmentally named and recognized that a new name seems desirable.

The name Denali, an Indian word meaning the highest or greatest, is the local name for Mt. McKinley and is in use among the Indians and a large segment of other Alaskans who prefer it to the name currently imposed on the mountain.

The position of the fault is here outlined as well as possible. Details of the geology are lacking, most of the geology is of a reconnaissance nature, and in many places the location of the fault is inferred from stratigraphic or geomorphic anomalies. This account is concerned mainly with the location of the fault and only incidentally with the stratigraphy.

Kuskokwim Region

At a point between the village of Arolik and Jacksmith Bay the Denali fault leaves the Bering Sea and forms the north face of the Kilbuck Mountains (Fig. 4). Here, covered by the alluvium of the Kuskokwim Flats, it strikes northeasterly. It passes between the Great Ridge and the Kilbuck Mountains in a trough in which flows the Middle Fork of the Eek River; passes under Eek Lake, the lower reaches of Canyon Creek; and forms a long trough in which the upper Kisaralik River flows. This trough forms a pass over the Kilbuck Mountains and is occupied then by the headwaters of the Kipchuck River, a tributary of the Aniak River. The course of faulting is difficult to follow to the northeast of this pass until the fault zone described by Cady *et al.* (1956, p. 90–93) is encountered about 15 miles from the pass. This fault zone consists of a number of long straight faults of steep dip and shows evidence of recent movement. Chief among these are the Atsaksovluk fault and the Boss Creek fault. The latter of these is easily projected to join the zone of faulting near Farewell, called the Farewell fault zone by these authors. Unfortunately about 60 miles of alluvium covers any easily recognizable traces of faulting between the Chuilnik Mountains and the Stony River, where the Farewell zone is distinguishable.

A very interesting member of this group is the Holitna fault, a thrust, the trace of which runs southwestward from Portage Creek, where it appears to join the Boss Creek fault, to the Gemuk River. The authors indicate that it might extend to the Tikchik Lake Region. It takes but little imagination to extend this feature through Togiak Lake and into the Bering Sea near the village of Togiak. In places where this fault is easily recognizable, Cady and his colleagues report that it dips between 20° and 30° to the northwest; a block lying between it and the Boss Creek fault was thrust over the land to the south. There are recent scarps nearly 20 feet high along the trace of this fault.

In the Kuskokwim Region, the Idiotarod-Nixon Fork alignment was noted by Mertie and Harrington (1924, p. 38). The zone appears to extend from the vicinity of Aniak in a northeasterly direction perhaps as far as the Tanana River. This appears to be a fault; the stratigraphic throw of which is reversed along the fault and is up on the southeastern side of the northeastern end and down on the southeastern side near the southwestern end. This reversal, the straight course of the fault, and the general

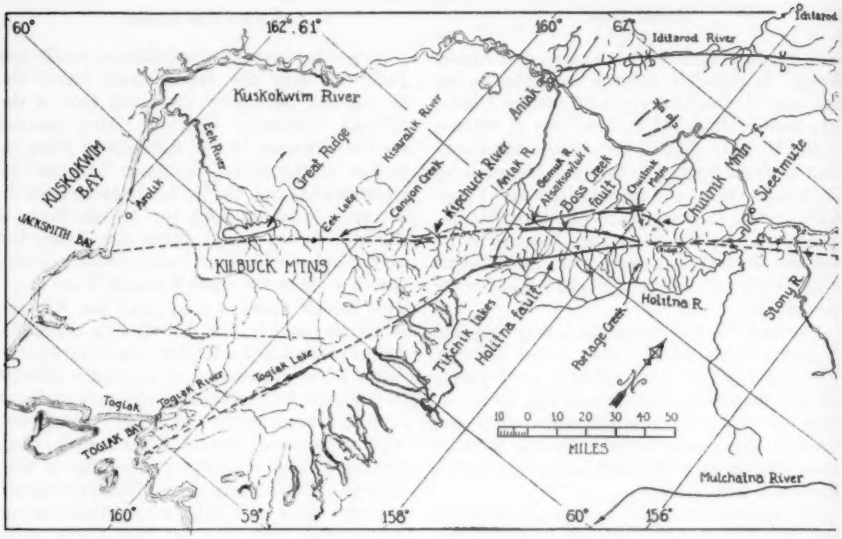

FIGURE 4.—COURSE OF THE DENALI AND

appearance of the topography lead to the postulation that it is a lateral fault subparallel to the Denali fault.

Mount McKinley to Nenana Glacier

From the point where the Farewell fault zone leaves the low lands of the Kuskokwim and enters the Alaska Range, the fault can be traced eastward along the northern front of the range as it delineates the magnificient northward-facing scarp of the Mt. McKinley massif. The fault begins to transect the range, forms, the trough in which Muldrow Glacier lies, passes through Anderson Pass, Easy Pass, and Foggy Pass, and is well south of the range front where it crosses the Alaska Railroad south of Windy. The trace of the fault is marked here by a line of long, straight stream channels and glacial valleys running parallel to the trend of the hills along the courses of Schist Creek, Bruskana Creek, and the Nenana Glacier as shown in Figure 6. The fault was recognized in this region by Moffit (1915) and included by Capps (1940) in later reports. The fault cuts Tertiary and Quaternary rock in the Mt. McKinley region. Just east of Mt. McKinley the south side seems stratigraphically downthrown, although the highest parts of the range lie to the south. The apparent stratigraphic throw is reversed near and to the east of the Nenana River. The appearance strongly suggests lateral displacement in addition to whatever vertical component of movement may exist.

There is another large fault subparallel to and north of the Denali Fault in this area; but the extent cannot easily be traced eastward past the Nenana River, although it probably goes farther.

Suspected Lake Clark Fault Zone

To the south of the Denali fault, near Chickaloon (Fig. 5) a large, subparallel fault called here the Lake Clark fault traverses Anthracite Ridge and possibly continues eastward through the northern Chugach Mountains to the St. Elias region. Westward it probably continues through Lake Clark, but it cannot be followed with confidence in either direction because of lack of geologic mapping. Capps (1935) presents a geologic map of the area surrounding Lake Clark but does not recognize such a fault, which although it is not precluded by the geology, possibly does not exist.

Thrust Faulting Along the Susitna-Chulitna Depression

The western side of the Susitna-Chulitna valley is marked by a bold, comparatively straight scarp that runs southwestward, from

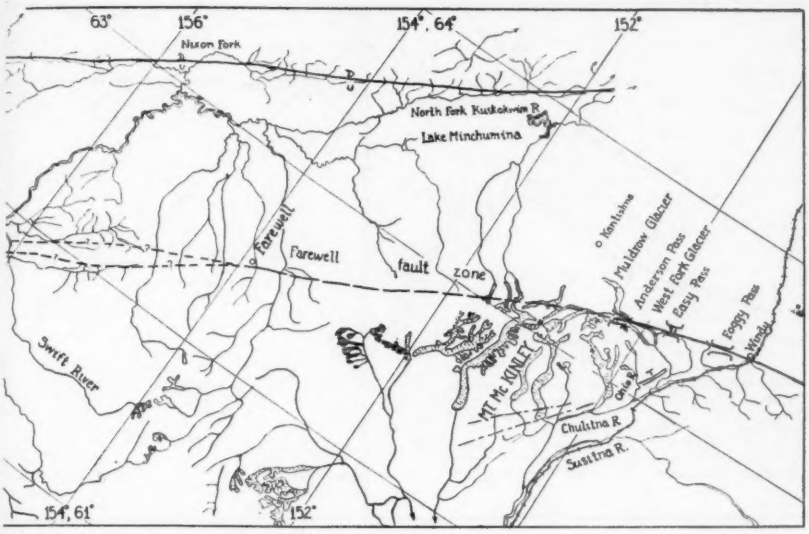

LAKE CLARK FAULTS IN WESTERN ALASKA

the intersection of the valley with the Denali Fault. It topographically resembles a fault scarp, and in at least one area thrust faulting has been observed.

Ross (1933, p. 307–309) has mapped a zone of thrusting between the Ohio River and the northwestward-flowing part of the Chulitna River. The zone is nearly 2 miles wide in which argillites of Triassic age have been shoved over rocks of Permian age. The thrusts dip in general 30°–45° to the northwest and strike to the northeast. An interesting feature of this zone is that some of the faults have horizontal grooves on the faces, indicating that the last movement was not up dip, but was lateral. The sense of the lateral movement cannot be determined from the description. The thrusts are shown in Figure 4; this author has indicated the possible extension of this type of faulting.

Nenana Glacier to Delta River

The region between the Nenana Glacier and Lower Black Rapids does not appear to have been geologically mapped. The fault probably passes under the middle reaches of the West Fork Glacier and Upper Black Rapids Glacier (Fig. 6). The possibility that the fault passes under or alongside the catchment basin of this glacier reopens the question as to the cause of its rapid advance in 1936 and 1937, (Hance, 1937, p. 782; Moffit, 1942, p. 146–158).

From Delta River to Alaskan Canadian Border

The Denali fault is recognized by Moffit (1912) just north of Miller's Roadhouse. Near the highway it separates Birch Creek Schist on the north from Carboniferous quartzite and Jurassic (?) intrusive rocks on the south. The fault passes under Canwell Glacier, to the east lies under the head of Gakona Glacier and Chistochina Glacier, forms an unnamed pass, determines the course of the Upper Slana River, and lies near Gillett Pass at the head of the Big Tokio River (apparently called Dry Tok Creek on later maps). The fault was recognized first in 1902 in this region by Mendenhall and Schrader (1903, p. 51) and Mendenhall (1905, p. 47, p. 83, 84).

In general the Birch Creek Schist on the north is faulted against the Mankomen Formation of Carboniferous age and the Tertiary Gakona Formation. The fault was thought to be a thrust dipping southward. Multiple faulting is recognizable between the west and middle forks of the Chistochina River.

Eastward, Moffit, *et al.* (1910, p. 46) recognized that a fault lies on the north of the Nutzotin Mountains, although they also invoked the possibility of a flexure without faulting. The

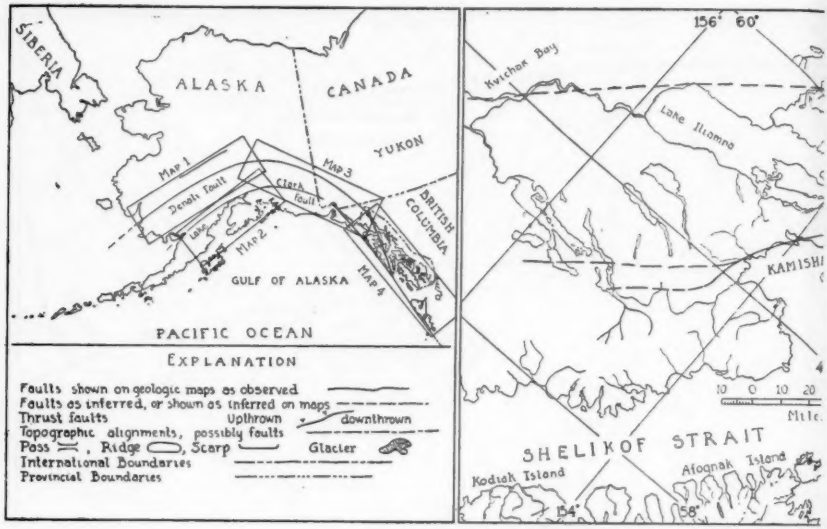

FIGURE 5.—INDEX MAP AND COURSE OF THE DE-

present author suspects that the fault crosses through the range near Mentasta Pass, (although in order to do this it must transect a large body of rock, shown as a single unit by Moffit (1954)) and connects the western portion of the fault with the Nutzotin scarp. This scarp is more than 60 miles long. To the south of the Nutzotins, Moffit, *et al.* (1910, p. 46) inferred a fault to lie between Carboniferous and Jurassic rocks in Cooper and Notch creeks. The alignment of Geohenda Creek, Platinum, and Lost Creeks suggests faulting, but it is not possible at the present stage of mapping to identify faulting with any certainty. In later work, Moffit (1938) and Moffit and Wayland (1943) give a little attention to these features but do not show faulting on their maps, although lateral faulting offers a reasonable explanation for the complex stratigraphic relations in that area.

In his monumental summary of more than 40 years field work Moffit (1954) has summarized the mapping in this region and recognizes that the Denali Fault extends from "some point west of the Delta River to the Little Tok and probably to Tetlin River" (p. 92). He says that in general the fault is a "zone of displacement and crushing, rather than a single plane of fracture and movement." The fault may extend westward to Mt. McKinley and eastward to Tetlin River (p. 177). He also suggested that it may branch around the Nutzotin Mountains and shows faults in Cooper and Notch Creeks. His interpretation differs in some details from that of this paper, but the main features of the locations are identical as they should be, because the author's interpretation is based in large measure upon Moffit's field work.

Canadian Border to Lake Kluane

Cairnes (1916) shows the section just east of the Alaska-Canada Boundary. Here it is clearly permissible to draw a fault between Gates Ridge, mapped as Cretaceous intrusive rocks and Cottonwood Hill to the south, mapped as Carboniferous sedimentary rocks. Gates Ridge diverts Baultoff and Beaver Creeks westward, the latter by about 6 miles. This ridge resembles the shutter ridges on strike-slip faults in parts of California. There is a small patch of lava in the fault zone in this section.

Bostock (1952) has published an excellent geologic map of the Shakwak Valley on a scale of 1 inch to 4 miles. He begins his inferentially plotted Shakwak Valley fault at the eastern end of Gates Ridge and continues it southeastward for 120 miles through the Shakwak Valley past the southeastern end of Lake Kluane. The following quote is from Bostock's work (p. 8, 9).

"The straight, steep front of Kluane Ranges along the southwest side of Shakwak Valley and

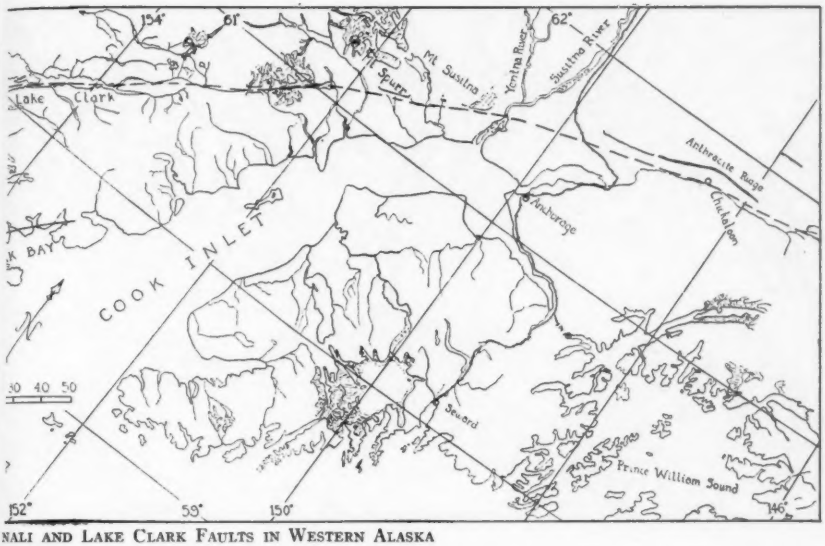

NALI AND LAKE CLARK FAULTS IN WESTERN ALASKA

the marked difference in the geology on each side of the valley, illustrated by the restriction of the old Yukon group rocks largely to the northeast and of the younger formations to the southwest, are evidence of a great fault zone along the valley, extending from west of White River southeastward beyond the mapped area to at least Dezadeash Lake (20, p. 28). The persistent drift-cover a mile or more wide everywhere along the valley prevents close study of the fault zone, but a general relative uplift of the Northeast side is indicated, though this may not represent the more recent movements along the fault.

"Examination of air photographs of the valley on the east side of Donjek River reveals a line of small, irregularly spaced, elongate mounds surmounted by relatively large trees traversing the slopes of tundra and stunted spruce (Plate IV). The mounds follow a nearly straight line along the general direction of the valley regardless of local changes in directions of slope or the interposition of glacial features, such as drumlinoid ridges, but are missing where the streams have been active recently, as on the flood plains of Donjek River and in the courses and alluvial fans of the creeks in line with the mounds.

"This line of mounds is most apparent on the east side of Donjek River, but can be traced at intervals from west of White River in the northwest to the far side of Kluane Lake in the southeast. The feature is believed to mark the trace of a fault along Shakwak Valley in which there has been movement in recent centuries. Although the bedrock geology indicates a general vertical displacement, the alignment of the mounds marking the fault suggests significant lateral movement."

The zone is multibranched in this area, and another fault probably lies to the southwest of the Shakwak Valley fault between Cottonwood Hill and Baultoff Mountain, down Miles Creek, up Hazel Creek, part of the west and east forks of the Koidern River, down upper Lynx Creek, Tetamagouche Creek and joins a short fault shown abutting against Halfbreed Creek. This alignment of valleys may be only coincidental, because formations at the head of Sanpete Creek are not shown offset. The Duke depression also appears to represent a fault trough. This is a third valley lying parallel to the Shakwak Valley and has, in general, unlike rocks on either side for over 100 miles. In fact, Bostock has shown a fault about 2 miles long in this depression and aligned with it. The author is of the opinion that the course of the Duke depression is fault-controlled.

Lake Kluane to Lake Dezadeash

Kindle (1953) has mapped the geology of the area from just south of Lake Kluane to the British Columbia Yukon Boundary. He continues Bostock's fault, between the Yukon Group of doubtful Precambrian age on the northeast and the younger Cretaceous Dezadeash Group on the southwest to Lake Dezadeash. Here he indicates that it branches.

One branch he continues across Lake Dezadeash in the topograph trough of the Shakwak Valley. This trough contains Frederick Lake

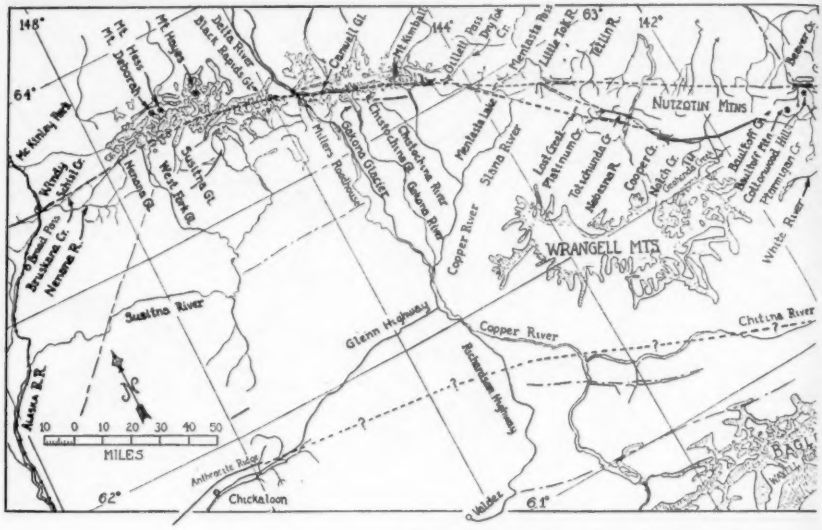

FIGURE 6.—COURSE OF DENALI FAULT IN CENTRAL

and part of Kusawa Lake. The trough continues past the border of his map and can be traced as far as Fan Tail Lake in British Columbia. The rocks on either side lie in the Yukon Group, here intensely intruded by the Coast Range Batholith. Kindle shows faulting along the sides of Kusawa Lake, but considering the lithologic similarity on both sides of this depression it would be hard to prove the existence of a fault in it. The trough is offset about 10 miles to the south where it is crossed, near Bennett, by another trough rising out of the head of Lynn Canal.

The other branch of the fault is carried down the Klukshu and Tatshenshini River to the British Columbia Border. The Yukon Group is on the east of the fault, the younger rocks to the west.

Although he does not show it clearly on his map, Kindle presents sufficient discussion and observation to indicate that the Duke depression is a fault-controlled feature. He suggests that faults lie along Cottonwood and Raft Creeks. The faulting in this region is between Triassic and Paleocene sedimentary rocks.

Lake Dezadeash to Lynn Canal

The next region south, the Squaw Creek-Rainy Hollow area, has been geologically mapped by Watson (1948). Whereas Watson's stratigraphy does not match well that of Kindle or Bostock, and he does not trace the fault out, it is clear from his map that it goes between the younger rocks on the west and the older rocks with igneous intrusions on the east. This line is marked by Tatshenshini River, Mansfield Creek and the Kelsall Rivers. Watson does not show the area around the Kelsall River as mapped, but the division between the two rock groups is clearly along the Kelsall River. Watson (1948, p. 52) discusses a prominent shear zone displaying extensive hydrothermal alteration of the rocks in the zone. This zone forms a bench to the east of Mansfield Creek. This zone is probably an expression of the great fault.

This portion of the fault is marked by the same sort of depression as farther north. The old Dalton Trail followed it, and the present Haines Cut-off Road is built a large part of the way in the trough.

The next geologic mapping to the south is in the Porcupine mining district (Wright, 1904; Eakin, 1916). This shows the same division between sedimentary and igneous rocks as is found farther north.

Lynn Canal

Wright and Wright (1908, p. 21–22) assume a fault, branched at the head of Lynn Canal (Fig. 7) lies in Lynn Canal and Chatham Strait. They base their reasoning on differences in geology on the two sides of the canal and on the

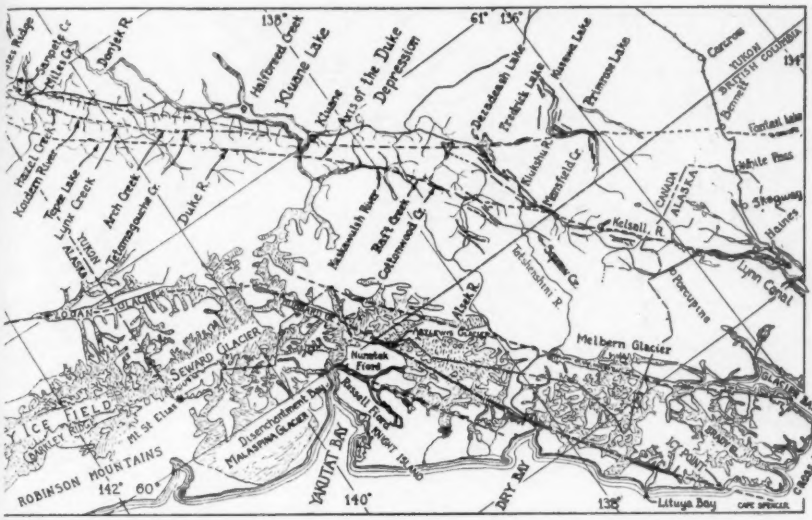

ALASKA, YUKON TERRITORY, AND BRITISH COLUMBIA

fact that this feature, more than 250 miles long and only 3–6 miles wide, traverses the general trend and "bedrock structure" of the mountains at an angle of about 30°.

This is about as far as the Denali fault can be traced on geologic and geomorphic inference.

Recapitulation

It is clear that a major zone of faulting, probably a continuous but multibranched fault, runs through the entire range from Cape Decision in Christian Sound to the Bering Sea. The feature crosses the mountains three times, from the southwest in the ocean it crosses to the north and east in British Columbia, re-enters near Mentasta Pass, passes to the south of the range between Mentasta Pass and Muldrow Glacier, and passes through the range again to form the scarp to the north and the west of Mt. McKinley and thence to the Bering Sea. In this 1300-mile course, it does not depart more than a few tens of miles from a circular arc with a radius of 620 miles (1000 km) and a pole at 54½° N. Lat., 149½° W. Long.

Other Possible Zones of Faulting in Southeastern Alaska

Faulting Along the Gulf of Alaska

To the west of Lynn Canal and Chatham Strait, are a number of odd topographic tendencies. The long straight west coast of the Baranoff and Chichagof Islands looks as if it might be determined by faulting. The presence of the volcanic cone of Mt. Edgecumbe on Kruzof Island, situated at a slight kink in the coast line, heightens the suspicion. The cone is surrounded by basaltic and andesitic lavas of Quaternary age (Knopf, 1912, p. 14–15).

A long trough occupied by a series of glaciers lies along the projection of this coast line to the northwest. From a few miles from Icy Point, near Cape Spencer, this feature trends roughly N. 30° W. for about 150 miles. The trough cuts across the heads of Lituya Bay, Dry Bay, Nunatak Fiord, and under the glacier at the head of Yakutat Bay. It is occupied in turn by the Artlewis and Hubbard Glaciers. This valley is anomalous in that it is so straight and lies parallel to the front of the range, (the front itself appears to be determined by faulting) rather than along the more natural drainage trends at right angles to the axis of the range. The long valley is the trace of an active fault, probably of lateral or oblique habit.

Kennedy and Walton (1946) thought that this trough marked the course of a fault. They show an inferred fault along the head of Lituya Bay between slates and greenstones on the west and schists and amphibolites on the east.

Movements in 1899

In their excellent work on the Yakutat Bay earthquake, Tarr and Martin (1912) give some

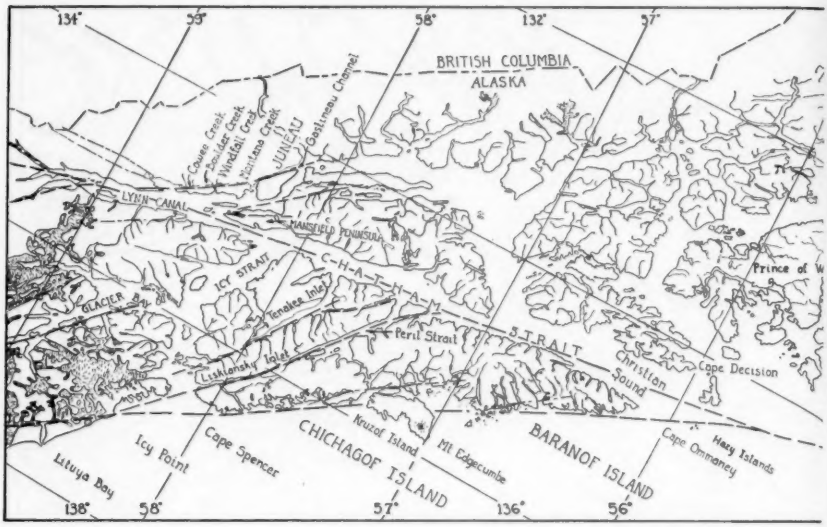

FIGURE 7.—COURSE OF DENALI FAULT IN

information that is of help in inferring the state of activity of this fault. Being excellent observers, they recorded everything that came to their attention whether they could explain it or not. They describe as minor faulting a series of steps and treads in a zone with a trend N. 40° W. (p. 37). These were on a rock hill at the head of Nunatak Fiord (Fig. 6). They were of unequal length, up to several hundred feet long. The zone contained some cross faults and grabens. The vertical component of motion was not very evident for the zone as a whole. The authors found this sort of faulting in several places, but they did not give exact locations. Martin concerned himself with the problem to some extent and concluded tentatively that the feature represented an oblique slip movement. Unfortunately, the zone was obscured by the glacier in the trough, so that the significance of the discovery was not realized. It is the authors opinion that the main motion of at least one of the major Yakutat Bay shocks occurred on this long troughlike feature. The uplift along the shore line represented secondary phenomena associated with the upthrusting of fault slices between Russell Fiord and Knight Island. This theory is strengthened by the reports of violent activity along the coast to the south and the report of a change in level near Cape Spencer, but it is unlikely that this theory will ever be proved.

Tarr and Martin also show a possible fault along Russell Fiord. This can be traced on topographic evidence for some distance past the head of the fiord. There is little doubt that the whole complex of faults for a considerable distance in all directions from Yakutat Bay took part in the movement. The anomalous advance of glaciers reported in the Glacier Bay Region, as well as the 1937 advance of the Black Rapids Glacier, may well have been due to fault displacement rather than the shaking down of snow.

Small-Scale Tsunamis in Yakutat and Lituya Bays

The small-scale tsunami that occurred in Yakutat Bay, described in Tarr and Martin (1912, p. 46–48) does not oppose the concept. It was three times as violent along the east side of Yakutat Bay as it was on the west side. It is possible that the sudden thrusting forward of the sides of Disenchantment Bay, in a northwesterly direction virtually shoved the land under the waters of the bay and caused them to lap up on first the east side and then to rush across the harbor to wash up on the west side.

Miller (1954, p. 1346) discusses two local tsunamis occurring in Lituya Bay. These have the same general nature as the type of wave observed in Yakutat Bay. Miller recognizes the fault at the head of the bay as active and attributes the waves to possible movement on

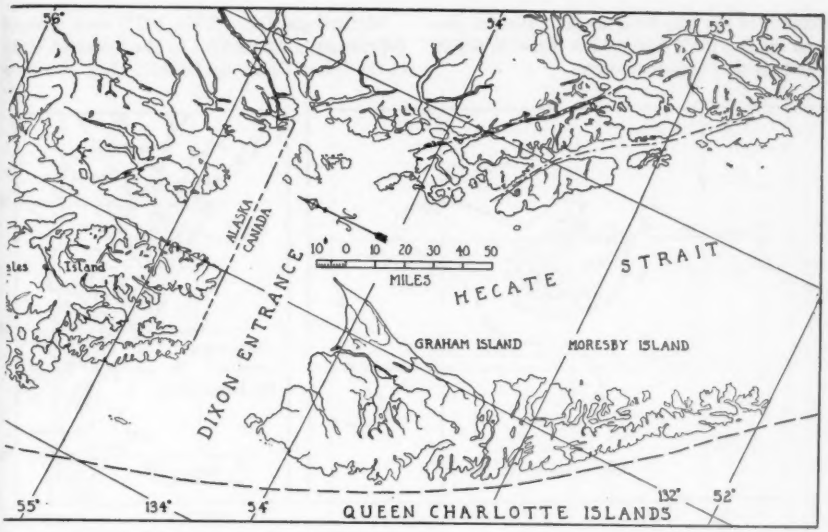

SOUTHEASTERN ALASKA AND BRITISH COLUMBIA

this fault. He is troubled, however, by the fact that no earthquakes are reported at the two dates he has fixed for the occurrence of the cataclysmic waves. It is conceivable that the dates he assigns are in error and that one of the waves occurred at the time of the Yakutat Bay earthquakes or some subsequent shock, or that earthquakes occurring on the dates assigned by Miller were missed or not properly located. It is also possible that the waves were not caused by earthquakes.

Other Faulting

Glacier Bay, the Melburne Glacier, and an alignment of river courses to the north present another linear feature subparallel to the fault in the glacial trough at the heads of Yakutat and Lituya Bays (Fig. 7). There are also a number of linear features in the archipelago, such as the trend of Peril Strait and Lisianski Inlet. In this case, the geology on either side does not preclude a fault, although none is drawn on the maps presented by Buddington and Chapin (1929) or Knopf (1912). The alignment of Cowee, Boulder, Windfall and Montana Creeks, and Gastineau Channel also strongly suggest an important lateral fault.

The region lying between the glacial trough, its coastward companion features, and the great fault through Lynn Canal, about as far north as Lake Kluane, contains most of the epicenters ascribed to this general part of Alaska and British Columbia. A few epicenters lie under the sea off the coast and may indicate additional zones of faulting lying offshore.

The determination of fault courses in the Archipelago and in the St. Elias ranges by topographic trends is a practice that cannot be pursued with confidence in view of the extensive glaciation that has taken place in the area and is still, in places, obscuring much of the bedrock geology. It seems wiser to avoid extensive speculation pending further detailed geologic mapping in that region. The faulting must play a very important role in determining the courses of glaciers, streams, and even the local seaways. This must be considered while doing geologic mapping in this area. Sainsbury and Twenhofel (1954) have discussed the faulting in this area and have published an abstract of their paper, in which conclusions similar to those expressed herein are detailed. Their work is based on long experience in the field and upon recent mapping and air-photo coverage.

FAULTING SOUTH OF DIXON ENTRANCE

Inference from Seismology

To the south of Dixon Entrance, a line of epicenters may be followed as it leaves the coastal mountains and extends, with but minor breaks, to a point near, but shoreward of, the undersea

extension of the San Andreas fault system. Between the two fault systems is a region in which no earthquakes appear to occur.

Menard and Dietz (1951–1952) show a closed depression lying parallel to the undersea scarp of the Queen Charlotte Islands. They also show

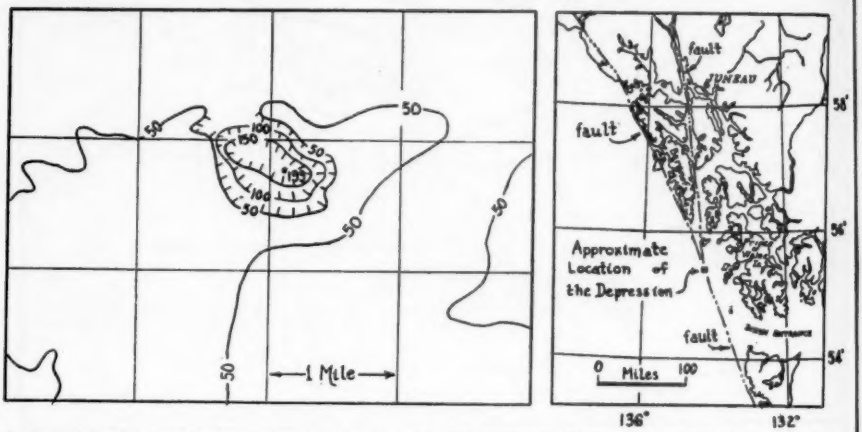

FIGURE 8.—SKETCH OF SUBMARINE DEPRESSION ON CONTINENTAL SHELF IN THE GULF OF ALASKA
The figure has been adapted from Murray (1941). The depths are in fathoms. Note the low relief of the ocean bottom in the vicinity of the depression. The grid is 1 statute mile on an edge. As accurately as can be deduced from Murray's small-scale map, the depression is on the main line of faulting.

Inference from Oceanography

The undersea topography south of Cape Ommaney shows some unusual features. A number of depressions partially cut across the continental shelf, and these often lead to deeper water on the inland side. A completely closed depression lies exactly on the projection of the fault through Chatham Strait and possibly at its intersection with the fault along the west coast of the Baranof and Chichagof Islands and in the glacial trough at the head of Lituya and Yakutat Bays. This depression has been discussed by Murray (1941, p. 336–337) and by Heck (1927). It is (Fig. 8) about 7500 feet by 12,000 feet and is about 900 feet deeper in the center than on the edges. Heck was of the opinion that it is a crater, but it may be instead a tectonic accident, a kind of undersea sag pond. Menard, on the other hand, has informed the author that this sort of depression is not unusual near shores such as Norway, Alaska, and Newfoundland.

The continental shelf is narrow in this region and to the west of the Queen Charlotte Islands, the 100-fathom contour lies only about 1 mile offshore. The narrowness of the shelf and the straightness of the western shore of these islands lead to the postulation that a fault defines the oceanward shoreline of the Queen Charlotte Islands.

an alignment of undersea topographic trends along the course of the fault; but these cannot be followed far beyond the Queen Charlotte Islands. Near the gap in the line of epicenters, at about Lat. 45°, Long. 130°, the topographic trends might be interpreted as indicating that thrust faulting or folding is taking place en echelon to the lines of epicenters.

Incidentally, it is at this point that Gutenberg and Richter (1935, p. 324) have deduced that the division between continental and Pacific Basin-type structure occurs.

GEODETIC FORMATION

Contemporary Changes in Land Level

There are over parts of Alaska, British Columbia, and the Yukon Territory, present changes in land level of sufficient magnitude to be measured. Montgomery (1948, p. 16) reports that the bench mark "Tidal 3" at Skagway has risen 2.14 feet in the years between two successive determinations of sea level, one covering the period 1908–1910, the other the period 1944–1946. The level lines run in 1943–1944 along the White Pass Yukon Railway did not agree with levels run in 1908–1910. The results indicated a tilt in which the northern end of the line dropped 4.9 feet in 115 miles. The bench mark at Big Delta was found to have

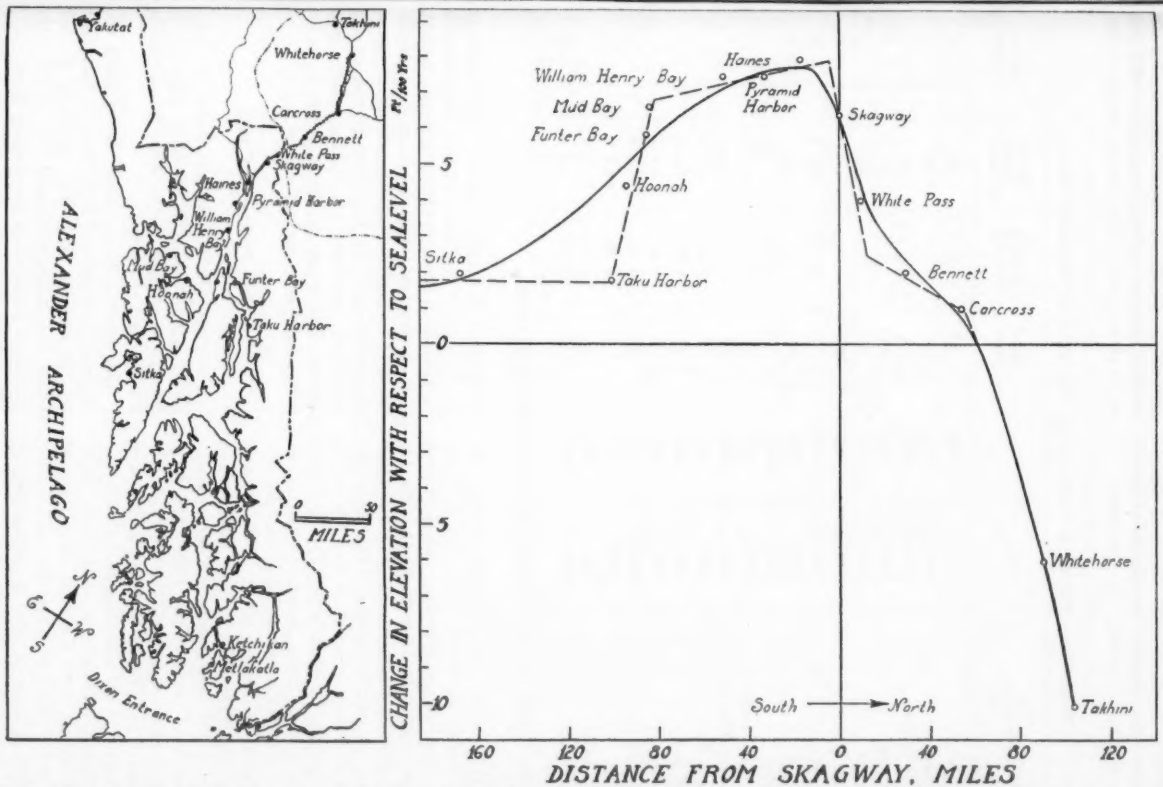

FIGURE 9.—CHANGE OF LAND ELEVATION IN PARTS OF ALASKA, YUKON TERRITORY AND BRITISH COLUMBIA, WITH RESPECT TO SEA LEVEL

This figure shows the data listed in Table 1. The distances are arbitrarily taken north and south of Skagway. The solid line represents an attempt to pass a smooth curve through the points, the dashed line is an alternative interpolation. South of Skagway, all the places plotted except Taku Harbor and possibly Funter Bay are to the west of the fault presumed to lie in Lynn Canal. In the second interpretation that portion of the Alexander Archipelago west of the fault might be being lifted as a block instead of there being a general upbowing of the Archipelago and downfold of the region to the north.

dropped 1.6 feet since 1923, a change of 8 feet per century; in this instance the possibility of thermokarst topographic development due to melting of permafrost must be considered.

paragraph, and unfortunately the observational periods are short. An interesting feature is the crochet of mean sea level observed in 1951–1952 at all three stations. The secular change reveals

TABLE 1.—CHANGES IN LAND LEVEL OBSERVED BY GEODETIC MEANS

Place	From	To	Period, years	Change in level, feet	Rate of change, ft/100 yrs.	Type of evidence
Big Delta	1923	1943	20	1.6	−8	L + T
Takhini	1908–10	1943	34	....	−10	L + T
White Horse	1908–10	1943	34	....	−6	L + T
Carcross	1908–10	1943	34	....	+1	L + T
Bennett	1908–10	1943	34	....	+2	L + T
White Pass	1908–10	1943	34	....	+4	L + T
Skagway	1908–10	1943	34	2.14	+6.3	L + T
Yakutat	1909	1950	41	1.7	+4	T + S
Haines	1890	1922	32	2.53	+7.9	S
Pyramid Harbor	1890	1922	32	2.37	+7.4	S
William Henry Bay	1890	1922	32	2.37	+7.4	S
Funter Bay	1890	1922	32	1.87	+5.8	S
Mud Bay	1902	1923	21	1.39	+6.6	S
Hoonah	1901	1923	22	0.96	+4.4	S
Taku Harbor	1890	1920	30	0.53	+1.8	S
Sitka	1893	1924–5	31	0.58	+1.9	S
Metlakatla	1883	1914	31	0.04	0.1	S
Ketchikan	1919	1953	34	0.00	0	T + S

L means leveling, T means tide guage, S means sea-level observations.

The U. S. Coast and Geodetic Survey has made available the details of the two levelings (Fig. 9). The extrapolation into change of level in feet per century is the author's and assumes that all differences are due to actual changes and not to errors of leveling, and that the vertical rate of change is sensibily constant for at least a century for each point. The land near Skagway is rising about 6 feet per century; at Carcross it is sinking about 9 feet per century.

Additional evidence is given in Woodworth and Haight (1927, p. 73–76) and incorporated in Figure 9. The data consist of observations of mean sea level made in the 1890's and early 1900's and again in the 1920's. Unfortunately the period of the 1899 earthquakes is embraced between most of the observations, but this may not be serious because some of the most vigorous movements were observed subsequent to 1899. Table 1 shows a compilation of the tide-gauge data, change of level as determined by leveling, and sea-level observations.

The U. S. Coast and Geodetic Survey has also made tide-gauge data available for Ketchikan, Skagway, and Yakutat. This information is illustrated in Figure 10. This involves the same sort of assumptions as in the preceding

an increase in height of about 4 feet a century of the land at Yakutat, whereas the elevation of Ketchikan remains comparatively constant.

It is clear that the region between Metlakatla and Carcross is rising, and the region to the north as far as Big Delta is sinking, the maximum upbowing is taking place near Haines. Unfortunately, there seems to be no data available to the east or west.

Post-Pleistocene Uplift

Twenhofel (1952) has summarized in a very useful manner all the available information concerning changes in the shore line along the Pacific coast of Alaska.

The general change from the southern end of the archipelago near Ketchikan to Aniakchak on the Alaska Peninsula, including Kodiak Island and Middleton Island, but excluding the stretch of coast along the Copper River delta and Prince William Sound, is that of uplift. Most of the evidence for uplift consists of marine deposits, usually derived from glacial debris, containing post-Pleistocene fossils, elevated from a few feet to 600 feet or more.

The evidence for subsidence in the Copper

River delta is that of terrestrial vegetation buried 20–40 feet below sea level and the existence of peat deposits 30 feet below sea level in rising and not sinking as might be suspected in proximity to the end of the Aleutian Trench. Twenhofel (1952, p. 536) points out that these

TABLE 2.—FIRST-MOTION DATA FOR NORTH PACIFIC EARTHQUAKES

Circumstances					Attitude		Movement		Remarks
Date			ϕ	λ	Strike 0	Dip 0	Horizontal	Vertical	
d	m	y							
13	04	49	46.9	122.6 W.	49 E.	83 NW.	L	R	H and S
					76 W.	12 SW.	R	R	pref.
06	07	34	41.5	124.5 W.	40 W.	84 NE.	R	sR	Byerly
23	06	46	49.8	124.9 W.	23 W.	60 NE.	R	N	H and M
					13 W. to 15 E.	31 W. to 36 NW.	—	N	
30	12	48	51.0	131 W.	65 W.	39 NE.	L	N	H and M
					59 E.	67 SE.	R	N	pref.
22	07	37	64.7	146.6 W.	37 E. to 30 E.	71 SE. to 64 SE.	L	sN	Adkins
16	10	48	64	148 W.	30 W.	78 NE.	—	N	pref. H and
					30 W.	12 SW.	—	N	M
27	09	49	60	149 W.	70 W.	72 NE.	—	N	H and S ex-
					70 W.	72 NE.	R	N	tension
					08 E.	57 NW.	L	N	indicated
01	04	46	53.5	163 W.	65 NE.	65 NE.	R	N	tsunami, H
					22 E.	85 NW.	L	sN	and M
									pref.
25	08	49	52.5	178 W.	09 E.	StpW.	L	N	H and S
					81 W.	90	R	—	
03	05	49	49	153 E.	06 W.	75 SW.	R	sR	H and S
					89 E.	71 NW.	L	R	depth of
									0.01 R
03	11	49	48	154 E.	67 W.	72 NE.	L	—	H and S
					25 E.	79 SW.	R	—	

Strike is measured from north. Stp means steep. In horizontal column, R means right lateral, L means left lateral, — indicates lack of evidence of horizontal movement. In vertical column, R means reverse, N means normal. A lower case s preceding the letter indicates that motion in that mode is slight compared to that in the other case.

Adkins refers to Adkins (1940), Byerly refers to Byerly (1938). H and S refers to Hodgson and Storey (1953), H and M refers to Hodgson and Milne (1951). Pref. indicates the preference given by the original authors, not necessarily that of St. Amand.

the bottom of Bering Lake. In the Prince William Sound region the primary evidence is that of drowned forests. Twenhofel ascribes this sinking to primarily tectonic processes rather than compaction of sediments.

I. C. Russell (1892, p. 24–26) describes a marine formation, thought to be of Pleistocene age, raised to heights as great as 5000 feet near Pinnacle Pass and in the Chaise Hills, just west of Yakutat Bay. Maddren (1914, p. 131–132) has related these to similar deposits 2000–4000 feet thick on the slopes of Robinson Mountains. Menard and Dietz (1951, p. 1280) cite these beds as described by Smith (1939, p. 59) in order to point out that the coastal region is beds are now thought to be Pliocene and therefore indicate less post-Pleistocene uplift than heretofore supposed.

Uplifted features such as those found along the southern coast of Alaska are missing from the northern coasts of Alaska, and the general tendency appears to be that of subsidence. Anthropologists have long postulated a land bridge across the Bering Straits, and it is very possible that such a bridge existed during and after the Pleistocene.

The apparent changes in land level are of course influenced by changes in the over-all level of the sea. It is difficult to assess this problem, because sea level may have changed mark-

edly since the Pleistocene and may be still slowly changing. The cause for the changes may be ascribed in part to this and in part to tectonic processes. It does not seem likely that unloading of the tremendous weight of Pleistocene ice is entirely responsible either because it would be the dip of the zone is steep. The appearance of the trough is similar to the path of the San Andreas fault in California, where it crosses hills and mountains.

In the high mountains, many streams are diverted from a normal course down the general

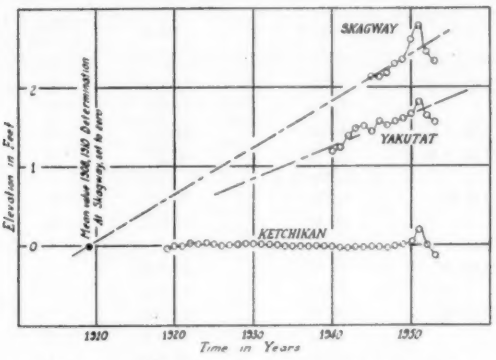

FIGURE 10.—CHANGE IN SEA LEVEL AT ALASKA PORTS
This figure shows the height above sea level that a hypothetical peg driven into a rock at sea level in 1909 would have as a function of time.

hard to explain the local downdropping, along the coast and in the interior, by this process.

It would be of tremendous interest to rerun level lines along the Richardson Highway and Alaska Railroad and to install tide gauges at other Alaskan Ports, along the Aleutian Islands, the Bering Sea Coast, and the coast of Kamchatka and Siberia.

TECTONIC SPECULATION

Nature and Movement of the Denali Fault

If one assumes that the great fault is a continuous feature, one must ask what the nature of the fault and the type of movement must be. It is likely that the fault is branched, or cut off, to the south of Lake Kluane, so the portion north of that point will be discussed first.

The nature and type of movement is unknown, but several clues that suggest that it may be a lateral fault are available. This idea has occurred to Clyde Wahrhaftig and R. B. Campbell.

The transverse profile of the fault zone is usually a trough, up to several miles in width, from which erosive agents have presumably removed rock crushed and weakened by the faulting. This condition prevails over most of its length. This phenomenon also indicates that slope of the land, to one parallel to the axis of the hill. Glaciers occupy a large portion of the trough. The trough furnishes a catchment basin for the glaciers, which in turn find it easier to flow along the trough for miles than to break out of it and pursue the gradient of the general hill slope.

Where the fault lies along, or at the foot of, a slope, the path is marked by a series of cols and buts. The shutter-ridgelike appearance of Gates Ridge has been mentioned.

The description by Bostock (1952, p. 8, 9) of the elongated ridges in the alluvium near Lake Kluane are extremely suggestive of lateral faulting. It appears as if several glacial and river vallays have been offset by the fault.

If the present elevation of the hills on either side of the fault was caused by vertical movement along the fault, then the vertical component of motion is not consistent along the length of the feature. Neither is the apparent stratigraphic throw of the fault always consistent with the present elevation of the land. The younger rocks lie in general along the south or west side of the fault, but in the Mt. McKinley region the highest mountains are on the south. Between the Nenana River and Mentasta Pass, the highest mountains are to the north, and the stratigraphic throw is more reasonable (assuming that the Wrangell Moun-

tains are predominately constructional volcanic features). In the Lake Kluane region, the highest land again lies on the side containing the younger rocks. The maps presented by Capps (1940) for the McKinley Park region show reversals of apparent stratigraphic throw over a distance of a few miles.

Direction of Faulting in Southeastern Alaska

Aside from the same general sort of argument and the rather hypothetical discussion for the Yakutat Bay shocks, the only evidence for direction of offset readily available is the first motion data furnished by Hodgson and Milne (1951, p. 237) for the Queen Charlotte earthquake of 22 October 1949 (Table 1). This yields a strike of N. 29° W., first motion is right lateral, and there is a slight tendency for the continent to overthrust the Pacific Basin.

Connection Between Denali Fault and Faulting in Southeastern Alaska

Juncture at Lake Dezadeash

Although the general trend of the Denali fault is curving, it possibly continues past the juncture with the fault up Lynn Canal. It is even possible that it is cut off and offset by the fault passing through the eastern arm of the canal. The juncture with the branch running towards Lake Kluane may well be an abutment rather than a smooth transition, or if smooth it may have been made so by progressive deformation.

Relation of Faulting Westward

The fault through Lynn Canal possibly bifurcates southward, one branch passes through Chatham Strait, and the other passes to the east of Mansfield Peninsula. The section passing through Chatham Strait no doubt connects with the fault zone running southward toward the San Andreas system, and northward past Yakutat Bay. At about the latitude of Yakutat Bay and to the north, an extensive westward topographic trend develops. Do the long linear ice bodies such as the Seward Glacier, and the Bagley Ice Fields lying along Barkley Ridge and Waxell Ridge, represent structural tendencies, possibly faults? Sharp and Rigsby (1954, p. 122), have called attention to these features and suspect that they are structural trends, possibly governed by thrust or steep reverse faults.

Present State of Activity

The Denali fault in the Alaska Range, appears to be currently active from west of Mt. McKinley to Mt. Kimball. It appears quiescent between Mt. Kimball and Lake Kluane, where it has been active in comparatively recent geologic time. South of Lake Kluane, seismic activity begins again. This activity may be due, not to the Denali fault, but to the northward projection of the fault system in southeastern Alaska.

The fault along the west coast of Baranof Island is active. The present state of activity here is not to be considered low simply because no very large shocks have occurred in recent years.

Connection with the San Andreas Fault System

Hiatus Between the San Andreas and Alaskan Faults

The line of epicenters connected with the Alaskan fault system appears to stop at a point near the end of the line of epicenters associated with the San Andreas fault system. This point is about opposite the northern end of the Basin and Range Province and the Columbia Plateau. Lava Fields. The line of closely spaced, dormant volcanoes that fringe the coast of the western United States stops at about this point as do the cordilleran earthquakes. It is tempting to think that the San Andreas system may have predated, or have been contemporaneous with the Basin Range orogeny and that the discontinuity represents a relative westward movement of the Sierran Block and the coastal ranges between this gap and the transverse ranges and subsequent extension in the block-faulted Basin Range and Columbia Plateau Provinces. If this is so, then the San Andreas system has been active since Miocene time or possibly earlier.

Other arguments, such as a change in crustal strength, to account for the discontinuity can, of course, be invoked.

Possibility of Rotational Movement

Is the Pacific Basin Being Shoved Under Alaska?

If the two systems represent one consistent system, some interesting possibilities arise. One

that the San Andreas and Alaska Complex is a gigantic tear fault, along which the Pacific Basin is being slid, relatively speaking under the Alaska Mainland and the Bering Sea.

region south of the Alaska Range has been and is still probably being rotated counterclockwise. If this is so, then it is possible that the Alaska Range between the Nenana and Delta

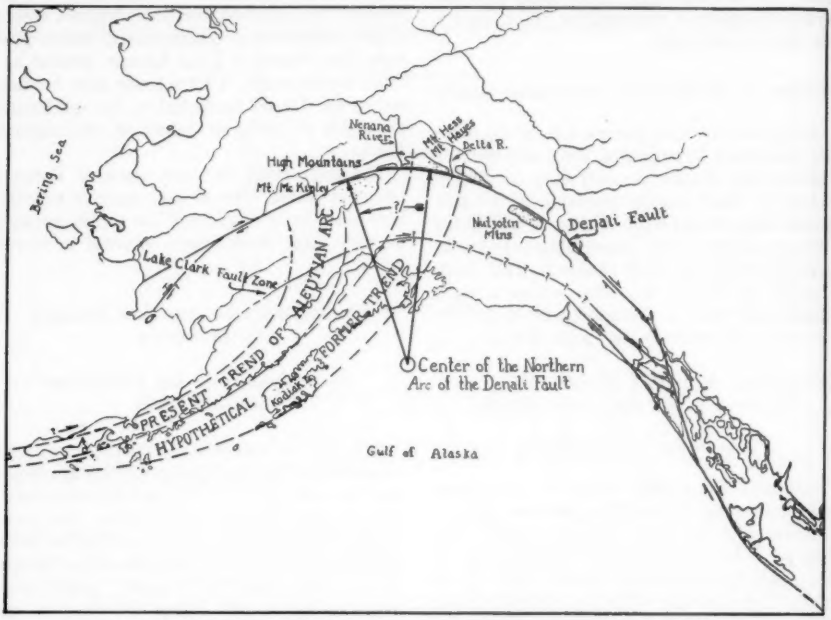

FIGURE 11.—SPECULATIVE CONSEQUENCE OF MOVEMENT ON THE DENALI FAULT

It is assumed that the fault has undergone right lateral displacement of about 150 miles. The massif of Mt. McKinley would then have fitted with the Mt. Hess-Mt. Hayes group, and the southern part of the territory would have undergone rotation.

Is the Pacific Basin Rotating?

On the other hand, if the whole system is a strike-slip fault having consistent right-lateral offset, then the whole of the western north Pacific Basin must be undergoing rotation. This argument may be invoked, even if the Denali fault and the southeastern Alaska complex represent structures of different age, that is to say if the Denali fault is an older feature.

The Denali fault is subparallel to a series of somewhat similar features between it and the Rocky Mountain Trench, which is itself very similar. If these are also strike-slip faults with the same sense of motion as the present San Andreas system, then the northern half of the continent has been undergoing rotation for a very long time.

If the motion is mainly right-lateral strike-slip along the whole of the Denali fault, the Rivers was once a continuous structure with the Aleutian Range, and the eastern end of the Aleutian Range has been shoved and twisted westward about 150 miles along the Denali fault (Fig. 11). This, however unreasonable sounding, is not beyond possibility. The width of the two segments is about right and the lack of high mountains behind the Denali fault in the Mt. Hayes-Mt. Hess region and to the north of Mt. McKinley is odd. Offsets of more than 225 miles since late Eocene time for the San Andreas system have been suggested (Hill and Dibblee, 1953, p. 449), and although these are not generally accepted, there have been no successful correlations across the San Andreas fault at lesser distances. Unless beds or other markers that could have been correlated have been destroyed or obscured, the land on either side of the fault has moved farther than the greatest distance over which correlation fails.

It is the author's opinion that Hill and Dibblee are more nearly correct than are their critics.

If the present rate of movement on the San Andreas system is applicable to the Denali fault, a purely arbitrary assumption, only 4×10^6 years would have been required for the movement to take place.

Do Pacific Arcs Undergo Lateral Motion?

Recent work by Hodgson and Milne (1951), Hodgson and Storey (1954), and unpublished work by Hodgson indicate that, on the basis of first-motion studies, the Pacific Arcs may be rotational strike-slip features. This is seemingly at variance with the hypotheses held by most geologists and supported by Benioff's (1954) analysis. The latter clearly indicates a complex zone of faulting extending to depth and usually dipping under toward the inside of the arc. Perhaps a rotational component of motion must be added to the apparent overthrusting tendencies to reconcile the two views. Coats (1950, p. 37) calls attention to an earlier paper by Knappen (1929) who made an exploration of the Aniackchak region on the Alaska Peninsula. Unfortunately Knappen left the survey before finishing his manuscript, and so the work is not complete. The important fact that he points out (p. 207) is that the predominant faulting is right lateral in nature. In general, the major structural feature is a great anticline of the Aleutian Range whose axis is northeasterly and closer to the Pacific Ocean than to the Bering Sea. The folds are broken by faulting and jointing. The largest faults are thrusts in which the northwestern block has sheared along a northeasterly line, moved northeastward a considerable distance and overriden the southeastern block to a slight or moderate extent. In other words, the movement has not been purely compressional or perpendicular to the strike of the fault, but the Peninsula has been subjected to shearing forces which tended to move the northwest side northeastward, and the thrusting and overriding have been incidental to a much more extensive horizontal movement.

The work of Robinson (1947) does not, on the other hand, furnish much evidence of such thrusting or extensive lateral faulting. It is likely, in the author's opinion, that some major lateral faults have been overlooked in past studies. They are very hard to detect in a volcanic or igneous terrain, and they must be actively looked for to be found. The major Aleutian faulting will probably prove to be a series of enechelon lateral faults which have volcanoes along tensional tear faults and subsidiary squeezing up of the ridge along thrusts and high-angle faults.

Further field work must be done to determine if this condition predominates over most of the Alaska Peninsula and perhaps the Aleutian Islands. If Knappen's observation is born out, it may well point the way to a solution to the problem of the nature of movement on Pacific Island arcs.

First Motion from Seismograms

The first motion data for a number of Alaskan and other north Pacific shocks have been collected in Table 2. Some of these do not tie in at all well with the general geologic structures. This is due in part to an imperfect knowledge of the geology; just as probably it is because a large percentage of earthquakes take place on subsidiary faults related to the main faults but possessing a different orientation and habit of movement. The main shock of the Kern County, California, series of 1952, on the oblique-slip, left-lateral, steep-reverse White Wolf fault might be cited as an example. It took place in a region dominated by the right-lateral, presumably vertical San Andreas fault, which has an orientation differing by almost 90°. This configuration is physically compatible with the movement of the San Andreas.

The motion as indicated by at least one of the solutions for almost all the earthquakes connected with the mainstream of activity, is consistent with the notion of counterclockwise rotation of the Pacific Basin between Baja California and the Kurile Islands. The suggested first motion is always at a slight angle to the strike of the arc at the epicentral region.

Menard's Theory of a Convection Cell

None of the ideas presented herein seems to the author to be at variance with the hypothesis of Menard (1956, p. 1179–1182) that a gigantic convection cell exists, or has existed, under the Pacific. The possibility of offset of the Sierra Nevada Mountains westward agrees with his Murray and Mendocino fracture zones, as he indeed indicates, and this suggests a Miocene or pre-Miocene age for the fracture zones. The strike-slip faults such as the San Andreas and the Denali fault seem logical as conjugate shear lines. If his convection cell has associated with

it a Coriolis force producing a rotation of the cell as is found in the atmosphere, then the whole pattern of the north Pacific deformation fits his hypothesis nicely. If such a force could exist what are direction and velocity of rotation and what effect has the dissipation of energy of rotation upon the length of the day and the pole of rotation? At first glance, downwelling in the Pacific would seem to better account for the direction of rotation but not as well for the small-scale features along the coasts.

Dates for the periods of activity of the Rocky Mountain Trench and the similar features lying between it and the Denali fault are not known. If these were indeed lateral faults, it would appear that they have been successively abandoned and that the convection cell has moved westward or decreased in size.

Is The Alaska Range an Inverted Pacific Arc?

Similarities and Differences

The Alaska Range has a few of the features of a Pacific structural arc, but it lacks a good many as well. The structure is arcuate in plan, and a line of epicenters follows the general trend of the range, except as noted between Long 142° and 145°. Some volcanoes inside the arc are active.

There are also significant differences. No deep shocks take place along the range. The epicenters fall on both sides of the zone instead of predominately inside it.

Tanana Valley

The ocean deep is missing. The Tanana Valley, however, provides a geomorphically analogous feature. This valley is a depression running parallel to the mountain front for hundreds of miles and ranges in width from a few miles to almost 100 miles. The silt-laden Tanana River flows for most of its length along the northern edge of the valley. The elevation of the valley floor is 400–500 feet in the vicinity of Fairbanks, almost a thousand miles from its base level, the Bering Sea. Wells drilled in the valley indicate that the bedrock lies, in places, well below sea level. It is difficult to imagine that the valley was cut by any erosional process. Even if the level of the sea were lowered several hundred feet, the valley could not be a cut feature. It must therefore be tectonic in origin and could possibly be the analogue of an ocean deep lying offshore of a normal Pacific Arc, although it is by no means as deep.

On the other hand, it might be pointed out that it may be a feature similar to the series of troughs that run along the west coast of North America, such as the Puget Sound Trough, the San Joaquin Valley, and the Imperial Valley.

The presence of some of the arcuate features and lack of others makes it impossible to form a judgment on this matter. The Alaska Range is usually spoken of as a "cap-range" formed at the junction of a system of intersecting structural arcs. That this is the case seems doubtful, in view of the internal structure and the fact that the structures to the east and south cannot really be considered arcs in the ordinary sense of the word.

Alternate Possibilities

Some possibilities to be considered are: it is not an inverted arc; it is an incompletely formed arc; it was formerly an arc but that only vestigial characteristics remain. Perhaps it is a clue to the formation of Pacific arcs, in that they may develop around curved portions of lateral faults. In any case, it is fortunate that the feature is on land where it can be easily examined. The tectonics of the Alaska Range forms an intriguing subject for speculation.

Suggestions for Further Work

Geologic Field Work

In any tectonic study success may be expected only when a unified approach, using the results of work in all the disciplines of science, is employed. Field studies are needed to determine the sense of motion and the nature of the Denali fault and the rest of the complex. From these, the general movements of the blocks of land involved might be deduced. More field work between Lake Dezadeash and Lynn Canal is needed to determine the type of connection between the Denali fault and that through Lynn Canal. Field work is needed between the Delta River and the Nenana Glacier to determine if the fault is continuous. More mapping is needed to the west of Mt. McKinley to determine the course of the fault between Mt. McKinley and the faults described by Cady *et al.* (1956) in the Kuskokwim. It will be years before a reasonably detailed answer will be available or that the whole of the

Denali fault system can be considered a single fault, or zone of faulting with certainty, and not a fortuitous concatenation of topographic and structural trends.

The structure of the Saint Elias, Chugach, and Aleutian ranges must be worked out to understand the juncture between the Aleutian arc and the faulting to the east. It will be necessary to learn more about the Wrangell Mountains because any complete tectonic theory of the Alaska Range must explain this group of volcanoes.

An analytical study of the stratigraphy of Alaska would throw light upon the age, history, and movement of the faulting.

Geophysical Studies

In view of the possibility of rotation of the land mass of south-central Alaska, and of the whole Pacific Basin, it might be fruitful to attempt to determine the direction of remanent magnetization of some of the sediments to see if evidence of rotation will show up there.

Geodetic studies should include periodic retriangulations and relevelings. Gravimetric studies to determine the state of isostatic compensation will be helpful. Installation of additional tide gauges is desirable.

The problem can also be attacked by installation of a well-equipped net of seismograph stations so that the precise location of epicenters becomes possible and so that detailed first motion studies and strain-release analysis of aftershock sequences can be made.

This work should include the Alexander Archipelago and the portion of British Columbia through which the faulting passes, as well as the rest of Alaska south of the Yukon River. Special attention should be given to the Chugach Range. A great deal of work could properly be espended in the Aleutian chain as well, and although the immediate economic interest would not be as great, the scientific results would certainly justify the effort.

References Cited

Adkins, J. N., 1940, The Alaskan earthquake of July 22, 1937: Seismol. Soc. America Bull., v. 30, p. 353–376

Benioff, Hugo, 1954, Orogenesis and deep crustal structure-additional evidence from seismology: Geol. Soc. America Bull., v. 65, p. 385–400

Bostock, H. S., 1952, Geology of northwest Shakwak Valley, Y. T.: Geol. Survey Canada Mem. 267, 54 p.

Bramhall, E. H., 1938, The Central Alaska earthquake of July 22, 1937: Seismol. Soc. America Bull., v. 28, p. 71–75

Buddington, A. F., and Chapin, Th., 1929, Geology and mineral resources of southeastern Alaska: U. S. Geol. Survey Bull. 800, 398 p.

Byerly, P., 1938, The earthquake of July 6, 1934, Amplitudes and first motions: Seismol. Soc. America Bull., v. 28, p. 1–13

Cady, W. M., Wallace, R. E., Hoare, J. M. and Webber, E. J., 1956, The Central Kuskokwim region, Alaska: U. S. Geol. Survey, Prof. Paper 268, 132 p.

Cairnes, D. D., 1915, District upper White River, Yukon: Geol. Survey Canada Mem. 50, No. 51, Geol. Ser. 191 p.

Capps, Stephen R., 1935, The Southern Alaska range: U. S. Geol. Survey Bull. 862, 101 p.

—— 1940, Geology, Alaska railroad region: U. S. Geol. Survey Bull. 907, 201 p.

Coats, R. P., 1950, Volcanic activity in the Aleutian Arc: U. S. Geol. Survey Bull. 974-B, p. 35–49

Eakin, Henry M., 1916, Porcupine gold placer district, Alaska: U. S. Geol. Survey Bull. 699, 29 p.

Gates, Olcott, and Gibson, William, 1956, Interpretation of the configuration of the Aleutian Ridge: Geol. Soc. America Bull. v. 67, p. 127–146

Gates, O., Fraser, G., and Snyder, G., 1954, Preliminary report on the Geology of the Aleutian Islands: Science, v. 119, p. 446–447

Gibson, William, and Nichols, Haven, 1953, Configuration of the Aleutian Ridge, Rat Islands—Semisopochnoi I. to West of Buldir I: Geol. Soc. America Bull., v. 64, p. 1173–1188

Gutenberg, B., 1956, Great earthquakes (1896–1903): Am. Geophys. Union Trans., v. 37, p. 608–614

Gutenberg, B., and Richter, C. F., 1935, On seismic waves, (2nd Paper): Gerl. Beitr. Z. Geop. 45, p. 280–360

—— 1949, 1954, Seismicity of the earth: 2d ed., Princeton Univ. Press, 310 p.

Hance, J. H., 1937, The recent advance of Black Rapids Glacier, Alaska: Jour. Geology, v. 45, p. 775–783

Heck, N. H., 1927, Some unusual submarine features in the North Pacific: Geog. Rev., v. 17, p. 448–452

—— 1938, Earthquake history of the United States: U. S. Coast and Geodetic Survey Pub. No. 609, 83 p.

Hill, M. L., and Dibblee, T. W., 1953, The San Andreas, Garlock and Big Pine faults, California: Geol. Soc. America Bull., v. 64, p. 443–458

Hodgson, J. H., and Milne, W. G., 1951, Direction of faulting in certain earthquakes in the North Pacific: Seismol. Soc. America Bull., v. 41, p. 221–242

Hodgson, J. H., and Storey, R. S., 1954, Direction of faulting in some of the larger earthquakes of 1949: Seismol. Soc. America Bull., v. 44, p. 57–84

Kennedy, George C., and Walton, Matt S., 1946, Geology and associated mineral deposits of some ultra-basic rock bodies in southeast Alaska: U. S. Geol. Survey Bull. 947-D, p. 65–84

Kindle, E. D., 1953, Dezadeash map area, Y. T.: Geol. Survey Canada Mem. 268, 68 p.
Knappen, Russell S., 1929, Geology and mineral resources of the Aniakchak district: U. S. Geol. Survey Bull. 797, 227 p.
Knopf, Adolf, 1912, The Sitka Mining district, Alaska: U. S. Geol. Survey Bull. 504, 32 p.
Maddren, A. G., 1914, Mineral deposits of the Yakutaga district: U. S. Geol. Survey Bull. 592, p. 119–153
Menard, Henry W., and Dietz, Robert S., 1952, Mendocine submarine Escarpment: Jour. Geology, v. 60, p. 266–278
—— 1951, Submarine geology of the Gulf of Alaska: Geol. Soc. America Bull., v. 26, p. 1263–1285
Menard, H. W., 1955, Deformation of the Northeastern Pacific Basin and West Coast of North America: Geol. Soc. America Bull. v. 66, p. 1149–1198
Mendenhall, Walter C., and Schrader, Frank C., 1903, Mineral resources of the Mt. Wrangell district Alaska: U. S. Geol. Survey Prof. Paper 15, 71 p.
Mendenhall, W. C., 1905, Geology of the central copper River region: U. S. Geol. Survey Prof. Paper 41, 133 p.
Merrell, Richard H., 1950, Distribution and frequency of Alaskan earthquakes: Seismol. Soc. America Bull. v. 40, p. 267–269
Mertie, J. B. and Harrington, G. L., 1924, U. S. Geol. Survey Bull. 754, 129 p.
Miller, Don J., 1954, Cataclysmic flood waves in Lituya Bay, Alaska, (Abstract): Geol. Soc. America Bull. v. 65, p. 1346
Moffit, F. H., Knopf, Alfred, and Capps, S. R., 1910, Mineral resources of the Nabesna-White River district, Alaska: U. S. Geol. Survey Bull. 417, 64 p.
Moffit, Fred H., 1912, Headwaters region of Gulkana and Susitna Rivers, Alaska: U. S. Geol. Survey Bull. 498, 82 p.
—— 1915, Broad Pass region, Alaska: U. S. Geol. Survey Bull. 608, 80 p.
—— 1938, Geology of the Slana-Tok district, Alaska: U. S. Geol. Survey Bull. 904, 52 p.
Moffit, Fred H., 1942, Geology of the Gerstle River district, Alaska: U. S. Geol. Survey Bull. 926-B, 160 p.
Moffit, Fred H. and Wayland, Russell G., 1943, Geology of the Nutzotin Mountains, Alaska: U. S. Geol. Survey Bull. 933-B, p. 103–199
Moffit, Fred H., 1954, Geology of the eastern part of the Alaska Range and adjacent areas: U. S. Geol. Survey Bull. 989-D, p. 65–218
Montgomery, R. H., 1948, Precise leveling on the Alaska Highway: Am. Geophys. Union Trans., v. 29, p. 13–16.
Murphy, Leonard M., 1950, United States earthquakes, 1947: U. S. Coast and Geodetic Survey Pub. 730, 62 p.
Murphy, Leonard M., and Cloud, William K., 1953, United States earthquakes 1951: U. S. Coast and Geodetic Survey Pub. No. 762, 50 p.
Murphy, Leonard M., and Ulrich, Franklin P., 1951a, United States earthquakes 1948: U. S. Coast and Geodetic Survey Pub. No. 746, 50 p.
—— 1951b, United States earthquakes 1949: U. S. Coast and Geodetic Survey Pub. No. 748, 63 p.
—— 1952, United States earthquakes 1950: U. S. Coast and Geodetic Survey Pub. No. 755, 47 p.
Murray, Harold W., 1941, Submarine mountains in the Gulf of Alaska: Geol. Soc. America Bull., v. 52, p. 333–362
—— 1945, Profiles of the Aleutian trench: Geol. Soc. America Bull., v. 56, p. 757–782
Robinson, G. D., 1947, Objectives, methods, and progress of Alaskan volcano investigations of the United States Geological Survey: Alaskan Volcano Inv. Rept. no. 2, p. 1–5
Ross, Clyde P., 1933, Mineral deposits near the West Fork of the Chulitna River, Alaska: U. S. Geol. Survey Bull. 849-E, p. 289–333
Russell, I. C., 1893, Second expedition to Mt. Saint Elias in 1891: 13th Annual Rept. U. S. Geol. Survey, Pt. 2, 91 p.
Sainsbury, C. L., and Twenhofel, W. S., 1954, Fault patterns in southeastern Alaska (Abstract): Geol. Soc. America Bull., v. 65 p. 1300.
St. Amand, Pierre, 1948, The Central Alaska earthquake swarm of October 1947: Am. Geophys. Union Trans., v. 29, p. 613–623
—— 1954, The tectonics of Alaska as deduced from seismic data (Abstract): Geol. Soc. America Bull., v. 65, p. 1350
—— 1956, Two proposed measures of seismicity: Seismol. Soc. America Bull., v. 46, p. 41–46
Sharp, R. P., 1946, Note on the geology of Agattu, an Aleutian Island: Jour. Geology, v. 54, p. 193–199
Sharp, Robert P., and Rigsby, George P., 1956, Some rocks of the central St. Elias Mountains, Yukon Territory, Canada: Am. Jour. Sci., v. 254, p. 110–122
Smith, Phillip, 1939, Areal geology of Alaska: U. S. Geol. Survey Prof. Paper 192, 100 p.
Tarr, Ralph S., and Martin, Lawrence, 1912, Earthquakes at Yakutat Bay, Alaska in Sept. 1899: U. S. Geol. Survey Prof. Paper 69, 135 p.
Twenhofel, William S., 1952, Recent shore-line changes along the Pacific Coast of Alaska: Am. Jour. Sci., v. 250, p. 523–548
Watson, K. DeP., 1948, Squaw Creek-Rainy Hollow area: British Columbia Dept. Mines Bull. 25, 74 p.
West, S. S., 1951, Major shear fractures of Alaska and adjacent regions: Am. Geophys. Union Trans., v. 32, p. 81–86
Woodworth, R. W., and Haight, F. T., 1927, Tides and currents in southeastern Alaska: U. S. Coast and Geodetic Survey Special Pub. 127, 145 p.
Wright, Charles W., 1904, The Porcupine placer district: U. S. Geol. Survey Bull. 236, 30 p.
Wright, Fred Eugene, and Wright, Charles W., 1908, Ketchikan and Wrangell mining districts: U. S. Geol. Survey Bull. 347, 210 p.

U. S. Naval Ordnance Test Station, China Lake, California and Seismological Laboratory, California Institute of Technology, 220 N. San Rafael, Pasadena, California, Contribution No. 721

Manuscript Received by the Secretary of the Society, March 1955

STRAIN-RELEASE MAP O

This illustration shows epicenters for the Alaskan region from Gutenberg and Richter (1954); Murphy (1950); Murphy and Cloud (1953; 1954); and Murphy and Ulrich (1951a; 1951b; 1952). The contour li units of square dep

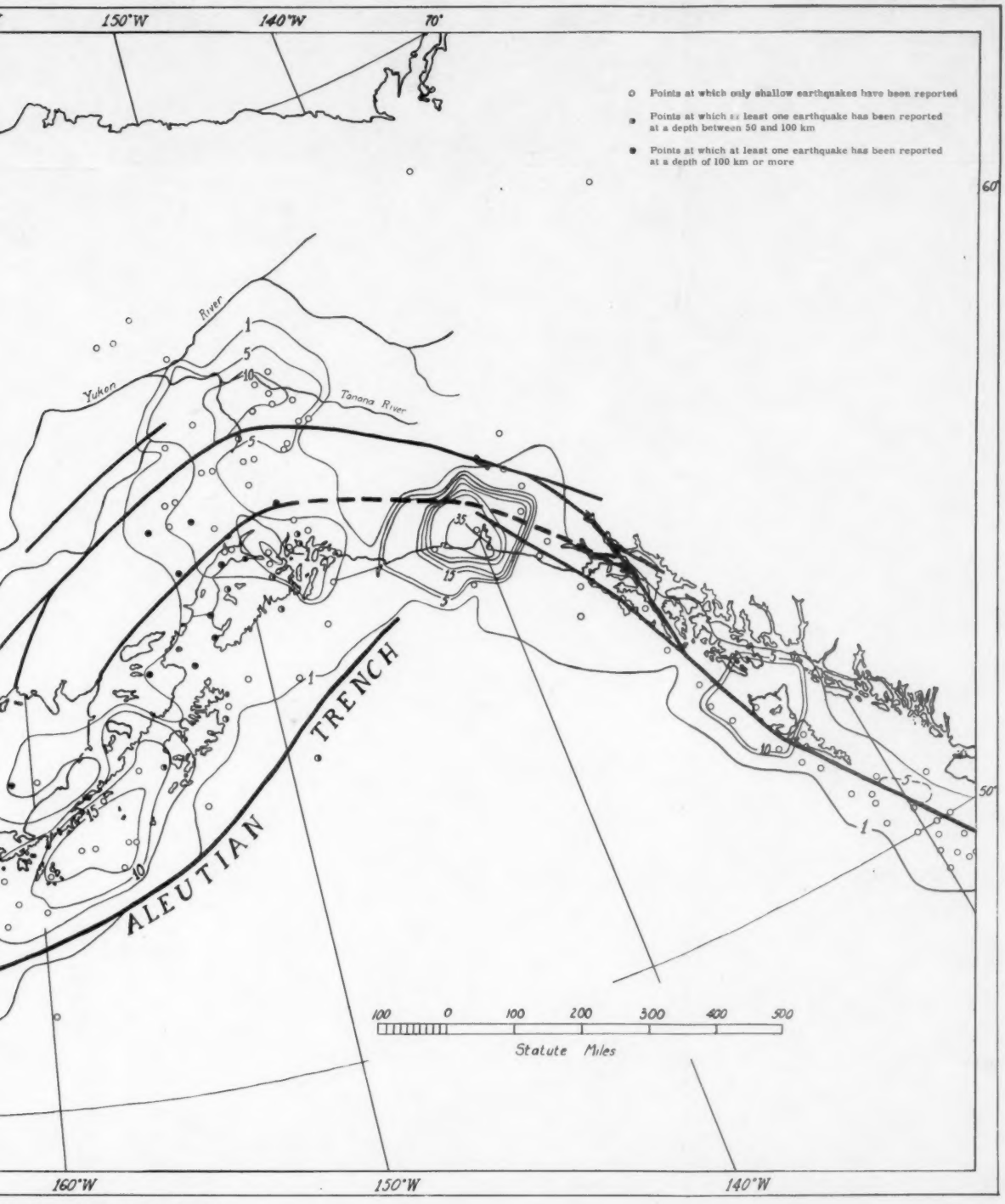
150°W
140°W
70°
Points at which only shallow earthquakes have been reported
Points at which at least one earthquake has been reported at a depth between 50 and 100 km
Points at which at least one earthquake has been reported at a depth of 100 km or more
60°
River
Yukon
Tanana River
ALEUTIAN TRENCH
50°
100 0 100 200 300 400 500
Statute Miles
160°W
150°W
140°W

MAP OF ALASKA

contour lines represent elastic strain released by earthquakes in units of equivalent earthquakes of the fourth magnitude per square degree per year.

BULLETIN OF THE GEOLOGICAL SOCIETY OF AMERICA
VOL. 68, PP. 1371-1410, 21 FIGS. OCTOBER 1957

UPLAND GRAVELS OF SOUTHERN MARYLAND

By John Schlee

Abstract

An upland capping of gravel and overlying silt (Pliocene ?) covers approximately 600 square miles of the Coastal Plain of southern Maryland. This sheetlike deposit, which successively overlaps older formations to the northwest, has a fairly constant thickness of 25–30 feet, and dips southeastward at approximately 5 feet per mile.

In the northern part of the upland, size and composition of the gravel show orderly changes eastward, which is also the direction of sediment transport as indicated by cross-bedding and gravel fabric. In the southern part of the area, facies changes are less orderly, and pronounced anomalies appear. These anomalies characterize both scalar and vector properties and therefore record a modification in conditions of deposition, probably induced by early Pleistocene climatic changes.

The upland deposits are fluvial in origin. They were probably deposited by a graded ancestral eastward-flowing Potomac River which, in the process of lateral corrasion, spread a veneer of channel gravel and flood-plain silt. Later side- and down-cutting combined with a gradual southeastward migration of the river, resulted in the present large, thin gravel sheet.

CONTENTS

TEXT

	Page
Introduction	1372
Acknowledgments	1373
Stratigraphy, lithology, and age of the upland deposits	1373
Stratigraphic nomenclature	1373
Lithology	1375
General	1375
Gravel member	1375
Loam member	1377
Age	1377
Sediment properties	1377
General	1377
Vectoral properties	1377
Cross-bedding	1377
Gravel fabric	1377
Scalar properties	1378
Size	1378
Lithology	1379
Sphericity	1383
Roundness	1383
Interrelations between scalar properties	1384
Spatial (facies) changes	1384
General	1384
Flow vectors and paleocurrents	1384
Size changes with distance	1385
Roundness and sphericity	1388
Lithology changes with distance	1389
Summary	1394
Origin of the upland deposits	1395
Previous hypotheses	1395
General	1395
Marine	1395
Alluvial fan	1395
Migrating "normal" river deposit	1396
Geologic history	1399
References cited	1399
Appendix A. Location of samples	1402
Appendix B. Size analysis—by weight per cent	1405
Appendix C. Pebble-count compilation	1407

ILLUSTRATIONS

Figure	Page
1. Sample locality and index map	1373
2. Contour map on the base of the upland deposits	1376
3. Areal distribution and trend of the cross-bedding data	1378
4. Rose diagram of the apparent dip readings	1378
5. Representative size histograms (11) and average histogram for the 72 size analyses	1380
6. Histogram of the modal size occurrence for sand and gravel	1381
7. Cumulative frequency distribution curves of sorting coefficients for selected environments	1381
8. Chert sphericity-roundness linear relation	1384
9. Areal occurrence of the maximum size grade for samples collected from the upland deposits	1385
10. Explanation of moving average computation procedure	1385
11. Moving average diagram of vectoral data	1386

Page

12. Moving average diagram for modal size data (gravel) in phi units 1387
13. Moving average diagram of vectoral data (arrows) and modal gravel size data (phi units) 1388
14. Size-distance exponential relationship for the upland deposits 1389
15. Distribution of anomalously large boulders in the upland deposits 1390
16. Distribution and per cent of minor rock types in the upland deposits 1391
17. Moving average diagram of quartzite content (16–32 mm) 1392
18. Moving average diagram of chert content (16–32 mm) 1393
19. Histograms of chert weathering changes .. 1394
20. Schematic diagram of Coastal Plain terraces by Shattuck (1902) 1396
21. Schematic diagram of paleocurrent trend during deposition of the upland deposits 1397

TABLES

Table Page

1. Previous and present nomenclature 1374
2. Size distribution of two pseudo bedding layers 1377
3. Comparison of vertical size distribution in the gravel member 1379
4. Composition of modern river gravel dredged from the Potomac River near Alexandria, Virginia 1382
5. Roundness values and lithologic content on gravel and sand fractions (3 localities) .. 1383
6. Values of the coefficient of size reduction .. 1389
7. Degree of chert weathering 1393

Introduction

The origin of the southern Maryland upland deposits is controversial. Previous studies which attempted to solve this problem have centered around geomorphic mapping of terrace levels. The present study concentrates on the petrology of the deposits. It is hoped that through the recording of sediment properties and facies changes and, the use of geomorphic data, the formation of these deposits might be understood. Quite apart from genetic considerations, the author was also interested in any interrelations among sediment properties.

The upland deposits of southern Maryland were selected because the type localities for two of the terraces are here and because of the widespread areal extent of the deposits. Inasmuch as they are widely exploited for gravel, fresh exposures in numerous pits are available for study.

The main area selected for study is the peninsula between the Patuxent and Potomac Rivers, including portions of Calvert, Prince Georges, Charles, and St. Marys Counties on the Coastal Plain. In addition, isolated exposures in Fairfax County, Virginia, Montgomery County, Maryland, and the District of Columbia were studied (Fig. 1).

The upland deposits occur mainly on the Coastal Plain where they form a plateau cap. Scattered patches of gravel and silt also are found on the Piedmont in Washington, D. C., at 410 feet and in Fairfax County, Virginia, at 518 feet. On the Coastal Plain, the upland deposits stretch southeastward as a fairly continuous gently undulating sheet; elevations range from 300 feet just south of Washington, D. C., to 90–120 feet in the southern part of St. Marys County; the average slope is 5 feet per mile. The present topographic surface of the upland slopes toward the river valleys of the Patuxent and Potomac (Hack, 1955, p. 31) and the dropoff ranges from 20 to 80 feet.

The gravel and associated silt cap gently dipping Tertiary and Cretaceous sediments. Because the underlying formation dips southeastward at steeper angles than do the younger terraces, the upland deposits overlie successively older formations to the west and northwest.

First geologic studies of the region date back to the early 1800's, but most of the definitive work was done in the last 75 years. (W J McGee, 1888; 1891; Darton, 1891; 1893; 1894; 1939; 1951; Cooke, 1930; 1932; 1941; Cooke *et al.*, 1952; Stephenson *et al.*, 1932; Dryden and Overbeck, 1948; Carr, 1950; Hack, 1955). In the present study, the writer visited 98 exposures (Fig. 1; Appendix A) and spent approximately 2 months on field work. At 72 exposures, channel samples were collected for detailed sedimentological study. At localities 84–95 (portions of Charles and St. Marys Counties) only pebbles count and determination of modal class of the gravel fraction were made. Light and heavy minerals in the size class of one-fourth to one-eighth mm were studied at 26 localities for descriptive purposes, whereas at 56 exposures, the direction of sediment transport was determined by cross-bedding or fabric analysis. Stations are 1–5 miles apart and are closer together toward the northwest, where facies changes were expected to be most pronounced, and where gravel pits are more numerous.

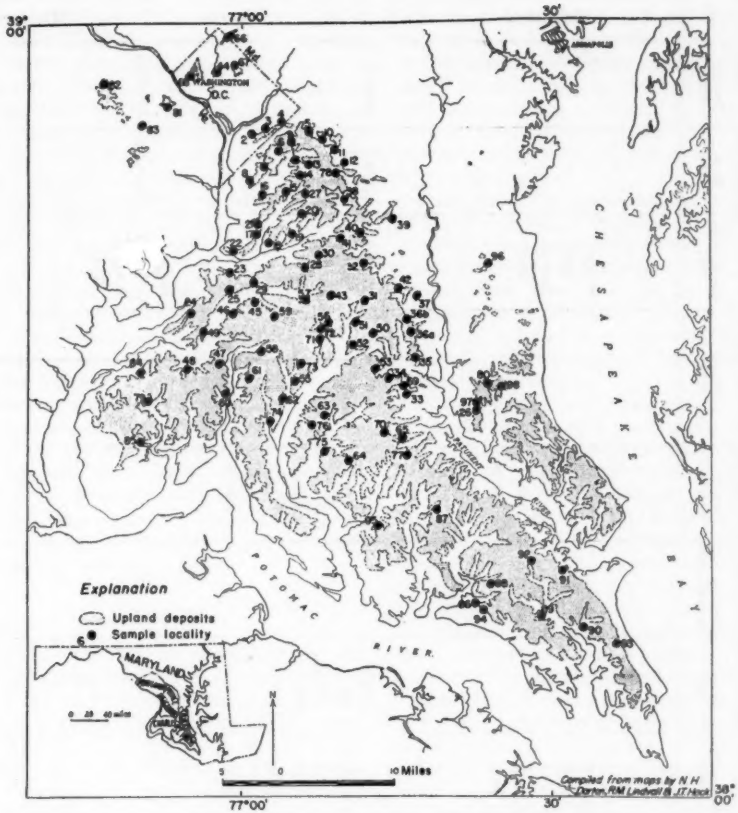

FIGURE 1.—SAMPLE LOCALITY AND INDEX MAP
See Appendix A for more precise location of the sample points.

ACKNOWLEDGMENTS

The study was financially assisted by the writer's parents and The Johns Hopkins University. The guidance, advice, and interest of Professor F. J. Pettijohn of The Johns Hopkins University and H. E. Vokes of Tulane University, Drs. L. Leopold and M. G. Wolman of the U. S. Geological Survey, and Dr. P. E. Potter of the Illinois Geological Survey, are gratefully acknowledged. In addition, the writer was assisted by numerous graduate students, among whom were D. E. Appleman and W. R. Power. The writer's mother, Hazel Schlee, made many of the sphericity and roundness determinations and fabric plots.

STRATIGRAPHY, LITHOLOGY, AND AGE OF THE UPLAND DEPOSITS

Stratigraphic Nomenclature

Table 1 summarizes the stratigraphic nomenclature in abbreviated form. For a more extensive review of the literature *see* Flint (1940, p. 758–770) and Dryden and Overbeck (1948, p. 6–13).

In this study, Hack's (1955, p. 26) designation of "upland deposits" is adopted. Inasmuch as pronounced physiographic (scarps) and sedimentologic breaks are absent in the upland deposits, the author feels justified in treating them as a single stratigraphic unit. This does not mean that the deposits are without physio-

TABLE 1.—PREVIOUS AND PRESENT NOMENCLATURE

McGee 1888	Darton 1894	Shattuck 1901	Clark 1915	Cooke 1930	Wentworth 1930	Darton 1939	Dryden and Overbeck 1948	Carr 1950	Darton 1951	Cooke *et al.* 1952	Hack 1955	Present study	Age
---?---	---?---	---?---	---?---	Sunderland	---?---			---?---		---?---	---?---	---?---	Pleistocene
Columbia Formation	Earlier Columbia Formation	Sunderland Formation	Brandywine Formation	Coharie Brandywine	Sunderland Formation		Sunderland and Brandywine Formation	Brandywine Formation		Sunderland Formation			
---?---	---?---	---?---	---?---		---?---	---?---	---?---	---?---	Tertiary				
Appomattox Formation	Lafayette Formation	Lafayette Formation			Tertiary terraces (Brandywine, *etc.*)	Gravel of High Plateau		and Bryn Mawr (?) gravel	Brandywine Formation	Brandywine Formation Bryn Mawr Formation	upland deposits	upland deposits	Pliocene
		---?---				---?---		---?---		---?---	---?---	---?---	Miocene

graphic breaks. Careful topographic surveys of the region by Hack (1955, p. 17) particularly in the Cedarville State Forest and the highway cuts on the Indianhead Access Road north of Piscataway Creek, establish that the gently sloping surface of the upland is broken by minor topographic breaks which he believes are associated with small unconformities within the upland deposits. Although the unconformities have not been seen, they have been detected by elevation differences of lithologic contacts within the upland deposits. Hack's survey indicates that, although there may be stratigraphic breaks, presumably caused by shifting of the ancient river channel and penecontemporaneous scour and fill, they are generally very small (10 feet near Cedarville) and difficult to trace for any distance; hence they do not qualify as mappable units.

Lower sets of terraces are adjacent to the upland (at 140–150 feet and 240–260 feet) in the Potomac River valley near Washington, and indeed, if the type locality of the Sunderland had been designated here rather than in Calvert County, its validity might have been much less in question.

Lithology

General.—The upland deposits cover approximately 600 miles in the region studied, and 500 of this is on the Potomac-Patuxent peninsula south of the Anacostia River. The upper surface of the deposits slopes steeply in the isolated outliers in Washington (29 feet per mile—Darton, 1951, p. 776) and Virginia (56 feet per mile) adjacent to the Fall Line. Southeast of Washington, D. C., the upland slopes 15 feet per mile, and ranges down to 2½ feet in St. Marys County (Clark, 1915, p. 501); the over-all slope for the whole sheet is 5 feet per mile.

The surface is essentially parallel to the base of the sheet except where erosion has thinned or removed some of the upland capping. The base of the deposits slopes gently southward at 5 feet per mile (Fig. 2). Because most of the compilation is based on well data (Otton, 1955, p. 248–307; Dryden and Overbeck, 1948, p. 154–171; Martin and Ferguson, 1953, p. 80–188), large variations in elevation account for the tortuosity of the contours, although both Hack and Otton postulate a subterranean ridge (trending northwest-southeastward down the Patuxent-Potomac peninsula) over which the upland deposits are draped. If present, it is certainly not pronounced (relief less than 20 feet near Hughesville, Md.), and the variation in basal elevations could be due to irregularities of the underlying surface or error of well drillers logs. The author believes the data show only a slope of the underlying surface to the south for most of the sheet, and southwest or west for that part of the sheet adjacent to the Potomac River valley.

Thickness of the upland deposits ranges from 10 to 30 feet (Hack, 1955, p. 10), though exceptional thicknesses up to 50 feet have been noted. Assuming an average thickness of 30 feet for the combined gravel and silt, for an area of 600 square miles, a minimum of about 3½ cubic miles of material was removed from the Piedmont and Appalachians during deposition of the upland deposits.

Hack (1955, p. 10) divided the Brandywine Formation as mapped in the Brandywine area, into an upper loam member and a lower gravel member. Such a subdivision proved applicable to the remainder of the deposits laterally continuous with those of the Brandywine area throughout the Patuxent-Potomac peninsula, hence this terminology is extended to the upland deposits. The contact between the members is gradational through 2–3 feet. In many portions of the upland, particularly near major rivers, the upper member is thin or absent, possibly as a result of the post-depositional erosion.

Gravel member.—The gravel member consists of pale-to dark-yellowish-orange (10YR 8/6–10YR 6/6 Hack, 1955, p. 12) to mottled pale-yellowish-brown poorly sorted gravel and sandy gravel, as well as very pale-orange (10YR 8/2) gravelly clay. The gravel member is fairly well stratified, and sedimentation units are easily recognizable. Units range from 6 feet to 2–3 inches thick; fine gravel characterizes the thinner beds. Where bedding is poor, sedimentation units up to 17 feet thick are present. Laterally, the beds range several hundred feet to 10 feet or less in the case of sand lenses. Trough or planar cross-bedding (McKee and Weir, 1953, p. 387) is present in about one-third of the exposures studied. Cosets up to 3 feet thick and sets up to 1½ feet thick (6 inches average thickness) were observed. Sand constitutes most sets, though small pebbly foresets are present in a few beds.

The gravel has a bimodal size distribution and consists of a gravel framework, averaging 61 per cent of the whole, and a matrix of sand, silt, and clay. Closework gravel predominates, and openwork seams are recorded in only 18 per cent of the exposures studied.

Typically the gravel is well indurated with a red silty sand matrix. In a few exposures, the gravel and associated sand are clean, well sorted iron free, and so poorly indurated that caving readily occurs.

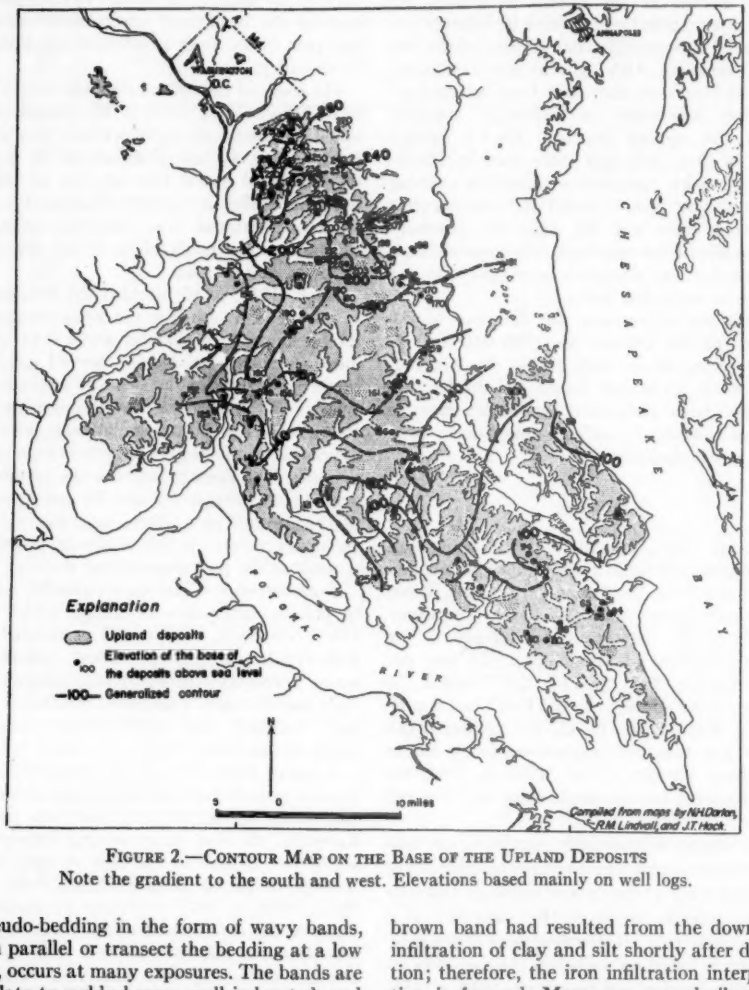

FIGURE 2.—CONTOUR MAP ON THE BASE OF THE UPLAND DEPOSITS
Note the gradient to the south and west. Elevations based mainly on well logs.

Pseudo-bedding in the form of wavy bands, which parallel or transect the bedding at a low angle, occurs at many exposures. The bands are chocolate to ruddy brown, well indurated, and a fraction of an inch thick. Between such layers the sand and gravel is light-colored and less well indurated; contacts may be either very sharp or gradational within a few inches. Such pseudo bedding and indeed many of the changes in induration could result from downward infiltration of clay and silt, or from infiltration of iron compounds through leaching of the overlying loam. Size analyses (Table 2) of two such contrasting layers reveal no significant difference in the weight percentage of clay such as might be expected if the indurated wavy dark-brown band had resulted from the downward infiltration of clay and silt shortly after deposition; therefore, the iron infiltration interpretation is favored. Moreover, secondarily introduced iron oxide (goethite? and hematite?) locally cements the sand and gravel along definite zones and in large irregular masses up to 3 feet across. Secondarily introduced iron compounds also stain the pebbles and produce a splotchy discoloration of the matrix.

The pebbles are mainly chert, quartzite-

sandstone, and "vein" quartz, whereas the sand matrix is almost all quartz and chert.

Loam member.—Overlying the gravel member is a pale-yellowish-brown (10YR 6/2) to grayish-orange (10YR 7/4) to moderate-yellowish-brown (10YR 5/4) massive loam. It is commonly mottled and grades into the underlying gravel in most localities (Appendix A, locality 61-Rose Hill, Md.), although in a few places a more pronounced break (Appendix A, locality 2) is present. The loam consists chiefly of compacted silt and some sand, clay, and scattered pebbles. According to Hack (1955, p. 13) A, B, and C soil horizons are expressed by changes in the sorting coefficient, median size, and clay content. The loam is very siliceous (90 per cent) and has 2–5 per cent heavy minerals (Hack, 1955, p. 13).

TABLE 2.—SIZE DISTRIBUTION OF TWO PSEUDO-BEDDING LAYERS

(Locality 7—in weight per cent)

Color of layer	2-1 mm	1-½ mm	½-¼ mm	¼-⅛ mm	⅛-1/16 mm	Less than 1/16 mm
Light-tan layer	2.3	19.5	61.0	5.3	2.3	9.6
Dark-brown layer	2.6	17.9	64.7	6.9	1.8	6.2

Age

The upland deposits or their equivalent (Table 1) are generally regarded as Pliocene(?) or Pliocene in age[1] (Wentworth, 1930, p. 27; Darton, 1939, Pl. 10; Cooke *et al.*, 1952, p. 40 and 46; Hack *et al.*, 1950, p. 2), because they overlie Miocene beds and are flanked by Pleistocene terraces (Wicomico, Pamlico, *etc.*). Wentworth (1930, p. 108) considers that the deposition may have required 25,000–50,000 years. Hack (1955, p. 37) postulates that deposition may have begun in late Miocene and continued on through the early Pleistocene.

That the upland deposits may be in part early Pleistocene is indicated by the position of the large (ice-rafted?) boulders adjacent to the Potomac River (*see* section Size Changes with Distance).

[1] The only "fossil" seen by the author was *Cassius madagascariensis spinella* Clench, found at the gravel-loam interface near Silver Hill, Maryland, by a steam-shovel operator. It is unlikely that a tropical marine form such as this, now found in the Florida Keys, was indigenous to the upland deposits; it may have been buried by Indians.

SEDIMENT PROPERTIES

General

The loam member was not investigated, but structures and textures of the gravel were studied at 98 localities. The properties examined were cross-bedding and gravel fabric, which have both direction and magnitude (vectoral properties) and size, mineralogy-lithology, roundness and sphericity, which have magnitude only (scalar properties).

Vectoral Properties

Cross-bedding.—Two kinds of cross-bedding predominate in gravel: planar, in which the lower bounding surfaces are essentially planes of erosion, and festoon or trough cross-bedding in which the lower plains are curved surfaces of erosion. The latter are rare and poorly developed.

Cosets range from 1 to 3 feet thick and generally do not extend laterally more than 20 feet, whereas sets, which are the more common, range from 2 inches to 2½ feet. The thickness of the sets seems to depend on the size of the material composing them. Where sand predominates, set thickness ranges from 2 inches to 2 feet and averages 6 inches; in the gravel cross-beds, thicknesses of 1¼ to 2½ feet are common.

Foreset inclination averages 21.1° and ranges from 5° to 38°. Cross-bedding (Fig. 3) is widespread; 86 cross-beds were measured at 38 stations. From one to five readings per station were made and averaged. The summations as shown in Figure 3, indicates sediment transport was mainly to the east and southeast (mean azimuth—125°).

Gravel fabric.—The paucity of cross-beds made it necessary to investigate the fabric of the gravel to determine the sediment-transport direction. Two methods (Schlee, 1957) were employed: marking the reorientation of pebbles from gravel exposures taken in the field (6 readings), and apparent dip measurements (40 readings). These two types of measurements (Fig. 4) suggest that the direction of sediment transport is southeasterly; the arithmetic mean azimuth is 151°, very similar to the 125° mean azimuth of the cross-bedding readings.

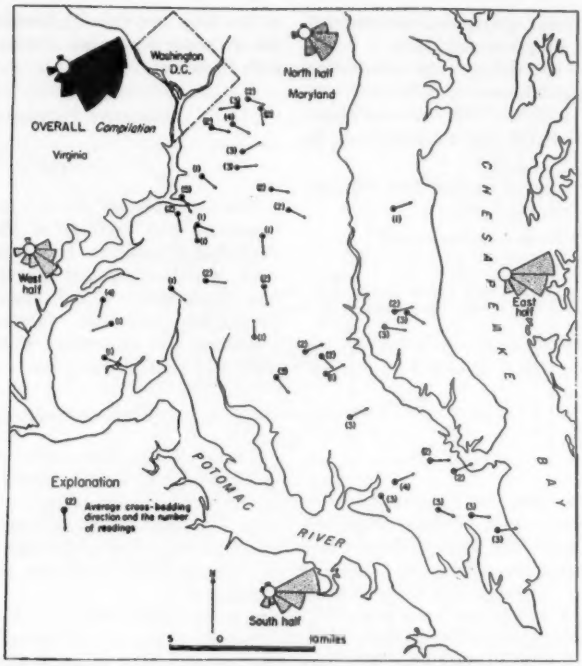

FIGURE 3.—AREAL DISTRIBUTION AND TREND OF CROSS-BEDDING DATA

Scalar Properties

Size.—One channel sample was taken at each of 72 stations; these samples were 26 feet or less in length and either continuous or discontinuous. All material larger than 2 mm was hand-sieved, and that smaller than 2 mm was sieved in a Ro-Tap for 10 minutes. Wentworth's empirical rule (Krumbein and Pettijohn, 1938, p. 31) respecting sample size was followed except where anomalously larger boulders (up to 8 feet long) were present. Wet sieving was employed where induration was so marked that it affected the size distribution by causing clots of smaller material to be retained in larger-sized sieves.

Vertical size variation generally is not pronounced as shown at three widely spaced localities (Table 3) where random samples were taken at the upper, middle, and lower portions of well-exposed sections of gravel. Lateral size variation is not pronounced within a single exposure. Cut-and-fill features and outlines of channels are rare.

In all but two analyses, the size distribution is bimodal (Fig. 5), and the primary mode is in the gravel fraction in 76 per cent of the samples. The frequency of occurrence of the modal-size class is illustrated in Figure 6. The bimodal distribution is caused by the lack of material in

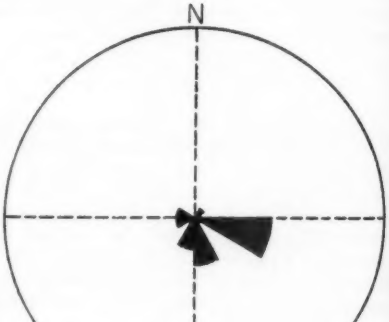

FIGURE 4.—ROSE DIAGRAMS OF APPARENT DIP READINGS

the 4- to 2-mm class, due either to a deficiency of this size material in the source area, or sorting action of the transporting medium which may have moved this size material to the sandy facies of the upland gravels east of the region sampled by the author. In any case, it seems fluvial environment for the whole sheet of gravel.

Sorting coefficients also suggest a fluvial origin for the upland gravels. These were calculated for 19 samples whose median size was 10 mm or larger. This large median size resulted

TABLE 3.—VERTICAL SIZE DISTRIBUTION COMPARISONS

Station	128–64 mm	64–32 mm	32–16 mm	16–8 mm	8–4 mm	4–2 mm	2–1 mm	1–½ mm	½–¼ mm	¼–⅛ mm	⅛–1/16 mm	< 1/16 mm
26 upper	....	1.6	1.6	12.6	19.9	16.7	11.6	18.2	10.8	4.6	1.3	1.2
26 middle	....	....	1.7	18.8	22.6	14.4	7.6	13.1	15.3	4.8	1.2	0.6
26 lower	....	....	2.6	16.0	19.9	12.7	5.9	14.1	24.1	3.3	0.6	0.7
41 upper	....	1.4	23.4	26.6	11.4	7.8	11.0	9.4	4.3	2.3	0.9	0.8
41 middle	....	3.8	23.3	23.8	11.4	7.6	8.2	12.6	6.2	1.7	0.6	0.6
41 lower	....	6.4	27.1	27.3	10.0	5.2	3.5	5.6	10.0	3.1	0.7	1.1
6 upper	12.6	31.2	13.7	8.2	5.5	3.7	4.3	8.5	8.2	2.7	0.8	0.7
6 middle	2.3	32.3	25.8	9.9	5.5	4.1	3.4	5.3	8.1	2.6	0.3	0.4
6 lower	....	27.2	23.3	14.2	9.1	7.1	6.0	8.7	3.2	.8	0.3	0.3

likely that the bimodal distribution may reflect in part the two loads (bed and suspended) carried by the transporting agent. The problem then arises as to whether the two loads were deposited simultaneously or at different times. Porosity-packing considerations suggest that the gravel and sand fractions were deposited contemporaneously. Theoretically, with loosest packing of large-size spheres—gravel, for example—32 per cent by weight of the total (Plumley, 1948, p. 544) could be composed of small-size spheres—sand, for example—which fill the interstices. Thus, this figure or larger might be expected if the gravel and sand had been deposited simultaneously. Forty-two of the 70 bimodal analyses have a sand fraction 32 per cent or higher; the average (arithmetic) weight percentage of sand, where the primary mode is in the gravel fraction, is 31.9 per cent (56 samples). The sparsity of open-work gravel beds also seems to suggest a similar conclusion.

Genetically, the bimodal distribution is characteristic of a fluvial environment. Of 31 histograms of river gravels (Wentworth, 1932, p. 30–37), only 6 were unimodal. Of 31 marine beach-gravel size analyses, only 3 were bimodal. If the upland gravels are composed of the estuarine Sunderland terrace (Cooke *et al.*, 1952, p. 46) and the fluvial Brandywine gravel, these differences should be apparent in the size analyses. There is no difference in the size distributions of the gravel previously mapped as Brandywine and Sunderland. Seventy of the 72 analyses are polymodal and thereby suggest a

in the inclusion of those samples with the widest range of size classes, and hence fairly large sorting coefficients were obtained. The Trask sorting coefficients (Pettijohn, 1949, p. 24) ranged from 2.22 to 10.15 and averaged 4.78. This is similar to Potter's 4.9 coefficient (Potter, 1955, p. 20) average for the Lafayette gravel and is more typical of a fluvial rather than a marine origin (Emery, 1955, p. 47). Marine gravels are better sorted and have a lower coefficient (1.13–2.14). Emery (1955, p. 47) also attempted to distinguish types of fluvial environments on the basis of the cumulative frequency distribution of sorting coefficients (Fig. 7). According to his analyses, stream gravels have a lower average coefficient (3.18) than alluvial fan gravels (5.33), though their ranges overlap considerably ((1.35–5.49 versus 2.50–8.95). Figure 7 shows the cumulative frequency distribution of sorting coefficients and shows the range of the 19 analyses from the upland gravels to be suggestive of an alluvial fan deposit.

Lithology.—The lithology is discussed on the basis of size of particles.

PARTICLES GREATER THAN 2 MM: The most abundant rock type is "vein" quartz, which occurs in all size grades. It is translucent to opaque, white, gray, or pink, and displays no discernible clastic texture. Pebbles surfaces are smooth, pitted or linearly streaked. Most of the vein quartz is probably from Piedmont crystalline and metamorphic rocks.

Quartzite-sandstone is present in all size

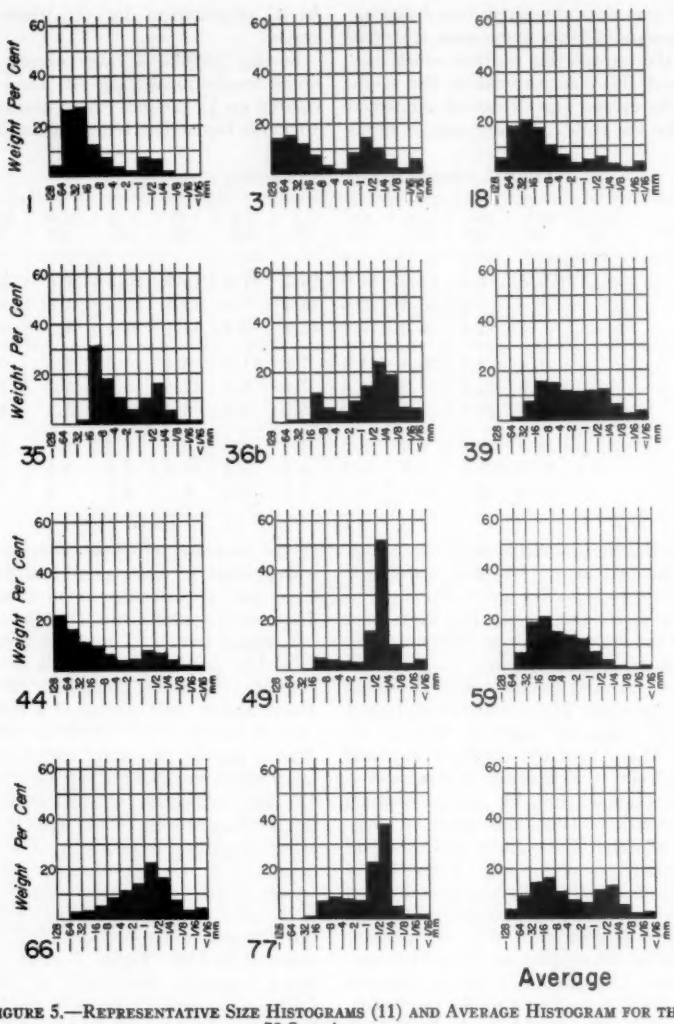

FIGURE 5.—REPRESENTATIVE SIZE HISTOGRAMS (11) AND AVERAGE HISTOGRAM FOR THE 72 SIZE ANALYSES

Size distributions can be unimodal (Size analyses 59 and 66) or polymodal (Size analyses 1, 18, 49, and 77). The primary mode can occur in the gravel fraction (Size analysis 35) or in the sand fraction (Size analysis 36).

grades and includes those particles in which individual clastic grains, or stained metamorphosed remnants are discernible. These rocks vary from friable to well indurated, depending on the parent material and on post-depositional weathering. Most of the pebbles are nearly pure quartz with surficial staining of iron oxide. Though generally unfossiliferous, a few of the pebbles display fossil brachiopod impressions which indicate a Devonian age: the source rock was probably the Oriskany sandstone. Other possible sources of quartzose sandstones and metaquartzites include the Weverton Quartzite, Antietam Sandstone, the Tuscarora Sandstone,

and the Pocono Sandstone of the Appalachian province. Of these, only the Weverton has been identified tentatively in the upland gravels. Thus, source areas of quartzite lie mainly in the Appalachian Mountains, and the closest

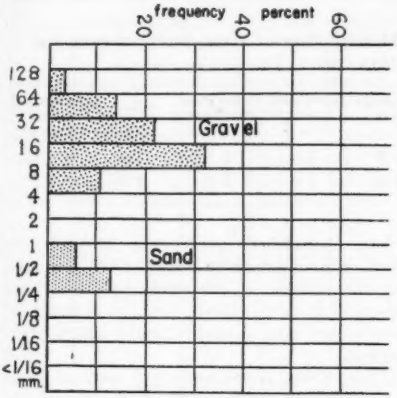

FIGURE 6.—HISTOGRAM OF THE MODAL SIZE OCCURRENCE FOR SAND AND GRAVEL

outcrop of the Weverton is about 36 miles northwest of the gravel sheet. Nearest occurrence of the Oriskany is approximately 80–85 miles from the northern part of the southern Maryland upland.

The chert-pebble types reflect many sources and the effects of post-depositional weathering Brown, gray, dark-gray, and bluish-gray varieties are found. Relict bedding and oolites are present in many of the cherts as are casts of fossils. The fossils identified include brachiopods, corals, and bryozoans from the lower Devonian (New Scotland and Shriver cherts). Other possible sources of chert include the Conococheague Limestone (Cambrian) and the Beekmantown Chert (lower Ordovician). Moreover, some pieces of Beekmantown Chert have been identified in the upland gravels by their internal rosette arrangement of the silica bands.

Much of the chert is badly weathered and so rotted that only a clayey chalklike residue remains. There is a slight tendency for the less weathered chert to occur in the more southerly portion of the gravel sheet. This may indicate that the amount of chert weathering is in proportion to the age of the gravel; the lower more southerly portion of the gravel deposits are probably younger than the upland gravels near Washington, D. C. (*see* section Lithology Changes with Distance). Other factors in chert weathering besides age are the presence or absence of iron oxide and the percentage of sand in the matrix.

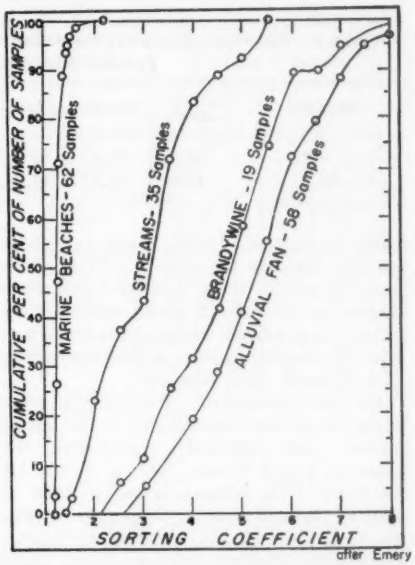

FIGURE 7.—CUMULATIVE FREQUENCY DISTRIBUTION CURVES OF SORTING COEFFICIENTS FOR SELECTED ENVIRONMENTS

Samples selected had a median diameter of 10 mm or larger.

Other rock types constitute a few per cent or less of the total (Appendix C). Dark-red to purplish-red thin-bedded siltstone and sandstone pebbles are present particularly in those localities adjacent to the Potomac River. The feldspar is thoroughly rotted, and much of the color is due to iron oxide. Possible sources for the material include the Juaniata Formation (upper Ordovician—75–80 miles from the northern part of the gravel sheet), the Catskill Formation (upper Devonian—80 miles distant) and Newark Series (30 miles distant). The Newark Series seems the most probable source not only because of its proximity to the upland deposits but also because of the large amount of feldspar and mica in both the pebbles and the Newark beds. The inability of sandstone to survive river transport is well illustrated by the Black Hills gravels (Plumley, 1948, p. 554), in

which nearly all the sandstone was destroyed after a transport distance of 30 miles.

A few pebbles of subarkosic micaceous glauconitic green and brown siltstone are also present. These may come from underlying Cretaceous and Tertiary formations which are highly glauconitic. Lastly, some very large boulders found in the western portion of the gravel sheet are badly weathered micaceous gneisses, crenulated with small quartzose folia, and cut by pegmatitic veinlets. Also noted were light-grayish-green cobbles of micaceous schist; most, however, were quartzite.

TABLE 4.—FREQUENCY PER CENT COMPOSITION OF MODERN RIVER GRAVEL DREDGED FROM THE POTOMAC RIVER NEAR ALEXANDRIA, VA.

Size (mm)	"Vein" quartz	Quartzite	Chert	Red sandstone	Green sandstone	Green stone and diabase	Clay	Gneiss and schist
8–16	60.2	12.2	13.4	5.8	3.4	1.8	1.4	1.8
16–32	45.0	37.2	18.0	4.9	7.8	3.9	1.9	1.5

The predominance of mature siliceous rocks is one of the unusual features of the upland gravels; such materials characterize the Lafayette gravel (Potter, 1955, p. 5), but not the Black Hills terraces (Plumley, 1948, p. 552). Is this difference in composition a function of the distance traveled or of pre-erosional weathering? Modern Potomac River gravel which comes from the same general source area, (Table 4) is quite different in composition from that of most of the upland gravels; it does bear a slight similarity to the younger portion of the deposit (Localities 84–86). This evidence, while not conclusive, appears to suggest that pre-erosional weathering caused the disintegration and decomposition of the more immature, mineralogically heterogeneous rock types in the source area.

PARTICLES LESS THAN 2 MM: Sands, silts, and clay constitute 38 per cent of the gravel member of the upland deposits. This material acts in part as a binding agent through adhesion and compaction in the finer grades, aided by infiltration and precipitation of iron oxides. The kinds and proportions of light and heavy minerals were determined at 21 localities. Grains were boiled for 5 minutes in hydrochloric acid to remove iron stains and thereby aid in mineral identification. They were mounted in Canada balsam.

Light minerals constitute 98 per cent of the sand fraction examined in the size grade of one-fourth to one-eighth mm. Quartz comprises 93 per cent of the light minerals and occurs in two forms. Nineteen per cent of the quartz grains have no overgrowths, are angular, and were probably derived by mechanical disintegration of "vein" quartz during transport as well as from the decomposed crystalline rocks themselves. Overgrowth quartz was probably derived from Applachian sandstones. The subangular outline is presumed to have been inherited from the source rock, as river transport is very slow in modifying the quartz grain outlines.

Chert forms approximately 5 per cent (one-fourth to one-eighth mm) of the grains. It occurs as subequant to bladed grains which are opaque to clear yellow in ordinary light; under cross nicols, the clear-yellow grains display the familiar microcyrstalline aggregate of chert with low interference colors. Feldspar (mainly potassium feldspar) forms 0.6 per cent of the size fraction studies; it is cloudy, subequant, and irregular in outline and is distinguished from inclusion-filled quartz by twinning and relief. Some muscovite and biotite (average—0.2 per cent) are also present.

Heavy minerals (S. G. greater than 2.8) were separated by the use of bromoform, boiled for 5 minutes in concentrated hydrochloric acid, and mounted in Canada balsam. One hundred grains per sample were counted to determine relative percentage of opaque versus non-opaque minerals and another hundred to determine the kinds and proportions of non-opaque heavy minerals.

Eighty three per cent of the heavy minerals are opaque. They are leucoxene (24 per cent of the 83 per cent), magnetite, and ilmenite. A minor amount of badly leached goethite was also noted.

Of the non-opaque minerals, zircon constitutes 65 per cent, tourmaline 8 per cent, and hornblende, actinolite, rutile, staurolite, sphene, augite, hypersthene are present in minor amount. Garnet, andalusite, monazite, sillimanite, epidote, cassiterite, biotite, chlorite, anatase, spinel, and glauconite are present in

trace amounts. The glauconite was probably derived from Tertiary and Cretaceous formations. The probable source of staurolite, andalusite, sillimanite, garnet, and kyanite was the gneisses and schists of the Piedmont. The p. 82), the siliceous rock types may have had higher initial sphericity. Because of its softness, limestone might be expected to attain a higher sphericity more quickly. Studies by Krumbein (1941b, p. 492) and Plumley (1948,

TABLE 5.—ROUNDNESS VALUES AND LITHOLOGIC CONTENT FOR GRAVEL AND SAND-SIZE MATERIAL

Size (mm)	Locality 41 (Cheltenham)					Locality 6 (Silver Hill)					Locality 26 (Bowens)				
	Frequency per cent		Roundness			Frequency per cent		Roundness			Frequency per cent		Roundness		
	"Vein" quartz and quartzite	Chert	Overall	"Vein" quartz and quartzite	Chert	"Vein" Quartz and quartzite	Chert	Overall	"Vein" quartz and quartzite	Chert	"Vein" quartz and quartzite	Chert	Overall	"Vein" quartz and quartzite	Chert
¼–⅛	96	4	.31	.31	.33	97	3	.34	.34	.28	94	6	.32	.32	.34
⅛–¼	95	5	.36	.36	.28	97	3	.35	.35	.28	93	7	.33	.33	.34
1–½	94	6	.37	.37	.37	92.5	7.5	.36	.36	.42	93.5	6.5	.35	.35	.37
2–1	95	5	.36	.36	.37	90.5	9.5	.35	.35	.34	93	7	.37	.37	.38
4–2	91	9	.40	.40	.42	93	7	.40	.40	.35	89.5	10.5	.40	.04	.41
8–4	88.5	11.5	.45	.46	.39	90	10	.45	.46	.42	85.5	14.5	.46	.46	.46
16–8	84.5	15.5	.45	.45	.45	88.5	11.5	.49	.49	.48	76.5	23.5	.44	.45	.40
16–32	...	...	...	...	...	72	28	...	...	...	...	...	...	...	...
32–64	...	...	...	...	...	79	21	...	...	...	...	...	...	...	...

rounded zircon and tourmaline indicate a sedimentary source, probably the Paleozoic rocks to the northwest.

Sphericity.—The sphericity was determined for pebbles of two size grades (16–32 mm and 32–64 mm) at 40 localities. The Zingg-Krumbein (Krumbein, 1941a, p. 68) was used to measure sphericity. Sample size determination was based on the statistical sampling theory of the standard error of the mean (Plumley, 1941, M.S. Thesis, Univ. of Chicago; Arkin and Colton, 1950, p. 116; Moroney, 1953, p. 137). In most cases, the measurement of approximately 20 pebbles per size grade was sufficient to give a mean sphericity of the accuracy desired (within 10 per cent of the "true" population mean).

The gravel has a fairly high sphericity, ranging from 0.70 to 0.76, particularly when compared to the Black Hills gravels where mean sphericity values range from 0.56 to 0.67 (Plumley, 1948, p. 556–557). This difference may be due to differences in rock types and to proximity to the source area. Plumley's measurements were on limestone pebbles, whereas the author's values are the weighted mean of three siliceous rock types. As initial shape has much influence (Wentworth, 1922, p. 561), however, demonstrate the sphericity changes to be very slow.

Roundness.—Roundness was determined on three main rock types for the 16- to 32-mm size grade (at 39 stations) and the 32- to 64-mm size grade (at 17 stations). Estimations of roundness were made using the visual roundness chart (Krumbein, 1941a, p. 68). Sample size was determined in the same manner as in the case of sphericity. Usually 40–100 determinations per size grade were sufficient to ascertain the roundness mean for the particular locality.

A fairly wide range of values are noted (0.48–0.77), and the average is 0.55 in the 16- to 32-mm grade and 0.59 in the 32- to 64-mm grade. The values are between 0.1–0.2 higher than those of Krumbein (1940, p. 655, 1942, p. 1385) and Potter (1955, p. 20). As in the case of sphericity, distance and lithology seem to influence the values obtained. Very rapid rounding occurs in the first few miles, the rate decreases thereafter (Plumley, 1948, p. 558; Krumbein, 1941b, p. 492). The higher roundness of the cherts (upland gravels) compared with those of the Lafayette gravel of western Kentucky (0.53 versus 0.42 in the 16- to 32-

mm class), suggests that the upland cherts were transported a greater distance.

Interrelations between scalar properties.—In the larger sizes, quartzite is the dominant rock type, whereas "vein" quartz is the chief constituent of the 16- to 32-mm size grade. In sand-size material (Table 5) quartzose detritus formed up to 97 per cent by count (based on three samples); chert formed the remainder (heavy minerals were not included). Such trends, with quartzose material dominant in the finer sizes may result from differences in abrasional resistance of the rocks or perhaps from initial differences in the relative amounts rock introduced at the source area.

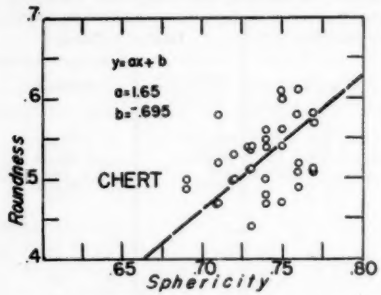

FIGURE 8.—CHERT SPHERICITY-ROUNDNESS LINEAR RELATION

In the smaller size grades, roundness determinations were made by use of a binocular and petrographic microscope (Table 5). A gradual decrease in roundness is present as finer and finer material is encountered. This relation was noted by Pettijohn and Lundahl (1943, p. 74) in beach sands and is valid for mature sands and gravel in general. Pettijohn (1949, p. 53) states, "The products of a long abrasion history show a close correlation between roundness and size. The larger sizes are better rounded." Presumably this correlation reflects the rate at which rounding occurs, being faster in the larger sizes.

In the two size grades studied, the pebbles were more spherical than rounded (average sphericity of 0.73; average roundness of 0.56). A linear relation between sphericity and roundness has been noted (Pettijohn, 1949, p. 408; Plumley, 1948, p. 561). In the upland gravels, the rounder pebbles also tend to be more spherical. The relation for "vein" quartz and quartzite pebbles in the 16- to 32-mm class is obscure. The values for chert were less scattered (Fig. 8). The roundness-sphericity relation seems to be of the type: $y = ax - b$, where y = roundness, x = sphericity, $a = 1.65$ and $b = -0.695$. Thus, for a 12 per cent change in sphericity, there is a 53 per cent change in roundness. The rate of change is considerably less than Plumley's values for limestone pebbles (12.3 per cent change in sphericity for 380 per cent change in roundness). Values of a and b are somewhat different from those calculated by Pettijohn and Lundahl (1943, p. 74), a = 2.2, 2.01 and $b = -1.27, -1.25$, for sand-size material. The coefficient of correlation (r)—a measure of the scatter—is 0.902; in a perfect positive linear relation, r equals 1 (Arkin and Colton, 1950, p. 80-81).

In the 16- to 32-mm grade, quartzite has a higher roundness than the other two rock types. The same relation is present in the 32- to 64-mm size class. This may reflect the ease with which the more friable quartzite was abraded.

SPATIAL (FACIES) CHANGES

General

The writer plotted both scalar and vectoral data on a series of maps to disclose systematic areal variations which might aid in interpreting the paleographic relations of the upland deposits.

The data can be present without any statistical modifications (Figs. 3, 9) and still show a trend or over-all direction. Or, it can be statistically grouped by the use of moving averages (Figs. 11, 12), which tends to "smooth out" irregularities caused by local and chance variation from locality to locality. The method was used by Potter (1955, p. 19) in the Lafayette gravel study to present size and cross-bedding data. In the present study, a grid divided into 1-inch squares was superimposed over a map of the formation. At each point of intersection of grid lines, the data from the stations falling within the four grid squares centered on the intersection, were averaged and the values placed at the point of intersection as shown in Figure 10. The values thus obtained were contoured.

Flow Vectors and Paleocurrents

Based on a compilation of the cross-bedding and gravel fabric data, an easterly to southeasterly direction of flow, which prevailed dur-

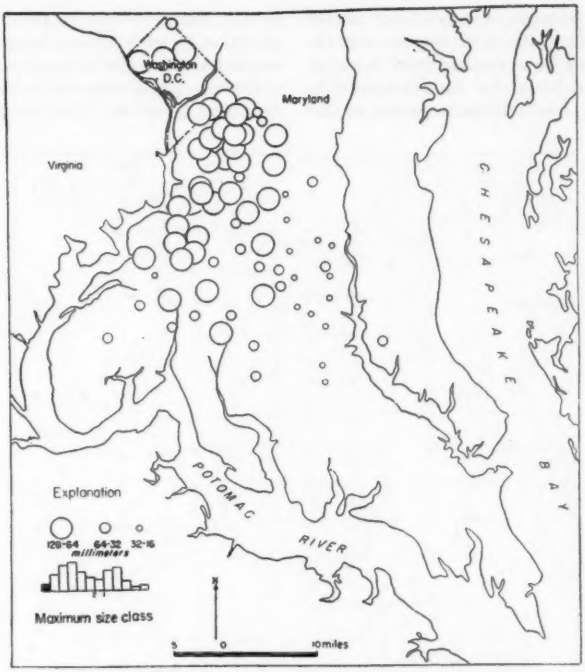

FIGURE 9.—AREAL OCCURRENCE OF THE MAXIMUM SIZE GRADE FOR SAMPLES COLLECTED FROM THE UPLAND DEPOSITS

ing deposition of the upland gravels, was established. This trend (Figs. 3, 11) is normal to the Potomac River in the northern part of the deposit and approximately parallel to the river in the southern part. The current flow tends to cross the peninsula subparallel to the contours showing the elevation of the formation base (Fig. 2). There seems to be no deviation in the direction of current flow pattern adjacent to the Patuxent River (Stations 26, 80 96, 98—Appendix A).

Size Changes with Distance

A decrease to the southeast of the maximum size class can be seen from Figure 9. Even more clearly, the same sort of change can be seen in the modal size of the gravel fraction (as expressed in phi units—negative log to the base 2) plotted through use of moving averages (Fig. 12). If Figures 11 and 12 are superposed (Fig. 13), the striking but normal relation between the paleocurrent direction and size diminution is obtained. In all parts of the gravel sheet, the fit is not perfect as can be seen in southern Charles and St. Marys Counties (southern part of the peninsula).

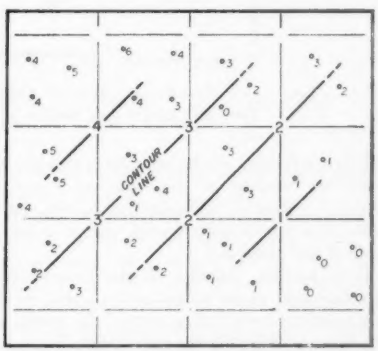

FIGURE 10.—EXPLANATION OF MOVING AVERAGE COMPUTATION PROCEDURE

The arithmetic average of the small size numbers in any four squares which intersect on a large size number, equals that large size number.

The orderly changes of modal size in the northern portion of the sheet suggest that the size change may be a mathematical function similar to those found for size diminution in modern rivers. The subequal spacing of the

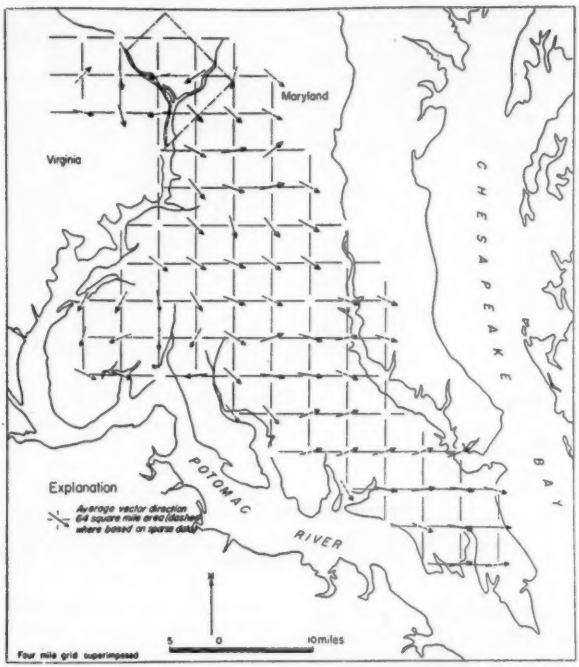

FIGURE 11.—MOVING AVERAGE DIAGRAM OF VECTORAL DATA
Over-all trend is very similar to that shown by the readings in Figure 3.

phi unit contours of distance indicates an exponential function of the form, $y = y_0 e^{-ax}$, where y = size at distance x from the source area, y_0 = size at source area, and a = coefficient of size reduction.

Four profiles, parallel to the current flow direction and as far as possible normal to the size contours were taken across the sheet. As can be seen (Fig. 14) the four points from each profile lie along a straight line. One line (shown in solid black, Fig. 14) represents the average as determined by the method of least squares.

The relation of size change is not new; the exponential function has been noted in ball-mill experiments and in modern rivers (Pettijohn, 1949, p. 397), but attempts to find similar such functions in ancient stream deposits have been unsuccessful (Plumley, 1948, p. 546, Potter 1955a p. 17). The genetic implication of such a function points to fluvial origin for the upland deposits.

Likewise, evaluation of the coefficient of size reduction (a) shows (Table 6) that is is of the same general order of magnitude as those for rivers (data for Table 6 is based on Pettijohn, 1949, Fig. 97, p. 397).

To obtain the value of a, in $y = y_0 e^{-ax}$, the value of y_0 (initial size) was assumed to be 128 mm. This value seems reasonable because it lies between the 160-mm diameter of the cobbles of the Rhine River study and 77-mm diameter of those of the River Mur study. From the slope of the line approximately 8 miles of travel is the "half distance"—that distance at which the diameter (modal size) is reduced to one-half of its initial value.

Thus, $y = y_0 e^{-ax}$, and $\frac{y}{y_0} = \frac{64}{128} = e^{-8a}$,

and taking the negative log of both sides, $-\log \frac{1}{2} = 8a$, $-(-.693) = 8a$, and therefore, $a = 0.087$

Such a derivation enables us to make some calculations concerning the distance to the source area. From the size-distance equation it is clear that cobbles 128 mm in diameter would have come from a place 8–16 miles northwest of the Fall Line. This would place the source area in granites, diorites, schists, gneisses, and quartzites of the Piedmont province. Most of the coarser fractions of the gravel, however, are "vein" quartz, quartzite, and chert, and contain little or no gneiss, schist, diorite, or granite. Inasmuch as the density differences between most of these rocks are small, sorting cannot be relied upon to account for the apparent loss of these rock types. Therefore, some other process such as weathering in the source area must have eliminated the multimineralic rocks and relatively enriched the quartzose rocks. The paucity of chert in the coarser sizes is to be expected inasmuch as its source lay much further to the northwest. In the 64- to 128-mm size grade, quartzite usually far exceeds "vein" quartz and chert. In the 32- to 64-mm size grade, quartzite percentages (Appendix C) are higher than chert percentages in 91 per cent of the counts. In smaller sizes 8- to 16-mm) this superiority is lost; in only 30 per cent of the pebble counts does quartzite exceed the chert present.

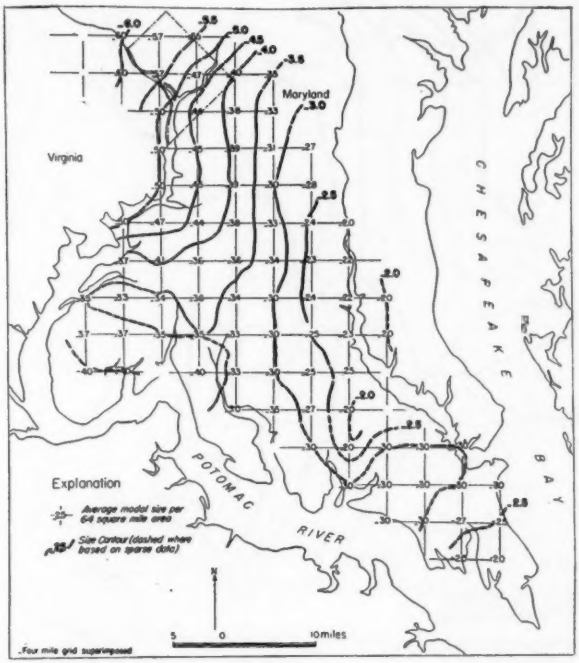

FIGURE 12.—MOVING AVERAGE DIAGRAM FOR MODAL SIZE DATA (GRAVEL) IN PHI UNITS
Notice particularly, the subequal spacing of the size contours.

As mentioned previously, anomalously course material occurs in the southern portion of the area so that size contours are no longer perpendicular to the paleocurrent vectors. Two explanations may account for these anomalies. First, the data are few in the southern portion of the peninsula; stations are approximately 5 miles apart. The moving average, therefore, is based on two or three stations per intersection and may not be truly representative of the deposits. Or, perhaps, a facies change exists in the gravels. Several other properties support this second contention. First, the gravel pits of this same area (southern Charles and St. Marys Counties) happened to contain ex-

tremely large boulders ranging from a cubic foot to more than 130 cubic feet (Fig. 15). These large boulders have been described by

altered. Climatic changes perhaps due to the advent of the Pleistocene, appear as a likely ultimate possibility. Such climatic changes also

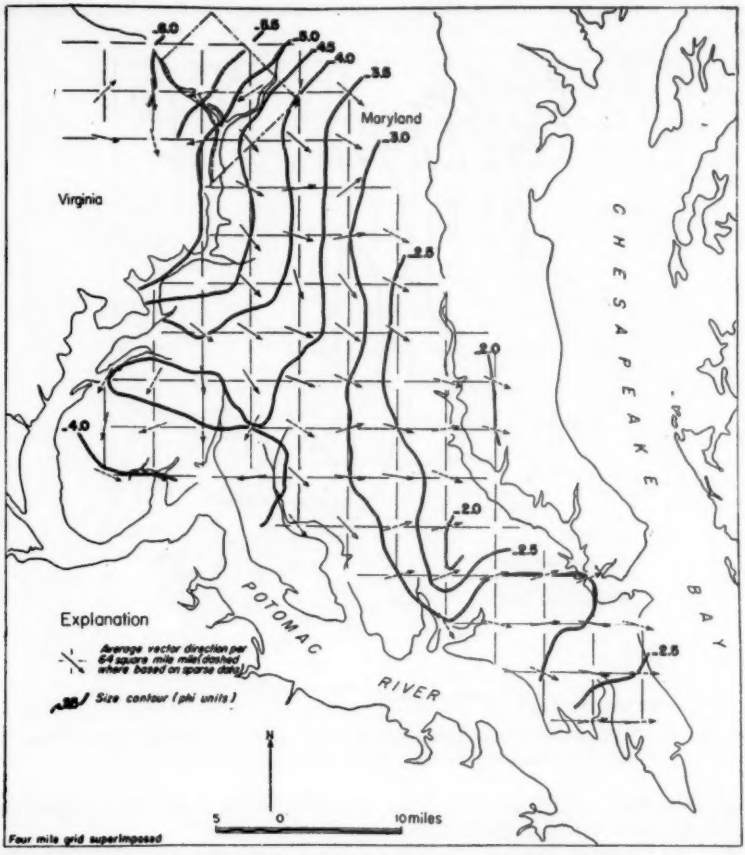

FIGURE 13.—MOVING AVERAGE DIAGRAM OF VECTORAL DATA (ARROWS) AND MODAL GRAVEL SIZE DATA (PHI UNITS)

Notice the normal relation between the arrows and the size contours.

Wentworth (1930, p. 46–47) who noted their proximity to the Potomac River and who attributed them to the "local action of river ice during colder climates than at present." Secondly, the minor rock types are also generally restricted to the Potomac side of the peninsula and to the lower elevations of the gravel sheet (Fig. 16). Taken together, they indicate a modification in the conditions during deposition.

Obviously, to effect such a facies change, the regimen of the dispersing agent was probably

may have formed the river ice needed to raft the large boulders as Wentworth has suggested.

The ancestral Patuxent River does not seem to have affected the size contours (Fig. 12) which seems to indicate that this river may have formed after the deposition of the gravel sheet.

Roundness and Sphericity

Roundness and sphericity show no systematic downcurrent variations. There is a

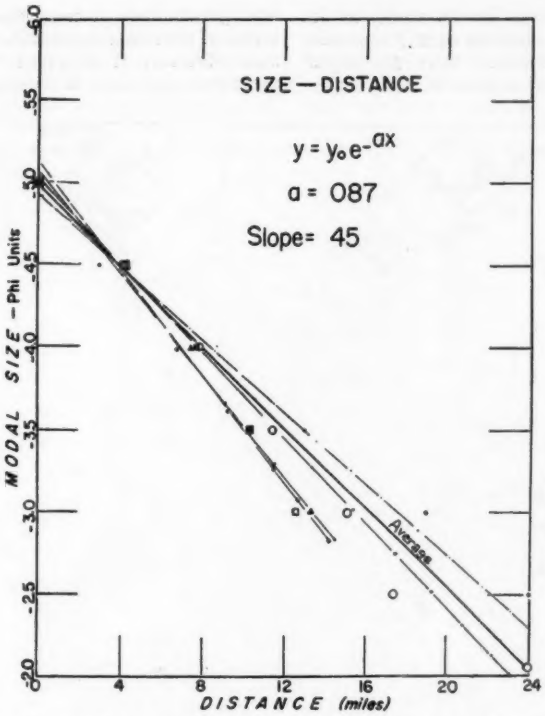

FIGURE 14.—SIZE-DISTANCE EXPONENTIAL RELATIONSHIP FOR THE UPLAND DEPOSITS

vague tendency for a southeasterly downcurrent increase in sphericity of quartzite pebbles in the 16- to 32-mm grade, but the magnitude of the change is only 0.05, which may not be statistically significant. Perhaps because the upland gravels are far enough removed from their source area, the roundness and sphericity values fluctuate erratically about some limiting value.

Lithology Changes with Distance

The proportions of the various major and minor rock types in the gravel show systematic areal variations which supplement the changes in the other sediment properties. These changes cannot be explained by rock ledges beneath the gravel sheet itself. All the gravel-sized material was derived from the rocks northwest of the Fall Line. The soft, partly consolidated Coastal Plain sediments contributed little or nothing. The changes in pebble lithology are irregular in places, but are generally systematic and fairly consistent from size grade to size grade (Figs. 17, 18). Likewise, they are generally consistent with patterns shown by current vector and size data.

TABLE 6.—VALUES OF COEFFICIENT OF SIZE REDUCTION

	Coefficient size reduction (a)
Largest Cobbles—Rhine River	.006
Mean Pebble diameter—River Mur	.010
Limestone	.007
Limestone—Abrasion mill	.016
Brandywine—Modal gravel size	.087

Moving average diagrams were made of the quartzite and chert amounts in three size grades (32–64 mm, 16–32 mm, and 8–16 mm). Inasmuch as they all tend to show the approximate pattern, only two of the more representative ones are included.

Quartzite (16–32 mm) content diminished to the east (Fig. 17) particularly in the north-

ern part of the area. To the south, in St. Marys County, the quartzite content is erratic, though notice particularly that the higher quartzite content is correlative with higher

mac gravels derived from the chert-bearing ledges of the folded Appalachians and that the main direction of transport was from the northwest by-passing Washington, D. C. The

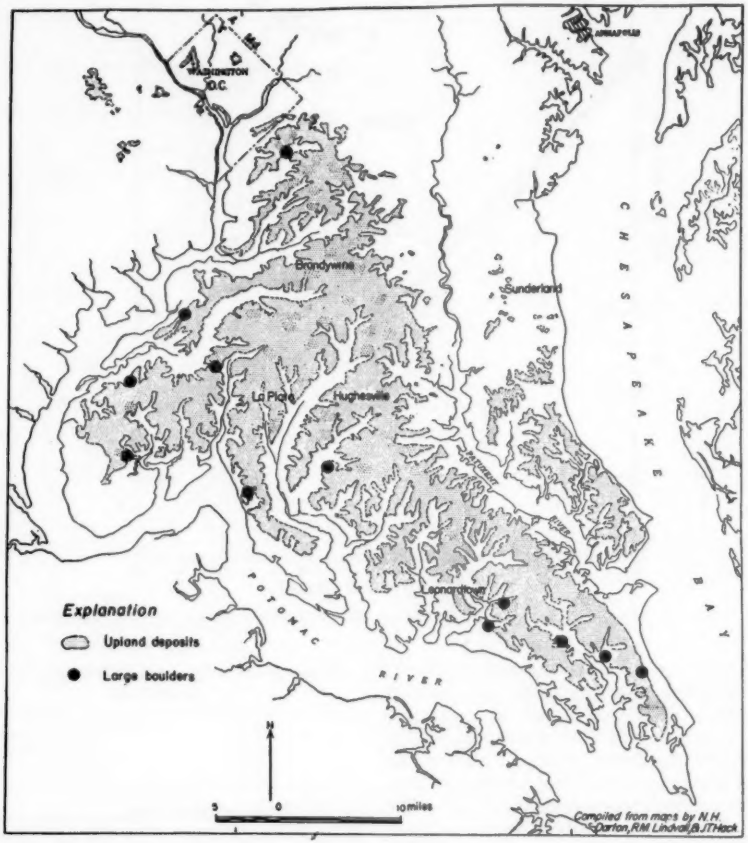

FIGURE 15.—DISTRIBUTION OF ANOMALOUSLY LARGE BOULDERS IN THE UPLAND DEPOSITS

values of the modal size (Fig. 12). Similar trends are present in the 32- to 64-mm and 8- to 16-mm grades.

Chert pebbles progressively increase in the downcurrent direction all three size grades. As shown in Figure 18, there is a paucity or a complete lack of chert in the terraces in Washington, D. C., and Silver Spring, Maryland, whereas in Virginia (Tysons Corners, and Fort Buffalo) chert is abundant. The chert content suggests that the main body of upland gravels in Virginia and southern Maryland are Pototerraces of the District of Columbia, on the other hand, were very probably deposited by a tributary, the drainage area of which was comparatively small and confined to non-chert-bearing rocks of the Piedmont.

In the 16- to 32-mm size class (Fig. 18), progressive down-current enrichment in the chert is observed in the northern portion of the peninsula. In southwestern Charles County and southern St. Marys County, anomalies in the chert content are present. Similar enrich-

ment of chert to the east is present in the 8- to 16-mm and 32- to 64-mm size grades.

What causes the diminution in quartzite and rise in chert content with distance? Such a change might be due to dilution, sorting, or abrasion. Dilution seems rather unlikely because little or no additional gravel-size material of the dominant lithologies could have taken place after the Fall Line was crossed. Sorting is difficult to imagine as the cause, inasmuch as chert and quartzite are not distinctly different in density. Shape differences are likewise not pronounced, and sorting on this basis would be difficult to justify. Abrasion seems a likely possibility, and its influence is indicated by the noticeably higher roundness values of quartzite. The clastic nature of the quartzite may have aided the abrasive process.

The areal distribution of the minor rock types has been touched on. Though minor in volume (24 per cent maximum at any locality), they are most abundant on the Potomac side of the gravel sheet, toward relatively lower elevations. Two of the heaviest concentrations (Fig. 16, solid circles) are in southwest Charles and southern St. Marys Counties—the same general region as the anomalies in the pebble lithology and modal size.

From distribution of minor rock types, modal size changes, and pebble composition,

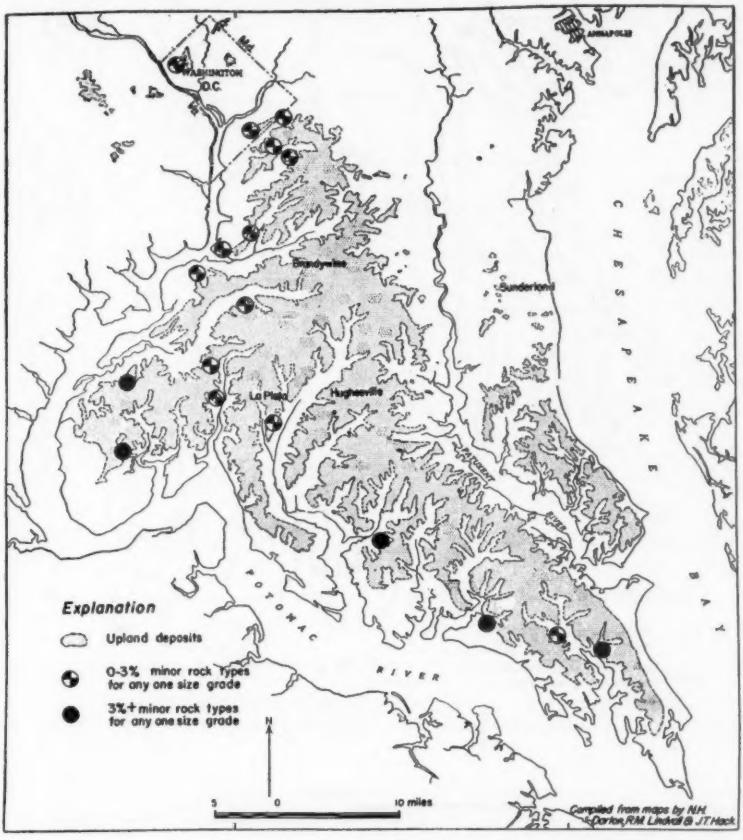

FIGURE 16.—DISTRIBUTION AND PER CENT OF MINOR ROCK TYPES IN THE UPLAND DEPOSITS

Notice the similarity between the distribution of the minor rock types and the anomalously large boulders.

it was seen that in the lower more southerly portions of the gravel sheet there appears to be a facies change with a coarsening of gravel size and a concomitant change in composition.

stages in the Frying Pan River area of Colorado.

The method is complicated, however, by (1) different chert sources at different times in the

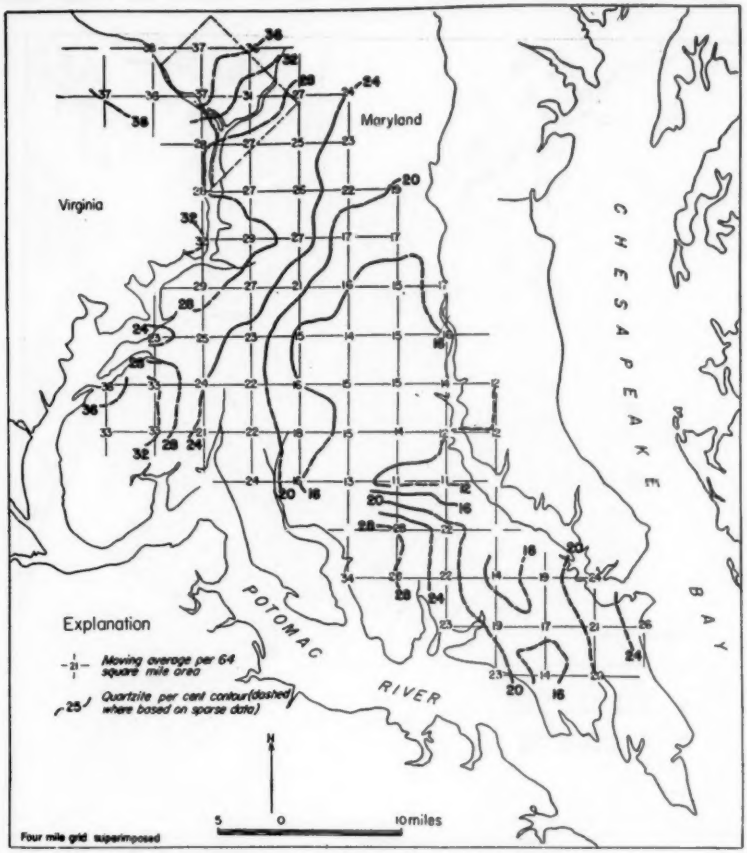

FIGURE 17.—MOVING AVERAGE DIAGRAM OF QUARTZITE CONTENT (16–32 MM)

With a composition more nearly like that of modern Potomac River gravels, it was expected that the southerly and lower portion of the upland sheet should be younger than the gravel to the north. To verify this, the degree of weathering of chert pebbles in different areas was studied. It was hoped that relative ages of the different portion of the upland gravels might be dated in this way. Such a method using granite porphyry pebbles and cobbles was used by Nelson (1954, p. 336) to delineate pre-Wisconsin and Wisconsin sub-

depositional history of the gravel, and (2) different post-depositional weathering history in different parts of the sheet. The first difficulty cannot be evaluated without a detailed study of the chert types to determine if they remain constant throughout the sheet. The second problem perhaps can be avoided by taking samples with similar matrices and coloration.

Three sets of samples were taken in the gravel member; two samples were taken near Leonardtown, a second set of three samples near La Plata, and the third set of three sam-

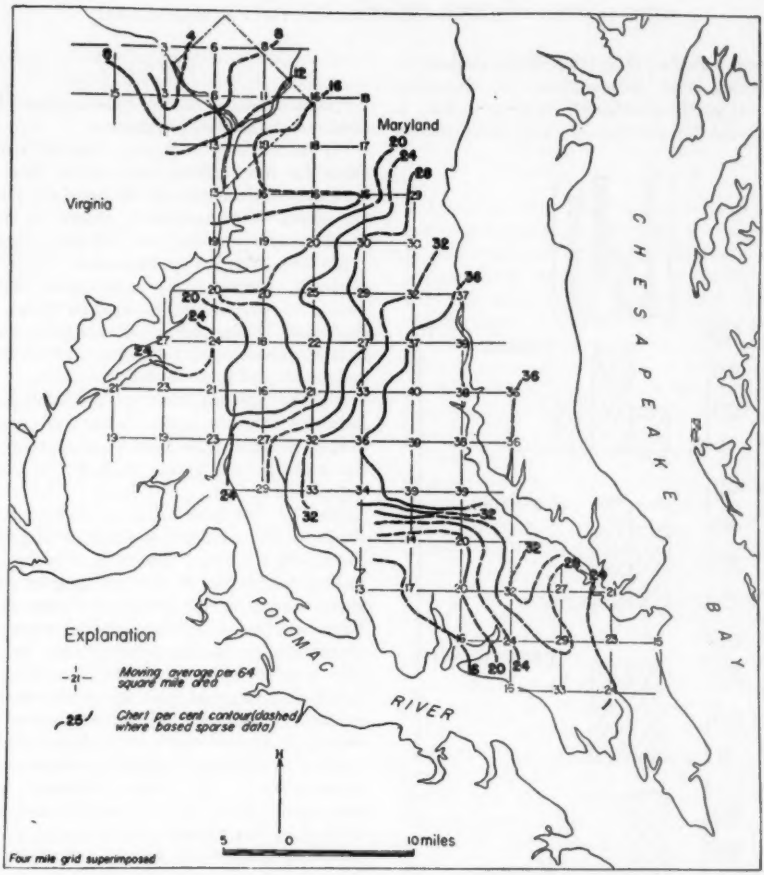

FIGURE 18.—MOVING AVERAGE DIAGRAM OF CHERT CONTENT (16–32 MM)

Note the eastward and southeastward change in chert content as also shown in quartzite content (Fig. 17) and size change (Fig. 13).

TABLE 7.—DEGREE OF CHERT WEATHERING

North ← → South

	Clinton					La Plata				Leonardtown			Potomac River—Alexandria Va. Smoot Sand and Gravel Co.	
Station No.	19	20	14*	Mean per cent with 14	Mean per cent without 14	65	63	47	Per cent	90	95	Per cent	f	Per cent
Unweathered	14	18	1	22	32	17	17	44	41	29	6	48	34	94
Partly weathered	35	27	17	53	62	19	32	25	55	28	13	52	2	6
Completely weathered	1	5	32	26	6	1	1	3	4	0	0	0	0	0

* Sample 14 contained an extremely high number of completely weathered chert pebbles which may indicate that stipulation 2 above may have been violated. Even excluding the sample, the trend is present.

ples near Clinton, Maryland. Three degrees of weathering were distinguished: (1) unweathered, (2) partly weathered, characterized by a white rind on the outside and unweathered

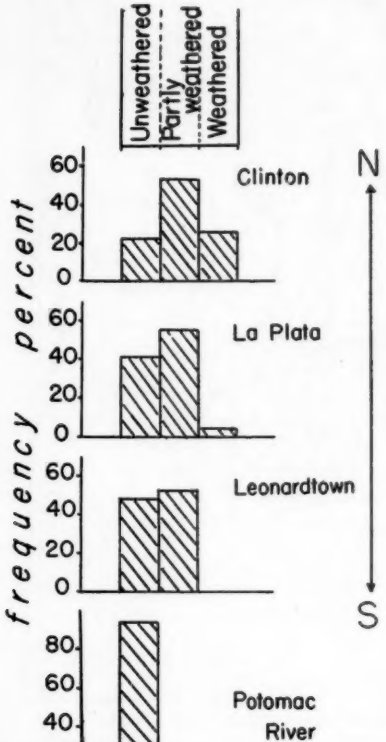

FIGURE 19.—HISTOGRAMS OF CHERT WEATHERING CHANGES

chert on the center, and (3) completely weathered, characterized by a clayey chalklike residue. Results are shown in Table 7 and Figure 19. For comparison, chert count from the modern Potomac River is included. Figure 19 shows the progressive increase in unweathered chert and the concomitant decrease in weathered chert southward, thus indicating a younger age for the southerly lower portion of the gravel sheet. The high deviation among samples in the same set indicates that more samples are needed.

Summary

Spatial relations of the upland gravels have disclosed the following points.

(1) An easterly sediment dispersal pattern exists for the northern part of the sheet and becomes southeasterly in the southern part of the sheet. The pattern is shown by cross-bedding, size changes, and lithology changes.

(2) The subequal spacing of the modal size contours suggests an exponential relation similar to that found for modern rivers. The coefficient of size reduction computed for the upland gravels, is of the same order of magnitude as that of modern rivers.

(3) The size-distance relationship further indicates that the source area was probably deeply weathered so that upon erosion, only the mature rock types reached the area of deposition.

(4) The last generalization is not strictly valid in the southern portion of the gravel sheet, where a facies change is indicated by a sudden fluctuation in size and pebble composition as well as the presence of anomalously large boulders, and immature rock types. The ultimate cause for the facies change was probably a colder climate. Furthermore, the chert weathering suggests that the southerly lower portions of the gravel sheet are younger than that part to the north at higher elevations.

(5) The sediment dispersal patterns in size, cross-bedding, and pebble lithology reveal that the Patuxent River or its ancestral equivalent does not appear to have taken part in the deposition of the upland gravels. On the other hand, the ancestral Potomac seems to have had much to do with the deposition of the upland deposits. First of all, the upland gravel is Potomac gravel, *i.e.* gravel which could have come only from the headwaters of the Potomac basin. It is distinguished by its high content of Paleozoic chert. The proximity of the river to the upland gravels further suggests that the two are related. Even though a large part of the course of the Potomac is now perpendicular to the flow vectors in the northern part of the sheet, the river is parallel to flow vectors in the southern part of the sheet. In addition, the general over-all trend of the Potomac is southeasterly, but like many of the larger rivers draining the Atlantic Seaboard, it turns to the right (southwestward) upon emerging from the Fall Line. The apparent parallelism of the present river and the paleocurrent vectors in western Charles and southeastern St. Marys Counties (Fig. 11)

serves to link the Potomac River with the gravel sheet. Moreover, the concentration of the minor rock types and the large boulders adjacent to the present course of the Potomac is striking and significant.

Lastly, when the conclusions from the scalar data are added, the picture is almost complete. Specifically, the bimodal size distribution is characteristic of a fluvial environment; a cumulative frequency plot of the sorting coefficients likewise displays a range of values consistent with a fluvial milieu.

All of this presents a strong case for a fluvial origin for the upland deposits based mainly on a petrologic approach to the problem. But, what have the previous studies disclosed?

Origin of the Upland Deposits

Previous hypotheses

General.—Any origin of the upland deposits must account for certain distinctive geomorphic and petrologic features which include:

(1) Lithologic association of loam and gravel
(2) Fairly uniform thickness of the deposit
(3) Poorly sorted character of the gravel
(4) Observed trends in the scalar and vector properties of the gravel
(5) Disparity between slope of the underlying and overlying surfaces of the formation and the direction of sediment transport
(6) Distribution of the minor rock types and anomalously large boulders
(7) Sheetlike areal distribution of the gravel

Marine.—Originally proposed by G. B. Shattuck (1901, p. 74–75; 1902, p. 73; 1906, p. 137; 1907, p. 99), the marine hypothesis holds that the upland deposits are a product of wave erosion of a Miocene coastline, and which through repetition four times of: (1) marine deposition, (2) uplift and subaerial erosion accompanied by entrenchment of river valleys, and (3) submergence and wave erosion, built a set of four terraces (Fig. 20). From highest to lowest they are the Lafayette (later named Brandywine), the Sunderland, the Wicomico, and the Talbot. The two highest terraces comprise "upland gravels". Later workers broadened and restated the hypothesis (Cooke, 1930, p. 577; Stephenson, 1912, p. 300–301), and the number of terraces recognized was increased to six (Cooke, 1930, p. 582). These and their elevations are:

Brandywine[2]	—270 feet
Coharie[3]	—215 feet
Sunderland	—170 feet
Wicomico	— 95 feet
Chowan	— 65 feet
Pamlico	— 25 feet

A marine origin was found untenable from a petrologic standpoint because the sorting is too poor; the bimodal size distribution does not appear characteristic of marine gravel. Moreover, the paleocurrent vector picture (Fig. 11) would require a marine current flowing normal to the coast and out to sea. Such an arrangement is particularly difficult to fit in with the configuration of the lower surface of the formation dipping as it does to the south and southwest (Fig. 2).

Lastly, if the upland deposits are in fact two or more separate terraces formed at different stands of the sea, the sediment properties might be expected to shift upon crossing the mapped contact (*i.e.* from one terrace to another). Such shifts were not apparent in the areas where geologic maps indicated that they might be anticipated. Geomorphic evidence (Campbell, 1931, p. 839; Flint, 1940, p. 760–762) failed to disclose scarps, beaches, spits or bars of linear continuity which would prove that the sea had previously stood at a certain elevation. Moreover, the fossil evidence fails to support the marine hypothesis. The younger terraces (Talbot) contain sea shells. Why then should not the "marine" Sunderland also contain marine fossils? Shattuck reports plant remains in the Sunderland and Brandywine terraces. Hay (1923, p. 345–348) found the remains of horses, elephants, and mastodons in the same terraces.

Indeed, in the past two decades, Cooke (1952, p. 37–46) has modified his views concerning Maryland Coastal Plain terraces so that the Brandywine (300–180 feet) and Bryn Mawr (350–518 feet) are now fluvial deposits, and the Sunderland (170 feet) is interpreted as a bayhead deltaic deposit. Cooke postulates a stand of the sea at 215 feet (Coharie).

Alluvial fan.—C. K. Wentworth (1930, p. 104) first proposed the alluvial fan origin for

[2] Cooke (1954, p. 204) has since substituted the name Hazelhurst terrace (270-foot level) for the Pleistocene Brandywine, but not for the Pliocene Brandywine which has a fluvial origin.

[3] Coharie—A designation used by Stephenson (1912, p. 273) for the marine terrace level at 215 feet in North Carolina and carried through to Maryland by Cooke (1930, p. 582).

Virginia gravels in part equivalent to the upland gravels of Maryland. He envisioned a large Potomac fan which began at Washington, D. C., and stretched to the south and east for 40–50 miles. Campbell (1931, p. 830) proposed the same origin for the southern Maryland upland gravels.

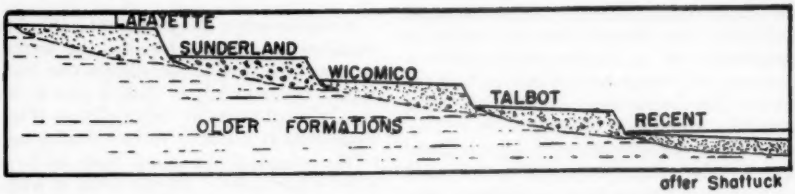

FIGURE 20.—SCHEMATIC DIAGRAM OF COASTAL PLAIN TERRACES BY SHATTUCK (1902)

Certain sedimentologic features support such a hypothesis. First, the sediment dispersal pattern, as discerned by cross-bedding and size data, is roughly fan-shaped. In addition, the sorting coefficient curve (Fig. 7) is similar to the one plotted by Emery (1955, p. 48) for alluvial fans. Other sedimentary features of the upland gravels are quite different from those of a fan. The peculiar association of silt grading down into gravel is widespread. The general lack of such features as torrential cross-bedding, and interfingering sand lenses and channel gravels do not support the fan hypothesis. Blissenbach (1954, p. 186) notes that fans have stratified deposits, pronounced channel cut-and-fill structure (observed in only three exposures in the upland deposits) and extreme variability in thickness of beds (up to 20 feet). He also notes the lenticular configuration of stream deposits in the fan, and the occurrence of unstratified mudflow deposits (due to sheet floods) interbedded with stream deposits. The upland gravels, though poorly sorted, are fairly well stratified.

Moreover, the fairly constant thickness of gravel from Virginia to southern Maryland makes it seem unlikely that the upland gravels are part of an alluvial fan; inasmuch as the alluvial fan is presumably the product of an aggrading stream system, it in most places shows a maximum thickness adjacent to the mountain front, and thins toward the outer edges.

Lastly, the present configuration on the base of the formation is difficult to imagine in terms of a fan or alluvial plain. The surface should slope to the east, but instead it slopes to the south and southwest (Fig. 2). The slope to the south might be accounted for by post-depositional silt, but inasmuch as the southwest slope merges imperceptibly into the south dip of the gravel sheet, streams in the alluvial fan would have had to have wandered to the southwest and to have cut a series of successively lower swaths to account for the southwest slope. This seems rather unlikely for an aggrading river system.

Collectively, these points negate an alluvial-fan hypothesis.

Migrating "Normal" River Deposit.—J. T. Hack (1955, p. 35) outlines the process of formation for the upland deposits as follows:

> "In the Coastal Plain, however, the ancestral Potomac flowed in the soft sediments, less resistant to erosion than the gravelly bed load of the river. For this reason, as the river meandered across the Coastal Plain, continually lowering its channel, it had a tendency to cut and erode the bank composed of Miocene sand more rapidly than the bank composed of gravel. As a result, in the Coastal Plain, the river has eroded a wide valley and kept it gently terraced and veneered with abandoned flood plain and channel deposits. The development of such a broad gently terraced valley is illustrated diagrammatically in figure 34, consisting of a series of hypothetical profiles illustrating stages in the development of an upland formed by lateral migration of degrading streams on a plain underlain by soft material, such as that of southern Maryland. The end result (profile F) is to produce a plain which slopes toward the major streams, and which is gently terraced by low scarps parallel to them."

It is difficult to envision a degrading river depositing a gravel sheet, but the process can be viewed at present in certain modern rivers. Mackin (1948) outlined the origin of the Shoshone River terraces in terms of the Shoshone itself. To quote Mackin (1948, p. 472),

> "The manner of origin of the terrace is indicated by the present activity of the stream, which is meandering on its valley floor. Some curves are slicing laterally at the base of vertical to overhanging rock walls, and some are shifting down valley from similar cut banks. As each meander shifts, it leaves behind a gravelly surface exposed at low water stage—it is safe to infer that the thickness

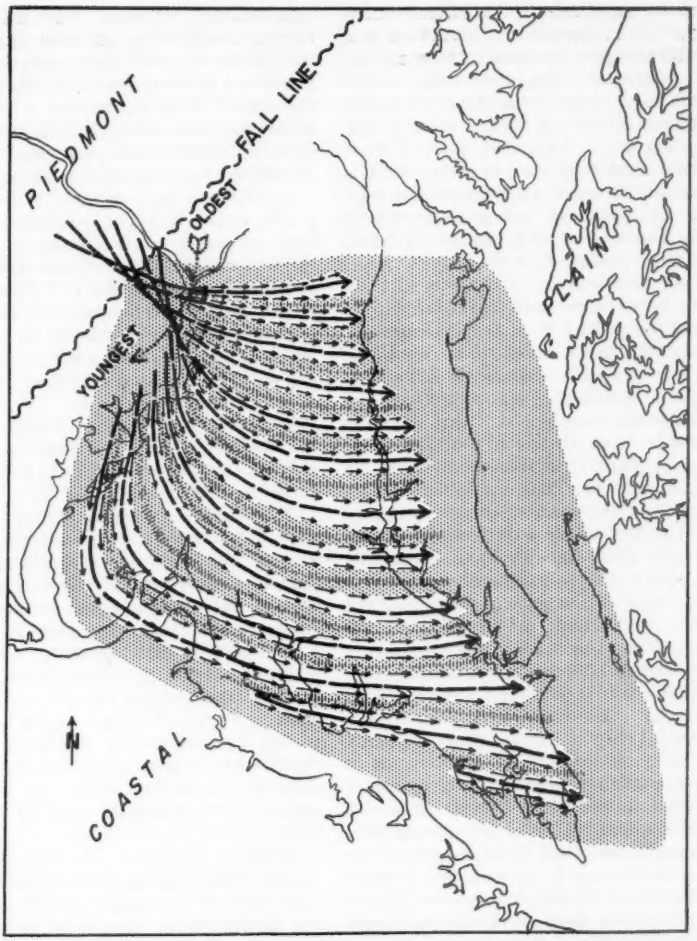

FIGURE 21.—SCHEMATIC DIAGRAM OF PALEOCURRENT TRENDS DURING DEPOSITION OF THE UPLAND DEPOSITS

of the channel is at least equal to the depth of the channel. It is evident that the gravel deposit grows by lateral accretion as the stream shifts, and if, as seems likely, it rests on a rock floor, then this floor must have been cut by the shifting stream, pari passu with deposition of the gravel. The gravel sheet represents the bed load; it is soon covered by fine silt and sand representing the finer fractions of the suspended load deposited by slow moving or ponded overbank waters, and later by slope wash and side-stream alluvial fans."

Through such a process, an association of channel gravel and overlying flood-plain silt is obtained along with a fairly constant thickness of gravel. These are the first two characteristics of the upland deposits which must be explained; what others can this process account for? The observed trends in scalar and vector properties can be explained by the same process combined with gradual downcutting; and when the spatial relations are added, the case for a fluvial origin for the upland deposits is nearly complete.

Only the sheetlike configuration of the deposit and the slope of the underlying surface

need to be explained. If the surface underlying the upland deposits dips southward, it is reasonable to expect the ancestral river to have flowed southward. Also, how does a river deposit a sheet of gravel the dimension of this one? A consideration of modern rivers (Happ *et. al.*, 1940, p. 27; Fisk, 1944, p. 6–9) shows that the normal flood plain or valley flat is a complex association of tributary alluvial fans, channel fill (sand, silt, and gravel), colluvial deposits (clay to boulders), channel lag (sand, gravel, and boulders), and splay deposits (sand, silt, and gravel). Equivalents of these deposits in all their ramifying interrelations were not recognized in the upland gravels. Moreover, the largest Shoshone terrace (Polecat) is only 3–5 miles wide and 20 miles long. As might be anticipated, the two problems can be logically explained by postulating a gradual migration from an easterly to southerly trend of the river (Fig. 21) adjacent to the Fall Line during downcutting. Thus, the initial outlines of the present Potomac valley were probably carved by successively lower swaths of the river which spread the gravel veneer much as Hack (1955, p. 35) has postulated.

This completes the genetic picture of the upland deposits except for the cause of the river migration. The cause of the migration is not known, but a number of possibilities exist. Hack (1955, p. 35) attributes the slip off to soft Coastal Plain sands which were more easily eroded than the gravel banks deposited by the river, and hence, as the rejuvenation of the river continued, slip off, cutting further and further to the south, became more and more pronounced. In order to appraise this mechanism, an additional factor, the anomalous course of the Potomac River, must be evaluated. The net result of the ancient migration, is that the Potomac now flows southeastward to the Fall Line and turns right (southwestward) onto the Coastal Plain roughly parallel to the Fall Line for 25 miles before resuming its southeasterly course. Such a course would not be unusual if it were not that other major rivers of the Middle Atlantic Coastal Plain follow the same pattern. The Susquehanna—*i.e.* its downed extension, the Chesapeake Bay—turns southwestward for 30–40 miles before a gradual southeasterly trend is reestablished; likewise, the Delaware River flows southwestward for 60 miles after leaving Trenton, New Jersey, before turning southeastward again. To the south, the James River has the same kind of anomalous course for approximately 10 miles. Did they all just happen to slip off in the same direction? Or, was there some additional factor which functioned as a *modus operandi* in combination with the slip-off slope mechanism to impart the anomalous river courses? Such factors might include: (1) coriolis force, (2) structural control, (3) offshore bars, (4) regional tilting.

Coriolis force was considered by Eakin (1910, p. 436) to be a factor in course deviation. This force supposedly causes a straight-line river to turn right (looking downstream) in the northern hemisphere due to rotational forces of the earth. It seems unlikely that such a force is effectively operative in this region, inasmuch as the rivers south of Virginia do not show the southward bend as do those up to the Hudson River.

Structural control seems doubtful because the over-all trend of the rivers is across the strike of the Coastal Plain beds, and the gradient is less than the dip of the beds.

The two remaining causes, regional tilting and offshore bars, were considered by Wentworth (1930, p. 13) who was perplexed by the same odd pattern of the rivers. The effect of bars has been used to explain anomalous river courses in the San Diego area (Hertlein and Grant, 1944, p. 18). Supposedly, offshore bars and ridges trending northeast-southwestward comprise the younger deposits of the eastern shore of Maryland (Carter and Sokoloff, 1951, p. 10). The writer finds it difficult to understand why offshore bars should cause the amount of deviation to increase toward the north, and to disappear south of the James River.

Regional tilting of the eastward-dipping Coastal Plain surface after deposition of the early phases of the upland gravels could give a net southeastward component of force and cause the river to meander in that direction. The effect of regional tilt on river courses is discounted by Cotton (1948, p. 337) who concludes that the net result of such tilt would be a higher bank on the more uplifted side, but no migration. But, if the valley were shallow the material in which it was cut was easy to erode, and if the tilting forced the river to one side, then Hack's mechanism might be able to operate. White (1953, p. 571) has utilized regional tilting from the north to explain the odd northeast-southwesterly tributary drainage pattern in Coastal Plain river in Virginia and North Carolina. Such tilting in Maryland might explain the pronounced development of such

southward-flowing tributaries as the Patuxent and Wicomico Rivers in Maryland Coastal Plain. The cause of the tilting is not known unless it might have been related to crustal adjustment due to formation of the Pleistocene ice sheet to the north. A complete study is needed before the cause-effect relations can be evaluated and the motivating forces discovered.

Geologic History

Data concerning the early stages of gravel deposition are obtained through integration of the Virginia outliers (above 300 feet) to the main sheet, trends in size-lithology data, and paleocurrent vectors. The isolated Virginia remnants of gravel above 300 feet which dip toward the main sheet in Maryland, suggest that they once may have been continuous with the sheet. In addition, the size trends and to a limited extent the lithologic trends continue into Virginia without a break. Cross-bedding and fabric direction indicate sediment transport from the west during the early stages of deposition. Events postulated in the later stages of deposition are based on the elevations of the base of the formation and size-lithology-vector data. The progressively lower elevations at which the anomalously larger boulders are found to the southeast may give an approximation of the river gradient during the early Pleistocene.

Marine conditions prevailed in the late Miocene. The shore line was located east of Washington, D. C. Because the marine sand beneath the upland deposits is not precisely dated, it is not possible to state exactly when the influx of gravel commenced. It is probably certain, as Hack (1955, p. 30) points out, that some of the earlier gravels were reworked to a limited extent by marine currents. Such reworking is indicated by the tendency for clean, well-sorted sections of gravel and sand to be situated more toward the eastern portion of the sheet. With rejuvenation of the eastward-flowing rivers due to landward uplift and/or oceanic withdrawal, deeply weathered debris from the Piedmont and Appalachians was incorporated into the load of the river. The ancestral Potomac which managed to remain near grade during the slow rejuvenation, slowly cut a shallow valley in soft easily eroded Coastal Plain sediments and, by lateral sidecutting, widened it and laid down a veneer of quartzose gravel. With continued downcutting and lateral sidecutting, the river slowly migrated to the south, deposited gravel at successively lower elevations, and removed Tertiary sands in the process. With continued migration, the ancestral Potomac slowly developed a southeasterly flow direction adjacent to the Fall Line while it maintained the same easterly trend in its downstream course (Fig. 21).

Definite changes were wrought in gravel deposition with the advent of the Pleistocene, perhaps because of a more rigorous climate. There was coarsening of the material, incorporation of immature rock types, and increasing inclusion of large boulders, the last probably rafted by river ice. The increase in the size of the load does not seem to be related to any increase in gradient. Indeed, if the lower and more southerly portions of the upland gravel sheet are correlative with the 250-foot terrace (Bailey's Cross Road, Virginia) or with a lower set, then the gradient of the river that deposited the lower more southerly portions of the sheet may have been less than that which deposited the older upland gravels (*i.e.* from Tysons Corner to Silver Hill and District Heights, Maryland). Such a relation would indicate that there may have been an increase in the discharge of the river, which with the same bed load would have tended to increase the cross-sectional area of the stream relative to the wetted perimeter and decreased the friction; thus an increase in velocity would allow for a temporary increase in the size of the material carried. But the river, because it was more than able to transport its load, would erode some additional material. This would decrease the slope. Erosion would continue until the velocity was so reduced that the river was just able to transport its load (Mackin, 1948, p. 494).

Formation of the continental ice sheets caused a marked lowering of the sea level with a subsequent phase of valley entrenching, very probably giving rise to the modern Potomac River valley, and effectively ending the upland phase of gravel deposition.

References Cited

Arkin, H., and Colton, R. R., 1950, Statistical methods: N. Y., Barnes and Noble Inc., 4th ed., 224 p.

Blissenbach, E., 1954, Geology of alluvial fans in semiarid regions: Geol. Soc. America Bull., v. 65, p. 175–190.

Campbell, M. R., 1931, Alluvial fan of Potomac River: Geol. Soc. America Bull., v. 42, p. 826–852.

Carr, M. S., 1950, The District of Columbia its

rocks and their geologic history: U. S. Geol. Survey Bull. 967, 59 p.
Carter, G. F., and Sokoloff, V. P., 1951, A study of soils and land forms of the Chesapeake Bay margins: Johns Hopkins Univ., Isaiah Bowman School of Geography, p. 1–37.
Clark. W. B., 1915, The Brandywine Formation of the middle Atlantic Coastal Plain: Am. Jour. Sci., 5th ser., v. 40, p. 499–506.
Cooke, C. W., 1930, Correlation of coastal terraces: Jour. Geology, v. 38, p. 577–589.
—— 1932, Southern Maryland: 16th Internat. Geol. Congr. (U. S.), Guidebook 12, Excursion B-7, p. 1–16.
—— 1941, Two shore lines or seven?: Am. Jour. Sci., v. 239, p. 457–458.
—— 1954, Carolina bays and the shapes of eddies: U. S. Geological Survey Prof. Paper 254-I, p. 195–206.
Cooke, C. W., *et al.*, 1952, Geology and water resources of Prince Georges County: Md. Geol. Survey Bull. 10, 258 p.
Cotton, C. A., 1948, Landscape as developed by the processes of normal erosion: N. Y., 2nd ed., John Wiley & Sons Inc., 509 p.
Darton, N. H., 1891, Mesozoic and Cenozoic formations of eastern Virginia and Maryland: Geol. Soc. America Bull., v. 2, p. 431–450.
—— 1893, On certain features in the distribution of the Columbia formation on the middle Atlantic slope: Am. Geologist, v. 11, p. 244.
—— 1894, Outline of Cenozoic history of a portion of the Middle Atlantic slope: Jour. Geology, v. 2, p. 568–587.
—— 1939, Gravel and sand deposits of eastern Maryland: U. S. Geol. Survey Bull. 906A, p. 1–42.
—— 1951, Structural relations of Cretaceous and Tertiary formations in part of Maryland and Virginia: Geol. Soc. America Bull., v. 62, p. 745–779.
Dryden, Lincoln, and Overbeck, Robert M., 1948, Geology of Charles County: Md. Dept. Geology, Mines and Water Res. p. 1–182.
Eakin, H. M., 1910, The influence of the earth's rotation upon the lateral erosion of streams: Jour. Geology, v. 18, p. 435–447.
Emery, K. O., 1955, Grain size of marine beach gravels: Jour. Geology, v. 63, p. 39–49.
Fisk, H. N., 1944, Geological investigation of the alluvial valley of the lower Mississippi River: Vicksburg, Miss. River Comm., War Dept., Corps Engineers, U. S. Army, 78 p.
Flint, R. F., 1940, Pleistocene features of the Atlantic Coastal Plain: Am. Jour. Sci., v. 238, p. 757–787.
Hack, J. T., 1955, Geology of the Brandywine area and origin of the upland of southern Maryland: U. S. Geol. Survey Prof. Paper 267A, 41 p.
Hack, J. T., *et al.*, 1950, The Coastal Plain geology of southern Maryland: Johns Hopkins Univ. Studies in Geology, no. 16, Guidebook 3, p. 1–56.
Happ, S. C., *et al.*, 1940, Some principles of accelerated stream and valley sedimentation: Dept. Agriculture Tech. Bull. no. 695, 134 p.
Hay, O. P., 1923, The Pleistocene of North America and its vertebrate animal from the states east of the Mississippi River and from Canadian provinces east of longitude 95°: Carnegie Inst. Washington D.C., pub. no. 322, 400 p.
Hertlein, L. G., and Grant, U. S., 1944, The geology and paleontology of the marine Pliocene of San Diego, California: Mem. San Diego Soc. Nat. History, v. 2, pt. 1 Geology, p. 18.
Krumbein, W. C., 1940, Flood gravels of San Gabriel Canyon, California: Geol. Soc. America Bull., v. 51, p. 639–676.
—— 1941a, Measurement and geological significance of shape and roundness: Jour. Sed. Petrology, v. 11, p. 64–72.
—— 1941b, The effects of abrasion on size, shape, and roundness of rock fragments: Jour. Geology, v. 49, p. 482–520.
—— 1942, Flood deposits of Arroyo Seco, Los Angeles County, California, Geol. Soc. America Bull., v. 53, p. 1355–1402.
Krumbein, W. C., and Pettijohn, F. J., 1938, Manual of sedimentary petrography: N. Y., Appleton-Century-Crofts, Inc., p. 31.
Mackin, J. H., 1948, Concept of the graded stream: Geol. Soc. America Bull., v. 64, p. 384–390.
Martin, R. O. R., and Ferguson, H. F., 1953, The water resources of St. Marys County: Md. Dept. Geology, Mines, and Water Res. Bull. 11, 194p.
McGee, W J, 1888, Three formations of the middle Atlantic slope: Am. Jour. Sci., 3d ser., v. 35, p. 367–388.
—— 1891, The Lafayette formation: U. S. Geol. Survey, 12th Ann. Rept., p. 353–521.
McKee, E. D., and Weir, G. W., 1953, Terminology for stratification and cross stratification in sedimentary rocks: Geol. Soc. American Bull., v. 64, p. 384–390.
Moroney, M. J., 1953, Facts from figures: London, Penguin Books, 472 p.
Nelson, R. L., 1954, Glacial geology of the Frying Pan River drainage, Colorado: Jour. Geology, v. 62, p. 325–343.
Otton, E. G., 1955, Groundwater resources of southern Maryland Coastal Plain: Md. Dept. Geology, Mines, and Water Res. Bull. 15, 347 p.
Pettijohn, F. J., 1949, Sedimentary rocks: N. Y., Harper & Bros., 526 p.
Pettijohn, F. J., and Lundahl, A. C., 1943, Shape and roundness of Lake Erie beach sands: Jour. Sed. Petrology, v. 13, p. 69–78.
Plumley, W. J., 1948, Black Hills terrace gravels: a study in sediment transport: Jour. Geology, v. 56, p. 526–577.
Potter, P. E., 1955, The petrology and origin of the Lafayette gravel: pt. 1—Mineralogy and Petrology: Jour. Geology, v. 63, p. 1–38.
Schlee, J. S., 1957, Fluvial gravel fabric: Jour. Sed. Petrology, v. 27, p. 162–176.
Shattuck, G. B., 1901, The Pleistocene problem of the north Atlantic Coastal Plain: Johns Hopkins Univ. Circ., p. 74–75.
Shattuck, G. B., *et al.*, 1902, Cecil County: Md. Geol. Survey, 315 p.
—— 1906, Pliocene and Pleistocene: Md. Geol. Survey, 287 p.
——1907, St. Marys County: Md. Geol. Survey, 205 p.
Stephenson, L. W., 1912, The Coastal Plain of North Carolina; the Cretaceous, Lafayette, and Quaternary formations: N. C. Geol. Survey, v. 3, p. 258–290.
Stephenson, L. W., *et al.*, 1932, Chesapeake Bay region: 16th Internat. Geol. Cong. (U. S.), Guidebook 5: Excursion A-5, 49 p.

Wentworth, C. K., 1922, The shape of beach pebbles: U. S. Geol. Survey, Prof. Paper 131-C, p. 75–83.

—— 1930, Sand and gravel resources of the Coastal Plain of Virginia: V. Geol. Survey Bull. 32, 146 p.

—— 1932, The mechanical composition of sediments in graphic form: Univ. of Ia. Studies, v. 14, no. 3, p. 1–127.

White, W. A., 1953, Systematic drainage changes in the Piedmont of North Carolina and Virginia: Geol. Soc. America Bull., v. 64, p. 561–580.

Grand Junction, Colo.

Manuscript Received by the Secretary of the Society, July 16, 1956

Appendix A.—Location of Samples

Sample Number

1. District Sand and Gravel Co. pit, 0.3 mile northeast of Maryland Route 5, 1 mile southeast of Gordon Corners, Maryland.
2. Northwest corner of 17th and Frankfort Streets, S. E., Washington, D. C.
3. Northeast corner of U St. and Branch Ave., S.E., Washington, D. C.
4. Behind Peoples Drugstore, Coral Hills Shopping Center, Bowen Road, Coral Hills, Maryland.
5. Forestville Sand and Gravel Pit, 1 mile east of District Heights on Walker Mill Road, Maryland.
6. Buffalo Sand and Gravel Co. pit, Gordon Corners, Maryland (intersection of Maryland Route 5 and 414).
7. Small pit north of St. Barnabas Road, west of Temple Hills, Maryland, near the Temple Hills Baptist Church.
8. Maryland Route 224, 0.5 mile south of Gilman Corners (intersection of Maryland Route 414 and 224).
9. Silver Hill Road, south of the highway, and 0.6 mile east of the junction of Maryland Route 218 and Silver Hill Road.
10. Abandoned pit of the Forestville Sand and Gravel Co. 0.4 mile south of Darcey Road, and Maryland Route 534 on Darcey Road (500 feet off of the road).
11. 0.5 mile east of the junction of Maryland Route 4 and Brown Station Rd. on Brown Station Rd. turn left on to Claire Rd. and proceed 400 feet along this road to the trench.
12. 0.8 mile northeast of the junction of Maryland Route 4 and Maryland Route 714, about 0.3 mile to the north of Maryland Route 4 on gravel road.
13. Abandoned pit opposite Military Air Transport Service base—Andrews Air Force Base, 0.5 mile west of junction of Maryland Route 218 and 337.
14. Camp Springs Cross Roads, 500 feet behind a large gray barn to the right of Maryland Route 5; enter from the northwest.
15. Paggetts Corners, take Temple Mills Rd. south from Paggetts Corners for 0.6 mile and turn right up gravel road by a white bungalow for 0.1 mile; outcrop is on the right of the road.
16. 6500 Bock Rd., S.E. near Palmers Corners, Maryland.
17. 1.6 miles south of Friendly, Maryland, just off Old Fort Rd., on macadam road to Tuckers Creek and Piscataway, Maryland.
18. 4.5 miles southwest of Clinton, Maryland, on Maryland Route 223, take gravel road to the left for 0.2 mile. Small pit off to right 400 feet off the gravel road.

Sample Number

19. 200 feet east of Box 358 of Thrift Road, 1 mile south of Hyde Field and Piscataway Rd.
20. Davis Sand and Gravel Corp., ¼ mile west of Surrattsville School, first abandoned pit on the lefthand side of the road.
21. Old Fort Rd., 0.9 mile south of Friendly, Maryland, opposite Providence Methodist Church on Thorne property.
22. Fort Washington Road, ⅛ mile east of the entrance to Fort Washington, Maryland, on the right-hand side of the road.
23. Smith's farm, Bryant Pt., Maryland, 1.4 miles northwest of Indianhead Access Road, south of Piscataway Creek.
24. 1.0 mile off of Maryland Route 224; take the Marshall Hall Rd. for 0.1 mile west from the Indianhead Access Road; turn off through the South Hampton Raceway arch (now a farm) for 1 mile to get to the pit.
25. Indianhead Access Road and Pine Road, 3.7 miles south of Piscataway Creek in Maryland.
26. Junction of Maryland Route 231 and Maryland Route 508 in Calvert County, Maryland.
27. 2.0 miles north of locality 20 on old Maryland Route 5 at the right hand side of the road going south.
28. 1.9 miles east of junction of Maryland Route 5 and McKendree Road on McKendree, on the right hand side of the road, 700–1,000 feet to the north.
29. 6.6 miles west of the junction of McKendree Road and Maryland Route 5, and 500′ south of McKendree Road (Mr. L. J. Higgs' farm).
30. 0.3 mile north of T B, Maryland; take gravel road in back of Kaiser-Willys dealer to the gravel pit.
31. Cedarville State Forest on Charles-Prince Georges County line, 0.4 mile east of Forest Headquarters.
32. 2.0 miles east of Brandywine on cross road between North Keyes Road and Maryland Route 381.
33. 2.8 miles east of Patuxent, Maryland, on Maryland Route 231.
34. 0.3 mile north of Maryland Route 231 on Maryland Route 381 near Patuxent, Maryland.
35. 1.0 mile south of Aquasco on Maryland Route 381.

36a. 1.3 miles south of Popular Hill, Maryland, on Maryland Route 381.

36b. Popular Hill, Maryland, 0.3 mile east of Maryland Route 381 on Maryland Route 382.

37. Junction of Maryland Route 382 and road to Baden and Westwood, Maryland.
38. On Woodyard Road, 2.0 miles northwest of Rosaryville, Maryland, and U. S. Route 301.

Sample Number

39. 0.5 mile east of Maryland Route 382 on Mataponi Creek Road and 1.0 mile southeast of Croom, Maryland.
40. Aist farm, 1 mile east of Cheltenham, Maryland, on gravel cross road between Maryland Route 382 and U. S. Route 301.
41. A. H. Smith Sand and Gravel Co., 2.2 miles north of Brandywine, Maryland, on U. S. Route 301.
42. Baden Road, 0.7 mile west of Westwood, Maryland, turn left on to gravel road for 0.2 mile and on the right is the gravel pit entrance.
43. Mattawoman Nike Station—gravel pit between the receiving and launching depots; turn east on road to Cedarville from U. S. Route 301 and proceed for approximately 1.0 mile to Nike entrance.
44. Colorado and 18th Streets, N.W., Washington, D. C.
45. Bolton, Maryland, 0.3 mile south of Maryland Route 228 (Berry Road).
46. On Benville-Bolton Road, 1.5 miles west of junction of Berryville-Bolton Road and road to Bealle, Maryland.
47. 1.0 mile south of Pomfret, Maryland, on road from Pomfret to Maryland Route 225.
48. 2.0 miles east of Mason Springs, Maryland, on Maryland Route 225.
49. 0.8 mile southeast of Pomonkey, Maryland, on Maryland Route 227.
50. 0.4 mile west of Gallant Green, Maryland, on Maryland Route 233.
51. East of St. Peters Church; 0.2 mile west of where Maryland Route 233 turns abruptly south, on 233.
52. 1.4 miles north of Bryantown, Maryland on Maryland Route 232.
53. 1.2 miles east of Masons, Maryland, off of road from Hughesville to Gallant Green, Maryland.
54. At the Junction of Maryland Route 5 and Maryland Route 488 southeast of Waldorf, Maryland.
55. 3.9 miles west of Locality 54 on Maryland Route 488.
56. 0.1 mile northeast of the junction of Maryland Route 233 and Maryland Route 5 on Maryland Route 233.
57. 1.0 mile west of U. S. Route 301 and 1.5 miles northwest of Waldorf, Maryland on unnamed road.
58. 0.9 mile east of U. S. Route 301 on Maryland Route 227.
59. 0.2 mile east of Berry, Maryland on Berry Road (Maryland Route 228), take gravel road off to the south (four yellow newspaper tubes) for a distance of 1.3 miles to the road cut.
60. 0.6 mile north of Maryland Route 6 at Rose Hill on the road to Maryland Route 225.
61. 0.7 mile north of the junction of U. S. Route 301, and Maryland Route 225 on U. S. Route 301 at the Parkway Tourist Center.
62. 4.0 miles southeast of La Plata, Maryland, on Maryland Route 6 just southeast of Newtown, Maryland.
63. 1.3 miles north of Maryland Route 6 on Maryland Route 232.
64. Ryceville, Maryland, 2.0 miles north of Budds Creek, Maryland. Travel 1 mile north of Wicomico, Maryland, and turn right on to dirt road and travel for 1.5 miles to locality 64a and 0.4 mile farther to locality 64b.
65. 1.6 miles east of Charlotte Hall on Maryland Route 6, turn left to gravel pit.
66. Montgomery Junior College, Silver Spring Maryland, under the overpass of the B. & O. Railroad tracks.
67. Fort Totten, Washington, D. C., northern part of park, north of the main earthworks.
68. Macomb and New Mexico Ave., N.W., Washington, D. C.
69. 3.3 miles east of Patuxent, Maryland, on road to Patuxent River Bridge (Maryland Route 231).
70. 3.4 miles south of Hughesville on the left hand side of the road (Maryland Route 5).
71. 2.1 miles southeast of Waldorf on Maryland Route 5, then 1.0 mile southeast on Maryland Route 693, then turn right and proceed 0.4 mile to gravel pit on the left hand side of the road.
72. 1.8 miles southeast of Waldorf on Maryland Route 5, turn right on to gravel road leading directly to the pit.
73. 1.9 miles southwest of Piney Church, Maryland, on the road to Brice, Maryland.
74. 1.8 miles south of Newtown on Maryland Route 588.
75. 2.8 miles south of Maryland Route 6 on Maryland Route 232, to the left hand side of the road, 500 feet from the road.
76. 0.3 mile west of Dentsville about 500 feet off Maryland Route 6.
77. 3.1 miles south of Charlotte Hall, Maryland, on Maryland Route 5, east side of the road.
78. 0.2 mile south of the East entrance to Andrews Air Force Base, turn left 0.1 mile on good gravel road to the pit and locked gate.
79. 1.5 miles north of Ironsides, Maryland, on Maryland Route 425, west side of road.

Sample Number

80. 2 miles east of Locality 26 on the north side of Maryland Route 231.
81. North Woodstock Ave. and 21st St., Lee Heights, Virginia.
82. Bliss Gravel Co., Tysons Corners, Virginia.
83. Fort Buffalo, Lee Blvd. and Leesburg Ave., behind Chevrolet garage, Virginia.
84. 0.5 mile north of Rison, Maryland, on Maryland Route 224.
85. 2.3 miles south of Ironsides, Maryland, on road to Grayton, Maryland, (Maryland Route 491).
86. Beauvue, Maryland, 4 miles due south of Leonardtown on Maryland Route 244.
87. 2.0 miles south of the junction of Maryland Route 234 and Maryland Route 5 on 5 to the east of the road.
88. Leonardtown Sand and Gravel Co.; 1.2 miles east of junction of Maryland Route 5 and Maryland Route 471 on 471.
89. Gravel pit, 8 miles south of the junction of Maryland Route 5 and 224 on 5, just west of Great Mills, Maryland.
90. 3.4 miles south of locality 89 on Maryland Route 5.

Sample Number

91. 1.6 miles north of railroad crossing just north of Lexington Park, Maryland, on Maryland Route 235.
92. Follow Hickory Hill Road west from St. Johns School (south of Hollywood, Maryland) for 1.4 miles and turn right on gravel road to get to the pit.
93. Evergreen Park; 1.0 mile south of the junction of Maryland Route 235 and road to Park Hall, Maryland, pit lies about 0.3 of a mile to the east of the highway.
94. 3.9 miles northwest of the junction of Maryland Route 244 and Chingville Road on 244.
95. 1.7 miles north of Hurry, Maryland, on the road to Chaptico, Maryland.
96. Mt. Harmony, Maryland, adjacent to the graveyard.
97. 0.2 mile north of Locality 26; just off (Southeast) of Maryland Route 231.
98. Junction of Maryland Route 2 and Maryland Route 231 west of Prince Frederick, Maryland, just south of the Amoco Service Station.

APPENDIX B.—SIZE ANALYSES—BY WEIGHT PER CENT

Locality	128–64 mm	64–32 mm	32–16 mm	16–8 mm	8–4 mm	4–2 mm	2–1 mm	1–½ mm	½–¼ mm	¼–⅛ mm	⅛–1/16 mm	<1/16 mm
1	4.3	26.3	27.3	12.8	7.3	3.6	1.9	7.5	6.6	1.7	0.4	0.3
2	11.3	20.1	20.2	12.0	6.5	3.4	4.0	5.1	6.7	4.5	2.2	4.1
3	14.4	15.4	17.3	7.4	3.2	1.9	8.1	14.1	10.2	5.4	1.9	5.6
4	1.8	9.2	12.6	11.6	7.8	5.7	9.4	15.9	10.9	6.0	3.1	5.7
5	0.6	11.4	30.7	15.5	8.2	5.2	4.5	12.4	7.1	2.7	0.9	0.7
6	6.2	18.4	23.0	14.4	6.2	3.0	3.3	7.2	11.3	4.5	1.2	1.2
7	10.2	23.9	23.4	10.5	6.6	5.6	4.0	6.4	6.0	2.8	0.3	0.3
8	10.4	11.1	8.5	6.9	3.7	2.2	6.3	12.1	12.4	10.0	9.0	7.3
9	3.1	20.5	32.8	9.7	5.0	4.0	6.5	9.8	5.3	2.0	0.6	0.8
10	....	4.2	15.0	22.4	14.7	9.2	5.5	11.6	9.0	4.3	1.8	2.3
11	....	3.8	10.9	23.6	14.6	8.4	5.9	10.5	10.2	6.4	2.4	3.5
12	1.5	8.7	15.4	17.1	12.8	8.6	6.2	14.6	8.9	4.0	1.2	0.9
13	12.6	10.7	20.1	15.4	7.1	5.5	5.6	7.1	6.4	4.7	2.1	2.8
14	3.4	3.7	16.1	18.6	10.5	7.4	7.1	17.1	11.3	2.4	0.8	1.3
15	0.8	8.4	18.7	17.6	9.6	5.9	5.8	15.0	11.6	4.3	1.2	1.1
16	5.7	16.6	14.3	10.7	7.2	5.8	7.9	12.0	10.0	5.2	2.1	2.4
17	15.4	24.4	16.7	11.4	6.4	3.9	4.1	6.5	5.8	2.1	1.0	2.3
18	5.1	18.0	20.4	17.6	10.5	6.6	3.2	4.6	5.8	2.9	1.4	3.7
19	4.4	15.0	16.9	15.5	10.4	6.3	5.3	11.2	11.5	2.1	0.9	0.7
20	....	7.5	24.7	20.1	11.9	7.5	4.8	9.7	9.1	2.7	0.8	1.1
21	5.3	19.9	18.8	15.0	7.1	3.9	2.6	8.6	9.7	5.4	2.0	2.2
22	13.0	20.0	15.9	11.3	6.7	3.9	3.2	7.0	11.7	3.9	1.3	1.4
23	9.3	19.6	13.3	9.0	5.5	3.7	4.1	10.9	15.5	4.1	1.8	3.0
24	14.8	18.6	16.4	13.1	7.1	3.8	3.6	7.4	9.1	3.2	1.1	1.8
25	4.1	10.5	19.3	11.7	8.0	6.0	3.3	8.2	12.2	9.0	4.1	3.6
26	....	0.5	2.0	15.8	20.8	14.6	8.4	15.1	16.7	4.2	1.0	0.8
27	1.2	5.4	18.2	27.2	15.3	9.3	6.3	8.5	4.8	2.3	0.6	0.8
28	....	7.6	28.4	19.1	10.9	6.6	3.8	8.2	10.6	3.0	0.8	0.9
29	8.6	25.2	22.4	11.0	8.0	4.8	2.9	7.3	6.4	1.8	0.8	0.9
30	2.5	5.5	16.8	19.4	13.3	8.9	4.9	12.0	13.4	1.9	0.6	0.8
31	....	0.8	22.4	26.9	12.4	6.9	3.8	8.5	13.8	3.8	0.4	0.3
32	....	0.4	7.3	16.0	13.2	9.9	6.4	13.9	26.8	4.5	0.7	0.8
33	....	....	0.3	13.2	14.4	12.5	7.2	14.3	23.3	7.5	3.3	3.9
34	....	....	1.9	15.2	19.6	17.9	14.4	17.0	7.3	3.8	1.4	1.5

APPENDIX B—*Continued*

Locality	128–64 mm	64–32 mm	32–16 mm	16–8 mm	8–4 mm	4–2 mm	2–1 mm	1–½ mm	½–¼ mm	¼–⅛ mm	⅛–1/16 mm	<1/16 mm
35	....	....	1.8	31.4	18.0	10.3	5.6	9.6	16.1	5.0	1.2	1.0
36a	....	....	3.7	20.1	22.7	16.7	11.6	11.8	10.0	1.7	0.6	1.1
36b	....	0.8	1.2	11.9	5.7	4.2	8.3	14.4	23.8	18.7	5.6	5.4
37	....	....	2.7	15.1	17.0	16.1	11.8	18.4	12.9	2.6	1.0	2.2
38	1.7	3.2	6.2	12.0	16.5	14.6	9.0	13.2	10.6	8.6	2.7	1.7
39	....	1.6	7.7	15.5	14.9	12.0	11.6	11.9	12.3	6.1	2.7	3.8
40	....	0.3	7.8	21.3	21.0	15.7	9.1	11.5	7.3	3.3	1.0	1.6
41	1.6	3.7	25.7	27.1	11.7	5.8	4.2	6.8	7.8	3.5	1.2	1.1
42	....	....	2.2	17.8	19.3	11.7	12.3	13.9	14.4	5.7	1.1	1.6
43	1.2	6.3	28.0	20.3	6.6	4.3	3.3	8.5	14.7	4.3	1.1	1.5
44	22.8	17.0	11.8	9.6	6.6	4.1	4.7	8.1	6.9	4.4	2.0	2.0
45	4.8	16.7	27.7	13.1	7.0	3.8	4.7	8.0	8.8	3.8	1.0	1.0
46	5.9	33.7	16.2	9.7	5.9	5.3	5.2	7.6	5.2	2.5	1.1	2.0
47	1.4	8.5	19.9	16.9	8.2	4.1	3.3	8.6	21.6	4.7	1.2	1.7
48	....	2.2	14.7	21.2	13.2	9.9	6.4	9.2	10.9	5.0	2.6	4.7
49	....		0.4	5.0	4.4	3.7	3.2	15.7	51.8	9.4	2.3	4.1
50	....		10.7	25.6	13.4	8.4	3.6	11.2	21.9	3.7	0.8	0.7
51	....	2.2	24.2	28.5	13.3	6.6	4.9	6.9	6.7	4.3	1.3	1.2
52	....	7.9	23.2	20.1	11.3	6.6	3.2	7.0	10.9	5.3	2.0	2.4
53	....		4.5	16.0	16.5	11.4	8.9	16.5	14.2	6.8	2.6	2.7
54	1.3	2.4	8.2	13.5	10.8	9.3	10.3	21.0	18.9	2.8	0.8	0.8
55	....	0.3	5.3	9.0	6.3	4.3	7.8	15.3	30.1	13.4	4.1	4.3
56	....	1.0	6.7	29.2	17.6	6.5	3.3	5.7	16.3	10.2	2.3	1.0
57	....	4.8	19.4	19.1	12.9	7.4	5.5	14.9	10.6	3.0	1.1	1.4
58	1.1	5.8	17.7	18.9	11.2	7.4	6.7	13.3	12.4	3.0	1.1	1.4
59	....	6.3	18.8	20.8	14.7	13.5	12.0	7.1	3.7	1.2	0.5	1.5
60	....	6.9	19.3	20.3	12.8	8.0	4.0	11.5	13.1	2.5	0.9	0.8
61	....	7.8	26.8	19.1	10.6	5.4	3.0	7.7	14.6	3.2	0.9	0.9
62	1.7	17.6	24.4	12.3	9.4	5.3	4.4	9.1	11.4	2.4	1.0	1.1
63	....	0.3	5.9	27.7	18.5	6.6	5.0	8.2	20.2	6.1	0.8	0.6
64	....	0.5	4.1	17.0	12.7	9.7	8.0	22.2	18.1	4.5	1.8	1.5
65	....	....	4.3	20.4	16.4	11.2	8.7	14.4	17.6	5.3	0.8	0.9
66	....	2.9	3.3	5.3	8.7	11.5	14.2	22.6	16.7	7.5	3.2	4.1
67	4.0	17.0	16.2	9.9	2.4	1.8	3.0	13.7	20.8	6.0	2.3	2.7
68	25.0	14.5	12.5	8.7	4.5	3.1	4.8	9.6	9.2	3.9	1.9	2.3
75	....	1.3	7.9	27.6	14.0	6.7	3.0	7.2	28.7	2.4	0.6	0.6
77	....	....	1.0	7.1	8.7	7.7	7.2	22.7	38.2	4.7	1.4	1.4
79	....	12.0	13.3	16.8	12.8	10.2	8.3	15.4	6.8			

Appendix C—Pebble Count Compilation

Locality	Size class (mm)	Frequency per cent			
		"Vein" quartz	Quartzite and sandstone	Chert	Misc.
1	32–64	31	49	20	
1	16–32	49	30	20	1.0 Dark-red sandstone
1	8–16	61	21	18	
2 (75)*	32–64	33	56	11	
2	16–32	57	36	7	
2	16–8	72.5	17	8.5	
3	64–32	27	59	14	
3	32–16	53	23	24	
3	16–8	68	16	16	
4 (24)	32–64	33	54	13	
4	16–32	62	25.5	12.5	
4	8–16	73	17	9.5	0.5 Dark-red sandstone
5 (81)	32–64	38	35	37	
5	16–32	57	30	13	
5	8–16	70.5	15.5	14.0	
6 (101)	32–64	20	59	21	
6	16–32	48	24	27.5	
6	8–16	70	12	17.5	
7 (152)	32–64	24	52	24	
7	16–32	59	29	12	
7	8–16	70.5	13.5	16.0	
8 (37)	32–64	32.5	65	2.5	
8 (195)	16–32	59	28	13	
8	8–16	72.5	20	7	
9 (123)	32–64	37	37	26	
9	16–32	53	32	15	
9	8–16	68	12.5	19.5	
10 (21)	32–64	28.5	52.5	19.0	
10	16–32	57	20.5	22.5	
10	8–16	67.5	13.5	19	
11 (6)	32–64	33	67	....	
11	16–32	78.5	16.5	5	
11	8–16	82.5	14	3.5	
12 (17)	32–64	17.5	53	29.5	
12	16–32	49.5	23	27.5	
12	8–16	73	9.5	17.5	
13 (113)	32–64	39	38	23	
13	16–32	52	33	15	
13	8–16	66	18	16	
14 (15)	32–64	47	20	33	
14	16–32	53	20.5	26.5	
14	8–16	66	12	22	
15 (58)	32–64	36	38	26	
15	16–32	48	33	19	
15	8–16	70	11.5	18.5	
16 (54)	32–64	30	65	5	
16	16–32	58	38	4	
16	8–16	86	9	5	
17 (70)	32–64	25.5	66	8.5	
17	16–32	49.5	32	18	0.5 Red sandstone
17	8–16	60.5	20	19.5	
18	32–64	36	48	16	
18	16–32	68.5	18	23.5	

Locality	Size class (mm)	Frequency per cent			
		"Vein" quartz	Quartzite and sandstone	Chert	Misc.
18	8–16	68.5	14	17.5	
19 (66)	32–64	38	50	12	
19	16–32	53	20.5	26.5	
19	8–16	71.5	11	17.5	
22 (75)	32–64	29	59	10.5	1.5 Green sandstone
22	16–32	45	33.5	19.5	2.5 Green sandstone 0.5 Red sandstone
22	8–16	51	20.5	26	2.5 Green sandstone
23 (86)	64–32	28	57	14	1.0 Red sandstone
23	16–32	46.5	33.5	18.5	1.5 Red sandstone
23	8–16	49	12	37	
26	16–32	52	12	36	
26	16–8	61	15	34	
31	16–32	57	14.5	28.5	
31	16–8	77	9	14	
32	16–32	54.5	14.5	31	
32	8–16	67	10.5	22.5	
35	16–32	68	8.5	23.5	
35	8–16	43.5	16	40.5	
39	8–16	71.5	12	16.5	
39 (181)	16–32	52	12	29	
41 (29)	64–32	34	32	34	
41	32–16	51	20	29	
41	16–8	79	9	12	
42	16–32	47	16.5	36.5	
42	8–16	75.5	7	17.5	
43	32–64	34.5	50	15.5	
43	16–32	58.5	14	27.5	
43	8–16	66	10	24	
44 (39)	32–64	21	79	0	
44	16–32	73	25.5	1.5	
44	8–16	83	14	3	
45	32–64	31	43	26	
45	16–32	56.5	22.5	21	
45	8–16	73.5	6.5	19	
47	16–32	56	29	15	
47	8–16	59.5	17	23	0.5 Red sandstone
48	16–32	51	22.5	26.5	
48	8–16	62.5	8	29.5	
49	8–16	61.5	22	16.5	
50	16–32	46.5	12	41.5	
50	8–16	73	8	19	
52	32–64	23	50	27	
52	16–32	61.5	15	23.5	
52	16–8	73.5	8	18.5	
53	16–32	53	17	39	
53	8–16	53	5	22	
54	16–32	59	14.5	26.5	
54	8–16	69	9	22	
58	16–32	71	17	12	
58	8–16	72.5	11.5	11	
60	16–32	56.5	21	22.5	
60	8–16	64	18.5	16.5	1.0 Red sandstone
62 (52)	32–64	32.5	54	13.5	0.5 Red sandstone

APPENDIX C—*Continued*

Locality	Size class (mm)	Frequency per cent			
		"Vein" quartz	Quartzite and sandstone	Chert	Misc.
62	16–32	45	26.5	28.5	
62	8–16	54.5	25	20	
63	16–32	54.5	9	36.5	
63	8–16	60	13	27	
64	16–32	55	11	34	
64	16–8	69	5.5	25.5	
65 (95)	16–32	49	11	40	
65	8–16	66	12.5	21.5	
66	8–16	88.5	1.5	10	
67	32–64	17	83	0	
67	16–32	52	48	0	
67	16–8	71	29	0	
68	32–64	21	79	0	
68	16–32	59	38	3	
68	8–16	70.5	23	6	0.5 Red sandstone
75 (93)	16–32	48.5	20	31.5	
75	16–8	65.5	14	20.5	
77	8–16	69	8.5	22.5	
79	8–16	65.5	14.5	20	
79 (132)	16–32	40	32	28	
82	64–32	19	66	15	
82	32–16	48.5	36.5	15	
82	16–8	65	21	14	
83	32–64	12	78	9	
84	64–32	25	61.5	13	0.5 Red sandstone
84	32–16	35	43	14	8.0 Brown sandstone
84	8–16	42.5	32.5	25	
85	64–32	22	63	7	5.0 Green sandstone 3.0 Red sandstone
85	32–16	56	25	16	3.0 Green sandstone
85	16–8	50	20	25	5.0 Green sandstone
86	32–64	29	45	11	6.0 Red siltstone 9.0 Brown siltstone
86	16–32	55	23	16	1.0 Clay 5.0 Brown siltstone
86	8–16	64	10	25	1.0 Brown sandstone
87	16–32	58	22	20	
87	16–8	72	7	21	
89	16–32	50	14	33	1.0 Red siltstone 2.0 Brown siltstone
89	16–8	68	13	18	1.0 Red siltstone
90	16–32	56	26	15	4.0 Brown siltstone
90	16–8	66	11.5	21	1.5 Brown siltstone
91	32–16	55	24	21	
91	8–16	68	10	22	
92	32–16	54	14	32	
92	8–16	67	5	28	
93	8–16	65.5	8.5	26	
94	8–16	64.5	16.5	19	
95	16–32	47	34	13	3.0 Red sandstone 3.0 Brown sandstone
95	16–8	65	8	22	2.5 Brown sandstone

* Number of pebbles counted; all others, 200 pebbles counted.

Short Notes

BULLETIN OF THE GEOLOGICAL SOCIETY OF AMERICA
VOL. 68, PP. 1411-1412, 1 PL. OCTOBER 1957

GIRVANELLA NOT A GUIDE TO THE CAMBRIAN

BY RICHARD REZAK

In a recent paper Scholten (1957, p. 156) refers to a personal communication by L. L. Sloss to the effect that the Bayhorse dolomite of Central Idaho is of Cambrian age and contains *Girvanella*. Unfortunately, the statement is worded in such a manner as to imply that the age assignment is based upon the occurrence of *Girvanella*. It should not be concluded that the presence of this genus is proof of the Cambrian age of the Bayhorse dolomite. The type species is from the Ordovician Craighead limestone of the Girvan District in Scotland (Nicholson and Etheridge, 1880, p. 23–24), and the genus is known to range from Cambrian through Lower Cretaceous (Pia, 1927, p. 38). *Girvanella* is not a guide to the Cambrian even though it may seem to be restricted to this system in southwestern Montana, and the presence of the genus in the Bayhorse dolomite of Cambrian(?) age has not been demonstrated with certainty.

Just what is *Girvanella*? Many geologists designate as *Girvanella* any concentrically layered pellet or pisolite that occurs in rocks of early Paleozoic age. This can be misleading. Many such pellets or pisolites are composed of *Girvanella*, but there are also many pellets that do not exhibit the microscopic characteristics required for the identification of the genus. The original description of the type species *G. problematica* Nicholson and Etheridge (1880, p. 23) states that it is composed of cylindrical tubes from 1/600th to 1/700th of an inch in diameter, twisted together in loosely vermiculate aggregations of a rounded or irregular shape. The microscopic tubules, not the pellets, constitute the genus *Girvanella*. Therefore, examination of thin sections is necessary before a positive identification can be made (Pl. 1). There is no indication in the paper by Scholten that Sloss identified the fossils from thin sections. C. P. Ross (1937, p. 13) states that two types of pellets occur in the formation, one composed of chert and the other dolomite. Each dolomite pellet consists of a single crystal grain of dolomite. The writer has examined a thin section of the dolomite pellets and finds no evidence to indicate the presence of *Girvanella*. The chert pellets could possibly retain some microscopic structures, but unfortunately no pellets are available to the writer at this time.

The affinities of this genus have been a matter of conjecture since it was erected in 1880. Its authors believed that it might be a rhizopod (Nicholson and Etheridge, 1880, p. 24). However, Rothpletz (1891, p. 301) placed the genus in the family Codiaceae (siphonous green algae) because of its apparent similarity to the genus *Sphaerocodium* Rothpletz. Later, Frémy and Dangeard (1935, p. 101) demonstrated that *Girvanella* is a synonym of the modern genus *Symploca* Kützing and as a consequence placed the genus in the division Cyanophyta (blue-green algae). Many geologists have accepted this latter interpretation of the genus; but the possibility still exists that more than one kind of organism is represented by specimens regarded as *Girvanella*.

The purpose of this note is not to present a comprehensive appraisal of the genus, but to point out that it is not a useful criterion of age. According to Scholten (1957, personal communication) it was not intended to imply that the age of the Bayhorse was established on the basis of *Girvanella* alone. Hence, no fossil evidence appears to exist at this time to confirm the Cambrian age of the formation.

References Cited

Frémy, P., and Dangeard, L., 1935, Sur la position systematique des Girvanelles: Soc. Linn. Normandie Bull., ser. 8, v. 8, p. 101–111.

Nicholson, H. A., and Etheridge, R., 1880, A monograph of the Silurian fossils of the Girvan District in Ayrshire, v. 1: Edinburgh and London, William Blackwood and Sons, 341 p.

Pia, Julius, 1927, Thallophyta, *in* Hirmer, Max, Handbuch der Paläobotanik: Munchen und Berlin, Verlag R. Oldenbourg, 708 p.

Ross, C. P., 1937, Geology and ore deposits of the Bayhorse region, Idaho: U. S. Geol. Survey Bull. 877, 161 p.

Rothpletz, A., 1891, Fossile Kalkalgen aus dem Familien der Codiaceen und der Corallinaceen: Deutsche geol. Gesell. Zeitschr., Bd. 43, p. 295–322, pls. 15–17.

Scholten, Robert, 1957, Paleozoic evolution of the geosynclinal margin north of the Snake River Plain, Idaho-Montana: Geol. Soc. America Bull., v. 68, p. 151–170, 7 figs., 1 pl.

U. S. Geological Survey, Federal Center, Denver, Colo.

Manuscript Received by the Secretary of the Society, May 2, 1957

Publication Authorized by the Director, U. S. Geological Survey

Plate 1.—*GIRVANELLA*

Figure 1.—*Girvanella* sp., Bromide formation, Bromide, Oklahoma. × 145. USGS Algae No. a632b. A well-preserved specimen.

Figure 2.—*Girvanella* sp., Gros Ventre formation, Beartooth Butte, Montana. × 145. USGS Algae No. a637a. Tubules partially destroyed by recrystallization.

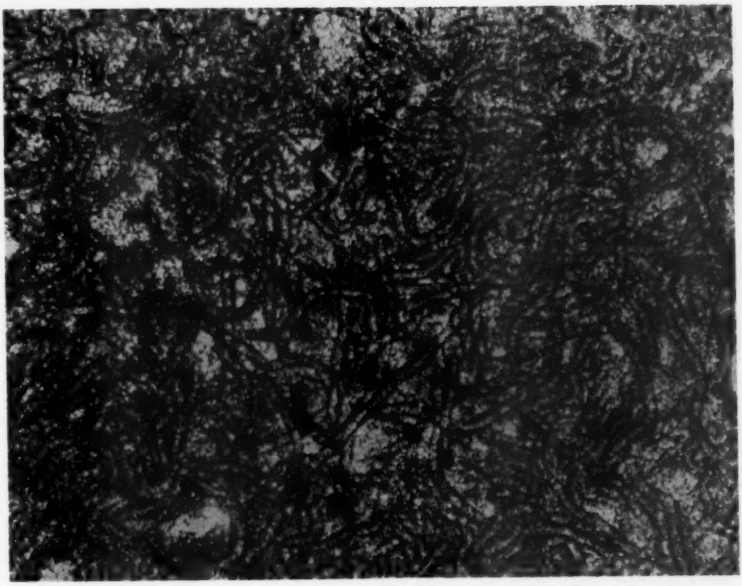

FIGURE 1

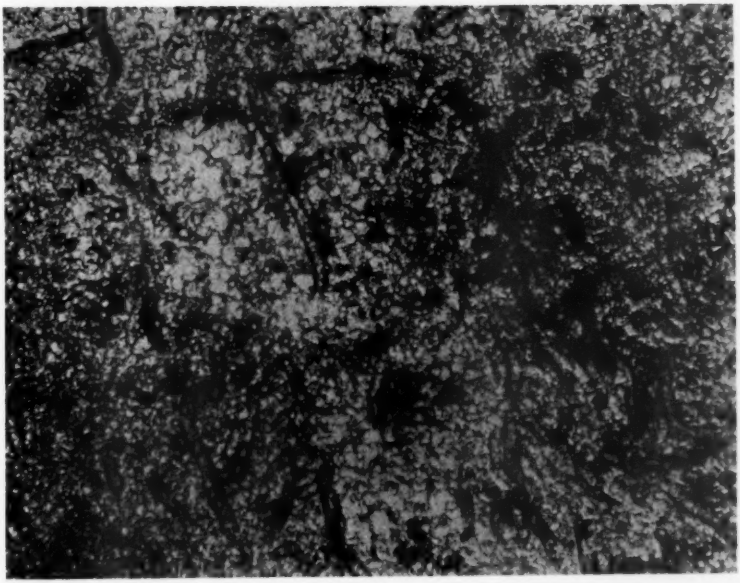

FIGURE 2

GIRVANELLA

BULLETIN OF THE GEOLOGICAL SOCIETY OF AMERICA
VOL. 68, PP. 1413-1414 OCTOBER 1957

MISCONCEPTION OF THE INTERMEDIATE REFRACTIVE INDEX

BY R. C. EMMONS AND R. M. GATES

It appears necessary to point up again a misconception in the optical procedure for the determination of a refractive index of a doubly refracting crystal (Emmons, 1943, p. 3). The misconception was applied and is endorsed recently in the Bulletin (Subramaniam, 1956, p. 235).

In the determination of the refractive indices of mineral grains by the immersion method, the grains must be in the extinction position, under which condition alone does the transmitted light have the value of one refractive index. In any other position between extinction positions, two refractive indices are available, each of which gives its own Becke line (or equivalent effect) and yields no intermediate value in ordinary crystalline material. The rotation on the microscope stage from one extinction position to the next causes one Becke line to increase in intensity and the other to decrease, but each retains its own identity and cannot blend with the other to give an intermediate value.

This principle may be checked readily in the laboratory by viewing the two independent Becke lines, or it may be proved theoretically as does Robertson (1934, p. 279) by means of the law of Malus.

The charts referred to by Subramaniam (1956) from Memoir 8 (Emmons, 1943, Pl. 10) may not be used as he uses them. They are applicable only to the changes in refractive index consequent on a change of vibration direction within a crystal and confined to an optical symmetry plane. For the present purpose that means a change resulting from a rotation on a horizontal axis only—the microscope stage has a vertical axis of rotation.

This recurring error of procedure has been pointed out in years past in an incidental way by others, buried under other titles. A modest search has not turned it up, but the writers recall that it has been taken care of.

References Cited

Robertson, J. K., 1934, Introduction to physical optics: New York, D. Van Nostrand, 422 p.

Subramaniam, A. P., 1956, Mineralogy and petrology of the Sittampundi complex, Madras State, India: Geol. Soc. America Bull., v. 67 p. 317–389.

Emmons, R. C., 1943, The universal stage: Geol. Soc. America, Mem. 8, 205 p.

UNIVERSITY OF WISCONSIN, MADISON 6, WIS.
MANUSCRIPT RECEIVED BY THE SECRETARY OF THE SOCIETY, JUNE 10, 1957